PNNL-25533
68592-RPT-001 Rev 0.0

Pacific Northwest
NATIONAL LABORATORY

Proudly Operated by Battelle Since 1965

Leading Indicator Process Development Report

October 2016

EC Golovich
MS Taubman
DS Daly
LA Mahoney
SK Cooley
J Bao
TM Brouns

Prepared for the U.S. Department of Energy
under Contract DE-AC05-76RL01830

PACIFIC NORTHWEST NATIONAL LABORATORY
operated by
BATTELLE
for the
UNITED STATES DEPARTMENT OF ENERGY
under Contract DE-AC05-76RL01830

PNNL-25533
68592-RPT-001, Rev. 0.0

Leading Indicator Process Development Report

EC Golovich
MS Taubman
DS Daly
LA Mahoney
SK Cooley
J Bao
TM Brouns

October 2016

Prepared for
the U.S. Department of Energy
under Contract DE-AC05-76RL01830

Pacific Northwest National Laboratory
Richland, Washington 99352

Summary

The Hanford Tank Farms has 177 underground tanks distributed across 18 tank farms that contain radioactive and chemical wastes from the Cold War era plutonium production missions. These tank farms contain either single-shell tanks equipped with passive breather filters on 1.0 to 1.5-m stacks or double-shell tanks which are actively ventilated through 6- to 12-m tall stacks. Chemical vapor emissions have been a concern at the tank farms despite efforts to understand and manage potential exposure to vapor emissions. An increase in reported symptoms suspected to be related to chemical vapor exposures during early 2014 led to a focused revitalization of the chemical vapors hazard management program to account for evolving conditions in the tank farms. The chemical vapors hazard management program is administered and implemented by Washington River Protection Solutions (WRPS), the U.S. Department of Energy's (DOE) Tank Operations Contractor. WRPS-led revitalization efforts included establishment of an independent Hanford Tank Vapor Assessment Team (TVAT) to examine hazardous chemical vapors management, related worker protection measures, and recommended actions. The recommendations of the TVAT (Wilmarth, et al., 2014) as well as other vapor control improvements are being implemented in a phased approach within WRPS' chemical vapors hazard management program[1] and include a series of projects and activities being executed by multi-disciplinary and multi-organization teams.

The chemical vapors hazard management program is guided by DOE's Integrated Safety Management System (ISMS), which defines the policies, objectives, and approach to ensuring protection of the public, worker and the environment (DOE, 2008). The five ISMS core functions, shown in Figure 1.1, define the structure for planning and implementing work activities that pose a potential hazard. The core ISMS function of "analyze hazards" is a focus of several key improvements to the chemical hazards management program and are represented by a series of projects and activities aimed at better identification and understanding of the vapor hazards. These activities include a) extensive headspace, source (e.g., stack or breather filter), and area characterization and monitoring, b) bench- and pilot-testing of a real-time vapor monitoring and detection system for potential tank farm deployment, c) updating the list of Chemicals of Potential Concern (COPCs) and corresponding exposure action levels to assure the most complete and recent tank farm data and chemical hazard information is being used, d) analysis of dispersion modeling methods to improve understanding of vapor plume migration and aerial extent of potential exposure, and e) identification of chemical vapor leading indicators (LIs) that can provide readily measurable early indication of vapor emissions ahead of other, more difficult to measure chemical vapors.

The Pacific Northwest National Laboratory (PNNL) is supporting WRPS' chemical vapors hazard management program improvement efforts with research, analysis, development, testing, and technical support in several of these key areas focused on better identification and understanding of the vapor hazards. The effort described in this report is one part of an overall vapors program at PNNL, specifically addressing the identification of chemical vapor leading indicators.

[1] WRPS. 2015. Implementation Plan for Hanford Tank Vapor Assessment Report Recommendations. Washington River Protection Solutions. Richland, Washington. http://wrpstoc.com/wp-content/uploads/2015/02/WRPS-1500142-Enclosure.pdf

The purpose of this work is to develop a process by which, concentrations of chemical species readily detected in near-real time in the field [e.g., ammonia (NH_3), nitrous oxide (N_2O), volatile organic compounds (VOCs), etc.] can be identified as LIs and indirectly suggest the presence of chemical species that are more difficult to measure. As LIs are identified for COPCs and knowledge of potential application increases, LI detection could serve as a means to alert staff of the presence of COPCs and help mitigate their risks in and around the tank farms.

Central to developing such a process is defining a technical basis for the relationship between potential LIs and the presence and semi-quantification of COPCs that may be difficult to measure. The principal tool for developing this basis is the statistical analysis of data from the tank farms in the Tank Waste Information Network System (TWINS) and other databases, including both the tank headspace characterization data and industrial hygiene monitoring samples. There are many aspects to consider, including selecting appropriate analytical tools, understanding what makes data suitable for this study, developing appropriate models (statistical, chemical transport, atmospheric drift and dispersion), and ultimately developing a selection criteria for LIs. There are a number of conditions within the tank farms that could alter the relationships between LIs and COPCs, including ventilation methods (passive ventilation in the single-shelled tank farms versus active ventilation in the double-shelled tank farms) or waste-disturbing activities as tank waste is sampled or retrieved. Understanding the time evolution of available data, in terms of diurnal and/or seasonal effects, is also instrumental to ensuring continued validity of specific LIs and the selection process in general.

This report describes the methods used to devise a process by which potential LIs could be identified and evaluated. A few key gaps and observations were identified throughout the initial evaluation of the data that can be combined into general themes.

Data Gaps: COPCs must be identified at the same time in the same location. The level of detail given for sample location varies from specific identification of particular tanks or exhausters to generic description limiting the ability to cross-reference samples. A standardized site-wide sample identification nomenclature is recommended to reduce the uncertainty of establishing related samples. All COPCs were not measured for every sample, meaning that analytical methods were used to only look at a select subset of the COPCs. It is recommended is that techniques are chosen so that all COPCs can be analyzed and reported for each air sampling event.

Vapor Sources: Nitrous oxide, hydrogen, ammonia and a number of VOCs are all characteristic chemicals from tanks, though none are unique to tank sources. Ammonia was positively detected in approximately 86% of the samples, while nitrous oxide and hydrogen were positively detected 62% and 76% of the time. Contributions from tanks and from non-tank sources may need to be identified in terms of multiple marker species and relative concentrations, so a more detailed multivariate statistical approach, such as factor analysis, is recommended to identify tank signatures.

Potential Leading Indicators: Overall, the available pairings indicate that both ammonia and nitrous oxide are strong candidates as LIs. Ammonia had pairings with 32 of the COPCs and nitrous oxide had pairing with 29 of the COPCs. The remaining COPCs did not have enough measurements to observe a pairing or relationship. The general trend for pairings with ammonia and nitrous oxide is that the majority of the paired data points fall above the 10% occupational exposure limit (OEL) level of the LI meaning that an alert on the LI would bound alerts for the COPC.

This distribution of data points results in low populations within the missed alert and true non-alert quadrants. Measured COPC concentrations can vary over a couple orders of magnitude for a particular LI concentration. Additional paired results with measured LI concentrations below the 10% OEL would give greater confidence in the probability distribution within the missed alert quadrant.

Acronyms and Abbreviations

AUC	area under the ROC curve
CFD	computational fluid dynamics
COPC	chemical of potential concern
DOE	Department of Energy
FY	fiscal year
IH	industrial health
ISMS	Integrated Safety Management System
LI	leading indicator
MDL	minimum detection limit
NDMA	N-nitrosodimethylamine
OEL	occupational exposure limit
PNNL	Pacific Northwest National Laboratory
ROC	receiver operating characteristic
SWIHD	Site-Wide Industrial Health Database
TBP	tributyl phosphate
THF	tetrahydrofuran
TVAT	Tank Vapor Assessment Team
TWINS	Tank Waste Information Network System
VMD&R	Vapor Monitoring, Detection and Remediation
VMDS	Vapor Monitoring and Detection System
VOC	volatile organic compound
WRPS	Washington River Protection Solutions

Contents

Figures

Tables

1.0 Introduction

The Hanford Tank Farms has 177 underground tanks distributed across 18 tank farms that contain radioactive and chemical wastes from the Cold War era plutonium production missions. These tank farms contain either single-shell tanks equipped with passive breather filters on 1.0 to 1.5-m stacks or double-shell tanks which are actively ventilated through 6- to 12-m tall stacks. Chemical vapor emissions have been a concern at the tank farms despite efforts to understand and manage potential exposure to vapor emissions. An increase in reported symptoms suspected to be related to chemical vapor exposures during early 2014 led to a focused revitalization of the chemical vapors hazard management program to account for evolving conditions in the tank farms. The chemical vapors hazard management program is administered and implemented by Washington River Protection Solutions (WRPS), the U.S. Department of Energy's (DOE) Tank Operations Contractor. WRPS-led revitalization efforts included establishment of an independent Hanford Tank Vapor Assessment Team (TVAT) to examine hazardous chemical vapors management, related worker protection measures, and recommended actions. The recommendations of the TVAT (Wilmarth, et al., 2014) as well as other vapor control improvements are being implemented in a phased approach within WRPS' chemical vapors hazard management program[1] and include a series of projects and activities being executed by multi-disciplinary and multi-organization teams.

The chemical vapors hazard management program is guided by DOE's Integrated Safety Management System (ISMS), which defines the policies, objectives, and approach to ensuring protection of the public, worker and the environment (DOE, 2008). The five ISMS core functions, shown in Figure 1.1, define the structure for planning and implementing work activities that pose a potential hazard. The core ISMS function of "analyze hazards" is a focus of several key improvements to the chemical hazards management program and are represented by a a series of projects and activities aimed at better identification and understanding of the vapor hazards. These activities include a) extensive headspace, source (e.g., stack or breather filter), and area characterization and monitoring, b) bench- and pilot-testing of a real-time vapor monitoring and detection system for potential tank farm deployment, c) updating the list of Chemicals of Potential Concern (COPCs) and corresponding exposure action levels to assure the most complete and recent tank farm data and chemical hazard information is being used, d) analysis of dispersion modeling methods to improve understanding of vapor plume migration and aerial extent of potential exposure, and e) identification of chemical vapor leading indicators (LIs) that can provide readily measurable early indication of vapor emissions ahead of other, more difficult to measure chemical vapors.

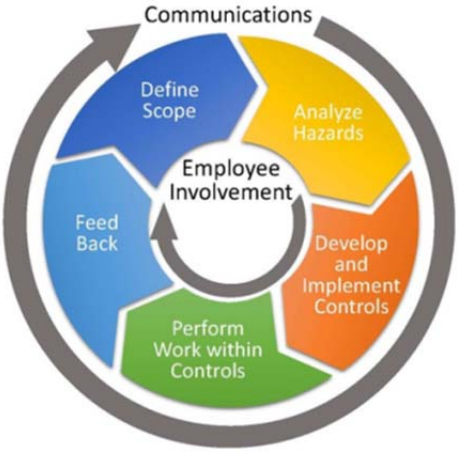

Figure 1.1. Integrated Safety Management System

[1] WRPS. 2015. Implementation Plan for Hanford Tank Vapor Assessment Report Recommendations. Washington River Protection Solutions. Richland, Washington. http://wrpstoc.com/wp-content/uploads/2015/02/WRPS-1500142-Enclosure.pdf

The Pacific Northwest National Laboratory (PNNL) is supporting WRPS' chemical vapors hazard management program improvement efforts with research, analysis, development, testing, and technical support in several of these key areas focused on better identification and understanding of the vapor hazards. The effort described in this report is one part of an overall vapors program at PNNL, specifically addressing the identification of chemical vapor leading indicators.

More than 1800 chemicals have been identified in the tanks over the last twenty or more years, with approximately 1,500 estimated to be in headspace, the primary source of tank emissions (Stock and Huckaby 2004). The remaining chemicals are stable in stagnant conditions and are found in the liquid waste. The chemical constituents of the tank vapors vary from tank to tank. Some tanks may have as many as 500 different chemical species present in the headspace. In 2006, the Industrial Hygiene Technical Basis team evaluated volatile chemicals for potential workplace risk and identified a set of chemicals of potential concern (COPCs) with corresponding occupational exposure limits (OELs) that provide guidance for monitoring vapor emissions within the tank farms (Meacham et al. 2006).[2] Many of these chemicals are difficult to measure, especially with available direct reading instruments that can provide real-time or near real-time detection. Using relationships between difficult and easier to measure COPCs (or non-COPC chemicals) may provide a means to infer more information about the difficult-to-detect COPCs. If chemical species (COPC or non-COPC) can be readily detected in near-real time at concentrations below their OELs or exposure action levels and correlate to or bound other COPCs at levels below their OELs, the easily measured species would be considered a LI.

The purpose of this work is to develop a process by which concentrations of chemical species readily detectible in near-real time in the field [ammonia (NH_3), nitrous oxide (N_2O), volatile organic compounds (VOC), etc.] can be identified as LIs of the presence and semi-quantification of chemical species that are more difficult to measure. As LIs are identified for COPCs and knowledge of potential application increases, LI detection could be a means to alert for those COPCs and help mitigate risks in the tank farms. Initially, it is expected that LIs would be identified for specific tank farms relationships, but as more data become available, LIs may be applied site wide.

The remainder of this report is organized as follows. Section 2.0 describes how the tank farms are divided into zones and how the relationship between LIs and COPCs can be affected. Section 3.0 describes the preliminary methods used to look for LIs in available data during development of the process. Section 4.0 discusses further method development for evaluating the alerting potential of LI candidates. Section 5.0 details the LI identification process. Section 6.0 describes the data sources and objectives to be used in the evaluation and validation of the LI identification process. Section 7.0 summarizes the conclusions of this work.

[2] The current list of 59 COPCs, dated 12/03/2008, is maintained on the WRPS industrial health and safety website.

2.0 Zones of Measurement

Defining the leading indicator process begins with an explanation of the tank farm and sources for detected vapors as it relates to potential LIs. Figure 2.1 illustrates the different zones of measurement in the Hanford tank farms. The top image shows two hypothetical tanks (*x* and *y*), each with its own solid and liquid contents (X), and headspace environment (A). In this illustration, tank *x* is shown with a breather filter or ventilation stack (B) and piping connecting to tank *y* with a hypothetical fugitive emission[1] (C). Also shown is a fenceline or boundary (D) around the region of interest that could be the tank farm or some other identified target region. The red dashed line around locations A and B of tank *x* indicates the initial focus of the LI process.

The lower image within Figure 2.1 identifies the relationships between various zones or regions (X, A, B, C, and D). The grayed annular regions represent the physical processes and phenomena impacting vapors as they move between these regions. Vapors evolve from the solid/liquid contents of the tanks (X). The tank headspace (A) is the primary reservoir of chemical vapors within the tank farm.[2] Vapors from the headspace (A) move passively to tank breather filters (B) or under negative pressure due to the stack ventilation (B), depending on the architecture of the tank, and can also become fugitive emissions (C). The intervening gray circle depicts processes that would change the nature or relative concentrations one might expect to see in region B relative to those within the headspace (A). These can include such things as catalytic or plating effects (e.g., deposition or condensation) through contact of vapors with metal piping, filter materials, etc. These same processes would also affect the vapors leading to fugitive emissions (C), although possibly in a different way.

Vapors from regions B and C can move to general geographical locations within the tank farm, and also can reach the boundary of the geographical region of interest, both of which are represented by D. The larger intervening grayed circle represents processes that could affect the concentrations and natures of vapors during this process. These include, but are not limited to, atmospheric transport phenomena and the impacts of humidity and sunlight, which may include breakdown or transformation of COPCs into other chemicals or COPCs. Interferents in the ambient surrounding air due the presence of vehicles, smoke, pollution, or other sources also have the potential to affect the concentrations and natures of vapors during this process.

[1] A fugitive emission may originate from non-breather filter or stack tank farm locations, such as a jumper pit, tank riser, or piping between tanks.

[2] Tank headspace composition depends on whether the liquid and solid material within the tank is in a quiescent or disturbed state. This difference could potentially affect COPC relationships and must be taken into account in the LI process.

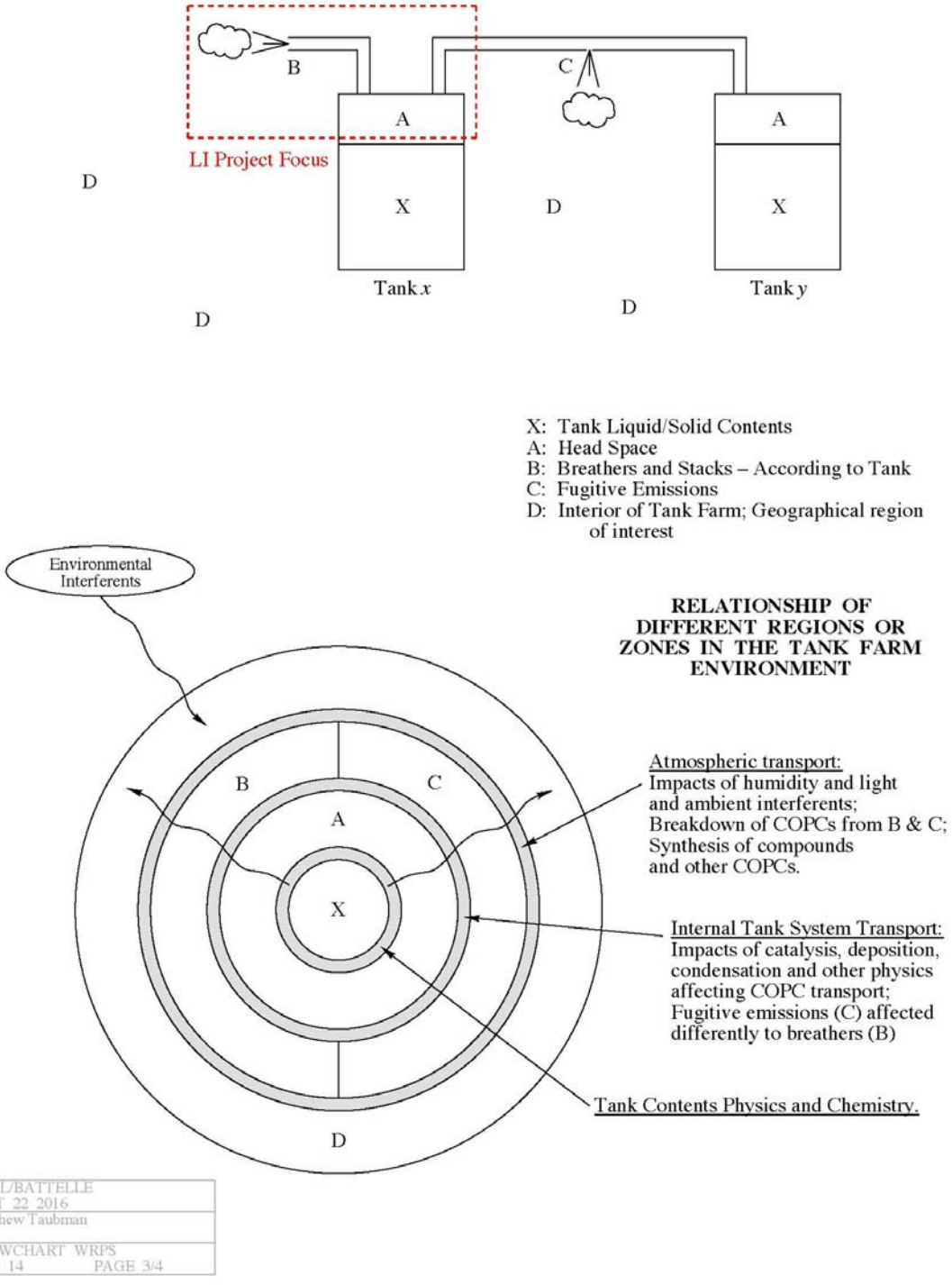

Figure 2.1. Schematic showing the relationship of different regions or zones in the tank farm environment as they relate to the identification of LIs

Confidently inferring the concentration of a COPC from measurements requires a probability model representative of the governing conditions and location. This unknown model may be estimated with relevant observations. The goodness-of-fit of the model's estimate depends on the number and representativeness of the samples, with the number of required samples increasing with the complexity of the model (i.e., a univariate probability model of COPC measurements will require fewer samples than a multivariate model of COPC and LI measurements). The straightforward approach is to sufficiently sample the governing conditions. A valid probability model may also be estimated by repurposing existing observations. The challenge to using existing observations for purposes other than the original intent is determining the conditions underpinning each observation, grouping observations sampled under similar conditions, and then identifying a group representative of the governing conditions and location.

The number and representativeness of existing measurements decrease as one moves outward from headspace to beyond the tank farm fence. Samples of tank headspace vapors (A) are the most numerous, and most easily grouped by conditions and location. Samples from breathers and stacks (B) are the second source of more easily grouped observations. Industrial hygiene samples have been drawn in general geographical regions (D). It is difficult, however, to pin down the conditions and locations underpinning these open-air samples to facilitate grouping and then identification with governing conditions and locations. Essentially, the numbers of samples decrease from headspace to farm fence while the ambiguity about their governing conditions increases. The data is opposite what is needed for understanding the atmosphere in which workers are exposed –a lot of accurate and precise data for tank headspace characterization and far less data obtained where operators work.

The most useful open-air COPC probability model would be built on open-air samples—likely a large number of open-air samples due to the complexity of the governing conditions and locations. The best evidence for a COPC-LI relationship, however, may be found in headspace samples from relatively simpler governing conditions, and the headspace model may be a good surrogate for the open-air model, suggesting that modeling out from the headspace is a sound approach.

This is so much the case that it would be extremely difficult to use just data at B to form LI relationships; data from headspaces (A) must be included in this process at this present stage. Finally, data taken in general geographical regions (D) are in open ambient conditions and are subject to atmospheric transport. Detected concentrations can vary wildly depending on the exact location of the sampling/measuring equipment and on the exact time of the measurement. Further, atmospheric conditions can affect chemical species differently, depending on affinity for humidity in the air and susceptibility to light. Breakdown and transformation of COPCs under the influence of ambient atmospheric factors such as light and humidity can result in COPCs, which are not present in headspaces (A) and must be considered.

The red dashed line around A and B of the left-hand tank (Figure 2.1) indicates the focus region of the LI identification process. Any relationships between COPCs and LIs are most likely to be established from measurements taken in these two regions; headspace and tank output through breather filter or stack ventilation. Data from regions A and B are expected to be the primary inputs for models developed due to the data available at the start of this project, although it is possible that inputs from C and D can be used if adequate data exist in the future. In any case, it is anticipated that the developed models can then be used to give estimates for LIs in other areas with limited data, including C and D.

3.0 Initial Spreadsheet Analysis of TWINS Data

An instinctive first approach to identifying LIs is to search for concentration relationships in time and location, between various pairs of chemicals observed in tank headspaces, at breather filters, and/or at stacks. Actual relationships are likely to be more complex, necessitating a fully multivariate approach where combinations of chemicals may indicate certain COPCs or discriminate among multiple COPCs. However, evaluating simple relationships between pairs of chemicals present in the tank vapors is of great value in the initial development and evaluation of a more evolved and complex process.

More data have been taken from the tank headspaces during characterization efforts than from industrial hygiene (IH) surveys. The availability of two sets of data taken from the headspaces, which are the emissions sources, or from locations downstream of the source such as breather filters, ventilation, and in-farm, allows some examination of how the pairwise relationship changes with distance from the source. Changes would be expected for various physical reasons, including reaction and deposition, and also because the existing IH data do not provide much information about time and location of measurement and so could lead to false correlation. The existing data were not numerous enough to allow IH data to be broken out into different zones (as in Figure 2.1) and separately examined, but IH data as a whole were correlated separately from headspace data. A further distinction between zones will be deferred until pilot test vapor data are available.

Because waste disturbances, whether through deliberate operations or spontaneous gas releases, can change the pattern of COPC release (Stock 2004), tank activity records were also used in examining the pairwise relationships. The headspace and IH concentrations data were not broken into separate sets for disturbed and non-disturbed conditions, but the concentration pairs occurring during disturbances were identified.

3.1 Analysis

The datasets used for analysis were the headspace and IH vapor-concentration data found through the Tank Waste Information Network System (TWINS).[1] To accommodate the multiple methods of viewing the importance of a given COPC, the initial spreadsheet-based selection process includes multiple scoring criteria in a process to rank potential LIs. The spreadsheet selection process is represented by the flowchart shown in Figure 3.1.

This pairwise search was based on the 59-COPC set in use at the time of this report and on potential indicator constituents. The approach made a set of assumptions about the qualities an indicator chemical would need to have. It would need to be readily measurable in the field. It would correlate strongly with one or more indicated COPCs over a range of concentrations from the detection level up through the historical maximum, with concentrations near the maximum being of particular interest because of their greater likelihood of exceeding the OEL. Ideally, the indicator would be non-toxic so that its presence, when measurable, would not increase the chances of causing an OEL to be exceeded. Barring that, it would be helpful (though not essential) if a toxic indicator was further from its OEL at its maximum

[1] The complete contents of each of these two datasets—for all tanks, dates, and chemicals—were downloaded on Jan. 29, 2016 as spreadsheets.

concentration than was the indicated COPC – again, to reduce the likelihood of needing to have the indicator exceed its OEL in order to predict that the indicated COPC would exceed its own OEL.

The inclusion of measurability as a criterion will be deferred until pilot test data are available. Therefore, for the present study the characteristics of a successful pairing were taken to include the following:

- one constituent in the pair is a COPC and has shown maximum concentrations that are significantly closer to, or more in excess of, its OEL than the other constituent, which may or may not be a COPC;
- there is consistent enough trending between the two constituents to suggest a physical reason for a dependable relationship between them; and
- data for the more OEL-challenging constituent show a wide range of concentrations, preferably including many that are less than the OEL, and also including the highest historically observed concentration.
- data include enough pairings taken during waste-disturbing activities to allow the effect of such activities to be included in whatever relationship between the paired chemicals is devised.

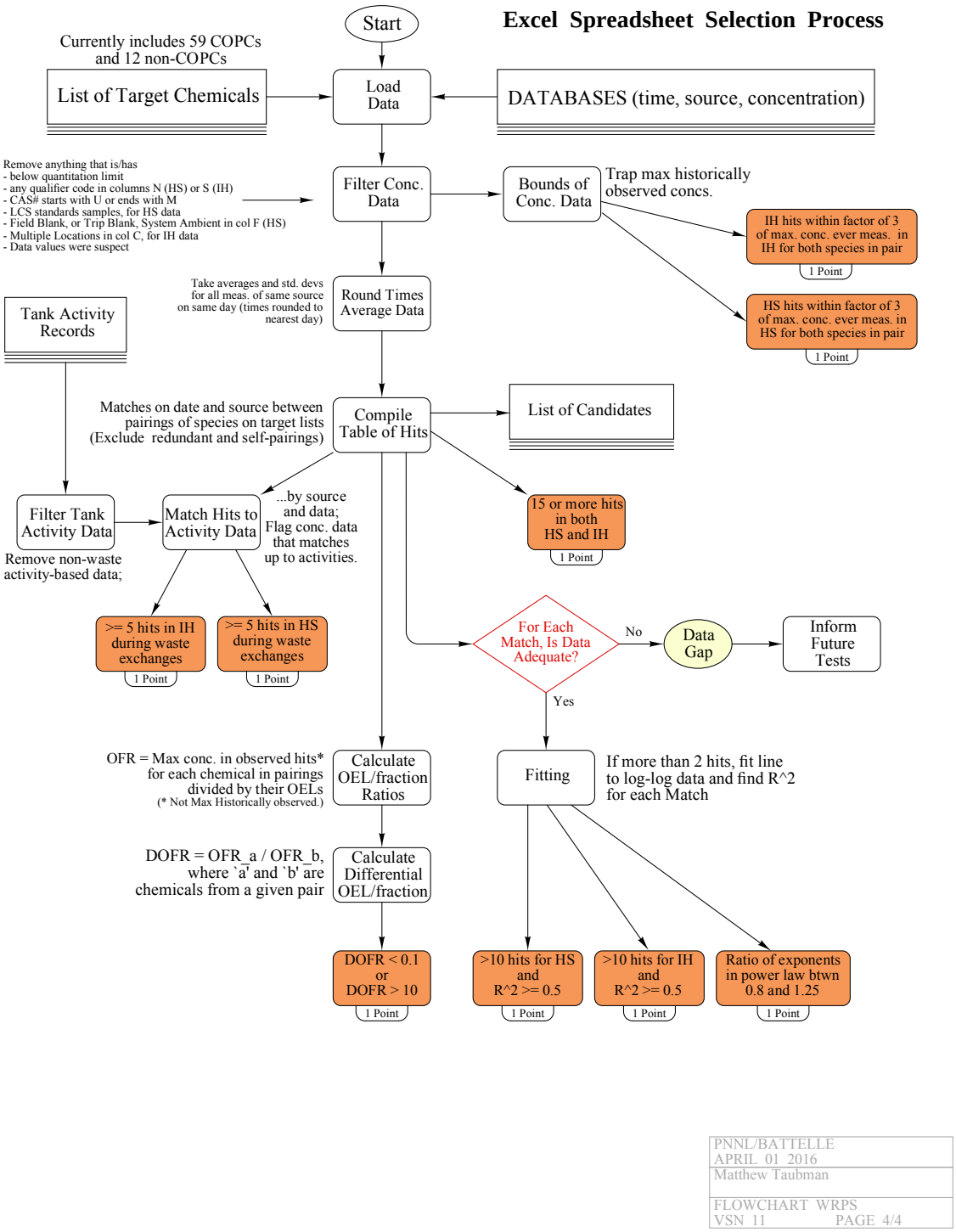

Figure 3.1. Flowchart representation of the macros used in the Excel spreadsheet analysis of TWINS and the IH database

3.1.1 Filter Data

The two datasets were filtered to remove data that might have quality issues or that were not pertinent to pairwise correlation. For the purpose of pairwise correlation, as distinct from the alert-probability-based approach described in Section 4, measurements were removed if

- the concentration was below the quantitation limit, since this often means that the chemical could not be proven to be present and since correlations between the detection levels of two chemicals are driven by the instrument's capabilities rather than the actual concentrations;
- any data qualifier code was present—these data were assumed to raise quality assurance questions, or to introduce extra measurement variability; therefore they were not considered in this initial phase of generating pairwise relations, but some will be considered in later phases;
- the CAS ID# started with U or began or ended with M—these were unknown-identity chemicals or mixtures of chemicals;
- the units in the headspace data were "% Recovery"—these were "LCS Standard" samples that never had concentrations reported and, as quality control samples, were not used;
- the headspace data were labeled as Field Blank, Trip Blank, or System Ambient—these were potentially useful as blank concentrations to subtract from the raw measurement, but were not used;
- the TWINS Multiple Location Flag was not blank—affected only one IH data point;
- the CAS # ID was interpreted by Excel™ as a date—this exclusion affected only three SO_2 data points in the IH dataset (SO_2 is not a COPC), and so was not considered significant in terms of finding indicators for COPCs;
- the measured concentrations were physically unreasonable or seemed to represent something other than a true measurement—five headspace points (for N_2O, CO_2, H_2, and total non-methane hydrocarbons) were removed for having a blank concentration or a concentration greater than 1,000,000 ppm (unphysical). Three points of IH data were removed for being upper bounds (acetaldehyde ceiling) rather than exact concentration measurements, and two points of IH data were removed for having sampling volumes that were implausibly small or large compared to what was typical for the sampling method and device.

As noted in the first bullet above, concentration measurements that are marked in a database as being below detection limits are not preferred for assessment of correlation. However, pairings in which only one chemical is above its detection limit are likely to be important in estimating what percentage of pairings may be above 10% of OEL, or any other chosen alert level. This approach will be discussed in Section 4 and Section 6.

After filtering, 18,329 lines of headspace data and 2,760 lines of IH data remained out of the original TWINS download of 116,923 lines of headspace data and 25,081 lines of IH data. Most of the deleted data were removed because the concentration was below the quantitation limit or a data qualifier code was present. Some calculations were carried out to fill in concentrations that were not supplied in numerical form in the IH dataset, based on available data in the dataset that were adequate to support concentration calculations.

3.1.2 Data Average

The sampling date/time was rounded to the nearest day for use in checking whether two chemicals were measured simultaneously and therefore could be linked to each other for correlation. This step made no difference for the IH dataset, in which survey time data were expressed only with a date. In the case of headspace data, many but not all measurements had a time as well as a date associated with them. For consistency with the lower time resolution of many of the data, the nearest day was used even when times were available.

For many samples, the concentrations of chemicals were measured more than once for a given source, day, and time. These multiple measurements were reduced to single concentrations by calculating an arithmetic average and standard deviation for the concentration of a chemical at a particular combination of source and day. Averages were preferred to maxima because the datasets included both samples where replicates were taken and samples with single measurements, and using maxima would have changed the relation between the former type and the latter type of samples.

The use of averaging meant that a set of several measurements for a source and date had the same weighting in subsequent correlation calculations as a single measurement would have had. This would distort the correlation if a true predictive correlation were to be created, but only a semi-quantitative gauge of the tendency of the pair of constituents to trend together was desired as part of this method development. In addition, it was not clear how to carry out pairings between, for example, an indicator sample with three measurements and an indicated-COPC sample with two measurements – whether it would count as six pairings, three, or two.

3.1.3 Hit List

For each pairing of constituents that was considered, a table of hits was compiled—hits defined as matches on date and source between the two constituents. The set of chemicals that were included contained all 59 COPCs plus 12 non-COPCs. The non-COPCs were chosen as those with plausible waste-chemistry relationships, per Stock (2004), and/or a relatively large amount of data. These non-COPC indicator candidates are identified at the bottom of Table 3.1.. Potential pairs were evaluated for all 59 COPCs with each other (self-pairings were not used) and all 12 of the non-COPCs. However, many of the possible pairings had no hits in one or both datasets because there were few or no records in the filtered data or because measurements of the two chemicals did not coincide in source and date. Out of 2,419 possible pairings, there were 377 pairings with one or more hits within the filtered headspace dataset and 606 such pairings within the filtered IH dataset. Many of the headspace and IH pairings overlap; as a result, the total number of pairings that included headspace, IH, or both was 705.

For each pairing that had more than two hits, the extent of correlation was determined by fitting a log-log line through all the hits, obtaining a power-law equation for the concentration of one constituent in terms of the other, and calculating the R^2 of the log-log fit. The headspace hits were fitted separately from the IH hits. Note that the objective of correlation was not to obtain an equation for direct use in modeling indicator-based predictions of COPC concentrations, but to obtain a semi-quantitative gauge of the tightness and consistency of a pairing trend over the whole concentration range represented.

The maximum historically observed concentration for each COPC and non-COPC was found over all the historical filtered headspace and IH datasets. In some pairings, these historical maxima were not among the data included in the hits.

3.1.4 Tank Activity

It was of interest to determine which of the hits coincided with waste transfer activities carried out in the tanks. Periods of tank activity could be approximately determined from the databases on TWINS[2] for tank activities that affected tank inventories. The activity databases required filtering to remove records for non-waste transfers such as water additions, apparent tank inventory changes that were artifacts of changes in level instrumentation, and other effects on inventory that did not include waste transfers. Additions of water were excluded because they would be likely to temporarily decrease releases, either by providing a more dilute liquid for gases and vapors to dissolve in, or because the added hydrostatic head would increase the pressure in retained-gas bubbles and decrease one of the driving forces that cause release. The intent was to flag the cases where waste-disturbing activity would be likelier to produce releases.

Hits in each pairing were matched to the periods of tank activity by source and date. Activity periods in each tank were checked against IH data for the specific tank, or non-specific locations in the same tank farm, such as exhausters, continuous-air monitor cabinets, etc., and (in the case of AW, AY, and AZ tanks) for the 702-AZ samples.

It should be noted that the tank activity data had low time resolution in some cases: a tank might be marked as involved in a transfer for a whole month, as if the transfer flow were continuous, even though the transferred volume was so small as to indicate that transfers occurred only during some intervals in the month. The low time resolution affected matching of both headspace and IH data to activities; some of the apparent matches are potentially spurious.

3.1.5 Usefulness Scoring

Pairings were scored so that they could be compared for potential usefulness. In this preliminary approach to pairing assessment, the following criteria (shown as orange boxes in Figure 3.1) considered in scoring:

(a) The pairing received 1 point when the maximum concentrations among the headspace hits were within a factor of 3 of the maximum concentrations ever measured in the headspace for each species in the pair. See the orange criterion box near the top right of the flowchart in Figure 3.1. The point scored reflects the importance of having a pairing relationship based on a dataset that captured the maximum concentration ever measured.

(b) Similarly, the pairing received 1 point when the maximum concentrations among the IH hits were within a factor of 3 of the maximum concentrations ever measured by IH for species in the pair. This criterion is also at the top right in Figure 3.1.

[2] Tank activity databases were downloaded on Jan. 29, 2016.

(c) If the pairing had 15 or more hits for the headspace dataset plus 15 or more hits for the IH dataset, it received 1 point. This criterion is shown near the center of Figure 3.1. The point scored reflects the importance of having a relatively large dataset from each type of location, headspace, and IH, allowing the two types of results to be compared.

(d) The pairing received 1 point if there were 5 or more hits from headspace samples taken during tank activities that involved waste changes (other than water additions). This criterion is on the left side of Figure 3.1. The point scored reflects the usefulness of having some activity-related measurements for comparison to measurements taken for a quiescent tank.

(e) Similarly, the pairing received 1 point if there were 5 or more hits from IH samples taken during tank activities that involved waste changes (other than water additions). This criterion is shown on the left side of Figure 3.1.

(f) For each chemical in the pairing and each dataset, the pairing's observed OEL-fraction ratio was calculated. This ratio was equal to the maximum concentration among the hits divided by the Hanford OEL for the chemical. Then, the observed-OEL-ratio for the first chemical in the pair was divided by that for the second chemical to get the differential OEL-fraction ratio for the pairing in that dataset. If the differential OEL-fraction ratio was greater than 10 or less than 0.1, the pairing received 1 point. Note that this differential OEL-fraction ratio was based on the maximum concentrations for the subset of data that were hits, not the maximum concentrations over all (filtered) measurements. This criterion is shown at the center of the bottom of Figure 3.1. The point scored reflects the usefulness of having one member of the pair (a potential indicator) that has historically been further from the OEL than the other. The assumption is that it is preferable, if possible, to have an indicator that can predict high concentrations of the indicated COPC without itself adding to the possibility of exceeding an OEL.

(g) If the pairing had more than 10 hits for headspace data and the log-log fit $R^2 \geq 0.5$, it was given 1 point. The point scored reflects the possibility that a reliable trend is present for the pair. The log-log fit (i.e. a power-law functional relationship between the vapor concentrations of two chemicals) was used because this form results from the dependence of release on the Henry's Law constant of the chemical. A Henry's Law constant for a chemical in electrolyte-free (salt-free) water has an dependence on temperature where the dominant term (JPL 2015) is of the form $exp(B/T)$, where B is an experimentally determined constant. The ratio of two Henry's Law constants can be expressed as one of the constants raised to some power that depends on the ratio of the B values for the two chemicals. Consequently, the vapor concentration of one chemical in a pair can be expressed as the other raised to a power. Over a range of temperatures, as seen in the tank population, the temperature-dependence of the Henry's Law constants tends to generate a power-law relation between two vapor-phase chemicals. The scatter around the line is caused not only by measurement variability but by variations in the dissolved concentrations of the two chemicals, the salt concentrations in liquids, and ventilation effects.

(h) Similarly, if the pairing had more than 10 hits for IH data and the log-log fit $R^2 \geq 0.5$, it was given 1 point.

(i) The pairing was given 1 point if the ratio of the exponents for the power-law correlations for headspace and IH was between 0.8 and 1.25. The point scored reflects the usefulness of having similar trends (i.e., possibly similar mechanisms) for both locations of measurements.

Table 3.1 identifies the target chemicals (59 COPCs and 12 non-COPCs), the OEL, the number of rows of data (measurements before averaging) in the filtered databases, the maximum concentration in the filtered databases, and the number of pairings that were determined. For many of the COPCs, there were no measurements remaining after filtering or there were so few that no conclusions could be drawn.

Table A.1 in Appendix A summarizes further detail on the scoring process by showing information for all the higher-scoring pairings. The pairings are arranged in descending order of score. A total of 3 pairings scored 7 out of 10 points by the criteria above, 14 scored 6 out of 10 points, 30 scored 5 out of 10 points, and the remaining 658 pairings for which there were any hits scored 4 or fewer points. The table contains one row for each pairing that scored 3 or more points out of the total of 10 possible points. Lower scores were considered to indicate that the evidence (to date) was inadequate to indicate a reliable pairing. Each column contains information related to one of the features for which a point could be assigned. Blank cells indicate that the pairing did not qualify for a point by the associated criteria. Non-blank cells show the information about the pairing that qualified it to score a point.

Figure 3.2 depicts a matrix view of the 705 pairings observed between the target chemicals (59 COPCs and 12 non-COPCs). Numbering for target chemicals follows the numbering given in Table 3.1. Pairings found in the headspace data are designated by “H”. Those found within the IH data are designated by “I”. Finally, pairings found in both sets of data are represented by “HI” within the matrix. The grey space in the matrix represents redundant pairing possibilities.

Table 3.1. Target chemicals[(a)]

COPC ID#	Chemical	Occupational Exposure Limit	Number of Data Rows in the Filtered Database		Maximum Concentration (ppm) in the Filtered Database		Number of Pairings That Score 3 or More Points; Notes*
			HS	IH	HS	IH	
1	Ammonia	25 ppm (17 mg/m^3)	814	269	2502	644	33
2	Nitrous oxide	50 ppm (90 mg/m^3)	715	89	53000	250	18
3	Mercury	0.025 mg/m^3	25	160	0.0149	0.0556	27
4	1,3-Butadiene	1 ppm (2.2 mg/m^3)	9	13	0.068	3.38	7
5	Benzene	0.5 ppm (1.6 mg/m^3)	252	24	0.067	0.0618	14
6	Biphenyl	0.2 ppm (1.3 mg/m^3)	0	3	n/a	0.00142	1
7	1-Butanol	20 ppm (61 mg/m^3)	445	119	22.0	6.4	22
8	Methanol	200 ppm (262 mg/m^3)	358	10	28	6.31	11
9	2-Hexanone	5 ppm (20 mg/m^3)	49	56	0.35	0.0888	18
10	3-Methyl-3-butene-2-one	0.02 ppm (0.069 mg/m^3)	0	0	n/a	n/a	0; no data
11	4-Methyl-2-hexanone	0.5 ppm (2.3 mg/m^3)	0	6	n/a	0.00295	0; < 4 hits
12	6-Methyl-2-heptanone	8 ppm (42 mg/m^3)	0	1	n/a	0.000179	0; < 3 hits
13	3-Buten-2-one	0.2 ppm (0.57 mg/m^3)	0	38	n/a	0.23	6
14	Formaldehyde	0.3 ppm (0.37 mg/m^3)	51	199	0.0656	0.273	18
15	Acetaldehyde	25 ppm (45 mg/m^3)	47	31	12	2.82	15
16	Butanal	25 ppm (74 mg/m^3)	76	103	7.6	0.471	21
17	2-Methyl-2-butenal	0.03 ppm (0.10 mg/m^3)	0	0	n/a	n/a	0; no data
18	2-Ethyl-hex-2-enal	0.1 ppm (0.52 mg/m^3)	0	0	n/a	n/a	0; no data
19	Furan	0.001 ppm (0.0028 mg/m^3)	2	18	0.016	0.0104	6
20	2,3-Dihydrofuran	0.001 ppm (0.0029 mg/m^3)	0	3	n/a	0.00068	0; < 4 hits
21	2,5-Dihydrofuran	0.001 ppm (0.0029 mg/m^3)	0	1	n/a	0.000122	0; < 3 hits
22	2-Methylfuran	0.001 ppm (0.0034 mg/m^3)	0	0	n/a	n/a	0; no data
23	2,5-Dimethylfuran	0.001 ppm (0.0039 mg/m^3)	0	0	n/a	n/a	0; no data
24	2-Ethyl-5-methylfuran	0.001 ppm (0.0045 mg/m^3)	0	0	n/a	n/a	0; no data
25	4-(1-Methylpropyl)-2,3-dihydrofuran	0.001 ppm (0.0052 mg/m^3)	0	0	n/a	n/a	0; no data
26	3-(1,1-Dimethylethyl)-2,3-dihydrofuran	0.001 ppm (0.0052 mg/m^3)	0	0	n/a	n/a	0; no data
27	2-Pentylfuran	0.001 ppm (0.0056 mg/m^3)	0	0	n/a	n/a	0; no data
28	2-Heptylfuran	0.001 ppm (0.0068 mg/m^3)	0	0	n/a	n/a	0; no data
29	2-Propylfuran	0.001 ppm (0.0045 mg/m^3)	0	0	n/a	n/a	0; no data
30	2-Octylfuran	0.001 ppm (0.0074 mg/m^3)	0	0	n/a	n/a	0; no data
31	2-(3-Oxo-3-phenylprop-1-enyl)furan	0.001 ppm (0.0081 mg/m^3)	0	0	n/a	n/a	0; no data

COPC ID#	Chemical	Occupational Exposure Limit	Number of Data Rows in the Filtered Database		Maximum Concentration (ppm) in the Filtered Database		Number of Pairings That Score 3 or More Points; Notes*
			HS	IH	HS	IH	
32	2-(2-Methyl-6-oxoheptyl)furan	0.001 ppm (0.0079 mg/m^3)	0	0	n/a	n/a	0; no data
33	Diethylphthalate	5 mg/m^3	0	26	n/a	0.0015	2
34	Acetonitrile	20 ppm (34 mg/m^3)	620	155	9	1.31	17
35	Propanenitrile	6 ppm (14 mg/m^3)	376	42	4.2	0.93	17
36	Butanenitrile	8 ppm (23 mg/m^3)	369	39	1.3	0.41	14
37	Pentanenitrile	6 ppm (20 mg/m^3)	111	25	0.251	0.35	5
38	Hexanenitrile	6 ppm (24 mg/m^3)	37	25	0.314	0.46	7
39	Heptanenitrile	6 ppm (27 mg/m^3)	0	2	n/a	0.000640	0; < 3 hits
40	2-Methylene butanenitrile	0.3 ppm (0.99 mg/m^3)	0	0	n/a	n/a	0; no data
41	2,4-Pentadienenitrile	0.3 ppm (0.97 mg/m^3)	0	0	n/a	n/a	0; no data
42	Ethylamine	5 ppm (9.2 mg/m^3)	0	18	n/a	0.0644	5
43	N-Nitrosodimethylamine	0.0003 ppm (0.00091 mg/m^3)	2	193	0.0233	0.257	5
44	N-Nitrosodiethylamine	0.0001 ppm (0.00042 mg/m^3)	0	17	n/a	0.000328	0
45	N-Nitrosomethylethylamine	0.0003 ppm (0.0011 mg/m^3)	0	74	n/a	0.000856	5
46	N-Nitrosomorpholine	0.0006 ppm (0.0028 mg/m^3)	0	53	n/a	0.000407	4
47	Tributylphosphate	0.2 ppm (2.2 mg/m^3)	2	7	0.0062	0.00478	3
48	Dibutylbutylphosphonate	0.007 ppm (0.072 mg/m^3)	1	2	0.0263	0.000165	0; < 3 hits
49	Chlorinated biphenyls	1 mg/m^3	0	0	n/a	n/a	0; no data
50	2-Fluoropropene	0.1 ppm (0.24 mg/m^3)	0	0	n/a	n/a	0; no data
51	Pyridine	1 ppm (3.2 mg/m^3)	34	24	0.147	0.083998	5
52	2,4-Dimethylpyridine	0.5 ppm (2.2 mg/m^3)	0	13	n/a	0.0568	1
53	Methyl nitrite	0.1 ppm (0.25 mg/m^3)	0	0	n/a	n/a	0; no data
54	Butyl nitrite	0.1 ppm (0.42 mg/m^3)	0	0	n/a	n/a	0; no data
55	Butyl nitrate	2.5 ppm (12 mg/m^3)	0	0	n/a	n/a	0; no data
56	1,4-Butanediol, dinitrate	0.05 ppm (0.37 mg/m^3)	0	0	n/a	n/a	0; no data
57	2-Nitro-2-methylpropane	0.3 ppm (1.3 mg/m^3)	0	0	n/a	n/a	0; no data
58	1,2,3-Propanetriol, 1,3-dinitrate	0.05 ppm (0.39 mg/m^3)	0	0	n/a	n/a	0; no data
59	Methyl Isocyanate	0.02 ppm (0.047 mg/m^3)	0	0	n/a	n/a	0; no data

Non-COPC ID#	Chemical	Occupational Exposure Limit	Number of Data Rows in the Filtered Database		Maximum Concentration (ppm) in the Filtered Database		Number of Pairings That Score 3 or More Points; Notes
			HS	IH	HS	IH	
60	Methane	---	484	3	299000	39	3
61	Hydrogen	---	946	5	68000	2400	1
62	TNMHC	---	214	0	285	n/a	1

Non-COPC ID#	Chemical	Occupational Exposure Limit	Number of Data Rows in the Filtered Database		Maximum Concentration (ppm) in the Filtered Database		Number of Pairings That Score 3 or More Points; Notes
			HS	IH	HS	IH	
					mg/m^3		
63	Methane, trichlorofluoro-	1000 ppm (5620 mg/m^3)	658	25	3.8	0.00708	5
64	Butane	800 ppm (1900 mg/m^3)	412	3	3.4	0.016	9
65	Methylbenzene	50 ppm (188 mg/m^3)	534	48	0.774	0.147	12
66	Tetrahydrofuran	200 ppm (589 mg/m^3)	545	27	1.31	0.071	14
67	Dichloromethane	---	85	18	0.617	0.0221	5
68	Ethanol	1000 ppm (1880 mg/m^3)	327	68	12.3	1.1	8
69	1-Propanol	200 ppm (491 mg/m^3)	617	53	5	0.0772	12
70	Dimethylmercury	---	22	20	2.68E-05	1.66E-05	6
71	Acetone	250 ppm (594 mg/m^3)	538	60	12.6	0.287	9

(a) The complete contents of each of these two datasets were downloaded on Jan. 29, 2016.

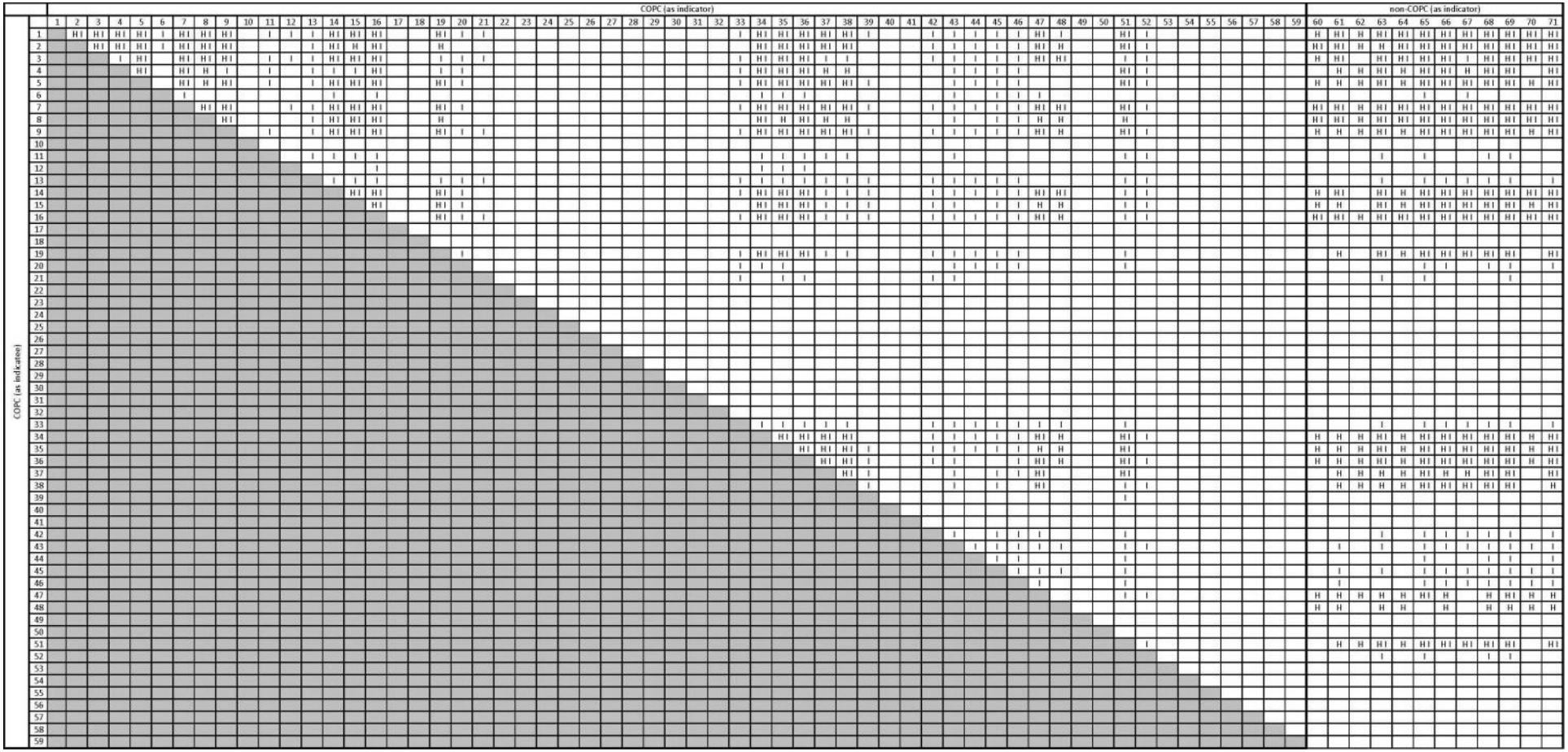

Figure 3.2. Matrix view of COPC and non-COPC pairings

Figure 3.3 is a log-log plot of the hit concentrations, OELs, alert level (10% of the OEL), and the overall maximum concentrations measured within the dataset for the butanal and butanenitrile pairing. The measurements are shown with squares for headspace data and triangles for IH data. The error bars on the points show one standard deviation for the set of concentrations measured at the same source on the same day, if there was more than one. When only one concentration was measured at that time and place, no error bar is shown. The log-log (power law) trend lines fitted to the hits in each dataset are shown by a thin solid black line for the headspace data and a finely dotted black line for the IH data. The tightness of grouping around both trend lines illustrates the high-R^2 criteria (criteria [g] and [h]), and the similar slope of the headspace and IH trend lines illustrates meeting criterion (i) for a reasonable matchup of behavior between the headspace and IH datasets.

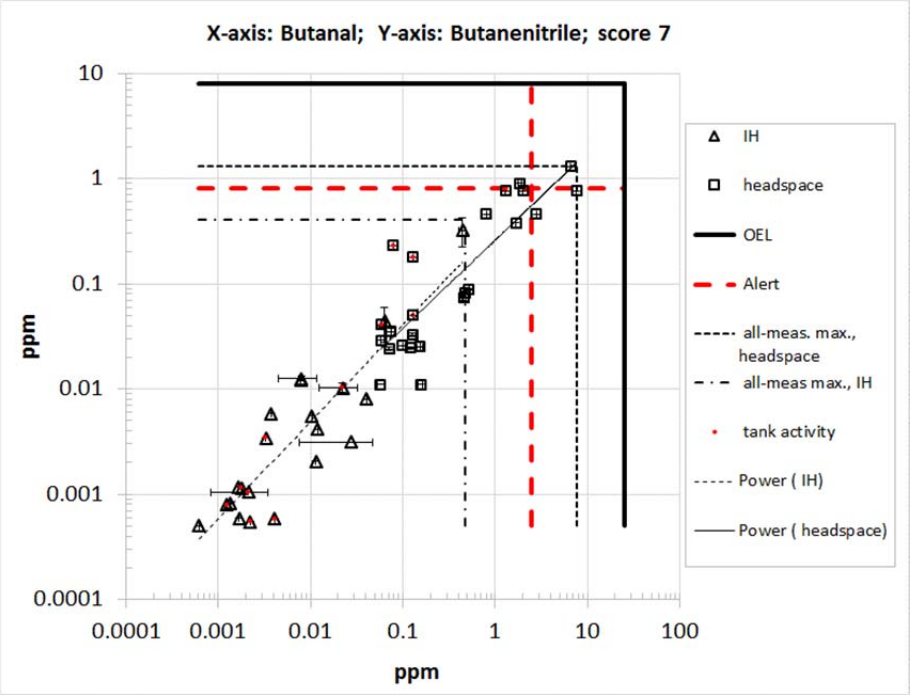

Figure 3.3. Pairing information for butanal and butanenitrile

The historical maximum concentrations for the two chemicals are shown by dotted small dashed black lines for the headspace data and dash-dotted black lines for the IH data. As can be seen, the maximum concentrations for both chemicals in both datasets fall on or not far below the historical maxima. This shows why criteria (a) and (b) were met, indicating that both headspace and IH datasets captured the maximum measurements.

Toxicological information also appears on the plot as thick, solid black lines that show the OELs for both chemicals. The historical maxima and the maximum hit concentrations fall below the OEL, but headspace concentrations have exceeded 10% of the OEL. The alert lines (thick, red dashed lines) show 10% of the OEL for each chemical. The nearly 1:1 slope of the concentration trends, and the fact that OELs are only a factor of 4 apart, shows why there is little distinction between the two chemicals in terms of degree of challenge to the OEL (i.e., how close their maximum concentrations come to the OEL). Because neither chemical is so much further from the OEL as to be a lower-challenge predictor for the higher-challenge chemical, neither the headspace nor the IH database met criterion (f).

It is worth noting that several tank farms are represented by the data in this pairing. The headspace data were dominated by C farm tanks, but there were also tanks from A, AX, BY, TX, TY, and U farms. Tanks AZ-101, B-101, C-103, and C-107 contributed the highest concentrations. The IH data were from C farm; the 702-AZ stack; AP and AW farm exhausters; individual tanks from AY, AZ, B, BX, and C farms, and three measurements inside the C farm. This set of tanks includes a range of waste types, tank waste temperatures, and ventilation conditions. Possible reasons for the close relationship of butanal and butanenitrile are an unconfirmed similarity of Henry's Law constants, similarity between reactions that generate them in the waste (Stock 2004), and perhaps measurements being made on the same samples by the same methods, which would decrease measurement-related variability.

Red dots on the points indicate data taken during tank activity periods, as defined by the filtered TWINS data for waste-related tank activities. Bear in mind that, as already noted, some of the database-defined activity periods probably included intervals of inactivity during which samples might have been taken. The two activity-marked headspace hits that lie well above the headspace trendline were for AX-101 and BY-105 on 9/10/2002. The activity-marked IH hits with the lowest concentrations were from the 702-AZ stack and the AW primary exhauster. In this particular example, the paired concentrations that coincided with tank activity did not consistently fall among the highest concentrations.

Finally, note that the plot can be thought of in terms of using the y-axis chemical as the indicator and the x-axis as the indicated COPC. The choice of which axis is the indicator, as plotted, is an artifact of the sorting in the data analysis algorithm. The scoring does not depend on which axis either chemical of the pair is assigned to.

3.1.6 Observations

Whether one chemical can be established as being an indicator for another depends on how many measurements of the two chemicals coincide in time and source. Variability of analysis in a given headspace at any time is so great that it was concluded that only time-coincident analysis can be considered. Given enough measurements, the extent to which a given chemical may serve as an indicator for another (a pairing) will depend on the degree to which they both tend to be generated in the waste by the same types of reactions, to be stored in gas phase or in liquid phase, and to undergo the same changes (reaction or condensation) in the period between their release from the waste and their contact with a receptor outside the tank. The reactions that produce volatile organics in the waste are too complex to address here, except in the most general way (Stock, 2004). The properties that are pertinent to storage, release, and transport can be discussed somewhat more specifically.

Table 3.1 shows that several COPCs have many pairings with other COPCs: ammonia (33 pairings), 1-butanol (22), butanal (21), nitrous oxide (18), 2-hexanone (18), formaldehyde (18), acetonitrile (17), propanenitrile (17), acetaldehyde (15), benzene (14), and butanenitrile (14). The non-COPC chemical with the most COPC pairings (of score 3 or greater) is tetrahydrofuran (THF), with 14 such pairings.

Although the non-COPCs that were chosen for analysis did not produce as many adequately scoring pairings with COPCs as the COPCs themselves did, there may be non-COPCs that would produce more pairings with COPCs than the ones chosen. Stock (2004) frequently mentions alkenes as in-tank reaction intermediates and products in a variety of reactions, with 1-butene receiving particular notice as a product/intermediate for reactions involving diluent hydrocarbons and tributyl phosphate (TBP). Stock also describes the branched ketone 3-octanone as a chemical marker for oxidation of the hydrocarbon

diluents, and 3-heptanone as a marker for oxidation of the diluents and of one of the phosphate esters. Other alcohols, aldehydes, and ketones not included among the COPCs may be worth testing for pairing.

Table A.1 suggests that the COPCs 1-butanol, butanal, and 2-hexanone would be worth further examination. They appear in a number of high-scoring pairings, and might, if co-measured with some of the COPCs, turn out to be LIs. The COPC, 1-butanol, is mentioned by Stock (2004) as being abundantly produced by butylphosphates such as TBP and its breakdown products, and might also be produced from the originally fed hydrocarbon diluents and the complexants. Butanal has similar sources. The source of 2-hexanone is not specifically discussed by Stock (2004), but it may be a marker like 3-heptanone and 3-octanone.

Previously Proposed Indicators

Ammonia and nitrous oxide have both been proposed as indicators, owing to their common occurrence and large number of measurements. Because of their differing Henry's Law constants, these two chemicals could be indicators for different types of releases—from inventory dissolved in liquid and from gas-phase inventory, respectively.

Ammonia has a moderately high Henry's Law constant, 60 M/atm in salt-free water at 25°C (JPL 2015); as such, most of the ammonia in any given tank is expected to be stored in dissolved form in the liquid, as was established by retained gas sampling (Mahoney et al. 1999). The predominance of storage in the liquid suggests that ammonia's releases depend as much, or more, on disturbances of the liquid (which increase the rate of transport to the headspace) than on gas-phase release mechanisms. This release from disturbed liquid was seen, for example, in the transfer from SY-101 to SY-102 (Mahoney et al. 2000), with dissolved ammonia being released from the stream flowing into SY-102. Ammonia-producing reactions are common and predominantly depend on the presence of nitrogen-containing organics, such as the complexants originally added to the tanks. A dependence on strictly inorganic sources such as nitrite and cyanate ions is also present, but less significant (Stock and Pederson 1997).

Nitrous oxide has a higher Henry's Law constant than other gases that are reaction products (e.g., 0.024 M/atm for N_2O versus 2.6×10^{-4} M/atm for H_2, in salt-free water at 25°C).. Nevertheless, most of the nitrous oxide inventory will be found in the gas phase, at least in waste layers where there are solids capable of retaining gas. Releases may depend either on liquid disturbance (of convective liquid waste layers) or gas-phase release mechanisms (from solids layers). The generation of nitrous oxide depends to some extent on the reduction of the inorganic nitrite ion (Stock and Pederson 1997) and also on the organic inventory. If the dependence on the nitrite ion or inorganic reactions is more substantial for nitrous oxide than for ammonia, or for volatile organics, that might cause nitrous oxide to be a less likely match for the majority of COPCs whose presence depends on organic reactions.

The highest pairwise scores for ammonia were in two pairings that score 6 points out of 10 (with acetaldehyde and 1-butanol), while the highest score for a nitrous oxide pairing is 4 out of 10 (with 1-butanol, formaldehyde, and butanal). It is worth noting that ammonia, with its moderately high Henry's Law constant, is a better match for these aldehyde COPCs and for 1-butanol, in terms of expected release mechanisms, than nitrous oxide. The three highest-scored pairings for ammonia and the two highest-scoring pairings for nitrous oxide are depicted in Figure 3.4 through Figure 3.8. The scatter produced by these pairings is substantial and not well defined by trend lines (i.e., spread of concentrations on the vertical axis for a single concentration on the horizontal).

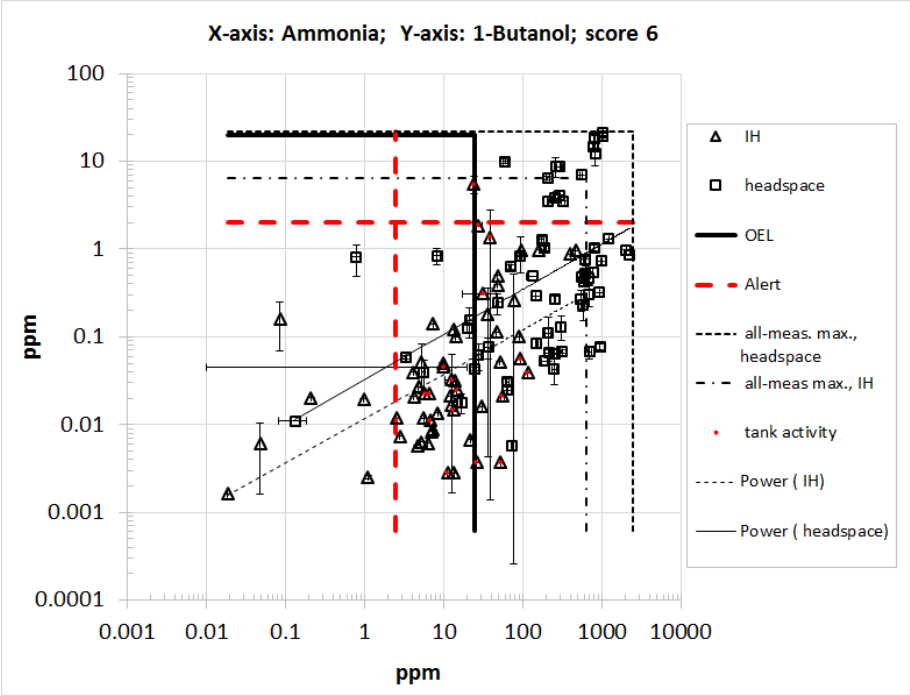

Figure 3.4. Pairing information for ammonia and 1-butanol

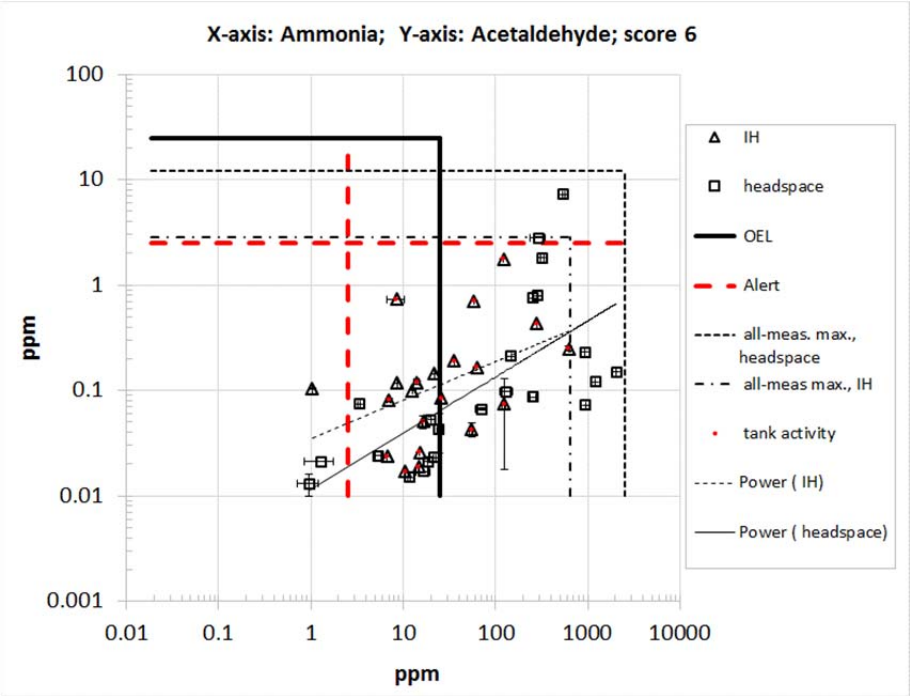

Figure 3.5. Pairing information for ammonia and acetaldehyde

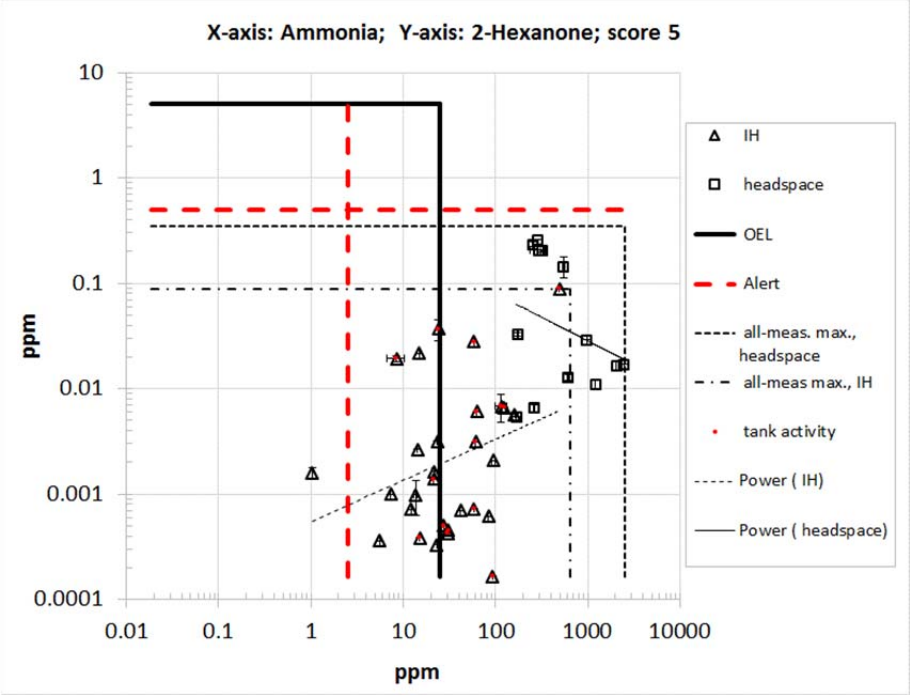

Figure 3.6. Pairing information for ammonia and 2-hexanone

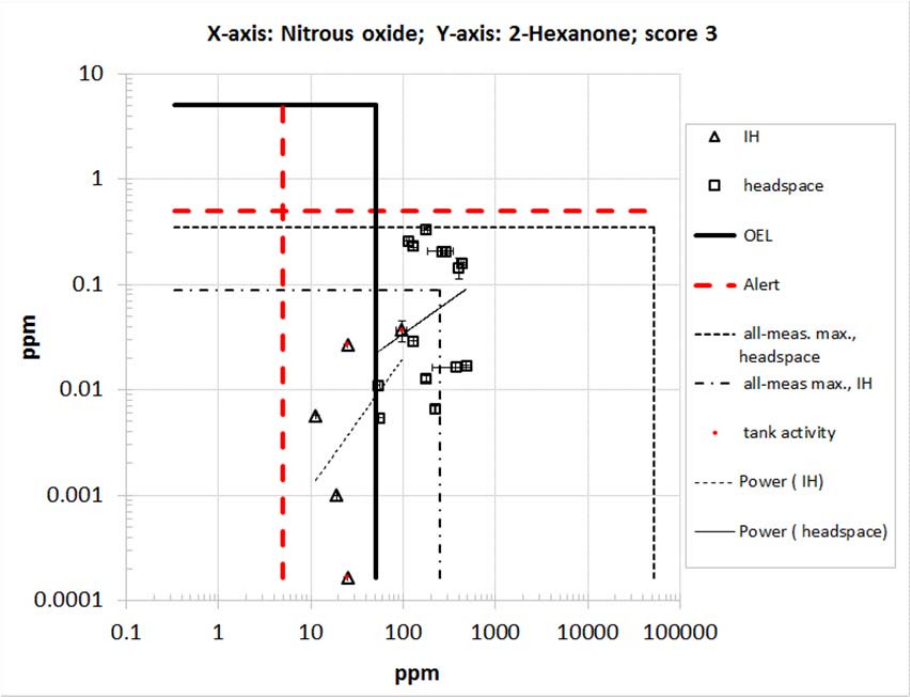

Figure 3.7. Pairing information for nitrous oxide and 2-hexanone

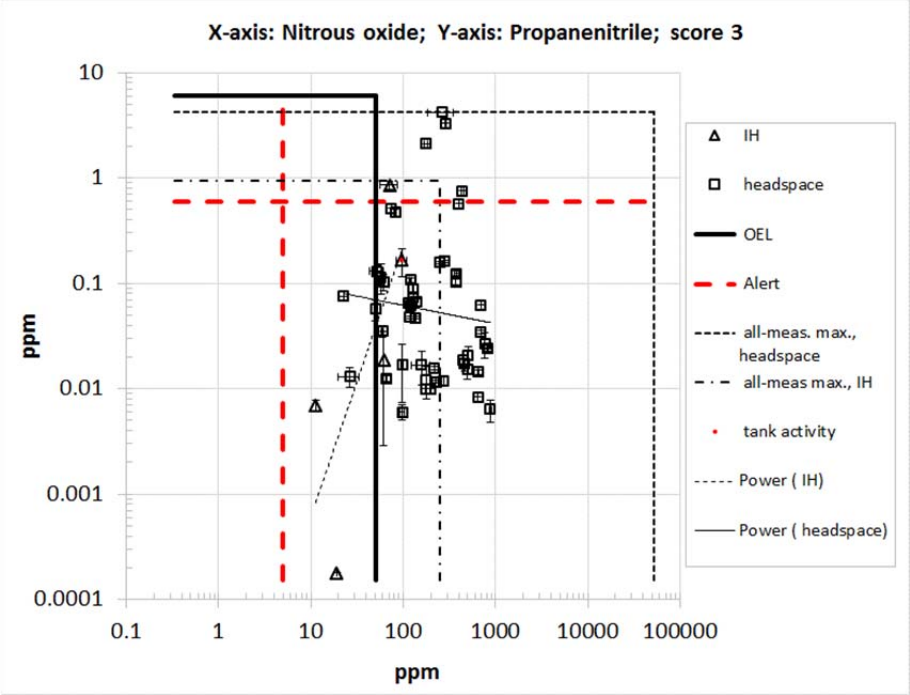

Figure 3.8. Pairing information for nitrous oxide and propanenitrile

Indicators of Low-OEL COPCs

Another question is whether pairwise relationships give clues to any potential LIs for the lower-OEL COPCs. Because there are more filtered data for formaldehyde and N-nitrosodimethylamine (NDMA) than for any of the other low-OEL COPCs, the top pairings for these two COPCs were reviewed.

The three highest-scoring pairings for formaldehyde are shown in Figure 3.9 through Figure 3.11 (THF, 1-propanol, and ammonia, respectively). As in preceding figures, measurements are shown with squares for headspace data and triangles for IH data, error bars on the points show one standard deviation, and the log-log trend lines for each dataset are shown by a thin, solid black line for the headspace data and a finely dotted black line for the IH data. The historical maximum concentrations for the two chemicals are shown by dotted black lines for the headspace data and dash-dotted black lines for the IH data. Toxicological information takes the form of the thick, solid black lines for the OELs and thick, red dashed lines at an alert point, assumed to be 10% of the OEL for each chemical.

The IH data for formaldehyde show scatter in all three cases, while the headspace data are less scattered for the THF and 1-propanol pairings (Figure 3.9 and Figure 3.10) than for the ammonia pairing (Figure 3.11). Also note the long vertical error bars on the data from the IH databases. These error bars show a tendency for formaldehyde measurements made within a day of each other to vary strongly, possibly because of tank activity. The absence of equally long horizontal error bars might mean more repeatability of the x-axis chemical measurements over the course of a day, or might only mean that only one measurement was taken that day.

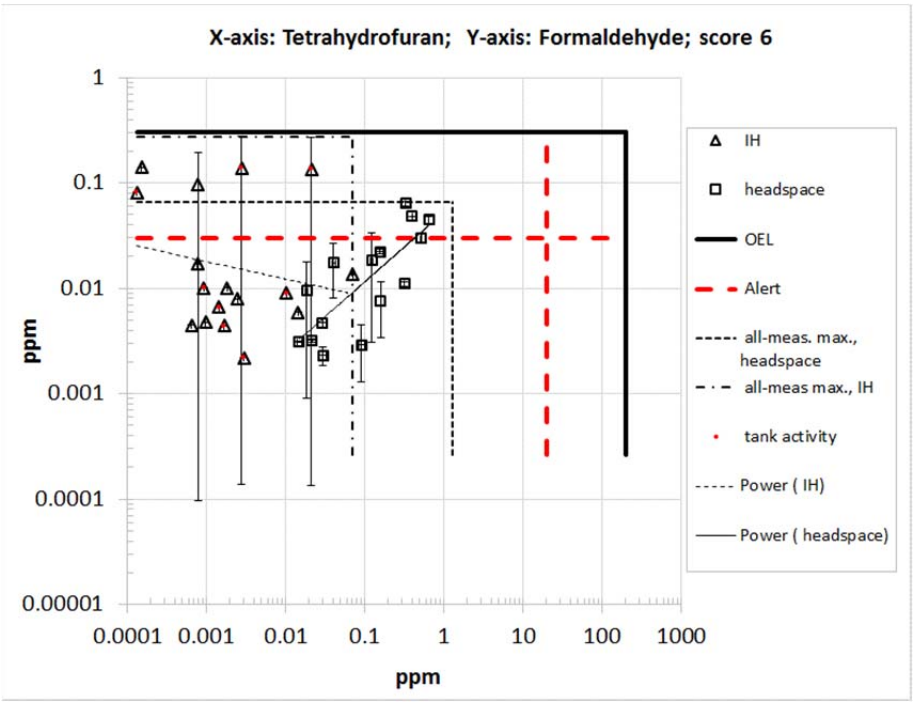

Figure 3.9. Pairing information for tetrahydrofuran (non-COPC) and formaldehyde

Formaldehyde is an unusual organic chemical in a number of ways. Its Henry's Law constant is very high: 3200 M/atm in salt-free water at 25°C (JPL 2015). It is an intermediate in a large number of reactions involving many types of organic feed material: complexants, phosphate esters, and hydrocarbon diluents (Stock 2004). It is very reactive; its releases are thought to come from volatilization during reactions that create and consume it, more than from an accumulating continuously present inventory. Whatever inventory is present at any time, it is expected to be almost entirely in the form of a hydrate (Stock 2004). Because of its unusual chemistry, formaldehyde may be difficult to pair with another indicator.

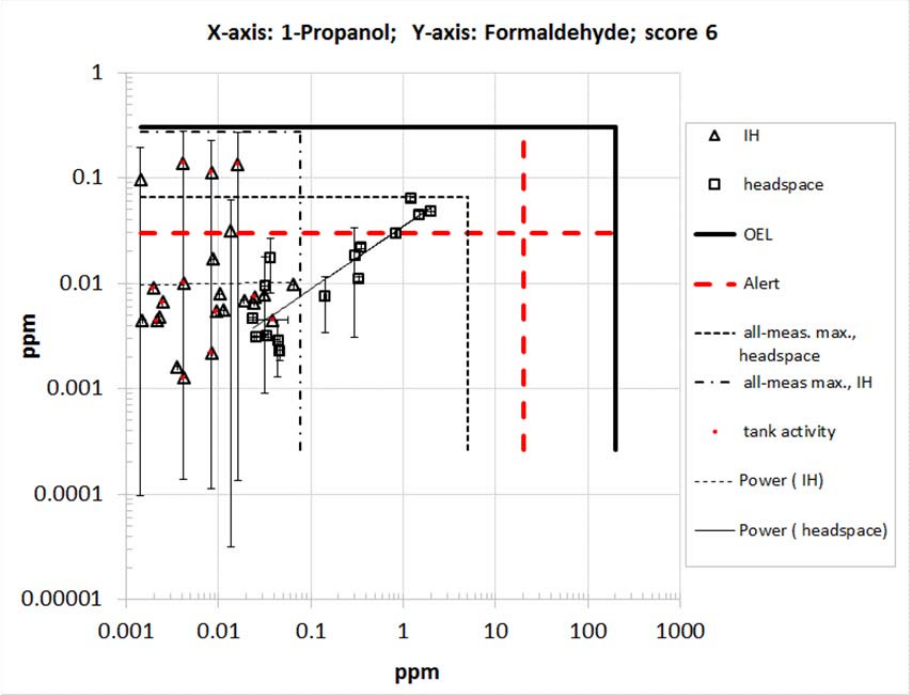

Figure 3.10. Pairing information for 1-propanol (non-COPC) and formaldehyde

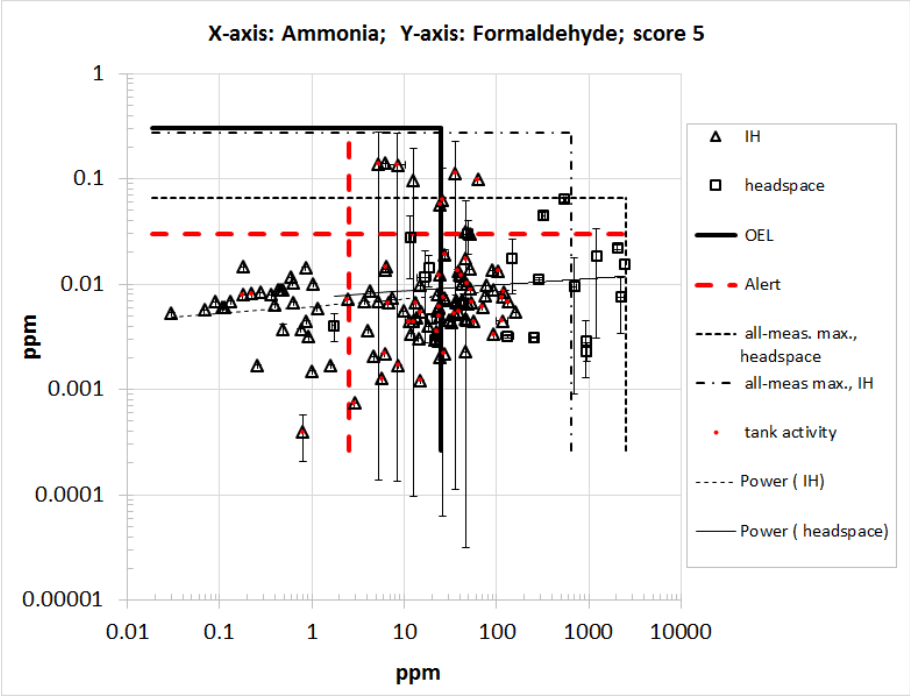

Figure 3.11. Pairing information for ammonia and formaldehyde

The two highest-scoring pairings for a potential indicator versus NDMA are shown in Figure 3.12 and Figure 3.13 (nitrous oxide and ammonia, respectively). As was the case for formaldehyde pairings, there is much scatter and no obvious trend in the NDMA pairings. NDMA has a high Henry's Law constant:

400 M/atm in salt-free water at 25°C (JPL 2015).. It might be better matched by chemicals that have a similar characteristic.

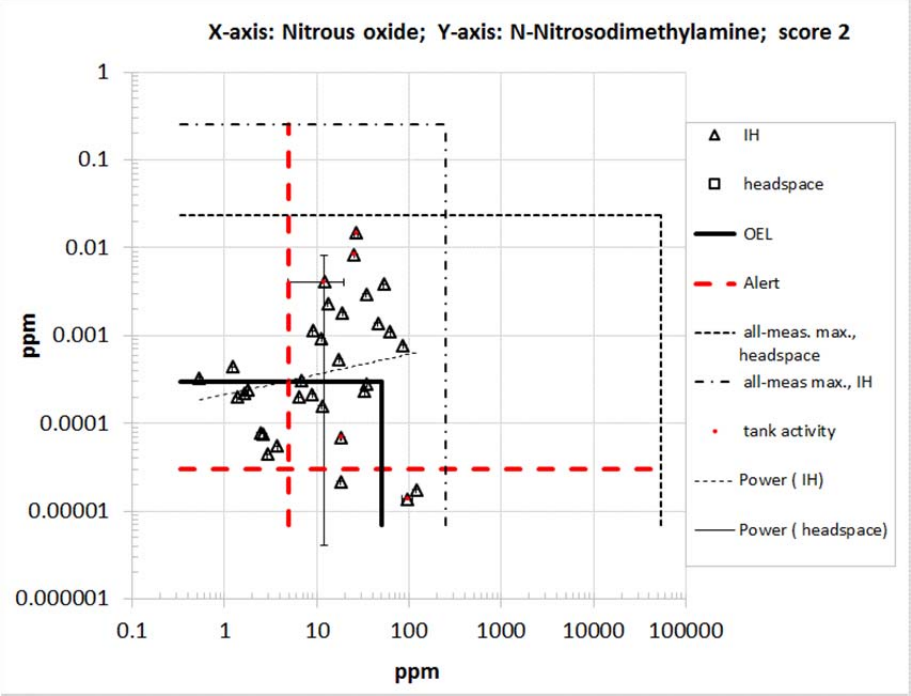

Figure 3.12. Pairing information for nitrous oxide and NDMA

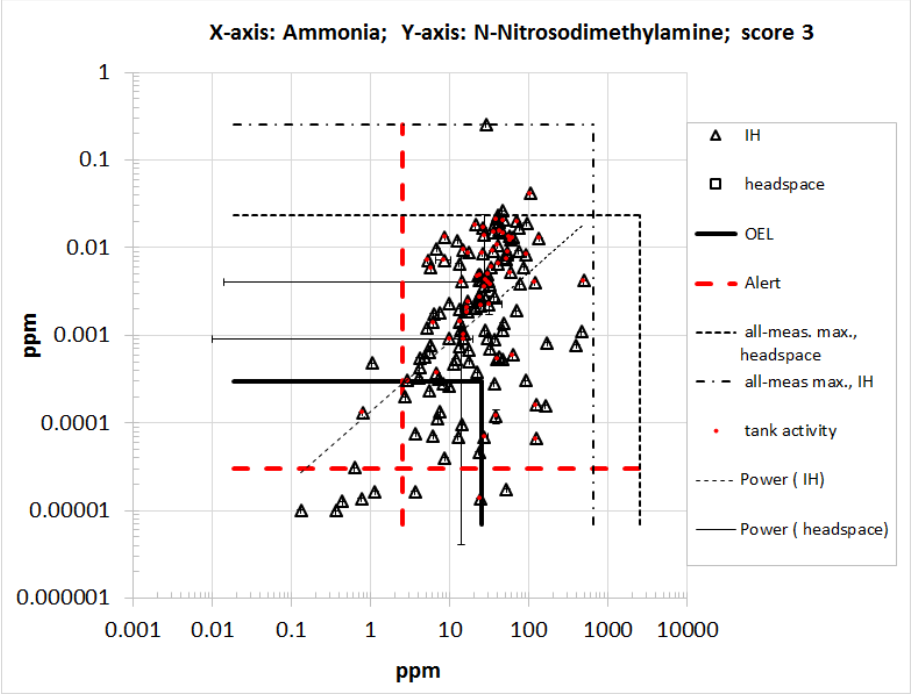

Figure 3.13. Pairing information for ammonia and NDMA

To check for the dependence of trends on sources (i.e. tank or tank farm), the IH data from the ammonia and NDMA pairing shown in Figure 3.13 are repeated in Figure 3.14, this time with the various sources distinguished from one another by symbols. Figure 3.14 shows some of the scatter in ammonia and NDMA comes from differences between sources, but that no individual tank-farm source shows a clear trend within its data. Figure 3.15 partially repeats Figure 3.11 for ammonia and formaldehyde and shows only the IH data with different sources distinguished by symbols. Here too there is scatter both within source groupings and among them.

Chemical Groups

Another possible approach to consider when identifying LIs is to investigate whether chemicals in the same family tend to cluster with each other. If there are such cases and one member of the family has a maximum concentration that is a lower fraction of its OEL than for other members, it may be able to serve as an indicator. Table 3.2 shows only the closely related chemical pairings from Table 3.1. Each of the columns represents the scoring criteria as described in Section 3.1.5. Only the pairing information that resulted in a point awarded is shown in the table for each of the criterion. As can be seen, the alkanenitrile COPCs have a tendency to trend with one another, but there is not much difference between them in terms of the maximum fraction of OEL observed among the hits (i.e., the challenge to OEL). The nitrosoamines are in a similar situation, since all have low OELs. The relationships within the aldehyde group and within the alcohol group may deserve further attention, though an assessment of the aldehyde group is hampered by having a relatively small number of hits.

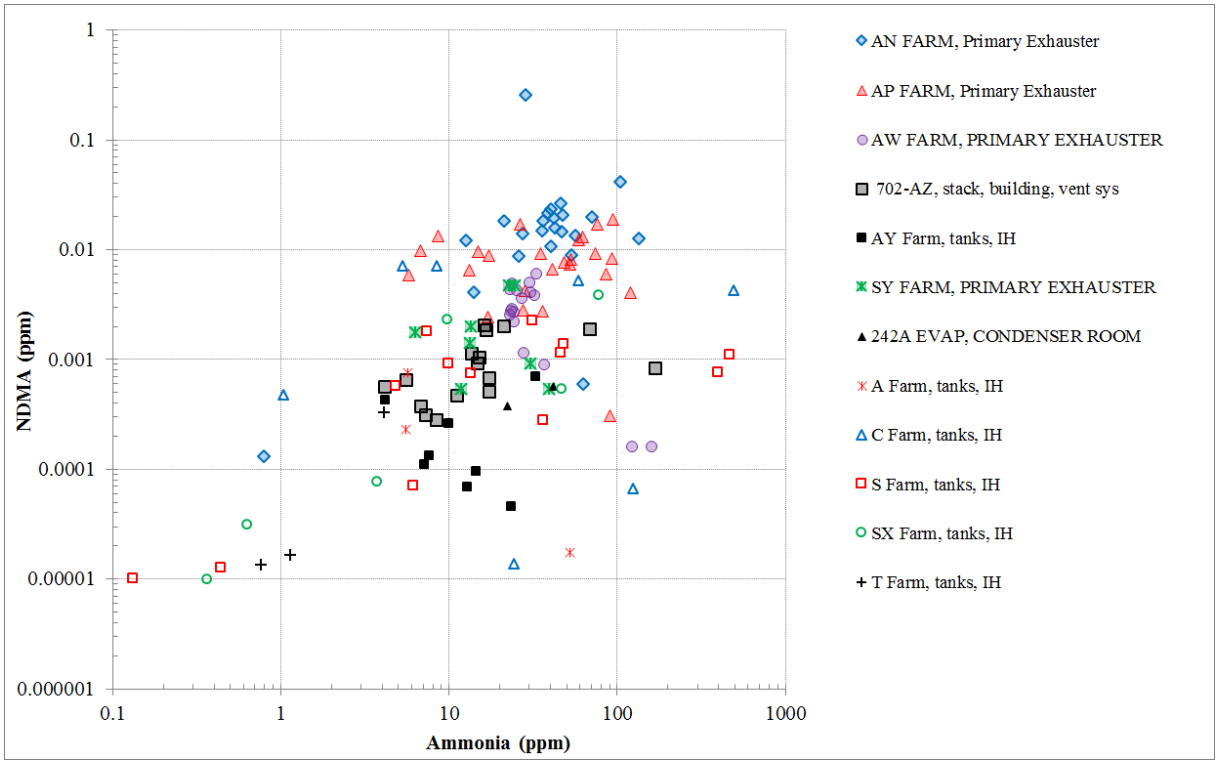

Figure 3.14. Effect of source on the ammonia and NDMA pairing

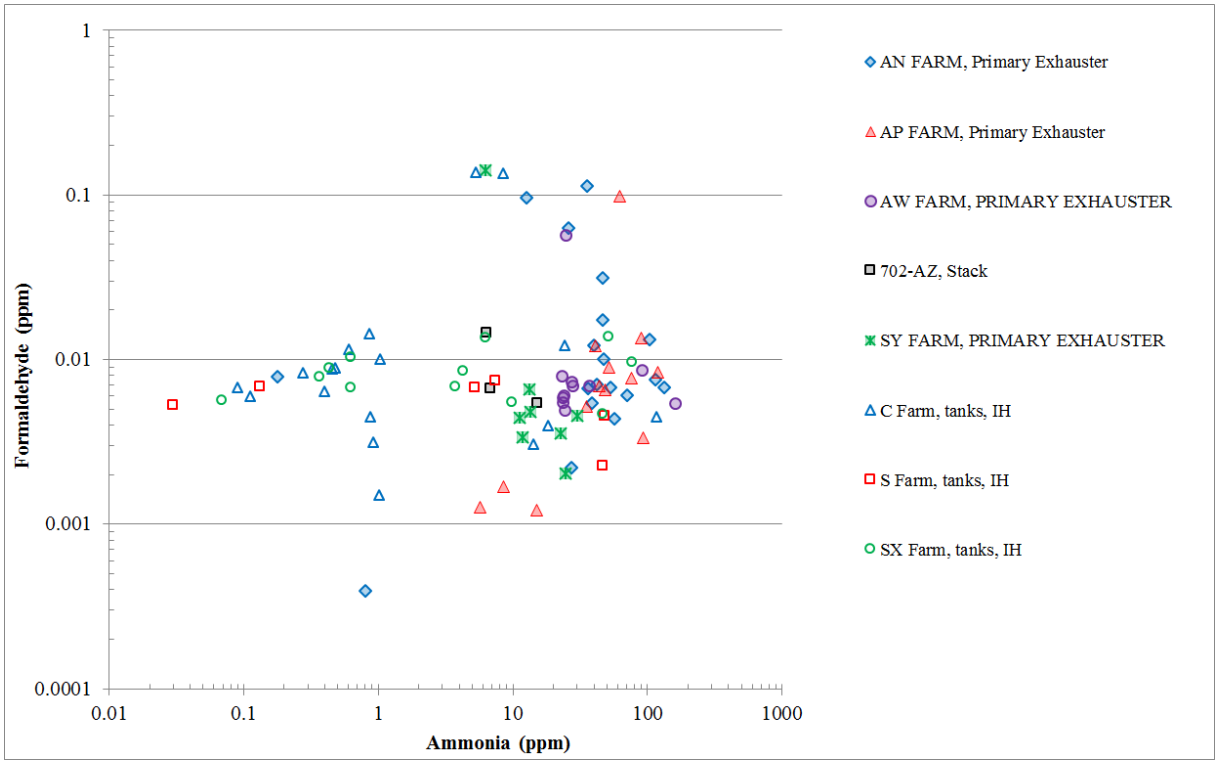

Figure 3.15. Effect of source on the ammonia and formaldehyde pairing

Table 3.2. Scoring information for the high-scoring pairings of chemicals that are structurally related[(a)]

x-Axis Chemical	y-Axis Chemical	Number of Hits in Each Dataset (Headspace and IH)	At least 10 Hits and High R^2		y vs. x OEL-Fraction Differential among Hits		Ratio of the All-Data Max x and y to the Max. x and y among Headspace Hits		Exponents in Headspace and IH, if Similar to Each Other	Percent of Hits That Were during Tank Activity		Total Score
			Head-space R^2	IH R^2	Head-space	IH	Head-space	IH		Head-space	IH	
Alkanenitriles												
Propanenitrile	Butanenitrile	53 & 18	0.73	0.79	---	---	1.0	1.3	0.7 & 0.8	---	33%	7
Butanenitrile	Pentanenitrile	---	0.64	0.90	---	---	1.9	1.3	0.8 & 1.0	---	---	5
Acetonitrile	Propanenitrile	68 & 18	0.77	---	---	---	1.0	---	0.9 & 0.7	---	---	4
Pentanenitrile	Hexanenitrile	---	---	0.89	---	---	1.1	1.1	1.1 & 1.1	---	---	4
Acetonitrile	Butanenitrile	---	0.52	---	---	---	1.0	---	---	---	33%	3
Propanenitrile	Hexanenitrile	---	0.72	---	---	---	---	1.1	1.0 & 1.0	---	---	3
Butanenitrile	Hexanenitrile	---	0.51	---	---	---	1.9	1.3	---	---	---	3
Aldehydes												
Formaldehyde	Butanal	---	0.63	---	---	0.009	2.7		---	---	40%	4
Formaldehyde	Acetaldehyde	---	---	---	---	---	1.7	2.0	---	---	60%	3
Nitrosoamines												
N-Nitrosodimethylamine	N-Nitrosomethylethylamine	---	---	0.71	---	0.003	---	1.0	---	---	55%	4
N-Nitrosodimethylamine	N-Nitrosomorpholine	---	---	0.50	---	0.001	---	1.0	---	---	53%	4
N-Nitrosomethylethylamine	N-Nitrosomorpholine	---	---	0.66	---	---	---	1.1	---	---	58%	3
Ketones												
2-Hexanone	3-Buten-2-one	---	---	0.59	---	132	---	---	---	---	38%	3
Alcohols												
1-Propanol	1-Butanol	73 & 17	0.75	0.66	42	367	1.1	---	---	---	41%	7
Ethanol	1-Butanol	60 & 23	---	---	103	47	1.2	---	---	---	22%	5
Ethanol	Methanol	---	0.70	---	14	31	1.2	1.1	---	---	---	5
1-Propanol	Methanol	---	---	---	---	243	1.0	3.0	---	---	---	3
Ammonia, ethylamine, and nitrosoamines												
Ammonia	N-Nitrosodimethylamine	---	---	---	---	44	---	1.3	---	---	43%	3
Ethylamine	N-Nitrosomethylethylamine	---	---	---	---	222	---	1.0	---	---	75%	3
Ethylamine	N-Nitrosomorpholine	---	---	---	---	53	---	1.0	---	---	78%	3

(a) Only pairing criteria that resulted in awarding a point are shown in the table.

The aldehyde-family formaldehyde and butanal pairing is shown in Figure 3.16. Note that in this case the lower-OEL chemical is on the x-axis, not the y-axis. There is no strong trend in the IH data for the pairing. The apparent trend in the headspace data may be nothing more than an artifact of the presence of a grouping of measurements from the C farm tanks at the top of the trend line, and another grouping of measurements from the S and U farms at the bottom of the trend line. The fact that butanal has much lower Henry's Law constant than formaldehyde (9.6 M/atm versus 3200 M/atm in salt-free water at 25°C) suggests that the apparent trend should be viewed with some skepticism, as it is not expected on the basis of physical release mechanisms.

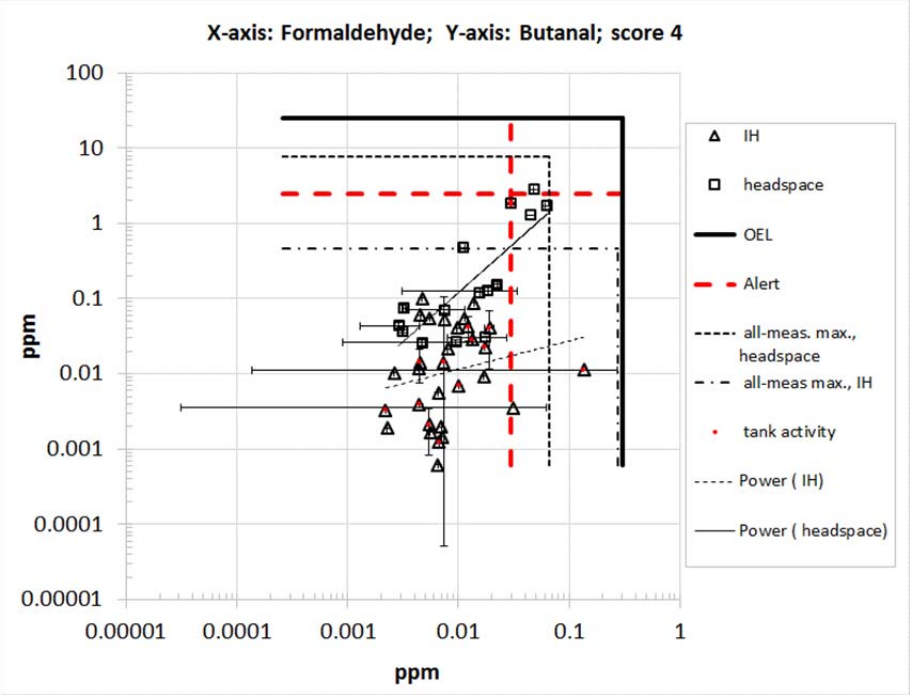

Figure 3.16. Pairing information for formaldehyde and butanal

Figure 3.17 shows the alcohol-family 1-propanol and 1-butanol pairing. Here there is a strong trend in the headspace data, and this trend is echoed in the IH data. The headspace data from Figure 3.17 are repeated in Figure 3.18, but with different sources distinguished by symbols. The measurements within each tank farm follow about the same trend as that followed by all the headspace data together. This pairing, which is of two straight-chain alcohols with only one carbon difference, appears to have a reliable link over many different sources.

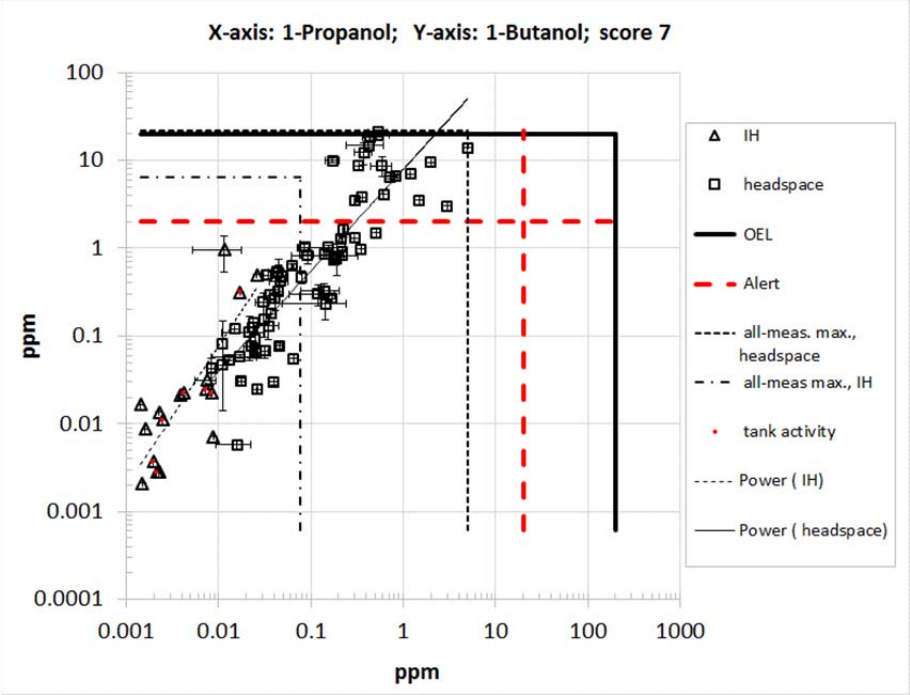

Figure 3.17. Pairing information for 1-propanol and 1-butanol

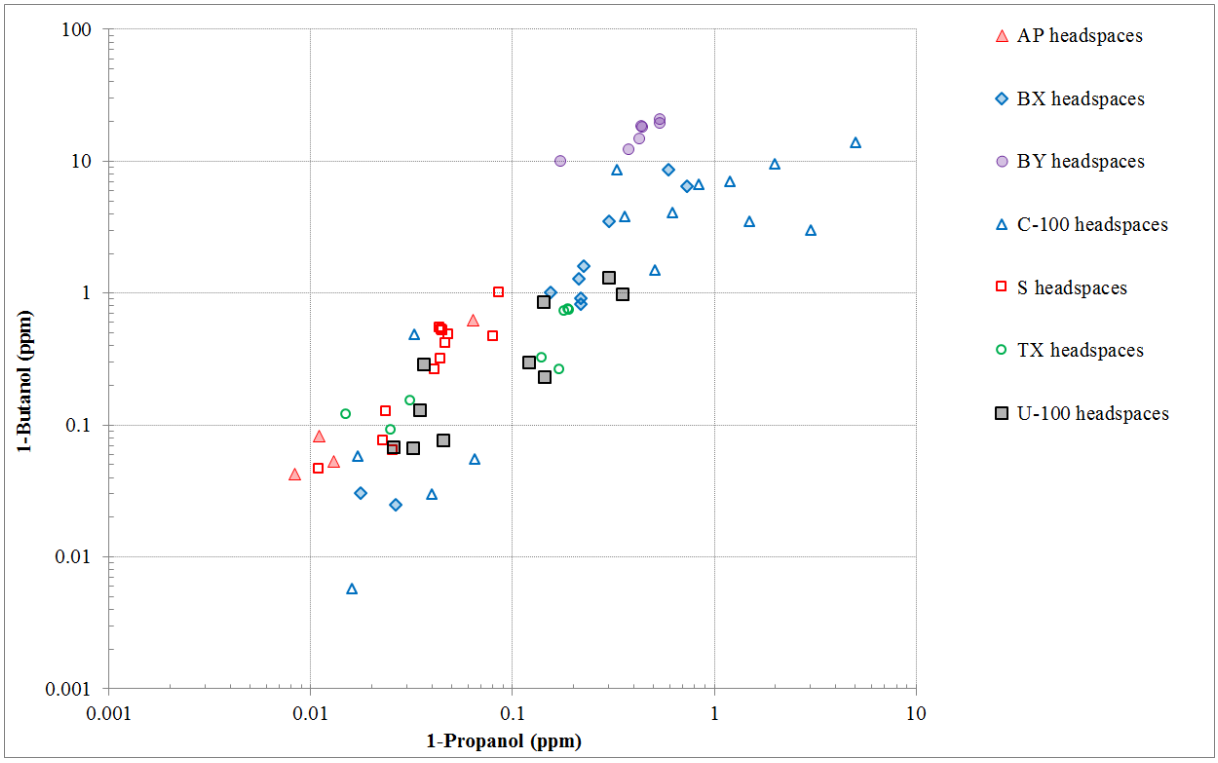

Figure 3.18. Effect of source on the 1-propanol and 1-butanol pairing

3.1.7 Summary

A few key observations were made throughout this initial analysis of the TWINS data that can be combined into general themes.

Time and Space

COPCs must be identified at the same time in the same location. If multiple samples are taken, but a timestamp and the associated location information are not recorded, COPC pairings cannot be identified between the multiple samples. The level of detail given for sample location ranges from specific identification of particular tanks or exhausters to generic description as "inside tank". The more generic the description limits the ability to cross-reference samples. Additionally, more detailed day/time information regarding tank activities will be required to identify tank activity effects on COPC pairing relationships.

This analysis found that ammonia paired with 33 COPCs within the filtered dataset. Nitrous oxide paired with 18 COPCs which were a subset of the 33 paired with ammonia. This is a promising observation, suggesting the possibility (in future work) of multivariate prediction using both NH_3 and N_2O.

Data Gaps

Not all COPCs were measured for every sample, meaning that analytical methods were used to look at a select subset of the COPCs. In the filtered dataset downloaded from TWINS on January 29, 2016, there were 25 COPCs that were not shown to have a pairing with another COPC (Figure 3.2). The lack of observed pairings does not strictly imply the pairing does not exist; rather there is a data gap for that pairing and those particular COPCs may not have been analyzed in the same samples.

Relationships

The apparent relationship trends observed in the site-wide population may not be the same as trends identified in the individual tank farms evaluated (Figure 3.14). COPCs within functional group families tend to trend well together and have shown similar data trends in site-wide data or individual tank farms (Figure 3.18). If chemicals in the same family are often analyzed by the same method, this would also remove some of the measurement variability.

4.0 Suitability Analysis

One thing that becomes apparent when attempting to analyze relationships between pairs of candidate chemicals from the TWINS database is that the relationship is best visualized on a log-log plot or processed in a log-log space. This is typical when relationships are more complex than linear, encompassing power law relationships between concentrations, or when variable ranges cover several orders of magnitude. However, even then, the relationship rarely reduces to a single line on such a plot; it is a scatter or band often spanning several orders of magnitude. Two questions arise: Why are the relationships like this? And how can such relationships be used to establish a leading indication from the presence of one chemical for that of the other? The reality of what the information on such a plot is conveying is that a given concentration of the potential LI may indicate a large range of potential concentrations of the COPC spanning, in some cases, several orders of magnitude.

The causal relationships between any pair of chemicals in question may in fact be tighter than what appears statistically after any given measurement process. The reasons for this can be many and varied, and include (1) varying circumstances between measurements of the two chemicals, or even different measurements of the same chemical; (2) the possibility that there are more complex relationships between one or both of the chemicals under investigation with other chemical species, whose concentrations are also varying; (3) differences in the decay of the two species, be that decay either chemical or radiological; and finally (4) different physics, such as affinity for materials in the environment and surroundings. All of these things can skew the apparent relationship between measured concentrations of two chemicals. Ultimately, however, the actual reasons are unknown, and in general irrelevant. One has to work with the statistical spread presented by the data.

Figure 4.1 shows a group of hypothetical data points, each having a measured COPC concentration value *Vc* and a measured LI value *Vi*, plotted on what is referred to herein as a quadrant diagram. In this figure, the data are seen as a cloud of points with a shape and size that depict a hypothetical relationship between the concentrations of the two chemicals in question. Data for pairs of chemicals in the TWINS and other databases may not give a cloud with anything like the density of the one depicted here, but this doesn't change the utility or function of this tool.

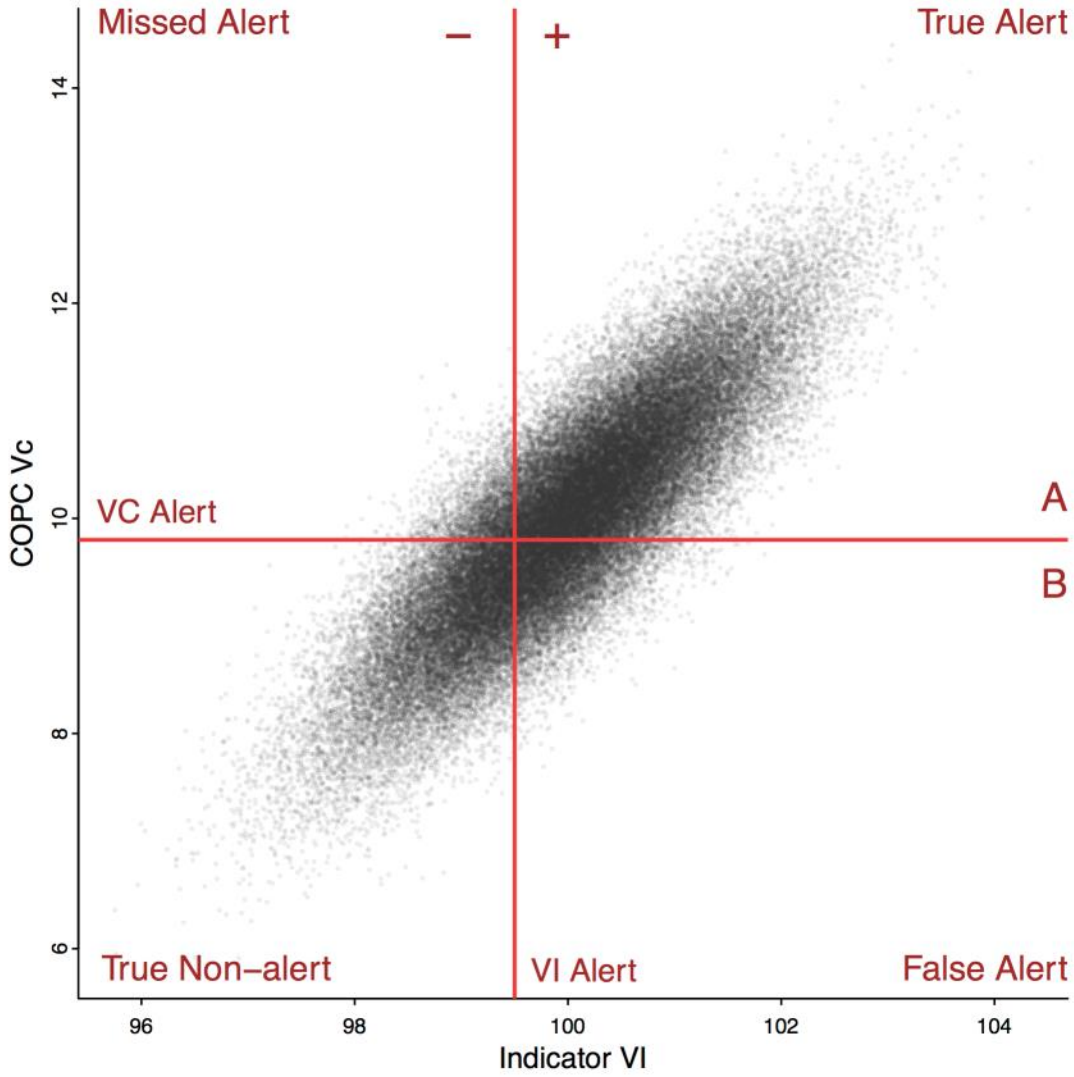

Figure 4.1. Quadrant diagram showing true and false alerts, missed alerts, and non-alerts

For any value of an LI concentration *Vi* on the horizontal axis, there is clearly a spread of COPC concentrations, *Vc*, on the vertical axis. This reflects the reality of the uncertainty in the predictive power of the LI given the available data. The *Vc* Alert level, or *Ac*, is the value set by health and safety or site management, as an exposure limit for workers, and as such is a number that users of this process are not anticipated to change. The LI alert level, *Vi* Alert or *Ai*, is a value that the users of the process can set to manage the risks and predictions provided by this tool. The crossing of these two levels now becomes the center of this plot and divides it into four quadrants. The upper right quadrant contains true alerts, for which the measured concentration is above the alert level, and the indicator above its threshold ($Vc > Ac$ and $Vi > Ai$). One can say in this case that the indicator is fulfilling its purpose by indicating a potentially hazardous exposure to the associated COPC. The bottom left quadrant contains true non-alerts, for which the measured COPC concentration is below the alert level and the indicator is below its threshold ($Vc < Ac$ and $Vi < Ai$). One can equally say that the purpose of the process is fulfilled here, in that there is no alert, and no potentially hazardous exposure risk. The lower right quadrant contains false alerts, or instances when the indicator is above its threshold ($Vi > Ai$), but there is no exposure risk from the COPC

(*Vc < Ac)*. The consequences of any alert can include evacuation of staff and shutting down of operations in scenarios applicable to the tank farms, which incurs expenses and takes time. However, if they happen too often, the cumulative cost of such false alerts can become prohibitive or their frequency could even shut down operations entirely. The remaining quadrant, the upper left, contains missed alerts. These more consequential instances are where there is no indicator alert (*Vi < Ai)*, but there is a potentially hazardous COPC exposure (*Vc > Ac)*.

An important distinction in nomenclature relating to the quadrature diagram is that of positive or negative rates, versus true or false alert rates. For example, true alert rate is often confused with true positive rate. These two are not the same entity, and confusing them can lead to overly optimistic expectations about the statistical performance of an alert system employing such a tool. A true positive rate speaks to the statistical performance of a test or metric (e.g., given 100 true cases, how many result in a positive test?). A true alert rate is about the statistical performance of a system employing this test (e.g., given 100 positives, how many result from true cases?). Similar statements also exist for the other three quadrants. The same could be said about the potential to confuse the terms "false alerts" and "false positives," or to think that these two terms mean the same thing. Table 4.1 summarizes and defines the nomenclature related to quadrant diagrams.

Table 4.1. Summary of quadrant nomenclature

Terminology		Definition
True Alert	$V_C > A_C \mid V_I > A_I$	Conditions unsafe and the system alarms
False Alert	$V_C < A_C \mid V_I > A_I$	Conditions are actually safe, but the system still alarms
True Non-Alert	$V_C < A_C \mid V_I < A_I$	Conditions are safe and system does not alarm
False Non-Alert (missed alert)	$V_C > A_C \mid V_I < A_I$	Conditions are unsafe, *but* the system does not alarm
True Positive	$V_I > A_I \mid V_C > A_C$	The system alarms and given conditions are unsafe
False Positive	$V_I > A_I \mid V_C < A_C$	The system alarms, but given conditions are actually safe
True Negative	$V_I < A_I \mid V_C < A_C$	The system does not alarm and given conditions are safe
False Negative	$V_I < A_I \mid V_C > A_C$	The system does not alarm, but given conditions are unsafe

The possibility of missed alerts may seem like something to be avoided at all costs. This would correspond to moving the vertical line, *Vi* Alert or value *Ai*, to the left so that there are no longer any points in the top left quadrant. This precisely describes the bounding behavior discussed earlier in this section, and is an acceptable mode of operation provided it doesn't result in excessive false positives such that operation is prohibitive or impossible. Note that the number of potential false positives in the lower right quadrant increases as the vertical line is moved to the left in Figure 4.1. Running with a non-zero number of points in the upper left quadrant is a compromise, allowing some small rate of missed alerts, but greatly reducing the number of false alerts to an acceptable level. Finding a value for *Ai* that gives such acceptable rates, in turn, depends on two things. First, the relationship between the potential LI and the COPC must be strong enough to give sufficiently low relative populations in the missed and false alerts quadrants of this figure. Second, the data used for this or any other analytical tool must be available and understood, in terms of their geographical and temporal locations and distributions, and also their reliability.

To expand on this concept, what interests all stakeholders in the tank farms is the understanding of what the chances are of certain conditions arising over given periods of time. The quadrant tool gives some insight into relative probabilities given appropriate data. For example, the probability that a worker

will interact with a COPC above a given alert rate is related to the number measurements where $Vc > Ac$ compared to the total number of measurements in some sample. However, as alluded to above, establishing rates per unit time depends on how all the measurements were distributed through time. This now reflects requirements into how the data are taken, where they are taken, how often, and with what regularity. If the measurements were taken in a different region or zone than where the worker was located during this time period, such an estimation would have to engage transport models giving probabilities of something seen in one place, appearing at another, and in what concentrations. In turn, such models would have to pull in a large range of both systematic and random factors, such as decay rates, reactivities and affinities of COPCs, wind directions, wind speed, solar heating (sub-factors including time of year, time of day, cloud cover and barometric conditions, etc.). Knowing and understanding these factors is much more about understanding the data than it is about understanding any given analytical or statistical tool, such as the quadrant plot. Similarly, making accurate assessments about establishing and using LIs is just as much about knowing how to use the process, and on which data, as it is about having confidence in this process itself. These statements also speak directly to the necessity of continually updating and maintaining databases so that such tools can be used to inform appropriate and relevant risk management decisions.

5.0 The Leading Indicator Identification Process

Implementation of a process predicting relationships between potential LIs and COPCs ultimately may take one or more of several forms, from a step-by-step procedure implemented by staff on limited data (as discussed in Sections 3.0 and 4.0) to a semi-autonomous computer program routinely monitoring a stream of data from automated sensors throughout the tank farms. The early stage of the process development takes the form of two flowcharts, as discussed in detail below.

Central to developing such a process is defining a technical basis for the relationship between potential LIs and the presence and semi-quantification of COPCs that may be difficult to detect and measure. At this time, the principal tool for developing this basis is the statistical analysis of data from the tank farms in TWINS and other databases, including both the tank headspace characterization data and IH monitoring samples. There are many aspects of this problem and resulting process to consider, including selecting appropriate analytical tools, understanding what makes data suitable for this study, developing appropriate models (statistical, chemical transport, atmospheric drift and dispersion), and ultimately developing a selection criteria for LIs. There are a number of conditions within tank farms that could alter the relationships between LIs and COPCs, including ventilation methods (passive ventilation in the single-shell tank farms versus active ventilation in the double-shell tank farms) or waste-disturbing activities as tank waste is sampled, transferred, or retrieved. Understanding the time evolution of available data, in terms of diurnal and/or seasonal effects, is also instrumental to ensuring continued validity of specific LIs and the selection process in general.

The process was developed with the intent of both allowing and requiring the user to determine the requisite decision parameters, and also where and upon what data it is to act. The results of the process must be understood in terms of where the user has chosen to use it. Refer again to the depiction of the different detection zones of the tank farms shown in Figure 2.1. For example, results of the process may be different if applied to data in the headspaces (A), as opposed to measurements at breather stacks and vents (B). It may also be different if data from both regions (A) and (B) are used together as equivalent (e.g., as seen in Figure 3.10). The benefit of this level of user discernment is that as datasets become available from the different regions within the tank farms, for whatever reason, one can process these data separately to identify potential LI candidates specific to those particular regions or zones. The two flowcharts representing the LI identification process are shown in Figure 5.1 and Figure 5.2.

5.1 LI Search Loop

The flowchart depicted in Figure 5.1 identifies the process for identifying LI candidates associated with individual COPCs. The structure of this flowchart is basically that of a do-loop for the current list of 59 COPCs. The loop moves from “Start” through each of these in turn, until the list is exhausted, at which point “End” is reached. The pink shaded area (dashed line box on the left-hand side of the figure) represents the chemical correlation algorithm used by the process to evaluate matches between COPCs and non-COPCs, which embodies a match search between pairs of chemical species, and a subsequent decision tree (consisting of multiple decision points) examining various properties of candidate matches. Several light blue boxes without explicit flow arrows are included within this region indicate sub-processes that are implicit in the algorithm or not part of the do-loop. These include “Input of New Data,” which embodies the process of reading in new data; “Pre-processing of DATABASES,” which embodies checks ensuring that field data (date, time, location, concentration, quality assurance flags, and other

selected metadata) are put into the correct form for combined analysis; and "Algorithm Improvement Subroutines," which is a placeholder for potential sub-processes to improve the algorithm's performance, but are as yet undefined.

The pink shaded area in this figure can be broadly thought of in three pieces, indicated by the tabs to the left of the figure. These are discussed separately in Sections 5.1.1, 5.1.2, and 5.1.3.

5.1.1 Match Identification

For a particular COPC, a database analysis is completed to identify COPC pairs found in the same location at the same time to generate a list of potential LI candidates for that COPC (represented by box labeled "Match Search"). If an adequate dataset is not established, that finding should be noted as a data gap and used to inform future testing (indicated by the red decision diamond "Is the Data Adequate" and subsequent actions to the right). For example, one sample with an observed pairing indicates that the two chemicals can be found together. Two data points potentially identify a relationship, but additional data points for a pairing give greater statistical significance to the relationship that can be inferred from the data.

If adequate data are not found at this decision point ("Is the Data Adequate"), then the data gap is noted and recorded to inform future tests ("Inform Future Tests"), and the do-loop continues to the next COPC.

5.1.2 Relationship Evaluation

After identifying a potential COPC/potential LI-pair, data are evaluated to determine if a sufficiently strong relationship exists, likely using a graphical representation of the measured concentration pairs from the database. This entails investigating potential relationships from the available data and determining if the trend is independent of circumstances (tanks, activity, etc.) or if there are multiple trends depending on circumstances (each tank farm shows a different trend). If no relationship exists, the gap should be noted for future consideration as more data become available. Other possible relationships between this COPC and other potential LIs can then be evaluated. There may be more than one result from the "Match Search" for a given COPC. Strictly speaking, a separate do-loop could be drawn for this, but this has been avoided in the interests of simplicity.

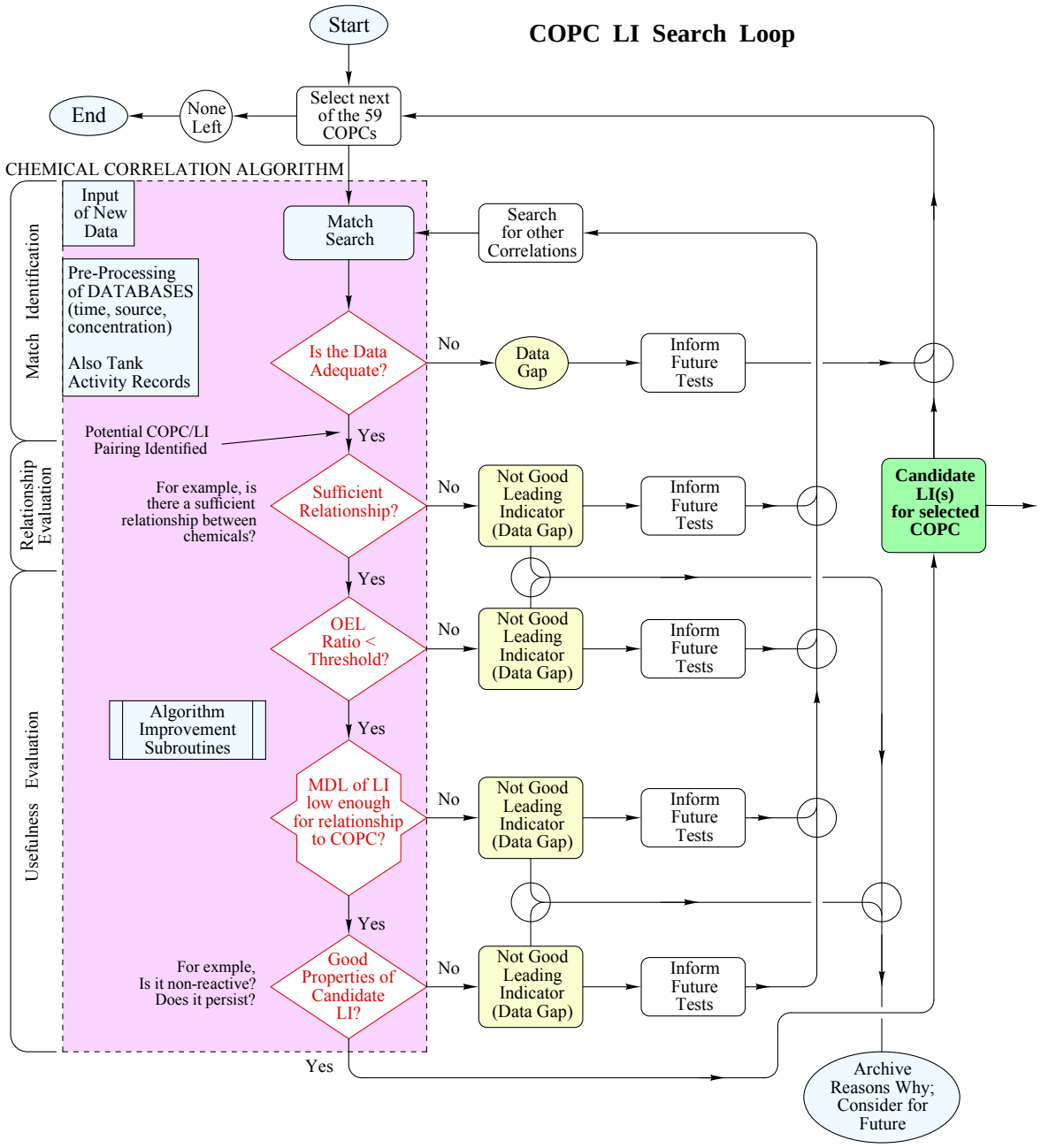

Figure 5.1. Flowchart of the COPC LI search loop

5.1.3 Usefulness Evaluation

If a pairing is identified with an adequate dataset and a relationship is observed, the OELs of the COPC/candidate-LI pairs are assessed with the minimum detection limits (MDLs) of the field equipment used to acquire available test data to determine the suitability of the LI for the COPC.

OEL Assessment

A good LI should present less of a hazard than the COPC it is indicating. Thus, if the OEL ratio of the two chemicals doesn't differ by more than a certain ratio, another LI may be sought. At this time, the ratio threshold has not been determined. This determination would need to be agreed upon by qualified staff (i.e., tank operations contractor management, IH representatives, etc.) and may be dependent on the pairing.

MDL Assessment

If the MDL of the candidate LI corresponds to a concentration greater than the OEL of the COPC (or some acceptable multiple of it), then another LI may be sought. In all steps through the process, the technical basis for why certain species are or are not chosen as potential LIs should be well documented and archived to inform future sampling or to revisit as new technology is employed within the tank farms.

LI Properties Assessment

Properties of each proposed LI species should be evaluated to confirm that it is a suitable candidate for the particular COPC. Reactivity, persistence, and potential effects from other COPCs or environmental interferent(s) are properties that could affect the application of the LI relationship.

5.2 Suitability Analysis

Candidate LIs determined from the search loop flowchart are then analyzed further to determine alert suitability. Figure 5.2 shows the second process flowchart, depicting statistical evaluation of candidate LIs for predictive bounding behavior capability and the potential for false alerts using statistical methods.

5.2.1 Bounding Indicator

A bounding indicator can be described as an LI, which when present at or above a predetermined concentration indicates the need for precautionary measures to prevent exposure to a COPC. This is bounding in the sense that this predetermined concentration is taken as an absolute alert level requiring a definite response. Such a bounding behavior can be adequate for preventing exposure of staff to potentially hazardous chemicals, but can also lead to the possibility of false alerts.

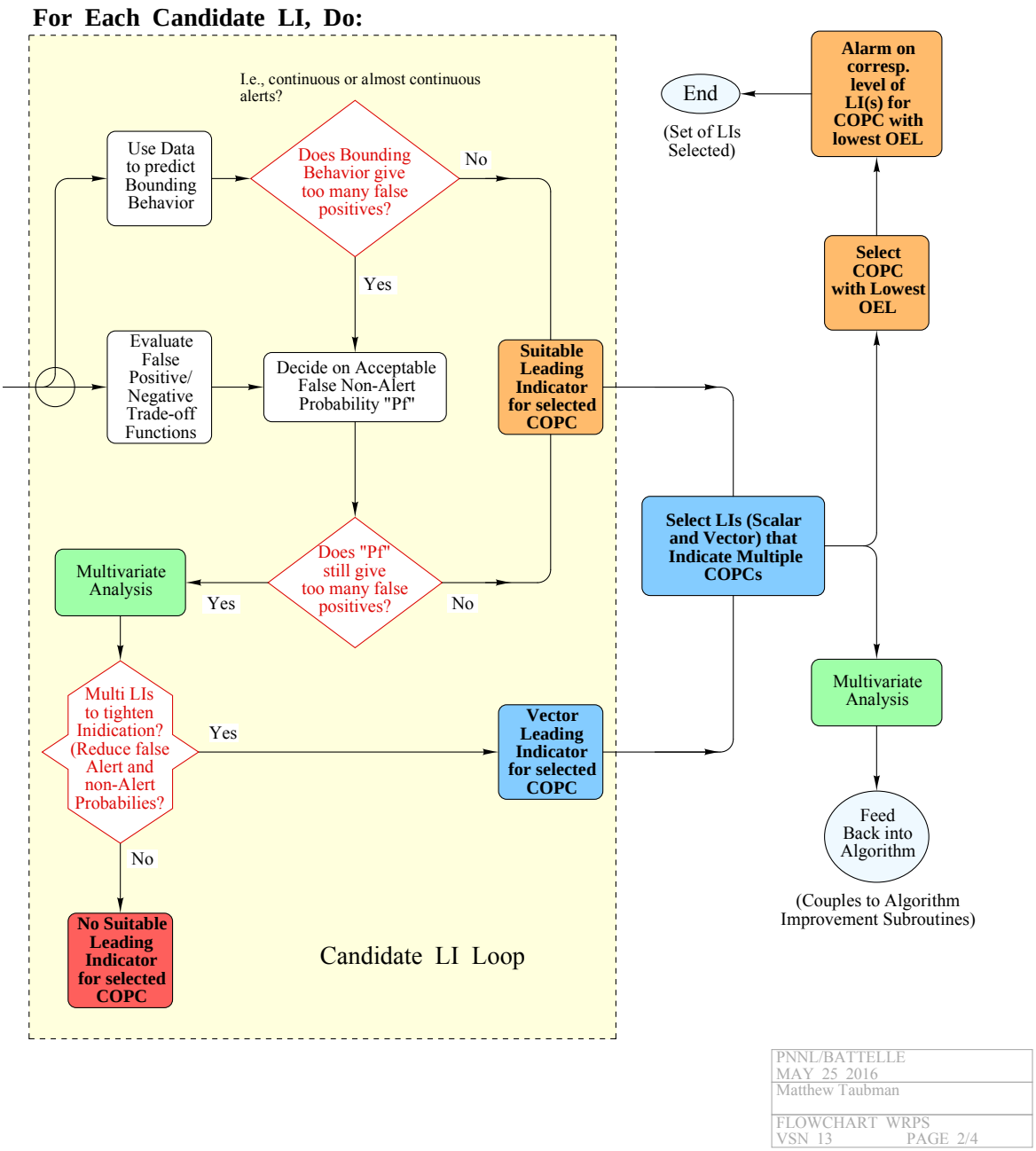

Figure 5.2. Flowchart depicting the LI suitability analysis

5.2.2 False Alerts

There will be a certain level of false alerts associated with the use of a bounding indicator due to the variation of potential concentrations of the COPC relative to the LI. If the level of false alerts given from bounding LI activity becomes burdensome, this can have a negative impact on the operations of the site. For example, an alert condition may exist for much of the time. If this is not the case, this leads to the orange box with text "Suitable Leading Indicator for selected COPC." Further to the right of this, the option of selecting groupings of LIs that indicate multiple COPCs is explored. In such cases, the COPC with the lowest OEL would be chosen to set LI alert levels.

Alternatively, if bounding use of an LI leads to unacceptable false positives, a different approach is warranted in order to establish an acceptable false negative rate to reduce the false positive rate to a manageable level. The LI Suitability Analysis flowchart depicts such possibilities, centered on relaxing the absolute nature of the above-described bounding use of an LI. This leads to standard statistical techniques such as four-quadrant analysis, in which rates of false positives and false negatives can be adjusted by the user-defined alert levels of the LI. This is embodied by the white box with text "Decide on Acceptable False Non-Alert Probability Pf." If the false non-alert probability (COPC is present, but no alert is given) is not too high, then the LI can be used in this statistical manner. Otherwise further multivariate analysis is required, including the possibility of using two or more LIs (see box with text "Vector Leading Indicator for selected COPC") to identify alert levels of COPCs in an acceptable way. Ultimately, it may be inevitable that given the available data, no LI(s) can be found for a given COPC.

The Hanford tank operations contractor holds the responsibility for deciding on alert levels, what constitutes too many false positive alerts, and an acceptable probability of false non-alert. If a single LI gives too many false positives relative to the acceptable false non-alert probability, multivariate analysis can be used to determine if a multiple LI vector approach can reduce the false alert and non-alert probabilities. At this time, a suitable multivariate approach has not been selected. Principal component analysis is one such method, although other approaches may be used as additional datasets become available.

6.0 Leading Indicator Process Validation

The primary objective of this report is to define a process through which chemical species known to be in tank farm emissions (including COPCs) are evaluated for their suitability for use as an LI, particularly for other difficult-to-detect COPCs. As additional data become available from future tank farm sampling and testing campaigns, the process may be re-evaluated and refined to include lessons learned from the new datasets. This includes defining the technical basis to state that adequate data sources are available and sound relationships exist between potential LIs and COPCs to be used in a correlating or bounding manner. Evaluation of the LI identification processes will identify limitations of the process based on the data currently available. The determination will also characterize circumstances when the LI identification process should be repeated and data re-evaluated for future LI searches, or additional data need to be obtained.

Another major objective of this work is to identify potential LI candidates for the COPCs or the data gaps that must be closed in order to identify potential LIs. Descriptions of data gaps within the available dataset will be given along with recommendations, if known, on how to close the gaps. In some cases, additional sampling efforts may be required. In others, a new means of detection could be the potential solution.

Success criteria for each of the major objectives are summarized below:

- Objective 1: Define and evaluate a process through which COPCs (or non-COPCs) are evaluated for their suitability for use as a LI for other COPCs.
  - Success Criterion 1-1. A limited number (e.g., handful) of readily detectable COPCs (or non-COPCs) are shown to effectively correlate to and/or bound other vapor COPCs.
  - Success Criterion 1-2. LIs are found to correlate and/or bound other COPCs at concentrations less than the OELs or exposure action levels of the LIs.
- Objective 2: Establish potential LI candidates or known data gaps that must be addressed for each of the 59 COPCs.
  - Success Criterion 2-1. If LIs for specific COPCs are not identified or are not bounding (i.e., below COPC OEL/action level), then the COPC is identified with gaps, indicating either data limitations or the need for an appropriately sensitive direct measurement method.

6.1 Evaluation of the LI Process

The LI identification process described in Section 5.0 was developed using data available from the TWINS database, including both the tank headspace characterization data and IH monitoring samples. To better evaluate the process, a larger dataset should be used with a multitude of sampling locations at regions A, B, and D (as shown in Figure 2.1), including samples and/or measurements taken at the same time/location for temporal and spatial relationships.

6.1.1 New Data Sources

There are several evolving datasets that could be potential inputs for this evaluation, including (1) pilot-scale VMDS testing to be initiated in 2016, (2) mobile laboratory data collection underway in 2016, (3) additional vapor headspace sampling and analysis being performed in 2016, and (4) vapor headspace data collected since ~2005 that are not currently available through TWINS, but may offer additional data for testing.

The database generated during the pilot-scale test at the AP and A/AX tank farms would be an ideal test case to evaluate the LI identification process with a multitude of sampling locations at regions A, B, and D (as shown in Figure 2.1), including samples and/or measurements taken at the same time/location for temporal and spatial relationships. The 241A Vapor Monitoring and Detection System Pilot-Scale Test Plan (241A-TP-043) describes the intensive data collection activities planned. These activities include analysis of air samples taken from the stacks, passive breather filters, and other locations within the farms (fugitive emission points). Also included is a suite of instruments to be deployed within the tank farms. All these data sources will provide valuable input to the LI identification analysis.

In addition to the pilot-scale tests, RJ Lee has been contracted to use their mobile laboratory with state-of-the-art proton transfer reaction—mass spectrometry and gas chromatography—mass spectrometry instrumentation to collect integrated and/or grab samples in multiple locations throughout AP and A/AX tank farms, as well as other locations on the Hanford Site. The tank farms are routinely monitored by IH through the analysis of grab samples. All of these data sources will be incorporated into the LI identification analysis as data become available.

A campaign to sample and analyze tank headspace is also planned. Additional vapor headspace sampling and analysis post 2005 would provide similar but more recent information than that collected from TWINS for process development.

6.1.2 Process Evaluation

To test, exercise, and refine the process defined in Section 5.0, one or more of the new data sources identified above will be used. Given new data availability, an additional but limited dataset is expected to be tested through the process in fiscal year (FY) 2016, followed by process refinement and additional testing in FY 2017. The principal steps for testing are as follows:

1. Acquire new vapors data from the tank farm contractor, and complete preliminary assessment of data completeness and adequacy for processing.

2. Process new data through the LI search loop described in Section 5.1 and depicted in Figure 5.1 to identify candidate LIs. The results of the LI search loop will be documented using the matrix shown in Figure 3.2 and Table 6.1. Figure 3.2 was expanded to include non-COPCs observed pairings and potential LI candidates, and those can be seen in the 12 columns on the right side of the matrix.

Table 6.1. Evaluation of COPC LI search loop for a single COPC

COPC:			Dataset:				
COPC ID #	COPC	Pairing Observed?	Number Data Points	Relationship Observed?	OEL Threshold Comment	Means for Detection/MDL Comment	Continue with Statistical Analysis?
1	Ammonia						
2	Nitrous oxide						
3	Mercury						
4	1,3-Butadiene						
5	Benzene						
6	Biphenyl						
7	1-Butanol						
8	Methanol						
9	2-Hexanone						
10	3-Methyl-3-butene-2-one						
11	4-Methyl-2-hexanone						
12	6-Methyl-2-heptanone						
13	3-Buten-2-one						
14	Formaldehyde						
15	Acetaldehyde						
16	Butanal						
17	2-Methyl-2-butenal						
18	2-Ethyl-hex-2-enal						
19	Furan						
20	2,3-Dihydrofuran						
21	2,5-Dihydrofuran						
22	2-Methylfuran						
23	2,5-Dimethylfuran						
24	2-Ethyl-5-methylfuran						
25	4-(1-Methylpropyl)-2,3-dihydrofuran						
26	3-(1,1-Dimethylethyl)-2,3-dihydrofuran						
27	2-Pentylfuran						
28	2-Heptylfuran						
29	2-Propylfuran						
30	2-Octylfuran						
31	2-(3-Oxo-3-phenylprop-1-enyl)furan						
32	2-(2-Methyl-6-oxoheptyl)furan						
33	Diethylphthalate						
34	Acetonitrile						

COPC:			Dataset:				
COPC ID #	COPC	Pairing Observed?	Number Data Points	Relationship Observed?	OEL Threshold Comment	Means for Detection/MDL Comment	Continue with Statistical Analysis?
35	Propanenitrile						
36	Butanenitrile						
37	Pentanenitrile						
38	Hexanenitrile						
39	Heptanenitrile						
40	2-Methylene butanenitrile						
41	2,4-Pentadienenitrile						
42	Ethylamine						
43	N-Nitrosodimethylamine						
44	N-Nitrosodiethylamine						
45	N-Nitrosomethylethylamine						
46	N-Nitrosomorpholine						
47	Tributylphosphate						
48	Dibutylbutylphosphonate						
49	Chlorinated biphenyls						
50	2-Fluoropropene						
51	Pyridine						
52	2,4-Dimethylpyridine						
53	Methyl nitrite						
54	Butyl nitrite						
55	Butyl nitrate						
56	1,4-Butanediol, dinitrate						
57	2-Nitro-2-methylpropane						
58	1,2,3-Propanetriol, 1,3-dinitrate						
59	Methyl Isocyanate						

3. Process promising candidates from the LI search loop (step 2 above) through the Suitability Analysis steps (Section 5.2 and Figure 5.2) to identify selected LIs for COPCs with the lowest exposure action level and/or OEL. The candidate LIs will be subsequently analyzed for bounding behavior and false positive/negative tradeoffs. Evaluation of LI suitability analysis for a particular COPC will be tracked and documented in Table 6.2.

4. Based on the analyses of steps 1 through 3 above, selected LIs will be recommended. In addition, recommendations and conclusions will be drawn from the analysis relative to data gaps or limitations that preclude identification of suitable LIs for specific COPCs. Recommendations on additional testing, data collection, statistical analysis, LI development process refinement, and/or alternate measurement system development will be made based on the results of the testing.

Gaps discovered throughout the process would be identified, such as inadequate data for COPCs, lack of relationship with other COPCs or non-COPCs given the current database. Table 6.1 and Table 6.2 can be used to track associated gaps for each COPC as they pertain to particular steps within the LI search loop. Recommendations on closure of identified gaps may also come out of the process. For example, additional sampling efforts or a new means of detection may be required for gap closure.

Table 6.2. Evaluation of LI suitability analysis for a single COPC

COPC:			Dataset:			
COPC ID #	Potential LI	Bounding Relationship?	Agreeable False Positive?	Agreeable False Negative?	Need Multiple LIs?	Use LI?
1	Ammonia					
2	Nitrous oxide					
3	Mercury					
4	1,3-Butadiene					
5	Benzene					
6	Biphenyl					
7	1-Butanol					
8	Methanol					
9	2-Hexanone					
10	3-Methyl-3-butene-2-one					
11	4-Methyl-2-hexanone					
12	6-Methyl-2-heptanone					
13	3-Buten-2-one					
14	Formaldehyde					
15	Acetaldehyde					
16	Butanal					
17	2-Methyl-2-butenal					
18	2-Ethyl-hex-2-enal					
19	Furan					
20	2,3-Dihydrofuran					
21	2,5-Dihydrofuran					
22	2-Methylfuran					
23	2,5-Dimethylfuran					
24	2-Ethyl-5-methylfuran					
25	4-(1-Methylpropyl)-2,3-dihydrofuran					
26	3-(1,1-Dimethylethyl)-2,3-dihydrofuran					
27	2-Pentylfuran					
28	2-Heptylfuran					
29	2-Propylfuran					
30	2-Octylfuran					
31	2-(3-Oxo-3-phenylprop-1-enyl)furan					
32	2-(2-Methyl-6-oxoheptyl)furan					
33	Diethylphthalate					
34	Acetonitrile					

COPC:			Dataset:			
COPC ID #	Potential LI	Bounding Relationship?	Agreeable False Positive?	Agreeable False Negative?	Need Multiple LIs?	Use LI?
35	Propanenitrile					
36	Butanenitrile					
37	Pentanenitrile					
38	Hexanenitrile					
39	Heptanenitrile					
40	2-Methylene butanenitrile					
41	2,4-Pentadienenitrile					
42	Ethylamine					
43	N-Nitrosodimethylamine					
44	N-Nitrosodiethylamine					
45	N-Nitrosomethylethylamine					
46	N-Nitrosomorpholine					
47	Tributylphosphate					
48	Dibutylbutylphosphonate					
49	Chlorinated biphenyls					
50	2-Fluoropropene					
51	Pyridine					
52	2,4-Dimethylpyridine					
53	Methyl nitrite					
54	Butyl nitrite					
55	Butyl nitrate					
56	1,4-Butanediol, dinitrate					
57	2-Nitro-2-methylpropane					
58	1,2,3-Propanetriol, 1,3-dinitrate					
59	Methyl Isocyanate					

6.2 Process Evaluation

An evaluation of the process was initiated using a query[1] from the Site-Wide Industrial Health database (SWIHD) that contained headspace samples from 2014 – 2016. The dataset used in the evaluation also included a more recent query[2] of the TWINS database to obtain any additional analytical results entered since a previous download in January 2016.

Records were filtered to keep only the primary and duplicate result types. Records from the TWINS database were filtered to remove those with data qualifier codes (B, F, S, T, and Y) that identified records associated with quality issues with the batch blank samples, suspect results, or non-defined laboratory specific flags. Records with data qualifier codes (D, E, H, J, M, N, Q, U, and X) remained in the dataset, but were only used as observational tools and not for any correlation determination. See Table 6.3 with descriptions of the quality codes found within TWINS database records. Records from the SWIHD database were filtered to remove those with data qualifier codes (a, B, c, L, and Y) that identified records associated with quality issues with the batch blank samples, suspect results, or non-defined laboratory specific flags. Records with data qualifier codes (E, J, N, Q, T, and <) remained in the dataset, as these data still provided information, but were not used to the full extent of data without codes. See Table 6.4 with descriptions of the quality codes found within SWIHD database records.[3]

[1] The complete headspace contents for all tanks, dates, and chemicals were downloaded on July 12, 2016 as spreadsheets

[2] The complete contents for all tanks, dates, and chemicals were downloaded from industrial health and headspace databases on June 20, 2016 as spreadsheets

[3] SWIHD data qualifier code descriptions were taken from 222-S Laboratory Guidance Document ATS-GD-1028, Rev. D-2

Table 6.3. TWINS data qualifier code descriptions

Data Qualifier Code	Description
B	Compound found in associated laboratory blank as well as sample
D	Target analyte reported is the result of a secondary dilution
E	Reported concentration was above the instrumental calibration range
F	Target analyte reported in sample was also found in the field blank above action limit
H	Analysis was performed after allowed analytical holding time had elapsed or analysis date is not available
J	Reported concentration was estimated
M	Target analyte was absent (not detected) from sample
N	Compound is a tentatively identified compound. Includes both chemical library matches, chemist identified compounds, and unknowns.
Q	Target analyte was detected, but at concentrations less than Vapor Program Required Quantitation Limits
S	Result suspect – see comment field
T	Target analyte reported in sample was also found in trip blank above reporting value
U	Compound was analyzed for but not detected above reporting value
X	Analytical laboratory did not have the approved quality assurance documentation, or that a significant quality assurance deficiency was associated with reported result
Y	Laboratory defined flag. This flag indicates that remarks pertinent to data quality are in the data report narrative or comment.

Table 6.4. SWIHD data qualifier code descriptions

Data Qualifier Code	Description
B	Each analyte in a batch where the preparation blank/method blank result for that analyte exceeded the criteria specified in the analytical method or project-specific work instruction
E	Each analyte result that exceeded the calibration range of the instrument
I	Result was determined via indirect calibration
J	Results that are considered estimates.
N	Compounds identified based on a library search. These tentatively identified compounds (TICs) are not target compounds and the results are only an estimate and not quantitative.
P	Polychlorinated biphenyl data
Q	Results that are considered to be qualitative based on method of result acquisition or instrument and analyte specific calibration issues
T	TIC compounds identified by library search or identified as unknowns after a library search. The results are only an estimate and not quantitative.
U	Analytes that were analyzed for, but were not detected, or were detected below the method detection limit
Y	User-defined flag applied to results that require verbal descriptions or qualifying comments
a	All results (both detected and non-detected) within a sample batch that included a laboratory control sample with a percent recovery for that analyte that was outside the customer or analytical method specified
b	Analyte results (both detected and non-detected) when the matrix spike, or post-digestion spike is outside the customer or analytical method defined range
c	Analyte results (both detected and non-detected) where the relative percent difference between duplicate samples, laboratory control sample duplicate or matrix spike duplicate was greater than the customer or analytical method defined
d	Customer-defined flag applied to data that exceeded the relative standard deviation criteria set by the customer on triplicate analyses
e	Customer-defined flag and is applied to analytes for which the sample result and the serial dilution result (normally a factor of 5) for that sample have a percent difference of greater than 10 percent
f	Customer-defined flag applied to results to indicate that the matrix spike or the post-digestion spike failed and the serial dilution passed
p	Customer-defined flag only applied to compounds initially identified as TICs.

COPC concentration records from the remaining filtered dataset are shown in Figure 6.1. The ratio of concentration values to the COPC OEL are plotted on a non-linear x-axis. This figure gives a useful snapshot of the available data in terms of measured concentrations relative to the OEL and number of data points available. The 10% OEL for each COPC is identified by the vertical red dashed line at the 0.1 mark on the x-axis. The OEL is identified by the vertical red solid line at the 1 mark on the x-axis. The dotted line at the 100 mark on the x-axis represents measurements that are 100 times or greater than the OEL. The x-axis was plotted on a non-linear scale with the maximum of 100 times the OEL shown to constrain the size of the figure. COPCs are aligned on the y-axis by maximum value-OEL ratio. CAS numbers are used to identify the COPCs rather than the names to maximize the space available to plot the data. A list

of CAS numbers and chemical names in the same order as shown on the y-axis is given in Table B.1 in Appendix B. Measurements less than MDL are indicated as downward pointing triangles while measurements greater than MDL are marked with upward triangles. The numbers listed in the column on the right are the number of data points remaining after filtering for that particular COPC. Within this filtered dataset, all COPCs have been reported above the 10% OEL value. Thirty-five COPCs have been measured at or above the OEL value and 8 of these have been measured at or above 100 times the OEL. There are 14 COPCs where some of the observed MDL values are greater than the OEL. Of these, 4 COPCs have observed MDL values at or above 100 times the OEL. Another 13 were found to have some MDL values above the 10% OEL. Thirteen COPCs were found to have less than 10 data points within this filtered dataset.

A similar plot of non-COPC chemicals identified within the filtered dataset is shown in Figure 6.2. Again the ratios of concentration values to the OEL are plotted on a non-linear x-axis. The OEL values given for most of these non-COPC chemicals were listed within the SWIHD database. Those that were not included within the SWIHD database were identified in literature (Meacham et al. 2006, Poet et al. 2006, and Poet and Timchalk 2006). Non-COPC chemicals without defined OEL values have not been included within this figure. The 10% OEL for each chemical is identified by the vertical red dashed line at the 0.1 mark on the x-axis. The OEL is identified by the vertical red solid line at the 1 mark on the x-axis. The dotted line at the 100 mark on the x-axis represents measurements that are 100 times or greater than the OEL. The x-axis was plotted on a non-linear scale with the maximum of 100 times the OEL shown to constrain the size of the figure. Measurements that were indicated to be less than MDL are indicated as downward pointing triangles. Non-COPC chemicals are aligned on the y-axis by maximum value-OEL ratio. The numbers listed in the column on the right are the number of data points remaining after filtering for that particular chemical. A list of CAS numbers and chemical names in the same order as shown on the y-axis is given in Table B.2 in Appendix B. There are a number of non-COPC chemicals that are identified within the dataset that may be useful in identification of tank vapor signatures or leading indicators.

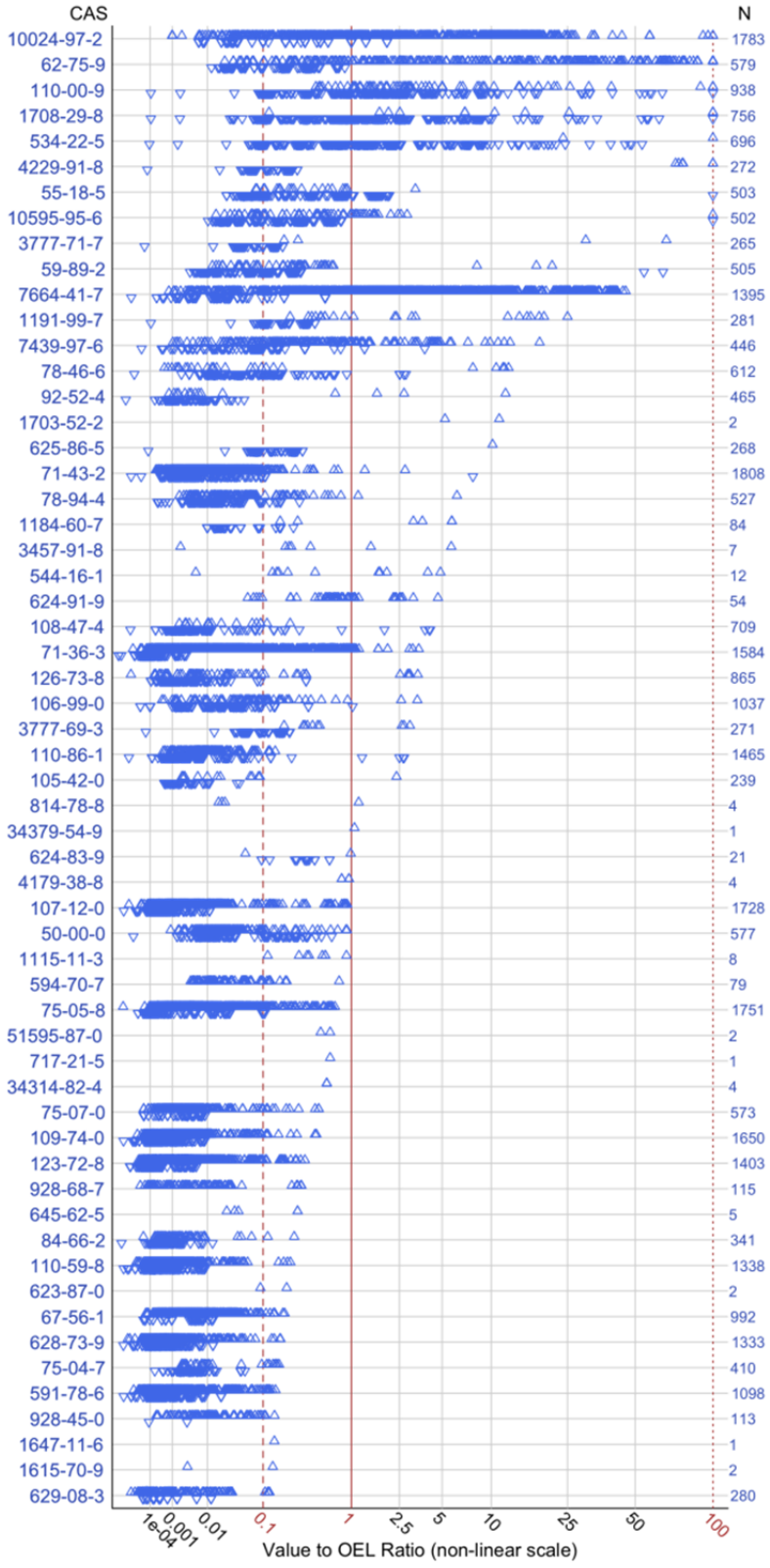

Figure 6.1. Filtered COPC:OEL ratios from TWINS industrial health samples and TWINS and SWIHD headspace samples. CAS IDs and chemical names are given in Table B.1

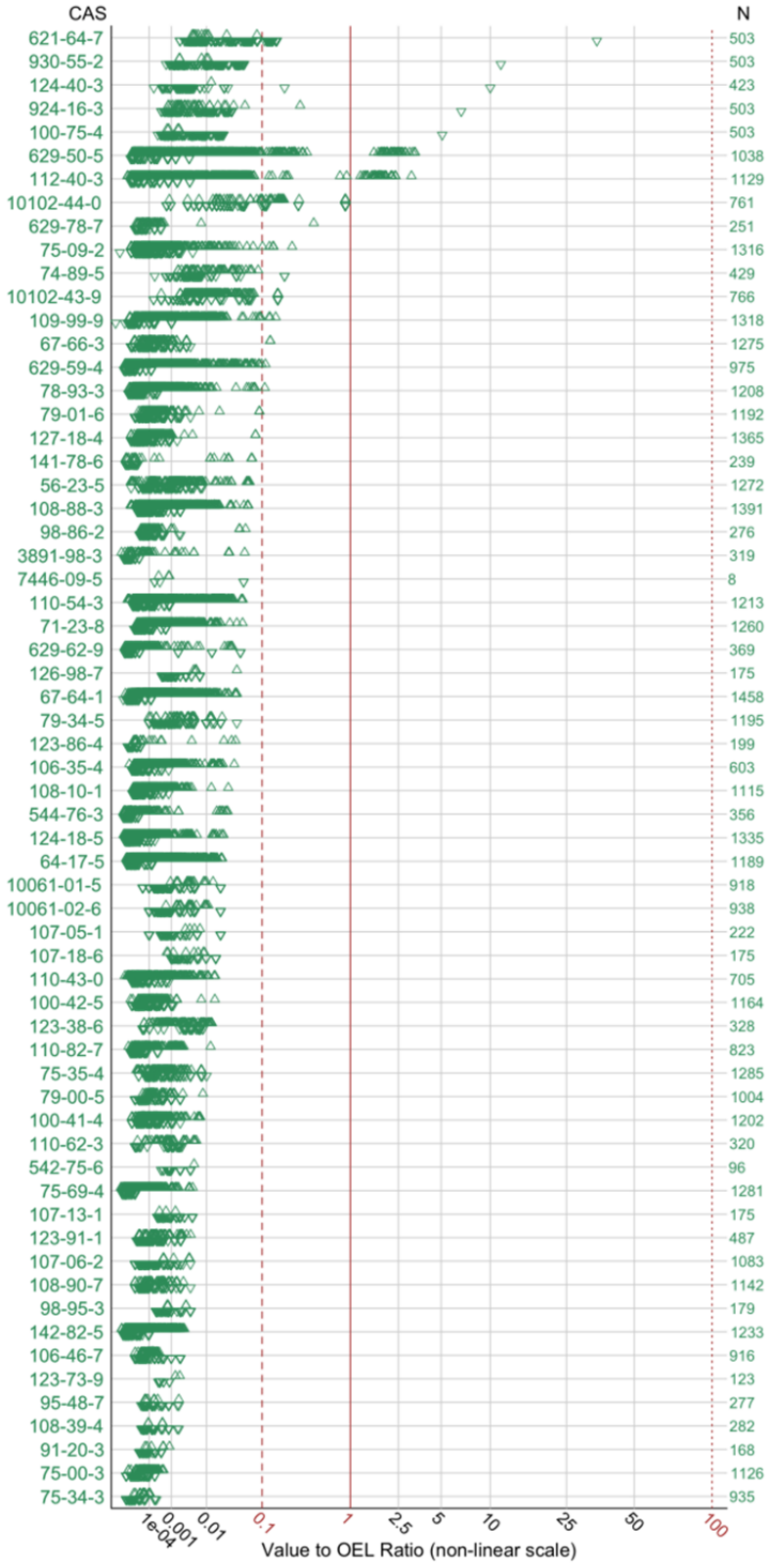

Figure 6.2. Filtered non-COPC:OEL ratios from TWINS industrial health samples and TWINS and SWIHD headspace samples. CAS IDs and chemical names are given in Table B.2

6.2.1 Tank Signature Investigation

In order to distinguish the source vapors (tank source vs. non-tank source), signatures of tank vapors, i.e., vectors of distinguishing chemical concentrations, must be identified. Available headspace samples were indexed and their chemical constituents were displayed in a signature format as a sample-by-chemical matrix (~5000 samples by ~1400 chemical identifications) in Figure 6.3. Color coding was used to represent chemicals with no report (yellow), a report of less than MDL (orange), or a report of a true detected result (brown). The goal of showing the matrix in Figure 6.3 was to illustrate that there are no consistent records of analysis (yellow coloring) for most chemicals throughout the years of analysis. The matrix was organized so that chemicals with the most records are shown on the left with the number of records decreasing toward the right. This allowed the matrix to be broken into smaller pieces of approximately 1200 samples and 80 chemicals per section. Figure 6.4 focuses on the top right corner of Figure 6.3. A list of CAS numbers and chemical names in the same order as shown on the x-axis is given in Table B.3 in Appendix B. Non-COPC chemicals have been italicized and comprise a majority of the list.

Nitrous oxide, hydrogen, ammonia and a number of VOCs are all characteristic chemicals from tanks identified in Table B.3, though none are unique to tank sources. An evaluation of the headspace dataset, including TWINS and SWIHD, for potential tank markers found that of the samples reporting ammonia analysis, ammonia was positively detected in approximately 86% of the samples and less than MDL reported for the remaining samples. Percentages of positive detection, greater than MDL, for nitrous oxide (62%) and hydrogen (76%) in the reported samples were lower than that for ammonia. Other chemicals with high percentages of positive detects, when the analysis was reported, include acetone (90%), trichlorofluoromethane (88%), and 1-butanol (88%). In non-headspace samples, the percentage of positive detects from reported samples decreases to approximately 40 – 60% for each of these chemicals. Contributions from tanks and from non-tank sources may need to be identified in terms of multiple marker species and relative concentrations. A more detailed multivariate statistical approach, such as factor analysis, would be necessary to identify tank signatures, but has not been completed at this time.

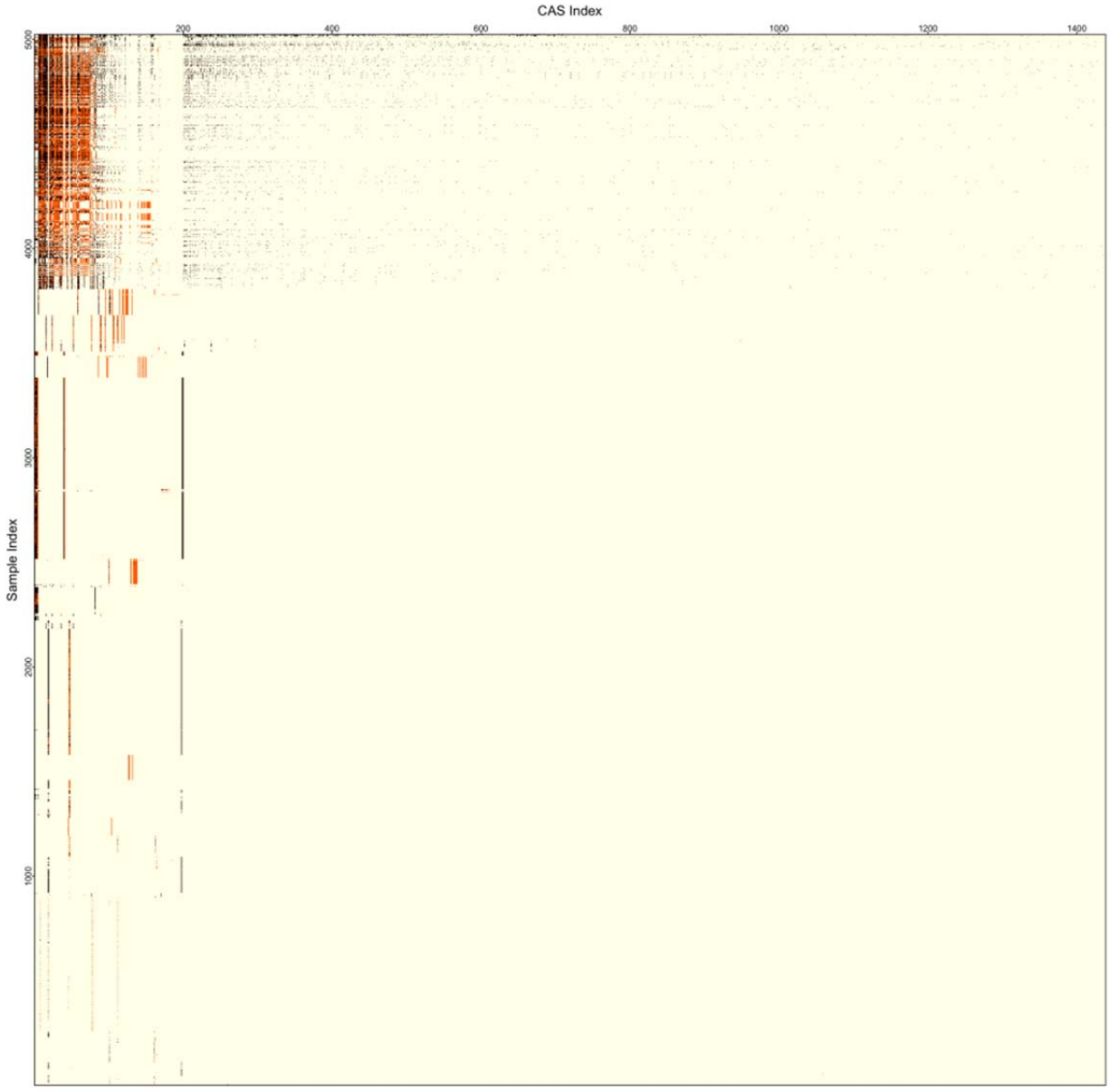

Figure 6.3. Indexed headspace samples and chemical analysis report matrix

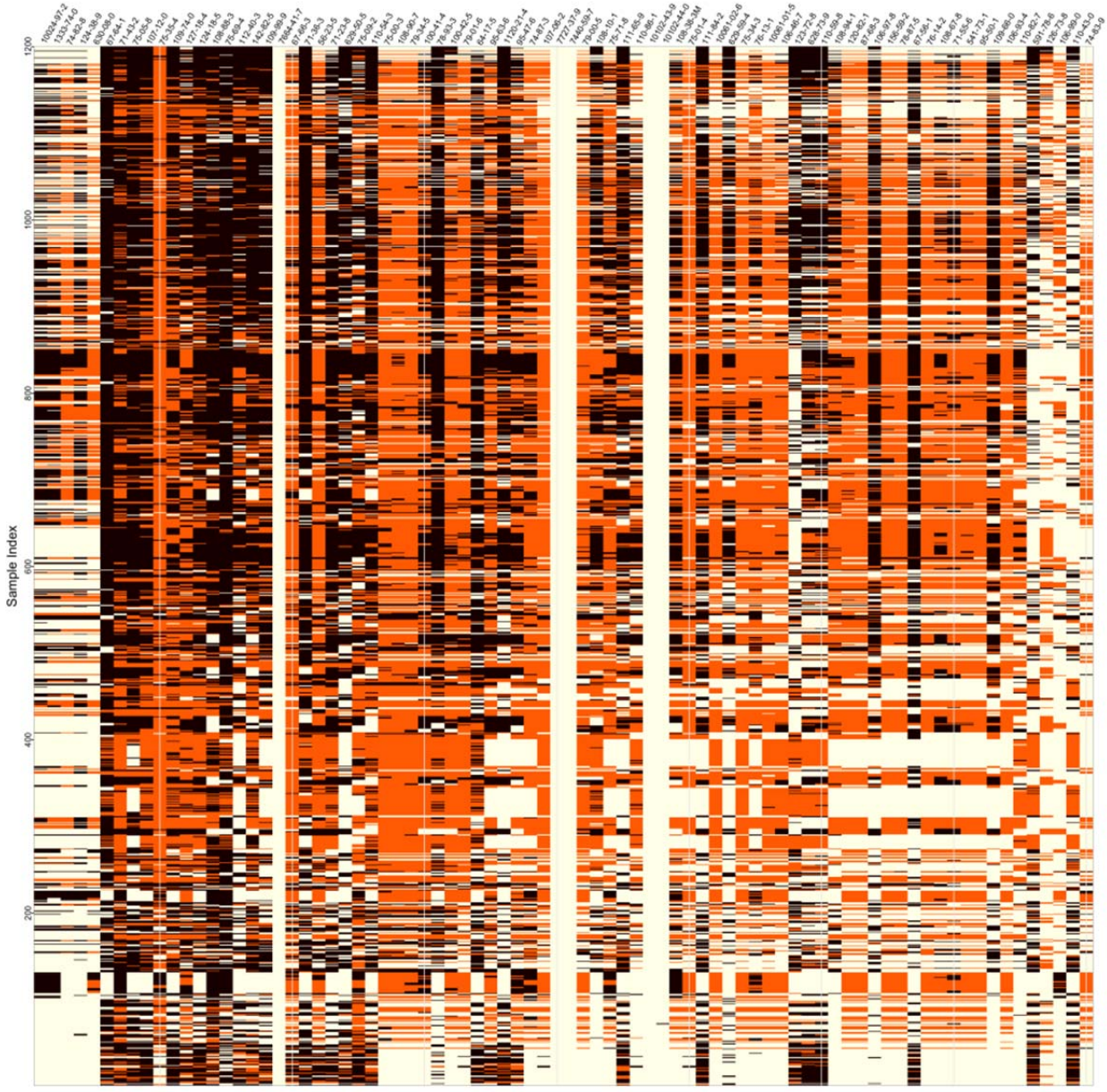

Figure 6.4. Insert from top-left region of the indexed headspace samples and chemical analysis report matrix in Figure 6.3

6.2.1.1 Potential Non-Tank Sources

Non-tank sources fall into the categories of combustion sources (vehicles, generators, controlled burns, wildfires, etc.), use of solvents and fuels for local work, and biogenic sources (local vegetation and animal wastes). A quick review of literature suggests that many articles specialize only in emissions of organics, criteria pollutants such as CO and nitrogen oxides, or greenhouses gases such as N_2O, so data from different sources will need to be combined. Both organic and non-organic marker species would need to be examined to find out what distinction can be made between non-tank sources and tank waste gases. The Environmental Protection Agency (EPA) database SPECIATE may provide valuable

information in this regard, but has not at this time been assessed to determine how many of the species of interest it contains.

Combustion sources

In general, combustion sources are distinguished by high production of carbon monoxide relative to methane and other VOC species. Simultaneous measurement of carbon monoxide and VOC might provide evidence of the significance of combustion products in a given air sample. However, there is great variability in the quantity and speciation of organics from combustion. A high ratio of CO to organics probably would not exclude the possibility of there being tank contributions to any particular chemical.

In addition, there is some potential for ambiguity in using CO as a combustion marker, because there is some evidence for CO production in the waste. Carbon monoxide was seen in gas generated by tests on simulated AN-107 waste (Bryan et al. 2004), although CO was not recorded in retained gas samples from actual waste (Mahoney et al. 1999). The CO/hydrocarbon ratios in tank headspaces would need to be determined to find out how they compare to combustion sources.

Much the same can be said for NO and NO_2. They are combustion markers, but they have been observed in many waste gas generation tests (Bryan et al. 2004) and also in retained gas samples (Mahoney et al. 1999).

One recent study (Kota et al. 2014) identified contributions from several broad source categories by using 18 volatile organic species; the study found that toluene and isomers of xylene were the most distinctive markers for tailpipe emissions. However, the organic speciation of tailpipe emissions depends on the type of vehicle, the mode in which it is operating (cold-startup versus fully warmed-up), and the age of the vehicle. Pang et al (2014) show the fleet-average tailpipe emissions for California vehicles from 1995 to 2003. There is substantial variation over the period, but toluene, ethene, trimethylpentane and isopentane stand out as high-percentage constituents in all years. All of these except ethene have been measured in tank headspace samples.

There is some information for speciation of emissions from open burning, as in natural cover fires and controlled agricultural burns (Lemieux et al 2004). Emissions of oxygenated compounds – methanol, 2,3-butanedione, acetaldehyde, acetone, formaldehyde, and methyl ethyl ketone are prominent. Furans, furfural, benzene, toluene, and xylene are also often substantial components. Again, many of these compounds have been measured in tank headspaces.

Solvents and fuels

Kota et al (2014) considered n-butane and isobutane to be markers for consumer and commercial solvent use because butane is used as an aerosol propellant. In their study, vehicle fuel evaporation was marked by isopentane (2-methylbutane). Methyl ethyl ketone was identified as an oxidation product of both n-butane and isopentane. Solvent use in the tank farms area would probably have a very limited and local effect on air samples.

Biogenic emissions

In the tank farms area, local vegetation may be a larger and more persistent contributor than any animal waste. Kota et al. (2014) found that isoprene (2-methyl-1,3-butadiene) was a strong marker for vegetation emissions, with methyl vinyl ketone and 2-methylprop-2-enal (methacrolein) being oxidation products of isoprene. Kesselmeier and Staudt (1999) note that the VOC emissions of vegetation often have lifetimes in the minutes to hours range – for example, isoprene has a lifetime of 3 hours in daytime and 1.5 hours at night – so oxidation products must be considered. Concentrations of isoprene in the atmosphere are given as being in the range of ppt (thousands of ppm) to several ppb, so they may not necessarily be a small part of VOC measured in air samples outside the tank. Kesselmeier and Staudt list many other alkanes, alkenes, organic acids, aldehydes, ketones, etc. that are emitted by plants. Where the authors give background concentrations for these compounds, the concentrations are sub-ppm.

Emissions from cattle wastes (Sun et al 2008) were found to contain methane, methanol, ethanol, ammonia, and volatile fatty acids (acetic and butyric acid were mentioned). Human wastes – as from local portable restrooms – would certainly contain many of these compounds as well.

6.2.2 Leading Indicator Evaluation

The focus of the recent analysis was to evaluate the use of ammonia and nitrous oxide as leading indicators for the other COPCs and to identify other potential leading indicators from the available data. The fifteen COPCs listed in Table 6.5 were found to have fewer than 10 measurements in the filtered database of headspace samples from TWINS and SWIHD and were not included in the following discussion. Additionally, a specific chlorinated biphenyl was not chosen to be included in this analysis at this time.

Table 6.5. COPCs with fewer than 10 measurements in the filtered headspace database

COPC #	CAS ID	Chemical Name
24	1703-52-2	Furan, 2-ethyl-5-methyl-
25	34379-54-9	Furan, 2,3-dihydro-4-(1-methylpropyl)-, (S)-
59	624-83-9	Methyl isocyanate
30	4179-38-8	Furan, 2-octyl-
32	51595-87-0	2-Heptanone, 6-(2-furanyl)-6-methyl-
31	717-21-5	2-Propen-1-one, 3-(2-furanyl)-1-phenyl-
26	34314-82-4	Furan, 3-(1,1-dimethylethyl)-2,3-dihydro-
50	1184-60-7	2-fluoro-1-Propene
56	3457-91-8	1,4-Butanediol, dinitrate
10	814-78-8	3-Buten-2-one, 3-methyl-
17	1115-11-3	2-Butenal, 2-methyl-
18	645-62-5	2-Hexenal, 2-ethyl-
58	623-87-0	1,3-dinitrate-1,2,3-Propanetriol
40	1647-11-6	Butanenitrile, 2-methylene-
41	1615-70-9	2,4-Pentadienenitrile

The basis of a leading indicator evaluation is a collection of sampled chemical signatures, i.e., a set of vectors of co-measured chemical concentrations. Historically, samples were drawn and the results recorded in the databases for only specific chemical analyses such as VOC or semi-VOC so that a complete chemical signature of the sampling event was not clearly identified. Therefore, a complete chemical signature of a sampling event was estimated by aggregating results from specific samples tagged with a specific location and time period. Here, a sampling event included all samples from a specific tank drawn between midnight to midnight due to limitations in the structure of the database. For many sampling events, concentrations of chemicals were measured more than once for a given source, day, and time. Multiple measurements, above MDL, were reduced to a single concentration by calculating a geometric mean for the concentration of a chemical at a particular combination of source, day, and time range (where available). Measurements at MDL were not used in calculations of the geometric mean.

The pairwise co-occurrence of chemicals within sampling event signatures were noted and Table 6.6 shows the identified pairings for ammonia with the other COPCs. Forty-two of the COPCs were identified with ammonia in sampling event signatures. Of those, 10 were found to have less than 10 paired data points; further analysis was not completed for those COPCs at this time. Table 6.7 shows the identified pairings for nitrous oxide. Forty-one of the COPCs were identified with nitrous oxide in sampling event signatures. Of those, 15 were found to have less than 10 paired data points; further analysis was not completed for those COPCs at this time.

A review of the relationship between a COPC and a potential LI includes a visualization of the available concentration measurements. Figure 6.5 shows a scatterplot of the filtered results of N-nitrosodimethylamine versus ammonia. These paired results have been separated into three categories. Red dots indicate where both the COPC and corresponding LI (ammonia in this example) were measured. Blue dots indicate one of two categories: one was measured and the other recorded as below MDL, or one was measured but the other was not recorded (or possibly not measured). The blue points represent missed opportunities for paired results. An estimate of the bivariate lognormal probability density over the paired results, not including <MDL measurements, is represented by a cloud of semi-transparent grey points. This plot is divided into four regions by the LI and COPC 10% OEL alert thresholds. These regions correspond to true non-alerts (green region), missed alerts (red), true alerts (blue), and false alerts (yellow) for the given LI and COPC. The detailed description of these regions can be found in Section 4.0. The proportions of the bivariate probability distribution in each region are estimates of the probabilities of a true non-alert, missed alert, true alert, and false alert. These proportions are listed in the extreme corners of the four regions. Scatterplots of all of the pairings for ammonia and nitrous oxide are shown in Appendix C. Figure 6.5 is an example where there is limited data below the LI alert line, making it hard to say the proportion of missed alerts and true non-alerts might change if there were more data at low LI concentration. The missed-opportunities (i.e., high COPC concentration at unspecified or <MDL LI concentration) suggest that this could be an important gap.

In addition to the scatterplot, a receiver operating characteristic (ROC)-like curve is a useful tool to review the LI-COPC relationship. This ROC-like curve displays the change, or trade-off, between the missed alert rate and true non-alert rate (or the false alert rate = 1 – true non-alert rate) as the LI alert level increases. A quicker rising ROC-like curve indicates better statistical performance, so given 2 ROC-like curves, the higher curve indicates the better performing leading indicator. The ROC-like curve results from fixing the COPC alert level at 10% OEL to partition the space into COPC-above-OEL and COPC-below-OEL regions. Then estimating and plotting the paired conditional probabilities, calculated from the logNormal estimate, of a true non-alert given the COPC-below-OEL region and missed alert COPC-

above-OEL region as the LI alert level increases from 0. For example, we, in essence, generate the ROC-like curve describing the statistical performance of ammonia as a leading indicator of nitrosodimethylamine by computing and plotting the proportions of points above and below the COPC alert level to the left of the vertical bar denoting the LI alert level from Figure 6.5 as it moves from left to right). The area under the ROC-like curve (AUC) is a scalar measure of the strength of the LI as an indicator of COPC level. Consequently, the LI with the higher AUC is a relatively better LI than one with a lower AUC. The ROC-like curve for N-nitrosodimethylamine and ammonia is shown in Figure 6.6. ROC-like curve plots for all of the pairings for ammonia and nitrous oxide are shown in Appendix C. As mentioned in the discussion of the scatterplot, the limited data below the LI alert line could result in a change in the ROC-like curve as more data becomes available.

Table 6.6. Evaluation of ammonia as a potential leading indicator

COPC:	**Ammonia**	**Data Set:**	TWINS headspace & industrial health download – June 20, 2016 SWIHD headspace download – July 12, 2016		
COPC ID #	**COPC**	**Pairing Observed?**	**Pairing Count[a]**	**Relationship Observed?**	**Continue Statistical Analysis?**
1	Ammonia	yes	431	yes	no, self-pairing
2	Nitrous oxide	yes	144	yes	yes
3	Mercury	yes	135	yes	yes
4	1,3-Butadiene	yes	40	yes	yes
5	Benzene	yes	139	yes	yes
6	Biphenyl	yes	11	yes	yes
7	1-Butanol	yes	263	yes	yes
8	Methanol	yes	96	yes	yes
9	2-Hexanone	yes	125	yes	yes
10	3-Methyl-3-butene-2-one	no, less than 10 measurements			
11	4-Methyl-2-hexanone	yes	5	no, less than 10 pairings available	
12	6-Methyl-2-heptanone	yes	32	yes	yes
13	3-Buten-2-one	yes	68	yes	yes
14	Formaldehyde	yes	145	yes	yes
15	Acetaldehyde	yes	83	yes	yes
16	Butanal	yes	189	yes	yes
17	2-Methyl-2-butenal	no, less than 10 measurements			
18	2-Ethyl-hex-2-enal	no, less than 10 measurements			
19	Furan	yes	53	yes	yes
20	2,3-Dihydrofuran	yes	13	yes	yes
21	2,5-Dihydrofuran	yes	4	no, less than 10 pairings available	
22	2-Methylfuran	yes	1	no, less than 10 pairings available	
23	2,5-Dimethylfuran	yes	1	no, less than 10 pairings available	
24	2-Ethyl-5-methylfuran	no, less than 10 measurements			
25	4-(1-Methylpropyl)-2,3-dihydrofuran	no, less than 10 measurements			
26	3-(1,1-Dimethylethyl)-2,3-dihydrofuran	no, less than 10 measurements			
27	2-Pentylfuran	yes	3	no, less than 10 pairings available	
28	2-Heptylfuran	yes	2	no, less than 10 pairings available	
29	2-Propylfuran	yes	2	no, less than 10 pairings available	

COPC:	Ammonia	Data Set:	TWINS headspace & industrial health download – June 20, 2016 SWIHD headspace download – July 12, 2016		
COPC ID #	**COPC**	**Pairing Observed?**	**Pairing Count[a]**	**Relationship Observed?**	**Continue Statistical Analysis?**
30	2-Octylfuran	no, less than 10 measurements			
31	2-(3-Oxo-3-phenylprop-1-enyl)furan	no, less than 10 measurements			
32	2-(2-Methyl-6-oxoheptyl)furan	no, less than 10 measurements			
33	Diethylphthalate	yes	39	yes	yes
34	Acetonitrile	yes	254	yes	yes
35	Propanenitrile	yes	150	yes	yes
36	Butanenitrile	yes	142	yes	yes
37	Pentanenitrile	yes	119	yes	yes
38	Hexanenitrile	yes	114	yes	yes
39	Heptanenitrile	yes	64	yes	yes
40	2-Methylene butanenitrile	no, less than 10 measurements			
41	2,4-Pentadienenitrile	no, less than 10 measurements			
42	Ethylamine	yes	17	yes	yes
43	N-Nitrosodimethylamine	yes	197	yes	yes
44	N-Nitrosodiethylamine	yes	11	yes	yes
45	N-Nitrosomethylethylamine	yes	55	yes	yes
46	N-Nitrosomorpholine	yes	41	yes	yes
47	Tributylphosphate	yes	25	yes	yes
48	Dibutylbutylphosphonate	yes	8	no, less than 10 pairings available	
49	Chlorinated biphenyls	not completed in this analysis			
50	2-Fluoropropene	no, less than 10 measurements			
51	Pyridine	yes	95	yes	yes
52	2,4-Dimethylpyridine	yes	6	no, less than 10 pairings available	
53	Methyl nitrite	yes	12	yes	yes
54	Butyl nitrite	yes	5	no, less than 10 pairings available	
55	Butyl nitrate	yes	22	yes	yes
56	1,4-Butanediol, dinitrate	no, less than 10 measurements			
57	2-Nitro-2-methylpropane	yes	23	yes	yes
58	1,2,3-Propanetriol, 1,3-dinitrate	no, less than 10 measurements			
59	Methyl Isocyanate	no, less than 10 measurements			

a. only measurements above MDL were included in the pairing count

Table 6.7. Evaluation of nitrous oxide as a potential leading indicator

COPC:	**Nitrous Oxide**	**Data Set:**	TWINS headspace & industrial health download – June 20, 2016 SWIHD headspace download – July 12, 2016		
COPC ID #	**COPC**	**Pairing Observed?**	**Pairing[a] Count**	**Relationship Observed?**	**Continue Statistical Analysis?**
1	Ammonia	yes	144	yes	yes
2	Nitrous oxide	yes	533	yes	no, self-pairing
3	Mercury	yes	37	yes	yes
4	1,3-Butadiene	yes	26	yes	yes
5	Benzene	yes	126	yes	yes
6	Biphenyl	yes	9	no, less than 10 pairings available	
7	1-Butanol	yes	174	yes	yes
8	Methanol	yes	119	yes	yes
9	2-Hexanone	yes	111	yes	yes
10	3-Methyl-3-butene-2-one	no, less than 10 measurements			
11	4-Methyl-2-hexanone	yes	4	no, less than 10 pairings available	
12	6-Methyl-2-heptanone	yes	34	yes	yes
13	3-Buten-2-one	yes	27	yes	yes
14	Formaldehyde	yes	33	yes	yes
15	Acetaldehyde	yes	67	yes	yes
16	Butanal	yes	127	yes	yes
17	2-Methyl-2-butenal	no, less than 10 measurements			
18	2-Ethyl-hex-2-enal	no, less than 10 measurements			
19	Furan	yes	42	yes	yes
20	2,3-Dihydrofuran	yes	6	no, less than 10 pairings available	
21	2,5-Dihydrofuran	yes	5	no, less than 10 pairings available	
22	2-Methylfuran	yes	2	no, less than 10 pairings available	
23	2,5-Dimethylfuran	yes	1	no, less than 10 pairings available	
24	2-Ethyl-5-methylfuran	no, less than 10 measurements			
25	4-(1-Methylpropyl)-2,3-dihydrofuran	no, less than 10 measurements			
26	3-(1,1-Dimethylethyl)-2,3-dihydrofuran	no, less than 10 measurements			
27	2-Pentylfuran	no	0	no, less than 10 pairings available	
28	2-Heptylfuran	yes	1	no, less than 10 pairings available	

COPC:	Nitrous Oxide	Data Set:	TWINS headspace & industrial health download – June 20, 2016 SWIHD headspace download – July 12, 2016		
COPC ID #	**COPC**	**Pairing Observed?**	**Pairing[a] Count**	**Relationship Observed?**	**Continue Statistical Analysis?**
29	2-Propylfuran	yes	1	no, less than 10 pairings available	
30	2-Octylfuran	no, less than 10 measurements			
31	2-(3-Oxo-3-phenylprop-1-enyl)furan	no, less than 10 measurements			
32	2-(2-Methyl-6-oxoheptyl)furan	no, less than 10 measurements			
33	Diethylphthalate	yes	12	yes	yes
34	Acetonitrile	yes	160	yes	yes
35	Propanenitrile	yes	135	yes	yes
36	Butanenitrile	yes	127	yes	yes
37	Pentanenitrile	yes	106	yes	yes
38	Hexanenitrile	yes	109	yes	yes
39	Heptanenitrile	yes	77	yes	yes
40	2-Methylene butanenitrile	no, less than 10 measurements			
41	2,4-Pentadienenitrile	no, less than 10 measurements			
42	Ethylamine	yes	1	no, less than 10 pairings available	
43	N-Nitrosodimethylamine	yes	55	yes	yes
44	N-Nitrosodiethylamine	yes	3	no, less than 10 pairings available	
45	N-Nitrosomethylethylamine	yes	8	no, less than 10 pairings available	
46	N-Nitrosomorpholine	yes	10	yes	yes
47	Tributylphosphate	yes	21	yes	yes
48	Dibutylbutylphosphonate	yes	6	no, less than 10 pairings available	
49	Chlorinated biphenyls	not completed in this analysis			
50	2-Fluoropropene	no, less than 10 measurements			
51	Pyridine	yes	53	yes	yes
52	2,4-Dimethylpyridine	yes	4	no, less than 10 pairings available	
53	Methyl nitrite	yes	14	yes	yes
54	Butyl nitrite	yes	5	no, less than 10 pairings available	
55	Butyl nitrate	yes	31	yes	yes
56	1,4-Butanediol, dinitrate	no, less than 10 measurements			
57	2-Nitro-2-methylpropane	yes	30	yes	yes
58	1,2,3-Propanetriol, 1,3-dinitrate	no, less than 10 measurements			
59	Methyl Isocyanate	no, less than 10 measurements			

a. only measurements above MDL were included in the pairing count

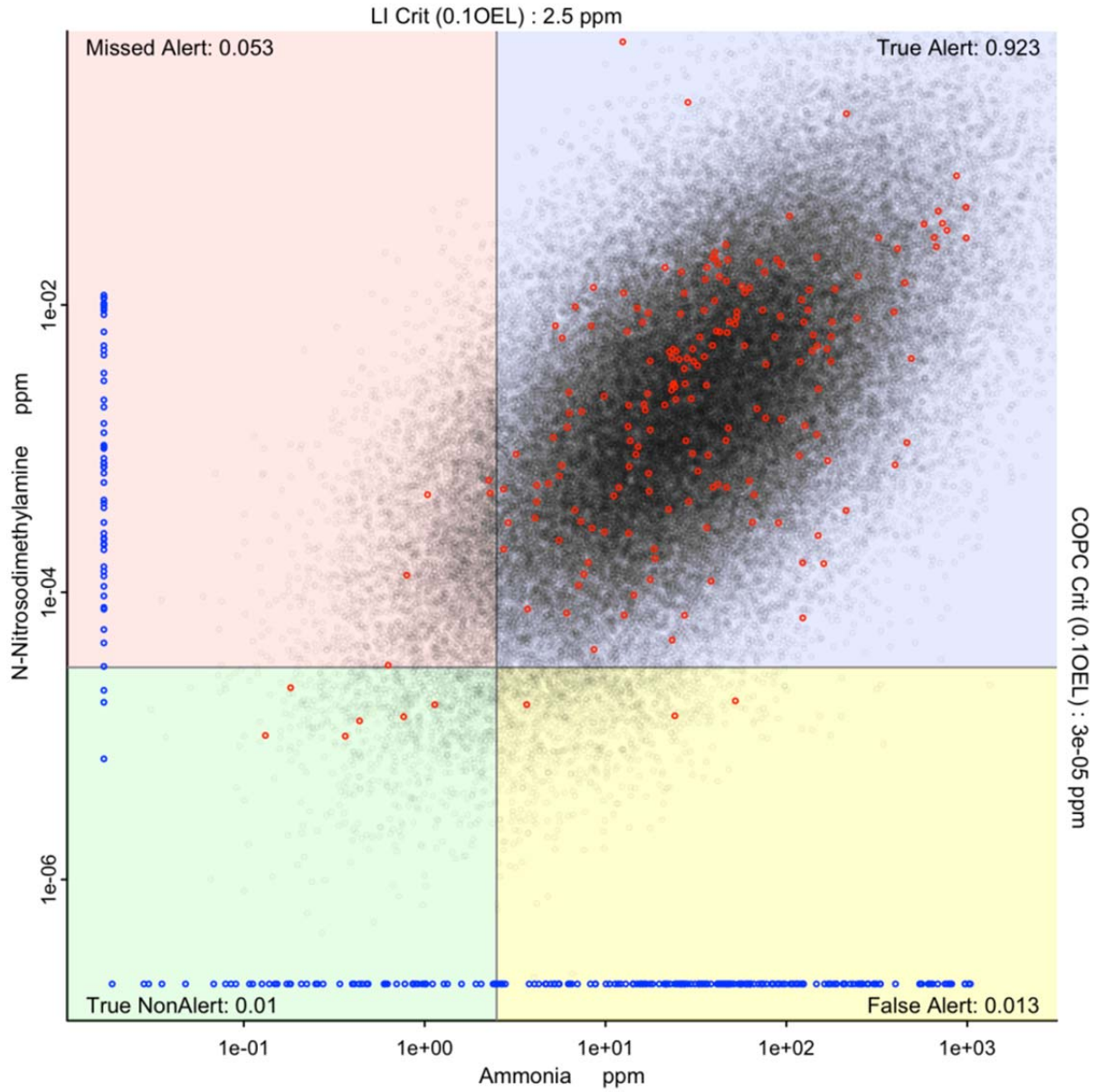

Figure 6.5. Scatterplot of N-nitrosodimethylamine and ammonia measurements (red dots), simulated points from the bivariate logNormal density estimate (transparent grey dots), and non-paired or MDL measurements (blue dots) with associated alert quadrants designated by 10% OEL indication lines for each chemical

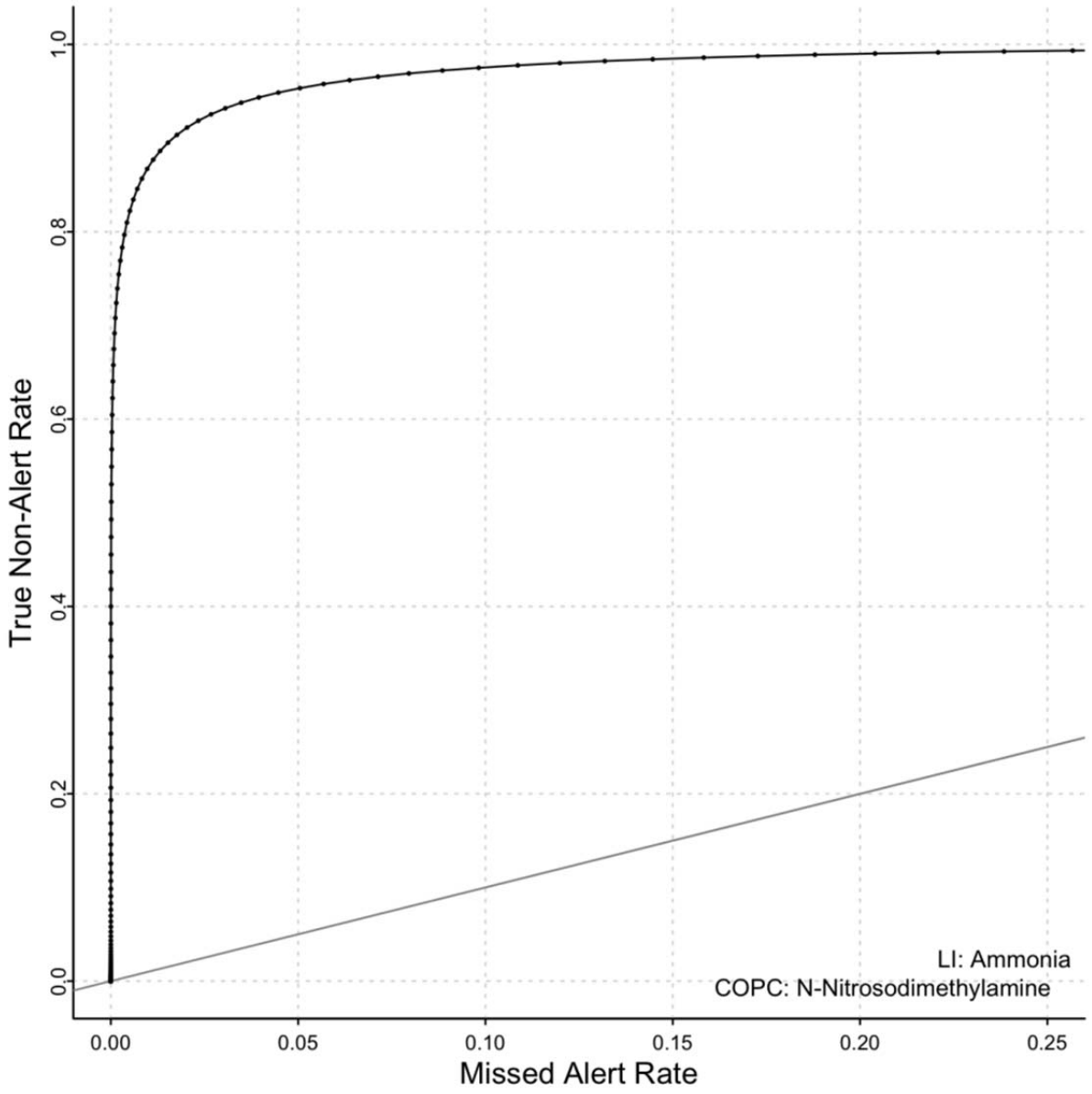

Figure 6.6. The ROC-like curve displays the change in statistical performance as a function of increasing LI alert level when using ammonia as a leading indicator for N-nitrosodimethylamine.

6.2.3 Summary of Evaluation

Overall, the available pairings indicate that both ammonia and nitrous are strong candidates as LIs. Ammonia had pairings with 32 of the COPCs and nitrous oxide had pairing with 29 of the COPCs. The remaining COPCs did not have enough measurements to observe a pairing or relationship. The general trend for pairings with ammonia and nitrous oxide is that the majority of the paired data points fall above the 10% OEL level of the LI meaning that an alert on the LI would bound alerts for the COPC.

This distribution of data points results in low populations within the missed alert and true non-alert quadrants. Measured COPC concentrations can vary over a couple orders of magnitude for a particular LI concentration. Additional paired results with measured LI concentration below the 10% OEL would give greater confidence in the probability distribution within the missed alert quadrant.

6.3 Computational Modeling Approaches

Modeling approaches are used across the site for verification purposes and predictive capabilities. It was thought that the use of computational fluid dynamics (CFD) simulations could provide additional verification as LIs are selected. In order to test this capability, a small dataset from smaller bench-scale experiments was modeled. A series of vapor release tests had been completed on January 21, 2016, at the west side of building 3430 and north side of building 3820 on the Pacific Northwest National Laboratory (PNNL) campus in Richland, WA. Ammonia (NH_3) and isobutylene (C_4H_8) were released. Ammonia was chosen because it is common to the tank farms in high levels (> 1ppm) and is commonly used as an indication of a chemical plume. Isobutylene was chosen as an inert surrogate for VOCs which are also common to the tank farms in high levels and used as tracer for chemical plumes in the tank farms.

Several sensors were located near the releasing point and recorded the concentration evolutions. A CFD simulation to mimic the bench-scale experiments was completed in commercial off-the-shelf CFD software STAR-CCM+®. STAR-CCM+ is a finite-volume-based multi-physics and complex geometries solver. It integrates the full procedure of CFD simulation, including mesh generation, physical problem solving, post-processing, and visualization.

6.3.1 Governing Equations

The transient pressure-velocity segregated solver was used to solve the mass and momentum conservation equations [Eqs. (1) and (2)]. The transient passive scalar model was used to solve the chemical species transport equation [Eq. (3)].

$$\frac{\partial \rho}{\partial t} + \frac{\partial}{\partial x_i}(\rho u_i) = \sum_{n=1}^{N} R_n \tag{1}$$

$$\frac{\partial \rho u_i}{\partial t} + \frac{\partial}{\partial x_j}\left(\rho u_j u_i\right) = \frac{\partial P}{\partial x_i} + \frac{\partial \tau_{ij}}{\partial x_j} + f_i + \rho g_i \tag{2}$$

$$\frac{\partial X_n}{\partial t} + \frac{\partial}{\partial x_i}(u_i X_n) = \frac{\partial}{\partial x_i}\left(D_n \frac{\partial X_n}{\partial x_i}\right) + \frac{R_n}{\rho} \tag{3}$$

where ρ is density, u_i is velocity, R_n is gas source/sink term, τ is stress, f_i is external force, P is pressure, g_i is gravity acceleration, D_n is diffusion coefficient, and X_n is gas component weight fraction. Reynolds-averaged Navier-Stokes equation with k-epsilon model was used for dealing with turbulence phenomena. The diffusivity D is modeled into two parts: molecular diffusivity and eddy diffusivity as:

$$D = D_m + D_e \tag{4}$$

where D_m is the molecular diffusivity, and D_e is the eddy diffusivity, which is assumed as $D_e = Sc_t \nu_t$. Sc_t is the turbulent Schmidt number, and ν_t is the eddy/turbulence viscosity in units of m^2/s.

6.3.2 Simulation domain and mesh

Figure 6.7(a) shows a satellite picture from Google Maps for the bench-scale test area. Because the satellite was not updated recently, a new building (3820) is missing, so a PNNL internal buildings map is shown in Figure 6.7(b). The red dot on the map is the approximate location of releasing point.

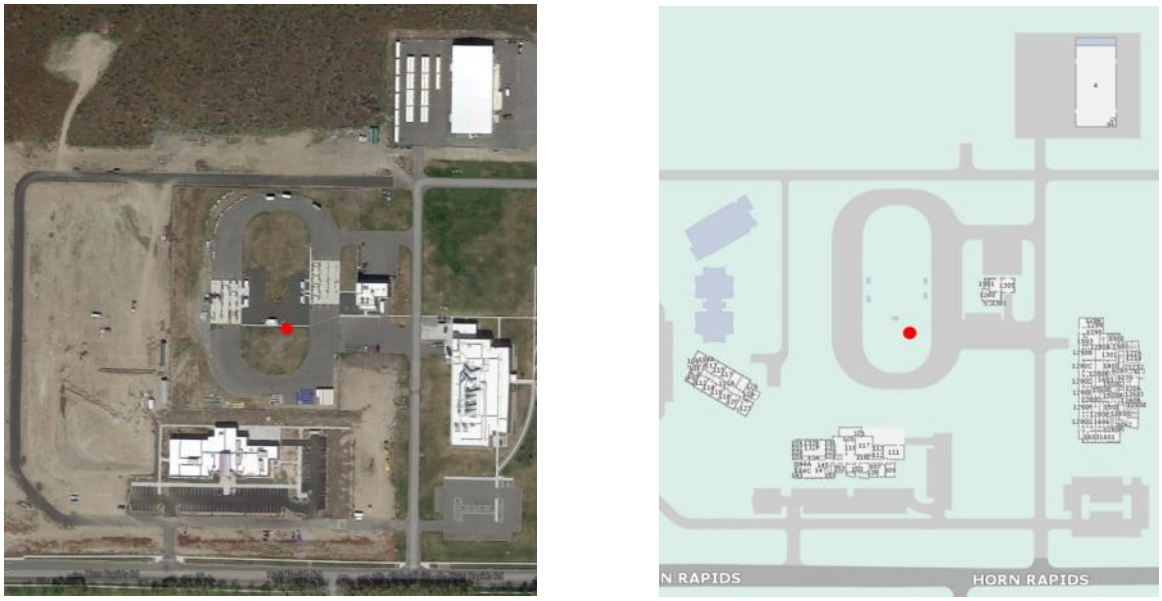

(a) (b)

Figure 6.7. (a) Satellite picture and (b) PNNL internal buildings map for the bench-scale test area. Red dot is the approximate location of releasing point.

The simulation used 1.36 million polyhedral mesh cells. The domain was 490 × 490 × 50 m, and five main buildings were modeled: 3850, 3820, 3430, 3440, and LSW. Figure 6.8 shows the three-dimensional domain (a), the top view of the mesh (b), and the enlarged area around the releasing source (c). The building surfaces were refined with 1 m mesh, the source surface was refined with 0.025 m mesh, and the domain around the releasing source was refined with 0.5 m mesh.

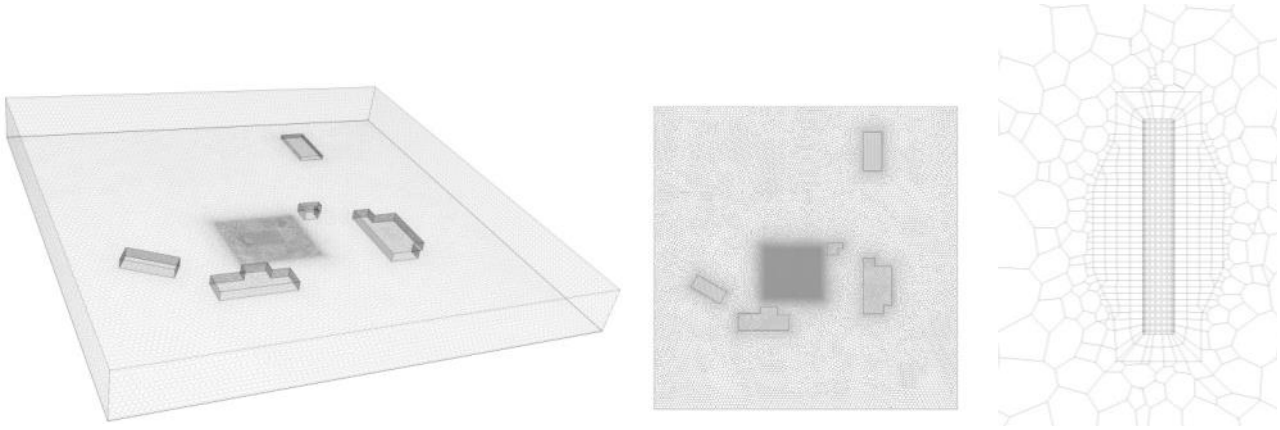

(a) (b) (c)

Figure 6.8. Mesh of the simulation domain

6.3.3 CFD Results

During the bench-scale experiment on January 21, 2016, 14:00 to 16:00, the wind was from the northwest with a velocity of 2.95 m/s. The wind direction was between south-southeast and south (28° counterclockwise from the south). Therefore, the north and west boundaries were set to velocity inlet with $u_x = 1.385\ m/s$ and $u_y = -2.605\ m/s$. The positive directions are north for x-axis, and east for y-axis. The south, east, and top boundaries were set to pressure outlet. Ten hours solution time was used to spin up the flow field to get a quasi-steady velocity profile. Figure 6.9 shows the velocity magnitude on the cross section 1.0 m from the ground, with blue representing slower velocities and red indicating faster velocities.

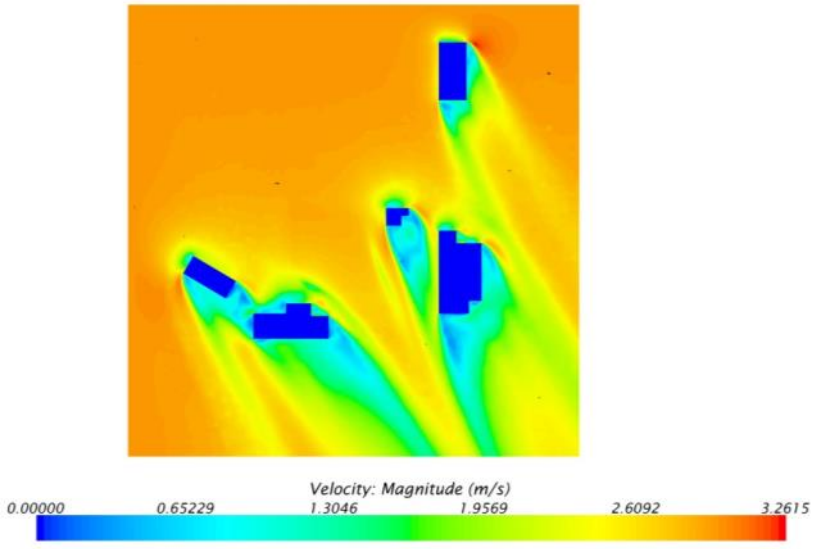

Figure 6.9. Velocity magnitude on the cross section 1.0 m from the ground

After 10 hours (36000 seconds) solution time spin up, NH_3 and C_4H_8 were released; the releasing rate is shown in Figure 6.10. The releasing simulation started from 36000 seconds. The entire gas release simulation period was divided in to four time period regions, marked as I, II, III, and IV. In region I (36000 to 36900 seconds), both NH_3 and C_4H_8 were released at the desired rate (0.058 g/s for NH_3, and 0.191 g/s for C_4H_8). The release rate for C_4H_8 linearly dropped[1] from 0.191 to 0.05 g/s in region II (36900 to 37500 seconds), while NH_3 release remained at 0.058 g/s. In region III (37500 to 37800 second), the release of C_4H_8 concluded while NH_3 continued at 0.058 g/s. Neither gas was released in region IV (37800 to 39000 second).

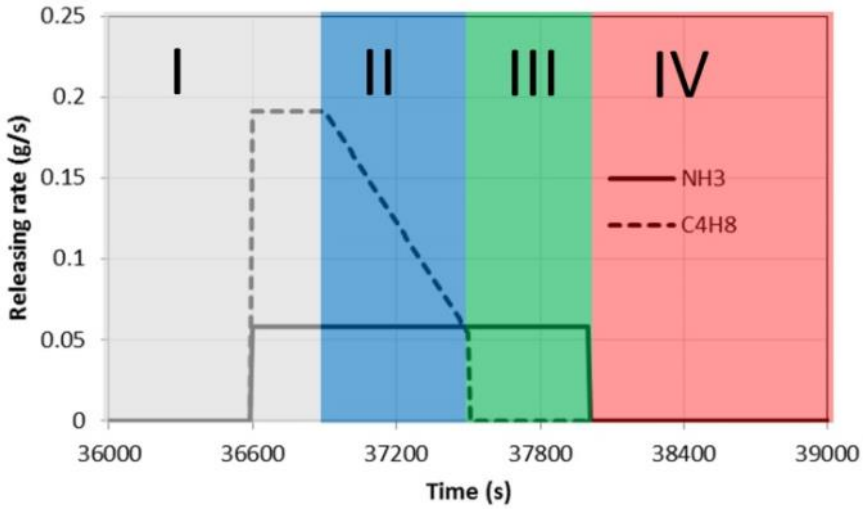

Figure 6.10. Releasing rate of NH_3 and C_4H_8

Figure 6.11 shows the plume cross section 1.0 m from the ground at 36901 and 37501 seconds for NH_3 (a and c) and C_4H_8 (b and d). There are 160 monitoring points around the releasing source in the simulation as the small dots shown in Figure 6.11. Eleven sensors operated during the experiments and locations are indicated in Figure 6.12. Figure 6.13 shows the simulated concentration evolution on these 11 points. The small oscillation of the concentration is caused by the low frequency and large-scale flow vortexes.

[1] The cylinder of C_4H_8 gas ran out of gas during the experiment (region III) and was ultimately shut off when the flow rate was unsustainable (region IV).

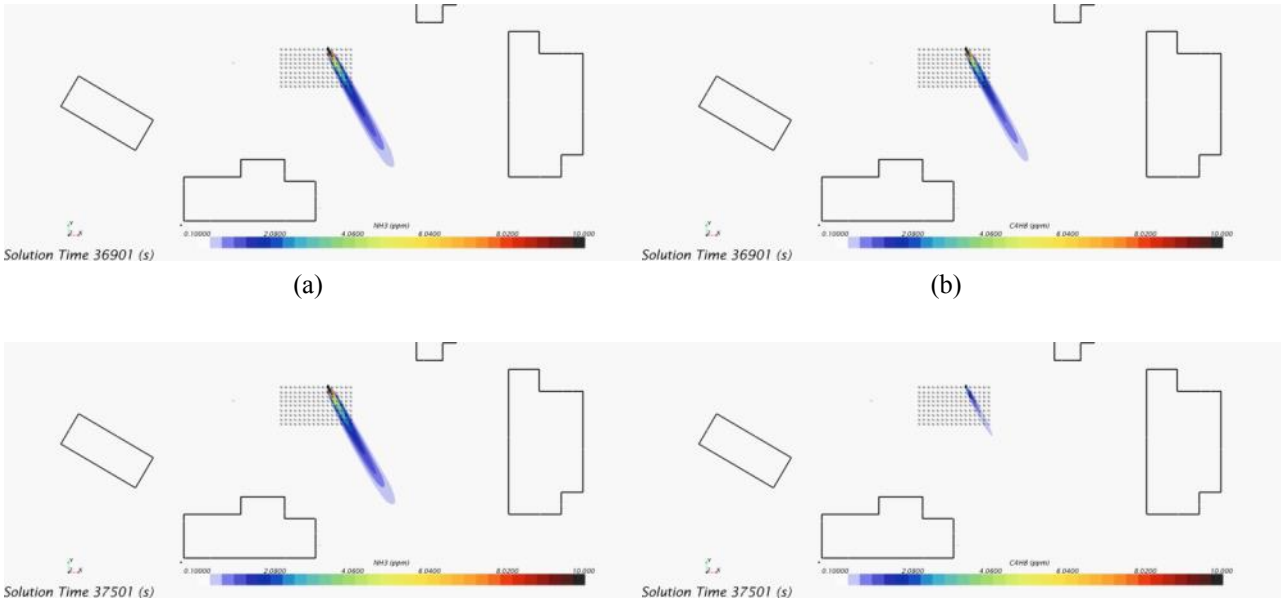

(a) (b)

(c) (d)

Figure 6.11. Plume distribution cross section 1.0 m from the ground: (a) NH_3 at 36901 seconds, (b) C_4H_8 at 36901 seconds, (c) NH_3 at 37501 seconds, (d) C_4H_8 at 37501 seconds

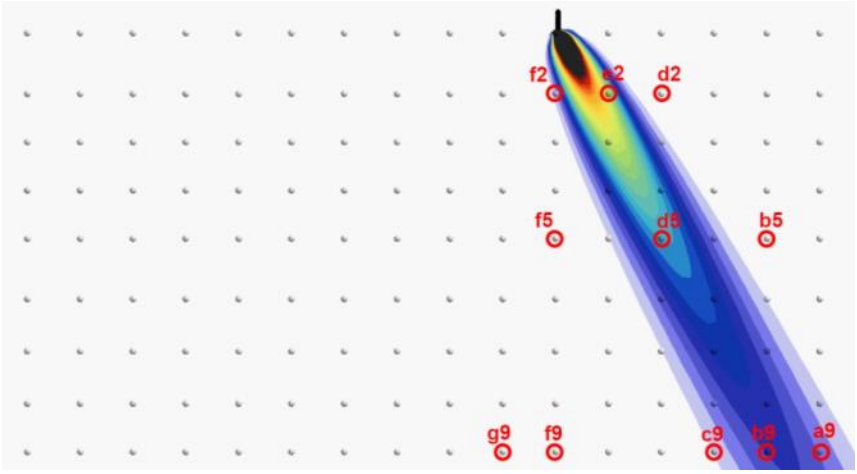

Figure 6.12. Activated sensor locations (red circles)

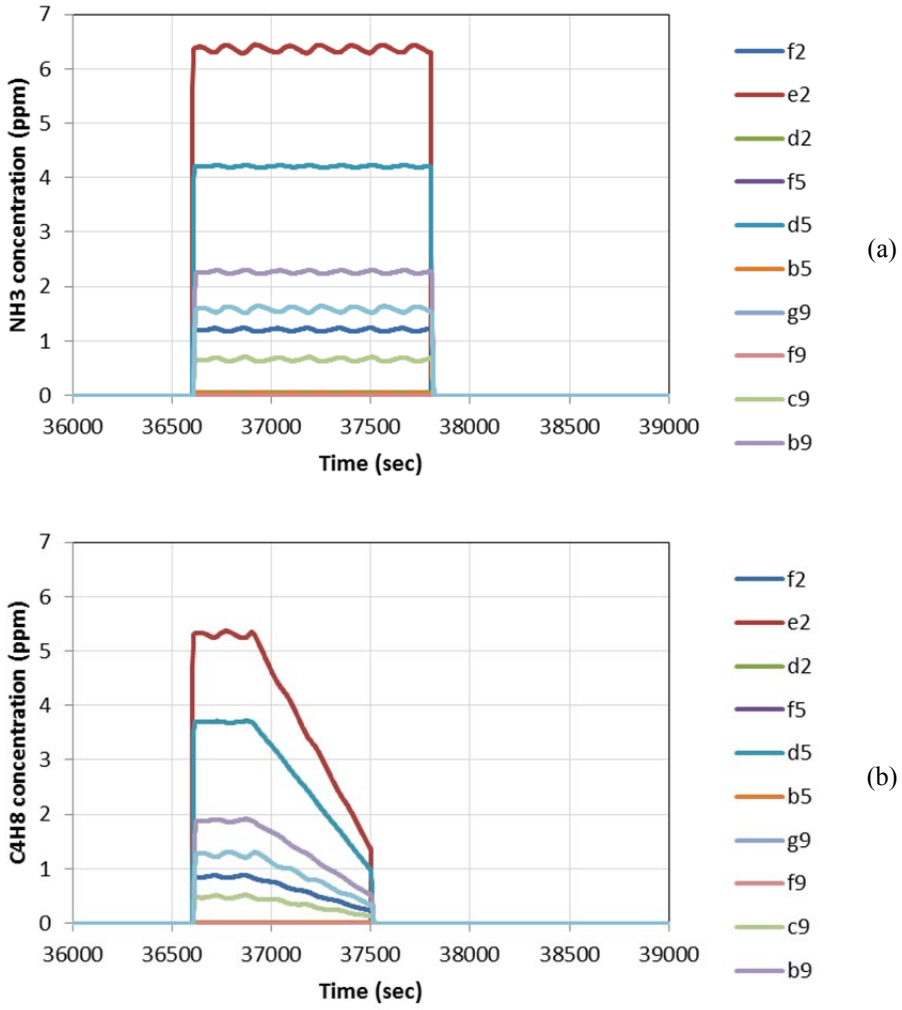

Figure 6.13. Simulated concentration evolutions of (a) NH_3 and (b) C_4H_8

Figure 6.14 shows the correlation between the NH_3 and C_4H_8 concentrations throughout the test simulation. The source releasing rates for NH_3 and C_4H_8 were not constant, so not all of the concentrations for these two species are well correlated. As mentioned above, the releasing periods were divided into four time period regions; the data on the correlation plot are shown in different color for each region. In region I, NH_3 and C_4H_8 concentrations are well correlated. In region II, C_4H_8 concentration gradually decreases, while the NH_3 concentration stays at an approximate constant value. In region III, C_4H_8 concentration rapidly drops to zero, while the NH_3 concentrations stays at an approximate constant value. In region IV, C_4H_8 concentration stays at zero, while NH_3 concentration rapidly drops to zero.

The simulation provides a good example to explain the correlation plots of the real measure data in the tank farms. Those plots include some non-correlated concentration points, which look like a vertical or horizontal line of data where one species's concentrations were zero. This is similar to the horizontal and vertical lines of points observed in the methane and N_2O measurements shown in Figure 6.5. CFD may be a helpful tool in verification of LIs.

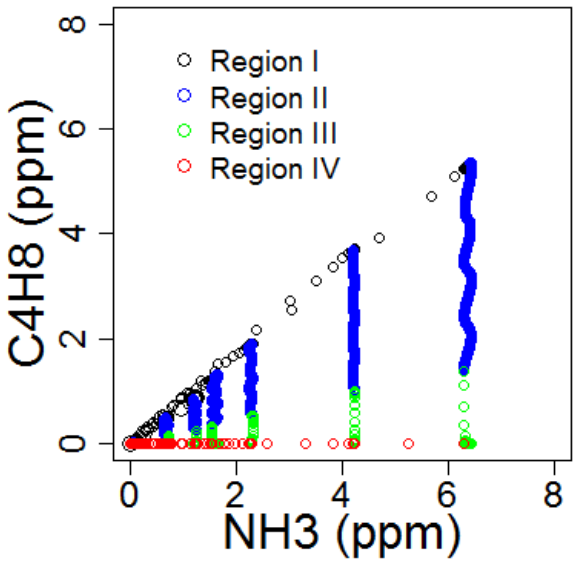

Figure 6.14. Correlation between NH_3 and C_4H_8 concentration during the simulated bench-scale tests

7.0 Conclusions

The leading indicator process shows promise for use at the Hanford Site. This report describes the methods used to devise the process by which potential LIs could be identified and evaluated. The current dataset, as downloaded from TWINS and SWIHD, has shown a number of match pairings of COPCs and non-COPCs. A few key gaps and observations were identified throughout this initial analysis of the data that can be combined into general themes.

Time and Space: COPCs must be identified at the same time in the same location. If multiple samples are taken, but a timestamp and the associated location information was not recorded, COPC pairings cannot be identified between the multiple samples. The level of detail given for sample location varies from specific identification of particular tanks or exhausters to generic description as "inside tank" which limits the ability to cross-reference samples. Additionally, more detailed day and time information regarding tank activities will be required to identify tank activity effects on COPC pairing relationships. A standardized site-wide sample identification nomenclature is recommended to reduce the uncertainty of establishing related samples.

Data Gaps: All COPCs were not measured for every sample, meaning that analytical methods were used to only look at a select subset of the COPCs. In the filtered datasets used in this analysis, there were COPCs that were not shown to have a pairing with another COPC. The lack of observed pairings does not strictly imply the pairing does not exist; rather there is a data gap for that pairing and those particular COPCs may not have been analyzed in the same samples. It is recommended that techniques are chosen so that all COPCs can be analyzed and reported for each air sampling event.

Relationships: The apparent relationship trends observed in the site-wide population may not be the same as trends identified in individual tank farms are evaluated. Though COPCs within functional group families tend to trend well together and have shown similar data trends in site-wide data or individual tank farms. Limited available data from individual tank farms will impact ability to identify tank farm specific relationships. The intensive data acquisition through the pilot-scale VMDS testing within the A and AP farms will allow the focused analysis within these two farms and a basis for comparison with the available site-wide data.

Detection Methods: Little focus has been placed on detection methods and/or detection limits within the process at this time. The data used throughout the generation and evaluation of this process have been from air sampling methods followed by laboratory-based chemical analysis. This technique provides greater chemical specificity and potentially lower detection limits than instrument within the field. Many of the deployed field instruments measure ammonia, nitrous oxide, and/or total VOC. Within the current dataset, there is not a total VOC measurement, so an evaluation of VOC as a leading indicator is not possible at this time.

Vapor Sources: Nitrous oxide, hydrogen, ammonia and a number of VOCs are all characteristic chemicals from tanks, though none are unique to tank sources. Ammonia was positively detected in approximately 86% of the samples, while nitrous oxide and hydrogen were positively detected 62% and 76% of the time. Other chemicals with high percentages of positive detects, when the analysis was reported, include acetone (90%), trichlorofluoromethane (88%), and 1-butanol (88%). In non-headspace samples, the percentage of positive detects from reported samples decreases to approximately 40 – 60%

for each of these chemicals. Contributions from tanks and from non-tank sources may need to be identified in terms of multiple marker species and relative concentrations, so a more detailed multivariate statistical approach, such as factor analysis, is recommended to identify tank signatures.

Potential Leading Indicators: Overall, the available pairings indicate that both ammonia and nitrous oxide are strong candidates as LIs. Ammonia had pairings with 32 of the COPCs and nitrous oxide had pairing with 29 of the COPCs. The remaining COPCs did not have enough measurements to observe a pairing or relationship. The general trend for pairings with ammonia and nitrous oxide is that the majority of the paired data points fall above the 10% OEL level of the LI meaning that an alert on the LI would bound alerts for the COPC.

This distribution of data points results in low populations within the missed alert and true non-alert quadrants. Measured COPC concentrations can vary over a couple orders of magnitude for a particular LI concentration. Additional paired results with measured LI concentration below the 10% OEL would give greater confidence in the probability distribution within the missed alert quadrant.

The pilot-scale VMDS testing will provide data with additional rigor through the use of a sampling plan that defines samples and their relationships (time, location, and activities) to one another. The pilot-scale VMDS testing will also include results from instruments not included in previous datasets (i.e., Fourier transform infrared spectroscopy instruments, direct read instruments, photoionization detectors, etc.) to challenge the LI identification process. Additionally, there are current scopes of work related to health process assessments and vapor modeling that must be included in the evaluation of potential LIs.

The tank farm environment is not static, so it is expected that periodic reviews of LIs will be needed. If a new set of sampling data becomes available from the tank farms that were not well characterized previously or during waste-disturbing activities, new LI relationships may be identified or bounding LI relationships may be expanded to other situations or tank farms. If tank waste composition has changed significantly due to transfers, previously identified LI relationships may no longer be correct. As the process is evaluated and refined, there may be other situations where a review is deemed necessary.

8.0 Quality Assurance

The PNNL Quality Assurance Program is based upon the requirements defined in the U.S. Department of Energy Order 414.1D, *Quality Assurance*, and 10 CFR 830, *Energy/Nuclear Safety Management*, Subpart A—Quality Assurance Requirements. PNNL has chosen to implement the following consensus standards in a graded approach:

- ASME NQA-1-2000, *Quality Assurance Requirements for Nuclear Facility Applications*, Part I, Requirements for Quality Assurance Programs for Nuclear Facilities.
- ASME NQA-1-2000, Part II, Subpart 2.7, Quality Assurance Requirements for Computer Software for Nuclear Facility Applications.
- ASME NQA-1-2000, Part IV, Subpart 4.2, Graded Approach Application of Quality Assurance Requirements for Research and Development.

The procedures necessary to implement the requirements are documented through PNNL's "How Do I…?" (HDI), a system for managing the delivery of laboratory-level policies, requirements, and procedures.

The project implements applicable quality requirements indicated in the statement of work through WRPS_CVST_02, *Project Specific Approach to Quality for Chemical Vapor Solutions Team Sub-Team Support Project*. The work described in this report was conducted following the requirements in WRPS_CVST_02. PNNL addressed internal verification and validation activities by conducting an independent technical review of the final data included in the report in accordance with WRPS_CVST_02. This review verified that the reported results are traceable, and that inferences and conclusions are soundly based.

9.0 References

Aneja VA, PA Roelle, GC Murray, J Southerland, JW Erisman, D Fowler, WAH Asman, N Patni. 2001. "Atmospheric nitrogen compounds II: emissions, transport, transformation, deposition and assessment," *Atmos. Env*. **35** (2001): 1903-1911.

Bryan SA, DM Camaioni, TG Levitskaia, BK McNamara, RL Sell, LM Stock. 2004. *Gas Generation Testing and Support for the Hanford Waste Treatment and Immobilization Plant*, PNWD-3463 (WTP-RPT-115), Battelle – Pacific Northwest Division, Richland, Washington.

EPA. 2004. *Update of Methane and Nitrous Oxide Emission Factors for On-Highway Vehicles*, EPA420-P-04-016, prepared by ICF Consulting for the Environmental Protection Agency.

JPL. 2015. *Chemical Kinetics and Photochemical Data for Use in Atmospheric Studies, Evaluation Number 18*, JPL Publication 15-10, NASA Panel for Data Evaluation, Jet Propulsion Laboratory, California Institute of Technology, Pasadena, California.

Kesselmeier J and M Staudt. 1999. "Biogenic Volatile Organic Compounds (VOC): An Overview on Emission, Physiology and Ecology," *J. Atmos. Chem* **33**: 23-88.

Kota SH, C Park, MC Hale, ND Werner, GW Schade, Q Ying. 2014. "Estimation of VOC emission factors from flux measurements using a receptor model and footprint analysis," *Atmos. Env.* **82** (2014): 24-35.

Lemieux PM, CC Lutes, DA Santoianni. 2004. "Emissions of organic air toxics from open burning: a comprehensive review," *Progress in Energy and Combustion Science* **30** (2004): 1-32.

Mahoney LA, ZI Antoniak, JM Bates, and ME Dahl. 1999. *Retained Gas Sampling Results for the Flammable Gas Program*. PNNL-13000, Pacific Northwest National Laboratory, Richland, Washington.

Mahoney LA, ZI Antoniak, WB Barton, JM Cobber, NW Kirch, CW Stewart, and BE Wells. 2000. *Results of Waste Transfer and Back-Dilution in Tanks 241-SY-101 and 241-SY-102*, PNNL-13267, Pacific Northwest National Laboratory, Richland, Washington.

Meacham JE, JO Honeyman, TJ Anderson, ML Zabel, and JL Huckaby. 2006. *Industrial Hygiene Chemical Vapor Technical Basis*. RPP-22491, Rev 1, CH2M Hill Hanford Group, Inc., Richland, Washington.

Olson LD. L David Olson to KW Smith. February 9, 2015. *Contract number DE-AC27-08RV14800 – Washington River Protection Solutions LLC Submits Implementation Plan for Hanford Tank Vapor Assessment Report Recommendations*. WRPS-1500142, Washington River Protection Solutions, Richland, Washington. http://wrpstoc.com/wp-content/uploads/2015/02/WRPS-1500142-IP-transmittal-letter-to-DOE-ORP.pdf.

Poet TJ, TJ Mast, and JL Huckaby. 2006. *Screening Values.for Non-Carcinogenic Haeford Waste Tank Vapor Chemicals that Lack Established Occupational Exposure Limits*, PNNL-15640 Rev. 0, Pacific Northwest National Laboratory, Richland, Washington.

Poet TJ and C Timchalk. 2006. *Proposed Occupational Exposure Limits for Non-Carcinogenic Hariford Waste Tank Vapor Chemicals*, PNNL-15736 Rev. 0, Pacific Northwest National Laboratory, Richland, Washington.

Stock LM. 2004. *Occurrence and Chemistry of Organic Compounds in Hanford Site Waste Tanks*. RPP-21854, Rev 0, CH2M Hill Hanford Group, Inc., Richland, Washington.

Stock LM and JL Huckaby. 2004. *A Survey of Vapors in the Headspaces of Single-Shell Waste Tanks*. PNNL-13366, Rev 1, Pacific Northwest National Laboratory, Richland, Washington.

Stock LM and LR Pederson. 1997. *Chemical Pathways for the Formation of Ammonia in Hanford Wastes*. PNNL-11702, Pacific Northwest National Laboratory, Richland, Washington.

Sun H, SL Trabue, K Scoggin, WA Jackson, Y Pan, Y Zhao, IL Malkina, JA Koziel, FM Mitloehner. 2008. "Alcohol, Volatile Fatty Acid, Phenol, and Methane Emissions from Dairy Cows and Fresh Manure," *J. Environ. Qual.* **37**: 615-622.

Vollmer MK, N Juergens, M Steinbacher, S Reimann, M Weilenmann, B Buchmann. 2007. "Road vehicle emissions of molecular hydrogen (H_2) from a tunnel study," *Atmos. Env.* **41** (2007): 8355-8369.

Wilmarth WR, MA Maier, TW Armstrong, RL Ferry, JL Henshaw, RA Holland, MA Jayjock, MH Le, JC Rock, and C Timchalk. 2014. *Hanford Tank Vapor Assessment Report*. SRNL-RP-2014-00791, Savannah River National Laboratory, Aiken, South Carolina.

Pairing Scoring

Appendix A

Pairing Scoring

Table A.1 summarizes scoring information for all the higher-scoring pairings. The pairings are arranged in descending order of score. A total of 3 pairings scored 7 out of 10 points by the criteria given in Section 3.1.5, 14 scored 6 out of 10 points, 30 scored 5 out of 10 points, and the remaining 658 pairings for which there were any hits scored 4 or fewer points. The table contains one row for each pairing that scored 3 or more points out of the 10 possible points. Lower scores were considered to indicate that the evidence (to date) was inadequate to indicate a reliable pairing. Each column contains information related to one of the features for which a point could be assigned. Blank cells indicate that the pairing did not qualify for a point by the associated criterion. Non-blank cells show the information that qualified the pairing to score a point.

For example, the first row in the table shows the following information for the butanal and butanenitrile pairing. In both datasets, the pairing's hits included maximum concentrations that were equal to or near the historical maximum concentrations over all data (hits or not): the ratio of historical to hit maxima was 1.0 for headspace data, and 1.3 for industrial health (IH) data (i.e., historical maximum 30% higher than maximum among hits). Thus, this pairing had some potential for capturing the behavior that defined historical maximum concentrations and scored points accordingly under criteria (a) and (b). Note that these ratios of maxima might have been for either the y or x chemical, whichever gave a higher ratio.

There were relatively many points in both datasets: the pairing therefore scored a point under criterion (c). A total of 33% of the IH hits (or 7 points) were from measurements during periods that were defined as tank activity periods, but fewer than five headspace measurements were taken during such periods. Therefore, the pairing scored a point under criterion (e), but not under criterion (d).

Neither dataset yielded hits that showed one chemical's maximum concentration, having a ratio to the occupational exposure limit (OEL) that was different from that of the other chemical by a factor of 10 or more. Thus, there was little differential between the two chemicals in terms of potential to reach or exceed the OEL. Because there was little toxicological advantage to using one as an indicator for the other, the pairing scored zero points (out of a possible 2) under criterion (f).

Both datasets also showed the two chemicals trending with each other in a relatively well-defined way, as shown by the high R^2 values for the power-law trend fits. Points were scored under criteria (g) and (h). The trends for the headspace and IH datasets had approximately the same slope (exponent of the power-law fit), suggesting that the mechanism's controlling release was similar under both headspace and IH sampling conditions. The pairing scored a point under criterion (i).

Table A.1. Scoring information for pairings of chemicals found in the vapor phase in Hanford tanks[(a)]

x-Axis Chemical	y-Axis Chemical	Number of Hits in Each Dataset (HS and IH)	At Least 10 Hits and High R^2		y vs. x OEL-Fraction Differential among Hits		Ratio of the All-Data Max x and y to the Max. x and y among Headspace Hits		Exponents in HS and IH, if Similar to Each Other	Percent of Hits That Were during Tank Activity		Total Score
			HS R^2	IH R^2	HS	IH	HS	IH		HS	IH	
Butanal	Butanenitrile	24 & 21	0.74	0.79	---	---	1.0	1.3	0.8 & 0.9	---	33%	7
Propanenitrile	Butanenitrile	53 & 18	0.73	0.79	---	---	1.0	1.3	0.7 & 0.8	---	33%	7
1-Propanol	1-Butanol	73 & 17	0.75	0.66	42	367	1.1	---	---	---	41%	7
Ammonia	1-Butanol	63 & 57	---	---	0.012	0.015	1.1	1.4	---	---	30%	6
Ammonia	Acetaldehyde	23 & 21	---	---	0.004	0.003	1.7	1.6	---	---	81%	6
Mercury	Acetonitrile	---	0.72	---	0.099	0.007	1.1	2.0	---	---	38%	6
1-Butanol	Butanal	29 & 36	0.82	---	---	0.032	1.6	2.1	---	---	28%	6
2-Hexanone	Butanal	20 & 22	0.74	0.62	---	---	1.0	2.4	---	---	36%	6
2-Hexanone	Propanenitrile	---	0.55	0.62	10	---	1.0	---	1.1 & 0.9	---	29%	6
2-Hexanone	Butanenitrile	22 & 16	0.83	0.72	---	---	1.0	---	1.0 & 0.8	---	44%	6
Methylbenzene	Ammonia	77 & 26	---	---	9820	6326	1.5	1.4	---	---	58%	6
Methylbenzene	1-Butanol	58 & 17	---	0.63	169	16	2.5	---	---	---	41%	6
Tetrahydrofuran	Formaldehyde	---	0.60	---	65	1319	2.0	1.9	---	---	47%	6
Ethanol	Butanal	29 & 17	---	0.52	69	---	2.8	---	0.7 & 0.8	---	29%	6
1-Propanol	Formaldehyde	---	0.76	---	21	1426	2.5	2.0	---	---	50%	6
1-Propanol	Butanal	41 & 25	0.88	---	12	---	1.0	---	---	20%	48%	6
Acetone	1-Butanol	74 & 19	0.68	---	32	42	1.6	---	---	---	37%	6
Ammonia	2-Hexanone	---	---	---	0.001	0.001	1.3	1.3	---	---	52%	5
Ammonia	Formaldehyde	20 & 112	---	---	0.002	0.073	1.0	---	---	---	39%	5
Ammonia	Butanal	20 & 57	---	---	0.001	0.001	---	1.4	---	---	35%	5
Ammonia	Acetonitrile	79 & 65	---	---	0.004	0.001	1.1	---	---	---	31%	5
Ammonia	Propanenitrile	42 & 20	---	---	0.008	0.004	1.1	---	---	---	35%	5
Ammonia	Butanenitrile	43 & 24	---	---	0.001	0.001	1.7	---	---	---	42%	5
Mercury	2-Hexanone	---	---	---	0.015	0.002	1.1	1.5	---	---	55%	5
Mercury	Formaldehyde	---	---	---	0.036	0.025	1.4	2.0	---	---	43%	5
Mercury	Acetaldehyde	---	---	---	0.046	0.007	2.4	1.9	---	---	79%	5
Mercury	Butanal	---	---	---	0.025	0.002	2.7	2.0	---	---	40%	5
1-Butanol	2-Hexanone	---	0.78	---	0.100	0.027	1.6	2.4	---	---	---	5
Acetaldehyde	Butanal	---	0.90	---	---	---	1.0	2.3	1.0 & 1.0	---	75%	5
Butanal	Acetonitrile	33 & 34	0.66	---	---	---	1.0	---	---	21%	29%	5
Butanal	Propanenitrile	19 & 25	0.81	---	---	---	1.0	1.1	---	---	28%	5
Butanenitrile	Pentanenitrile	---	0.64	0.90	---	---	1.9	1.3	0.8 & 1.0	---	---	5
Butane	Butanal	---	0.77	---	78	41	1.1	---	---	17%	---	5
Methylbenzene	Butanal	28 & 17	---	0.64	58	---	---	---	---	21%	59%	5
Tetrahydrofuran	Mercury	---	---	---	1709	26011	2.5	2.0	---	---	46%	5
Tetrahydrofuran	2-Hexanone	---	0.79	---	21	36	2.0	---	1.2 & 1.0	---	---	5
Tetrahydrofuran	Butanal	---	0.51	---	91	---	2.0	---	---	14%	67%	5
Ethanol	Ammonia	56 & 25	---	---	8776	21594	1.2	---	---	---	44%	5

x-Axis Chemical	y-Axis Chemical	Number of Hits in Each Dataset (HS and IH)	At Least 10 Hits and High R^2		y vs. x OEL-Fraction Differential among Hits		Ratio of the All-Data Max x and y to the Max. x and y among Headspace Hits		Exponents in HS and IH, if Similar to Each Other	Percent of Hits That Were during Tank Activity		Total Score
			HS R^2	IH R^2	HS	IH	HS	IH		HS	IH	
Ethanol	1-Butanol	60 & 23	---	---	103	47	1.2	---	---	---	22%	5
Ethanol	Methanol	---	0.70	---	14	31	1.2	1.1	---	---	---	5
1-Propanol	Ammonia	72 & 37	---	---	10144	14326	2.8	---	---	---	51%	5
1-Propanol	Mercury	---	---	---	448	61367	2.5	2.0	---	---	50%	5
1-Propanol	Acetaldehyde	---	0.85	---	19	363	1.0	---	---	---	83%	5
1-Propanol	Acetonitrile	---	---	---	18	13	1.0	---	---	6%	54%	5
Acetone	Ammonia	92 & 24	---	---	2755	15267	1.6	---	---	---	54%	5
Acetone	Acetaldehyde	---	0.75	---	15	31	1.6	---	---	---	100%	5
Acetone	Butanal	30 & 17	0.53	---	---	---	1.6	---	0.8 & 0.9	---	41%	5
Ammonia	Methanol	---	0.61	---	0.001	0.008	1.5	---	---	---	---	4
Ammonia	Pyridine	---	---	---	0.005	0.004	---	1.3	---	---	29%	4
Nitrous oxide	1-Butanol	52 & 20	---	---	0.050	---	---	2.6	---	---	35%	4
Nitrous oxide	Formaldehyde	24 & 22	---	---	0.016	0.042	---	---	---	---	23%	4
Nitrous oxide	Butanal	---	---	---	0.009	0.009	---	2.6	---	---	40%	4
Mercury	Butanenitrile	---	---	---	0.025	0.001	1.4	---	---	---	41%	4
1-Butanol	Formaldehyde	---	0.60	---	---	---	2.3	1.9	---	---	33%	4
1-Butanol	Acetonitrile	64 & 38	---	---	---	0.091	1.1	---	---	---	26%	4
2-Hexanone	Formaldehyde	---	---	---	---	61	1.0	2.4	---	---	40%	4
3-Buten-2-one	Butanenitrile	---	---	0.85	---	0.035	---	1.3	---	---	50%	4
Formaldehyde	Butanal	---	0.63	---	---	0.009	2.7	---	---	---	40%	4
Acetaldehyde	Propanenitrile	---	0.59	---	---	0.056	1.0	---	0.7 & 0.7	---	---	4
Acetonitrile	Propanenitrile	68 & 18	0.77	---	---	---	1.0	---	0.9 & 0.7	---	---	4
Pentanenitrile	Hexanenitrile	---	---	0.89	---	---	1.1	1.1	1.1 & 1.1	---	---	4
N-Nitrosodimethylamine	N-Nitrosomethylethylamine	---	---	0.71	---	0.003	---	1.0	---	---	55%	4
N-Nitrosodimethylamine	N-Nitrosomorpholine	---	---	0.50	---	0.001	---	1.0	---	---	53%	4
Methane	Nitrous oxide	---	---	---	nonCOPC	nonCOPC	1.0	1.0	---	---	---	4
Hydrogen	Nitrous oxide	---	0.63	---	nonCOPC	nonCOPC	---	1.0	---	---	---	4
Methane, trichlorofluoro-	Ammonia	---	---	---	26210	703525	1.0	---	---	---	55%	4
Butane	1-Butanol	---	0.75	---	269	1250	1.1	---	---	---	---	4
Methylbenzene	Butanenitrile	---	---	---	16	28	1.5	---	---	---	86%	4
Tetrahydrofuran	Ammonia	---	---	---	13778	10181	1.1	---	---	---	47%	4
Tetrahydrofuran	1-Butanol	---	0.77	---	233	70	1.5	---	---	---	---	4
Tetrahydrofuran	Acetaldehyde	---	0.67	---	144	274	2.0	---	---	---	---	4
Tetrahydrofuran	Acetonitrile	---	---	---	99	274	1.5	---	---	6%	---	4
Dichloromethane	Benzene	---	0.57	---	nonCOPC	nonCOPC	2.0	---	---	---	---	4
Ethanol	Formaldehyde	16 & 29	---	---	61	3550	---	---	---	---	34%	4
Ethanol	Acetaldehyde	---	0.65	---	109	796	2.8	---	---	---	---	4
1-Propanol	2-Hexanone	---	0.53	---	---	13	1.0	---	---	---	55%	4
Acetone	Mercury	---	---	---	143	36929	1.6	---	---	---	54%	4
Acetone	Formaldehyde	20 & 30	---	---	---	1842	1.6	---	---	---	33%	4
Acetone	Acetonitrile	103 & 17	---	---	14	---	1.6	---	---	---	29%	4
Ammonia	Nitrous oxide	73 & 28	---	---	---	---	---	2.1	---	---	21%	3

x-Axis Chemical	y-Axis Chemical	Number of Hits in Each Dataset (HS and IH)	At Least 10 Hits and High R^2		y vs. x OEL-Fraction Differential among Hits		Ratio of the All-Data Max x and y to the Max. x and y among Headspace Hits		Exponents in HS and IH, if Similar to Each Other	Percent of Hits That Were during Tank Activity		Total Score
			HS R^2	IH R^2	HS	IH	HS	IH		HS	IH	
Ammonia	Mercury	---	---	---	0.008	---	---	1.0	---	---	45%	3
Ammonia	1,3-Butadiene	---	---	---	0.002	0.015	---	---	---	---	56%	3
Ammonia	Benzene	---	---	---	0.001	0.014	2.1	---	---	---	---	3
Ammonia	Hexanenitrile	---	---	---	0.001	0.002	---	---	---	---	54%	3
Ammonia	N-Nitrosodimethylamine	---	---	---	---	44	---	1.3	---	---	43%	3
Nitrous oxide	2-Hexanone	---	---	---	0.007	0.004	---	2.6	---	---	---	3
Nitrous oxide	Propanenitrile	---	---	---	0.040	0.074	---	2.6	---	---	---	3
Nitrous oxide	Pentanenitrile	---	---	---	0.003	0.027	---	2.6	---	---	---	3
Nitrous oxide	Hexanenitrile	---	---	---	0.005	0.040	---	2.6	---	---	---	3
Mercury	1-Butanol	---	---	---	---	0.022	2.3	---	---	---	21%	3
Mercury	Methanol	---	---	---	0.025	0.090	1.3	---	---	---	---	3
Mercury	Propanenitrile	---	---	---	0.078	0.000	2.0	---	---	---	---	3
Mercury	Ethylamine	---	---	---	---	0.001	---	1.0	---	---	82%	3
Mercury	N-Nitrosomorpholine	---	---	---	---	0.037	---	1.0	---	---	58%	3
Mercury	Tributylphosphate	---	---	---	0.007	0.010	1.1	---	---	---	---	3
1,3-Butadiene	1-Butanol	---	---	---	12	0.018	1.5	---	---	---	---	3
Benzene	Butanal	---	---	---	---	0.079	1.0	---	---	45%	---	3
Benzene	Furan	---	---	---	119	1872	1.0	---	---	---	---	3
1-Butanol	Furan	---	---	---	23	1192	2.6	---	---	---	---	3
1-Butanol	Pentanenitrile	---	---	---	0.045	0.033	1.2	---	---	---	---	3
1-Butanol	Hexanenitrile	---	---	---	0.064	0.048	1.5	---	---	---	---	3
2-Hexanone	3-Buten-2-one	---	---	0.59	---	132	---	---	---	---	38%	3
2-Hexanone	Acetaldehyde	---	0.52	---	---	---	1.0	---	---	---	63%	3
2-Hexanone	Furan	---	---	---	309	2137	1.3	---	---	---	---	3
2-Hexanone	Acetonitrile	21 & 16	0.68	---	---	---	1.0	---	---	---	---	3
3-Buten-2-one	Butanal	---	---	---	---	0.015	---	1.1	---	---	38%	3
3-Buten-2-one	Propanenitrile	---	---	0.78	---	---	---	1.1	---	---	26%	3
Formaldehyde	Acetaldehyde	---	---	---	---	---	1.7	2.0	---	---	60%	3
Formaldehyde	Acetonitrile	---	---	---	---	---	1.0	2.4	---	---	31%	3
Formaldehyde	Propanenitrile	---	0.67	---	---	0.085	1.3	---	---	---	---	3
Formaldehyde	Ethylamine	---	---	---	---	0.040	---	2.8	---	---	70%	3
Acetaldehyde	Furan	---	---	---	317	176	---	2.3	---	---	---	3
Acetaldehyde	Acetonitrile	---	---	---	---	0.094	1.0	---	---	---	71%	3
Acetonitrile	Butanenitrile	---	0.52	---	---	---	1.0	---	---	---	33%	3
Propanenitrile	Hexanenitrile	---	0.72	---	---	---	---	1.1	1.0 & 1.0	---	---	3
Propanenitrile	N-Nitrosodimethylamine	---	---	0.64	---	1470	---	---	---	---	38%	3
Butanenitrile	Hexanenitrile	---	0.51	---	---	---	1.9	1.3	---	---	---	3
Ethylamine	N-Nitrosomethylethylamine	---	---	---	---	222	---	1.0	---	---	75%	3
Ethylamine	N-Nitrosomorpholine	---	---	---	---	53	---	1.0	---	---	78%	3
N-Nitrosomethylethylamine	N-Nitrosomorpholine	---	---	0.66	---	---	---	1.1	---	---	58%	3
Methane	1-Butanol	---	---	---	nonCOPC	nonCOPC	2.3	---	---	---	---	3
Methane	Methanol	---	---	---	nonCOPC	nonCOPC	1.3	---	---	---	---	3

x-Axis Chemical	y-Axis Chemical	Number of Hits in Each Dataset (HS and IH)	At Least 10 Hits and High R^2		y vs. x OEL-Fraction Differential among Hits		Ratio of the All-Data Max x and y to the Max. x and y among Headspace Hits		Exponents in HS and IH, if Similar to Each Other	Percent of Hits That Were during Tank Activity		Total Score
			HS R^2	IH R^2	HS	IH	HS	IH		HS	IH	
TNMHC	1-Butanol	---	0.80	---	nonCOPC	---	1.1	---	---	---	---	3
Methane, trichlorofluoro-	Mercury	---	---	---	13598	2040556	---	1.5	---	---	---	3
Methane, trichlorofluoro-	Benzene	---	---	---	243	879	---	---	---	9%	---	3
Methane, trichlorofluoro-	Butanal	---	---	---	632	99	---	---	---	21%	---	3
Methane, trichlorofluoro-	Acetonitrile	---	---	---	920	862	---	---	---	5%	---	3
Butane	Ammonia	---	---	---	26066	96476	1.1	---	---	---	---	3
Butane	Mercury	---	---	---	1236	516	1.2	---	---	---	---	3
Butane	Methanol	---	---	---	36	400	1.1	---	---	---	---	3
Butane	2-Hexanone	---	0.81	---	18	---	1.1	---	---	---	---	3
Butane	Formaldehyde	---	0.54	---	59	---	1.2	---	---	---	---	3
Butane	Acetaldehyde	---	0.90	---	124	---	1.1	---	---	---	---	3
Butane	Acetonitrile	---	---	---	114	---	1.1	---	---	7%	---	3
Methylbenzene	Nitrous oxide	---	---	---	3560	586	---	2.9	---	---	---	3
Methylbenzene	Mercury	---	---	---	780	10475	---	---	---	---	69%	3
Methylbenzene	Methanol	---	---	---	23	12	2.5	---	---	---	---	3
Methylbenzene	2-Hexanone	---	---	---	18	37	---	---	---	---	77%	3
Methylbenzene	Formaldehyde	---	---	---	82	569	---	---	---	---	36%	3
Methylbenzene	Acetaldehyde	---	---	---	184	249	---	---	---	---	86%	3
Methylbenzene	Acetonitrile	---	---	---	41	---	1.5	---	---	6%	---	3
Methylbenzene	Propanenitrile	---	---	---	145	18	---	---	---	---	63%	3
Tetrahydrofuran	1,3-Butadiene	---	---	---	22	15111	2.3	---	---	---	---	3
Tetrahydrofuran	Benzene	---	---	---	15	129	1.4	---	---	---	---	3
Tetrahydrofuran	Methanol	---	---	---	31	23	1.5	---	---	---	---	3
Tetrahydrofuran	Propanenitrile	---	---	---	157	44	1.5	---	---	---	---	3
Tetrahydrofuran	Butanenitrile	---	---	---	36	28	1.5	---	---	---	---	3
Tetrahydrofuran	Pyridine	---	---	---	41	1088	1.8	---	---	---	---	3
Dichloromethane	Ammonia	---	---	---	nonCOPC	nonCOPC	2.4	---	---	---	---	3
Dichloromethane	1-Butanol	---	---	---	nonCOPC	nonCOPC	2.0	---	---	---	---	3
Dichloromethane	Formaldehyde	---	---	---	nonCOPC	nonCOPC	---	2.0	---	---	---	3
Dichloromethane	Pyridine	---	---	---	nonCOPC	nonCOPC	2.1	---	---	---	---	3
Ethanol	Mercury	---	---	---	1280	91215	---	---	---	---	39%	3
Ethanol	2-Hexanone	---	---	---	16	18	2.8	---	---	---	---	3
1-Propanol	Benzene	---	---	---	---	235	1.0	1.9	---	---	---	3
1-Propanol	Methanol	---	---	---	---	243	1.0	3.0	---	---	---	3
1-Propanol	Furan	---	---	---	9688	25951	---	---	---	---	56%	3
1-Propanol	Propanenitrile	---	---	---	28	---	1.0	---	---	---	42%	3
Dimethylmercury	Ammonia	---	---	---	nonCOPC	nonCOPC	1.0	---	---	---	---	3
Dimethylmercury	Mercury	---	---	---	nonCOPC	nonCOPC	1.1	---	---	---	---	3
Dimethylmercury	1-Butanol	---	---	---	nonCOPC	nonCOPC	2.3	---	---	---	---	3
Dimethylmercury	Methanol	---	---	---	nonCOPC	nonCOPC	1.3	---	---	---	---	3

x-Axis Chemical	y-Axis Chemical	Number of Hits in Each Dataset (HS and IH)	At Least 10 Hits and High R^2		y vs. x OEL-Fraction Differential among Hits		Ratio of the All-Data Max x and y to the Max. x and y among Headspace Hits		Exponents in HS and IH, if Similar to Each Other	Percent of Hits That Were during Tank Activity		Total Score
			HS R^2	IH R^2	HS	IH	HS	IH		HS	IH	
Dimethylmercury	Formaldehyde	---	---	---	nonCOPC	nonCOPC	1.4	---	---	---	---	3
Dimethylmercury	Butanal	---	---	---	nonCOPC	nonCOPC	2.7	---	---	---	---	3
Acetone	Methanol	---	0.52	---	---	40	1.6	---	---	---	---	3
Acetone	Furan	---	---	---	418	9804	2.1	---	---	---	---	3

(a) Only pairing criteria that resulted in awarding a point are shown in the table.

I

Process Evaluation Chemical Identification Tables

Appendix B

Process Evaluation Chemical Identification Tables

This appendix has the chemical identification tables associated with each of the figures in Section 6.1.2 Process Evaluation.

Table B.1. Chemical identification of CAS IDs from filtered COPC:OEL ratios shown in Figure 6.1 listed in decreasing order of COPC:OEL ratio

CAS	Chemical Name
10024-97-2	Nitrous Oxide
62-75-9	N-Nitrosodimethylamine
110-00-9	Furan
1708-29-8	2,5-Dihydrofuran
534-22-5	2-Methylfuran
4229-91-8	2-propylfuran
55-18-5	n-Nitrosodiethylamine
10595-95-6	N-Nitrosomethylethylamine
3777-71-7	2-heptylfuran
59-89-2	n-Nitrosomorpholine
7664-41-7	Ammonia
1191-99-7	2,3-Dihydrofuran
7439-97-6	Mercury
78-46-6	Dibutylbutylphosphonate
92-52-4	1,1 biphenyl
1703-52-2	Furan, 2-ethyl-5-methyl-
625-86-5	2,5-Dimethylfuran
71-43-2	Benzene
78-94-4	3-Buten-2-one
1184-60-7	2-fluoro-1-Propene
3457-91-8	1,4-Butanediol, dinitrate
544-16-1	Nitrous acid, butyl ester
624-91-9	Nitrous acid, methyl ester
108-47-4	2, 4-Dimethylpyridine
71-36-3	1-Butanol
126-73-8	Tri-n-butylphosphate
106-99-0	1,3-Butadiene
3777-69-3	2-Pentylfuran
110-86-1	Pyridine
105-42-0	4-Methyl-2-hexanone
814-78-8	3-Buten-2-one, 3-methyl-

CAS	Chemical Name
34379-54-9	Furan, 2,3-dihydro-4-(1-methylpropyl)-, (S)-
624-83-9	Methyl isocyanate
4179-38-8	Furan, 2-octyl-
107-12-0	Propanenitrile
50-00-0	Formaldehyde
1115-11-3	2-Butenal, 2-methyl-
594-70-7	Propane, 2-methyl-2-nitro-
75-05-8	Acetonitrile
51595-87-0	2-Heptanone, 6-(2-furanyl)-6-methyl-
717-21-5	2-Propen-1-one, 3-(2-furanyl)-1-phenyl-
34314-82-4	Furan, 3-(1,1-dimethylethyl)-2,3-dihydro-
75-07-0	Acetaldehyde
109-74-0	Butanenitrile
123-72-8	Butanal
928-68-7	6-Methyl-2-heptanone
645-62-5	2-Hexenal, 2-ethyl-
84-66-2	Diethylphthalate
110-59-8	Pentanenitrile
623-87-0	1,3-dinitrate-1,2,3-Propanetriol
67-56-1	Methanol
628-73-9	Hexanenitrile
75-04-7	Ethylamine
591-78-6	Methyl n-butyl ketone
928-45-0	Butyl nitrate
1647-11-6	Butanenitrile, 2-methylene-
1615-70-9	2,4-Pentadienenitrile
629-08-3	Heptanenitrile

Table B.2. Chemical identification of CAS IDs from filtered non-COPC:OEL ratios shown in Figure 6.2 listed in decreasing order of COPC:OEL ratio

CAS	Chemical Name
621-64-7	n-Nitrosodipropylamine
930-55-2	n-Nitrosopyrrolidine
124-40-3	Dimethylamine
924-16-3	n-Nitrosodibutylamine
100-75-4	n-Nitrosopiperdine
629-50-5	n-Tridecane
112-40-3	Dodecane
10102-44-0	Nitrogen Dioxide
629-78-7	n-Heptadecane

CAS	Chemical Name
75-09-2	Methylene Chloride
74-89-5	Methylamine
10102-43-9	Nitric Oxide
109-99-9	Tetrahydrofuran
67-66-3	Chloroform
629-59-4	n-Tetradecane
78-93-3	2-Butanone
79-01-6	Trichloroethylene/Trichloroethene
127-18-4	Tetrachloroethylene
141-78-6	ethyl acetate
56-23-5	Carbon Tetrachloride
108-88-3	Toluene
98-86-2	Acetophenone
3891-98-3	2,6,10-Trimethyldodecane
7446-09-5	Sulfur Dioxide
110-54-3	n-Hexane
71-23-8	1-Propanol
629-62-9	n-Pentadecane
126-98-7	Methyl Acrylonitrile
67-64-1	Acetone
79-34-5	1,1,2,2-Tetrachloroethane
123-86-4	n-Butyl acetate
106-35-4	3-Heptanone
108-10-1	Methyl isobutyl ketone
544-76-3	n-Hexadecane
124-18-5	Decane
64-17-5	Ethanol
10061-01-5	cis-1,3-Dichloropropene
10061-02-6	trans-1,3-Dichloropropene
107-05-1	Allyl Chloride
107-18-6	Allyl Alcohol
110-43-0	2-Hepatanone
100-42-5	Styrene
123-38-6	Propionaldehyde
110-82-7	Cyclohexane
75-35-4	1,1-Dichloroethene
79-00-5	1,1,2-Trichloroethane
100-41-4	Ethyl Benzene
110-62-3	Valeraldehyde
542-75-6	1,3-Dichloropropene
75-69-4	Trichlorofluoromethane
107-13-1	2-Propenenitrile

CAS	Chemical Name
123-91-1	1,4-Dioxane
107-06-2	1,2-Dichloroethane
108-90-7	Chlorobenzene
98-95-3	Nitrobenzene
142-82-5	N-Heptane
106-46-7	1, 4-Dichlorobenzene
123-73-9	2-Butenal, (E)-
95-48-7	o-cresol
108-39-4	m-cresol
91-20-3	Naphthalene
75-00-3	Ethyl Chloride
75-34-3	1,1-dichloroethane

Table B.3. Chemical identification of CAS IDs from the top-left region of Figure 6.3 that is expanded and shown Figure 6.4

CAS	Chemical Name
10024-97-2	Nitrous Oxide
1333-74-0	*Hydrogen*
74-82-8	*Methane*
124-38-9	*Carbon Dioxide*
630-08-0	*Carbon Monoxide*
67-64-1	*Acetone*
71-43-2	Benzene
75-05-8	Acetonitrile
107-12-0	Propanenitrile
75-35-4	*1,1-Dichloroethene*
109-74-0	Butanenitrile
127-18-4	*Tetrachloroethylene*
124-18-5	*Decane*
108-88-3	*Toluene*
75-69-4	*Trichlorofluoromethane*
112-40-3	*Dodecane*
142-82-5	*N-Heptane*
109-99-9	*Tetrahydrofuran*
7664-41-7	Ammonia
67-66-3	*Chloroform*
71-36-3	1-Butanol
56-23-5	*Carbon Tetrachloride*
71-23-8	*1-Propanol*
629-50-5	*n-Tridecane*

CAS	Chemical Name
75-09-2	*Methylene Chloride*
110-54-3	*n-Hexane*
75-00-3	*Ethyl Chloride*
108-90-7	*Chlorobenzene*
79-34-5	*1,1,2,2-Tetrachloroethane*
100-41-4	*Ethyl Benzene*
78-93-3	*2-Butanone*
100-42-5	*Styrene*
79-01-6	*Trichloroethylene/Trichloroethene*
64-17-5	*Ethanol*
95-63-6	*1,2,4-Trimethylbenzene*
1120-21-4	*n-Undecane*
95-47-6	*ortho-xylene*
74-87-3	*Methyl Chloride*
107-06-2	*1,2-Dichloroethane*
7727-37-9	*Nitrogen*
7440-59-7	*Helium*
79-00-5	*1,1,2-Trichloroethane*
108-10-1	*Methyl isobutyl ketone*
75-71-8	*Dichlorofluoromethane*
111-65-9	*N-Octane*
110-86-1	Pyridine
10102-43-9	*Nitric Oxide*
10102-44-0	*Nitrogen Dioxide*
108-38-3M	*m,p-xylene*
75-01-4	*Vinyl chloride*
111-84-2	*Nonane*
10061-02-6	*trans-1,3-Dichloropropene*
629-59-4	*n-Tetradecane*
75-34-3	*1,1-dichloroethane*
76-13-1	*1,1,2-Trichloro-1,2,2-trifluoroethane*
10061-01-5	*cis-1,3-Dichloropropene*
106-46-7	*1, 4-Dichlorobenzene*
123-72-8	Butanal
628-73-9	Hexanenitrile
110-59-8	Pentanenitrile
108-94-1	*Cyclohexanone*
120-82-1	*1,2,4-Trichlorobenzene*
87-68-3	*Hexachlorobutadiene*
106-97-8	*Butane*
156-59-2	*cis-1,2-Dichloroethene*
78-87-5	*Propylene Dichloride*

CAS	Chemical Name
67-56-1	Methanol
76-14-2	*1,2-Dichlorotetrafluoroethane*
108-67-8	*Mesitylene*
71-55-6	*1,1,1-Trichloroethane*
541-73-1	*m-Dichlorobenzene*
95-50-1	*o-dichlorobenzene*
109-66-0	*N-Pentane*
106-93-4	*1,2-Dibromoethane*
110-82-7	*Cyclohexane*
591-78-6	Methyl n-butyl ketone
126-73-8	Tri-n-butylphosphate
106-99-0	1,3-Butadiene
110-43-0	*2-Hepatanone*
74-83-9	*Methyl bromide*

Italicized chemical are non-COPC chemicals

I

Ammonia and Nitrous Oxide LI Evaluation Figures

Appendix C

Ammonia and Nitrous Oxide LI Evaluation Figures

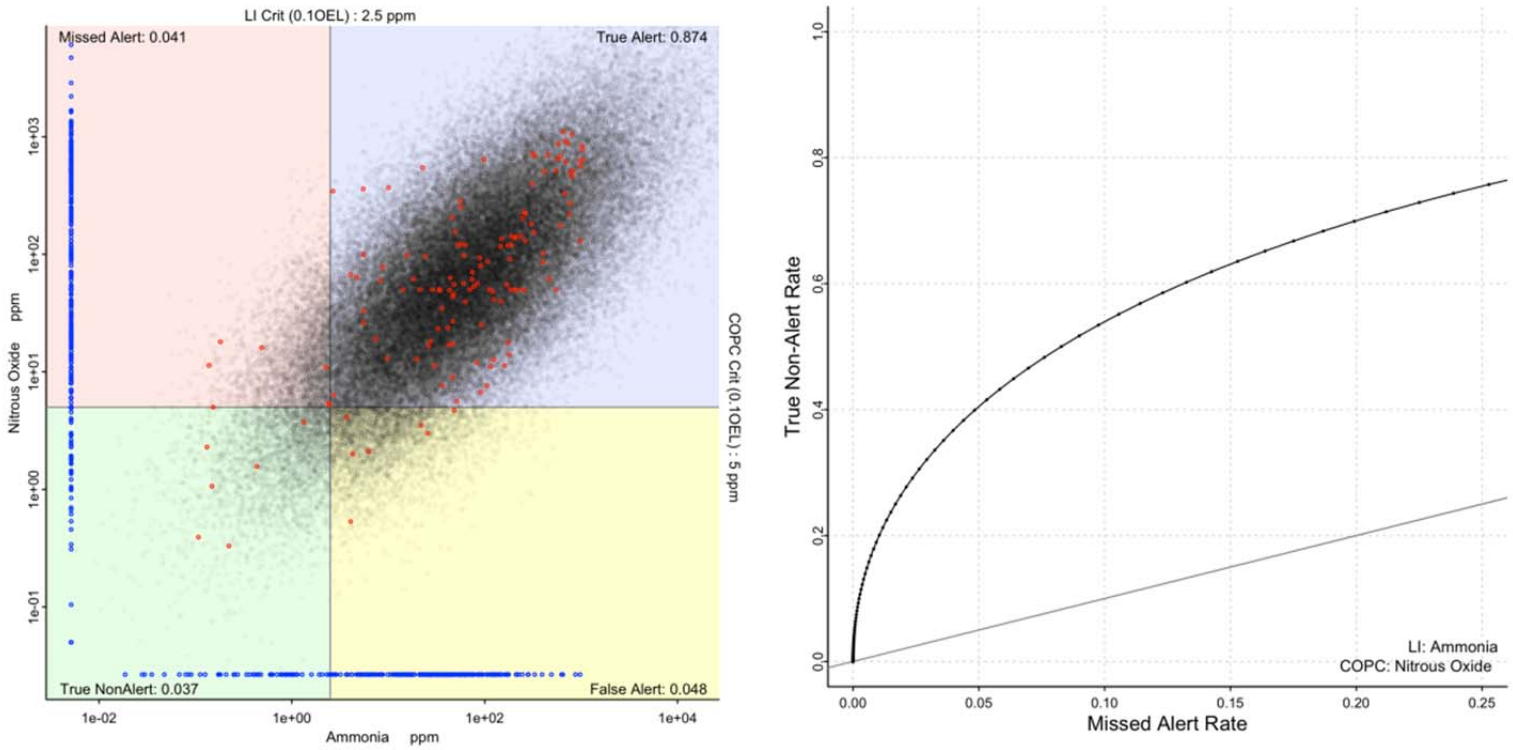

Figure C.1. Left: Scatterplot of nitrous oxide and ammonia measurements (red dots), probability density estimate (black dots), and non-paired or MDL measurements (blue dots) with associated alert quadrants designated by 10% OEL indication lines for each chemical. Right: ROC-like curve displays the change in statistical performance for nitrous oxide and ammonia in terms of paired true non-alert and missed alert probabilities obtained by increasing the LI alert level and noting the changes in these two.

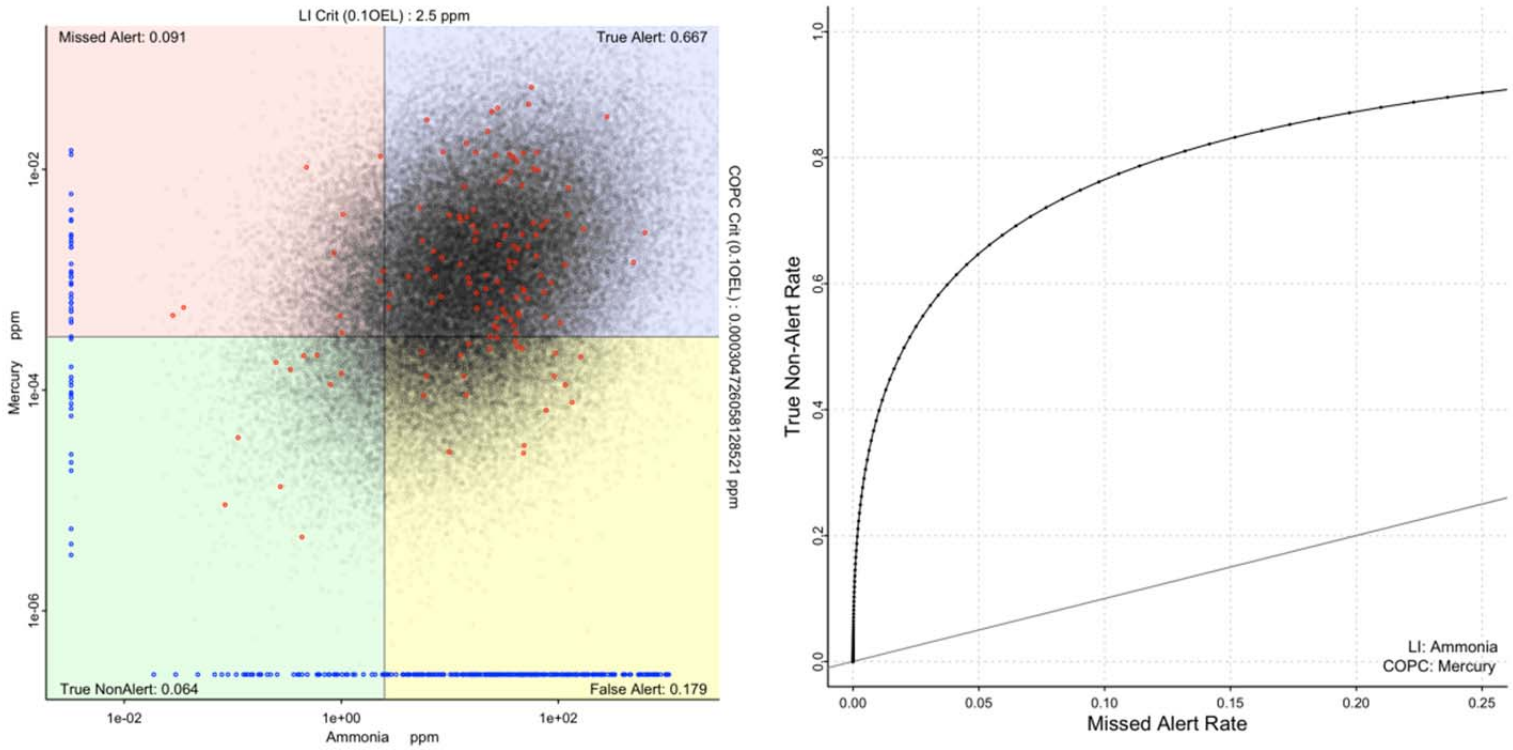

Figure C.2. Left: Scatterplot of mercury and ammonia measurements (red dots), probability density estimate (black dots), and non-paired or MDL measurements (blue dots) with associated alert quadrants designated by 10% OEL indication lines for each chemical. Right: ROC-like curve displays the change in statistical performance for mercury and ammonia in terms of paired true non-alert and missed alert probabilities obtained by increasing the LI alert level and noting the changes in these two.

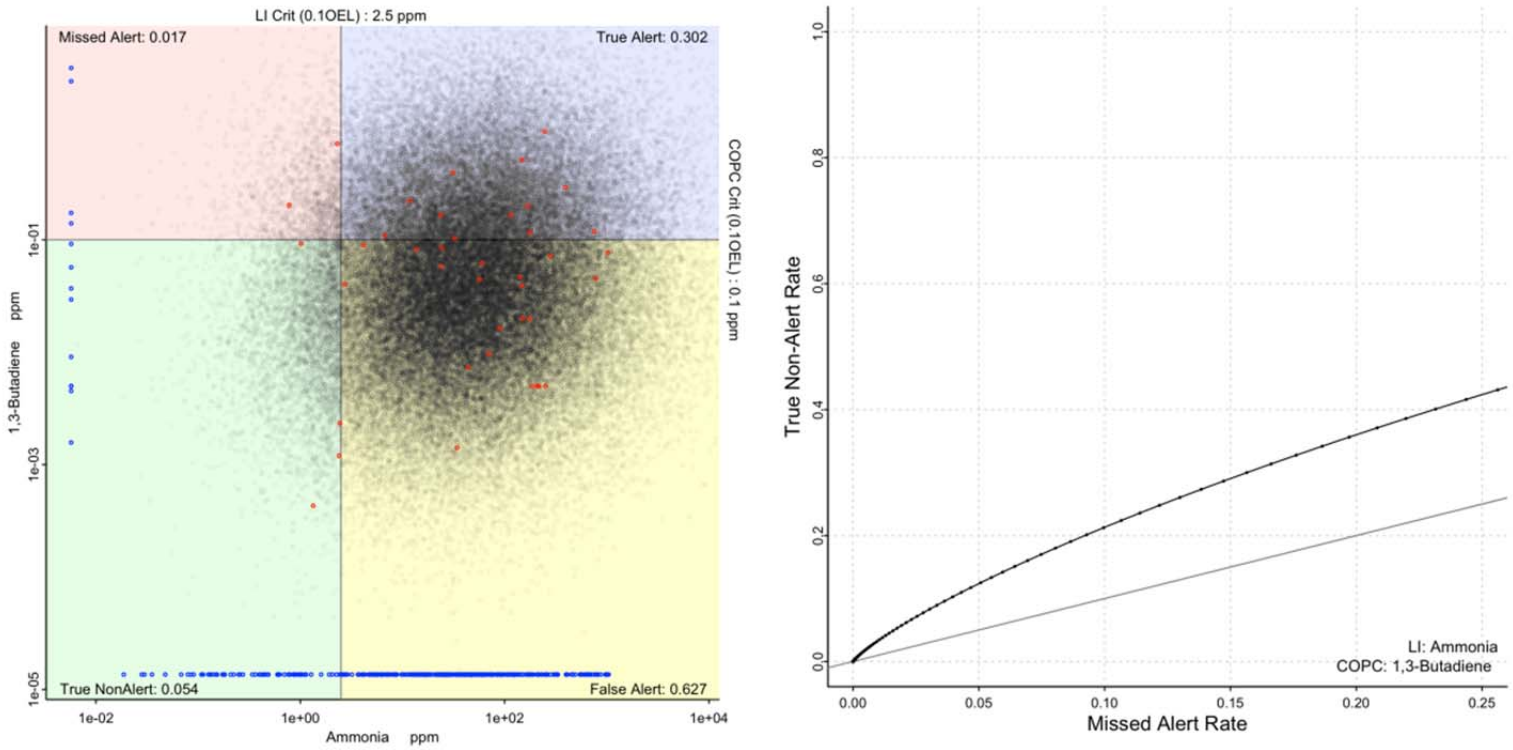

Figure C.3. Left: Scatterplot of 1,3-butadiene and ammonia measurements (red dots), probability density estimate (black dots), and non-paired or MDL measurements (blue dots) with associated alert quadrants designated by 10% OEL indication lines for each chemical. Right: ROC-like curve displays the change in statistical performance for 1,3-butadiene and ammonia in terms of paired true non-alert and missed alert probabilities obtained by increasing the LI alert level and noting the changes in these two.

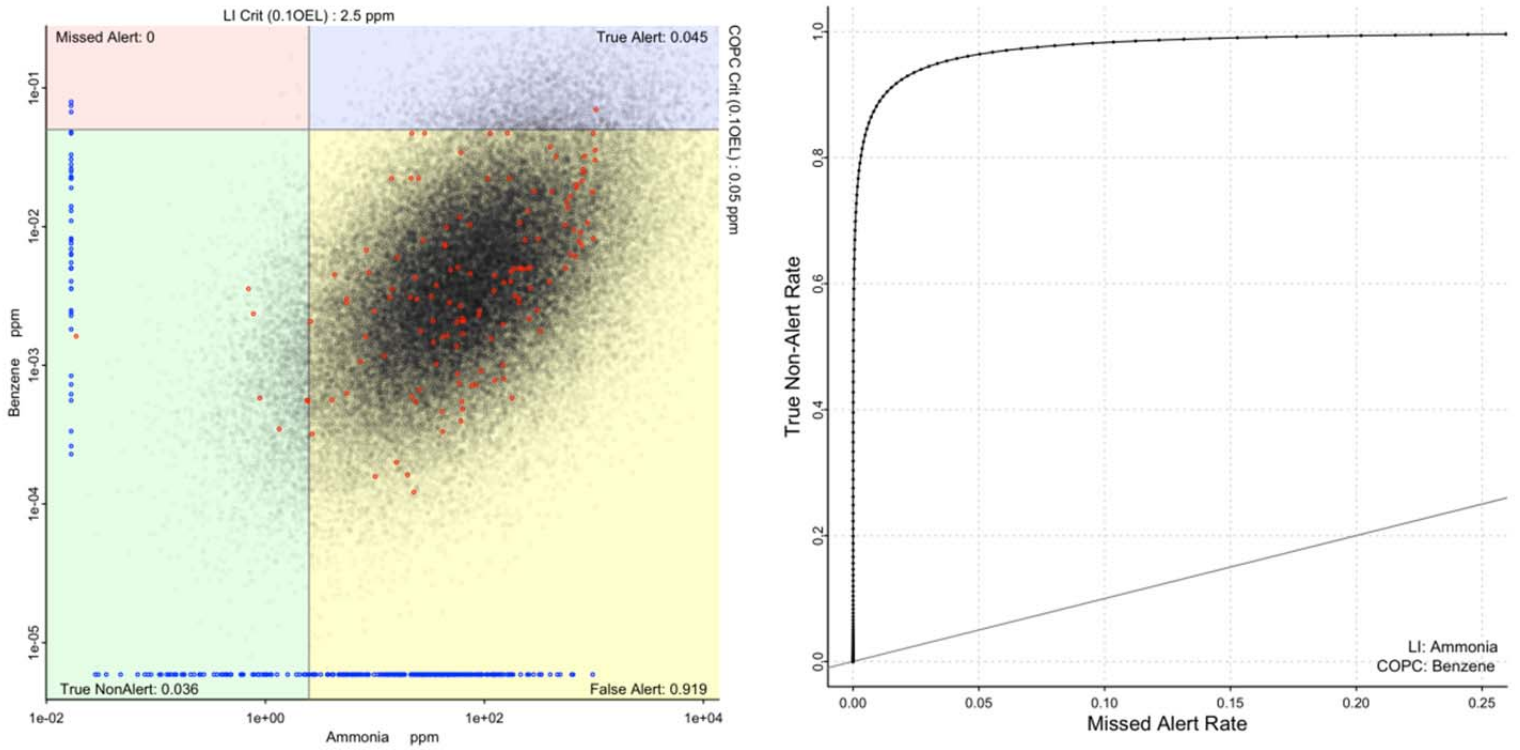

Figure C.4. Left: Scatterplot of benzene and ammonia measurements (red dots), probability density estimate (black dots), and non-paired or MDL measurements (blue dots) with associated alert quadrants designated by 10% OEL indication lines for each chemical. Right: ROC-like curve displays the change in statistical performance for benzene and ammonia in terms of paired true non-alert and missed alert probabilities obtained by increasing the LI alert level and noting the changes in these two.

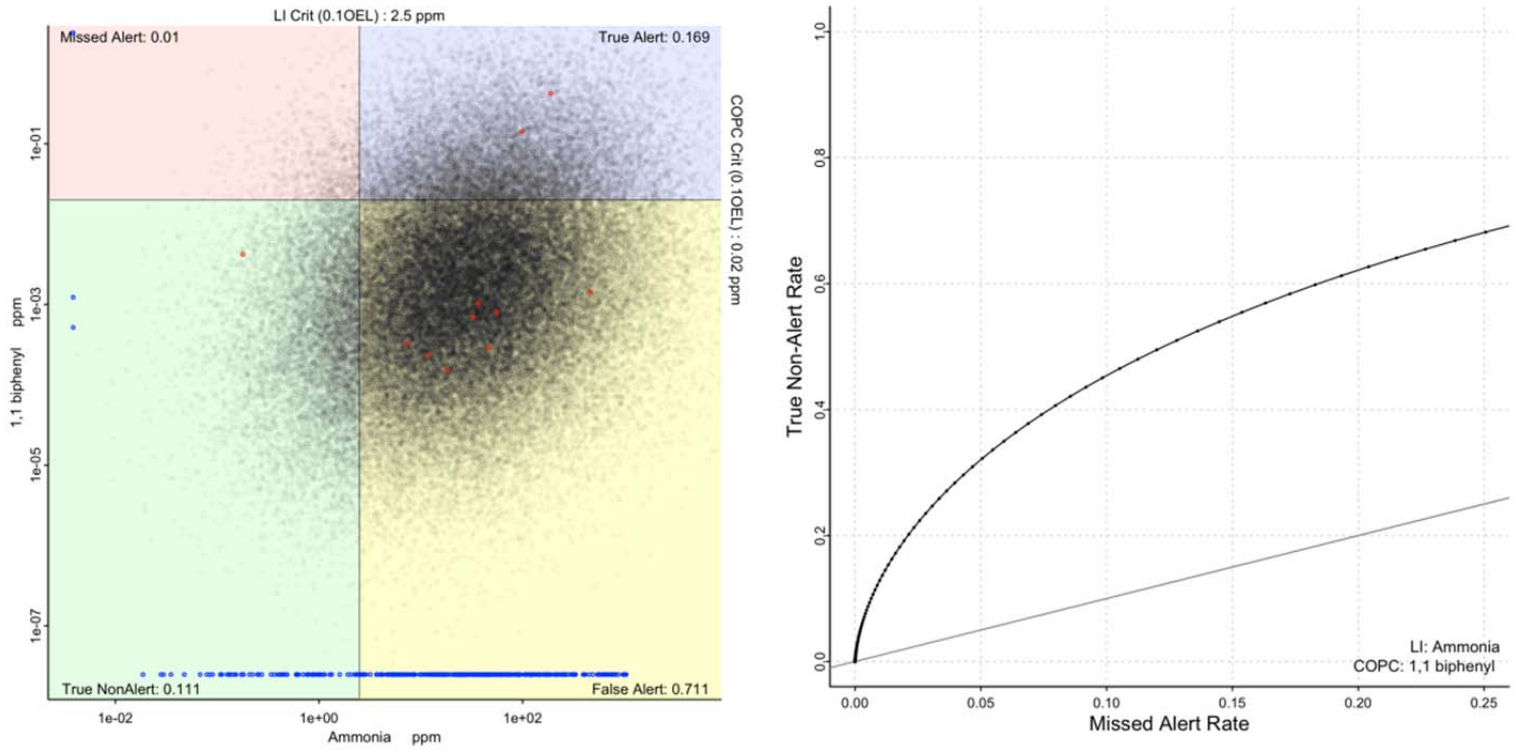

Figure C.5. Left: Scatterplot of 1,1 biphenyl and ammonia measurements (red dots), probability density estimate (black dots), and non-paired or MDL measurements (blue dots) with associated alert quadrants designated by 10% OEL indication lines for each chemical. Right: ROC-like curve displays the change in statistical performance for 1,1 biphenyl and ammonia in terms of paired true non-alert and missed alert probabilities obtained by increasing the LI alert level and noting the changes in these two.

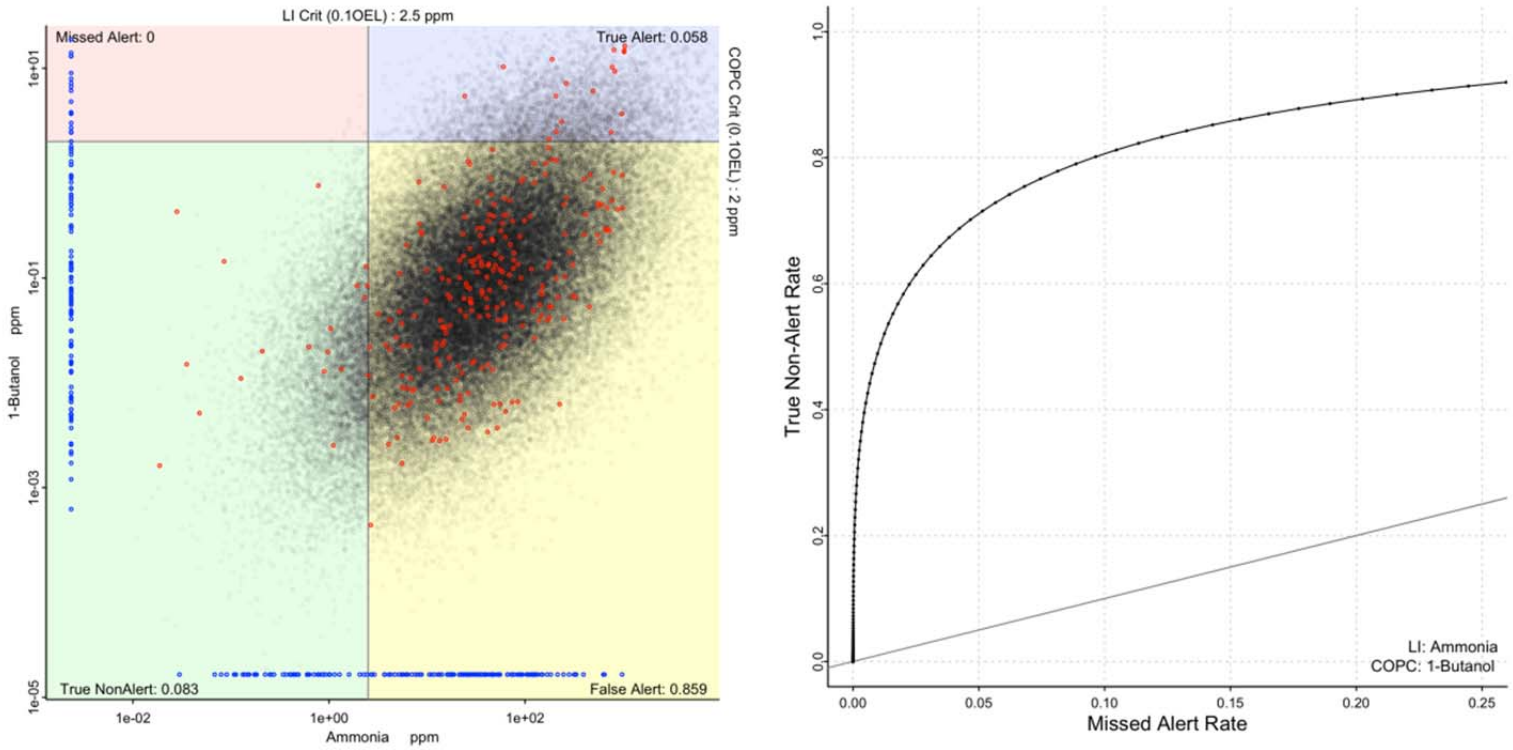

Figure C.6. Left: Scatterplot of 1-butanol and ammonia measurements (red dots), probability density estimate (black dots), and non-paired or MDL measurements (blue dots) with associated alert quadrants designated by 10% OEL indication lines for each chemical. Right: ROC-like curve displays the change in statistical performance for 1-butanol and ammonia in terms of paired true non-alert and missed alert probabilities obtained by increasing the LI alert level and noting the changes in these two.

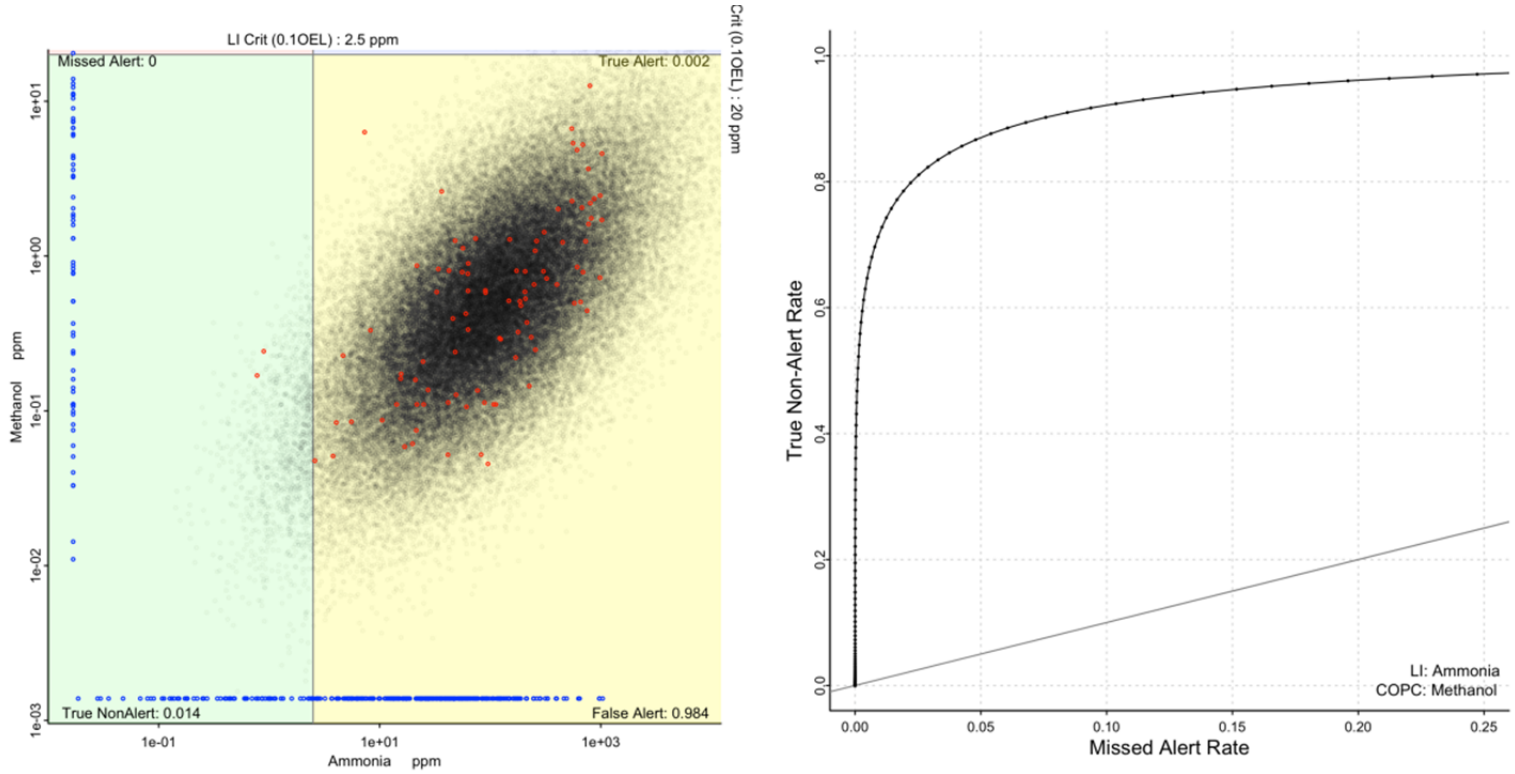

Figure C.7. Left: Scatterplot of methanol and ammonia measurements (red dots), probability density estimate (black dots), and non-paired or MDL measurements (blue dots) with associated alert quadrants designated by 10% OEL indication lines for each chemical. Right: ROC-like curve displays the change in statistical performance for methanol and ammonia in terms of paired true non-alert and missed alert probabilities obtained by increasing the LI alert level and noting the changes in these two.

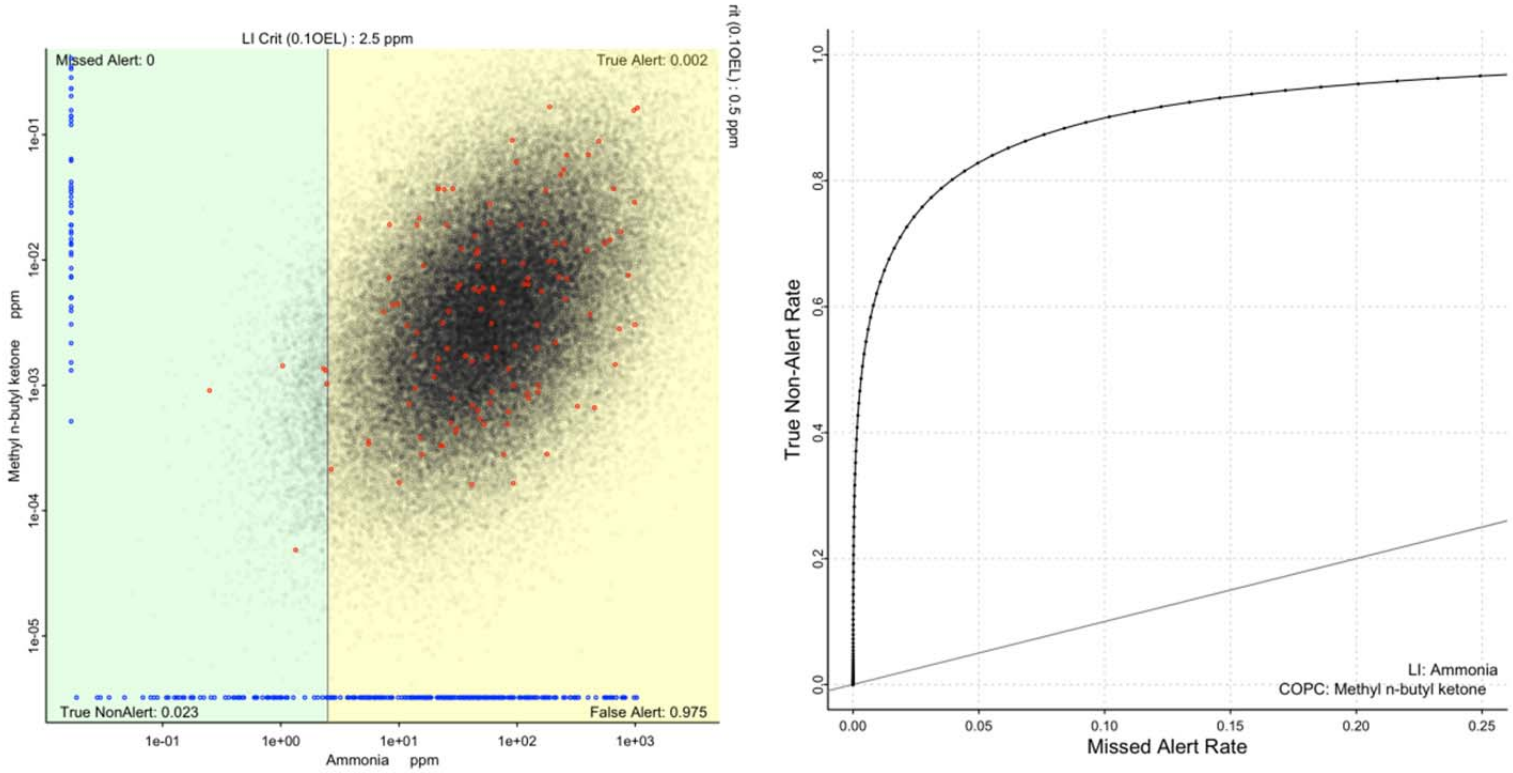

Figure C.8. Left: Scatterplot of methyl n-butyl ketone and ammonia measurements (red dots), probability density estimate (black dots), and non-paired or MDL measurements (blue dots) with associated alert quadrants designated by 10% OEL indication lines for each chemical. Right: ROC-like curve displays the change in statistical performance for methyl n-butyl ketone and ammonia in terms of paired true non-alert and missed alert probabilities obtained by increasing the LI alert level and noting the changes in these two.

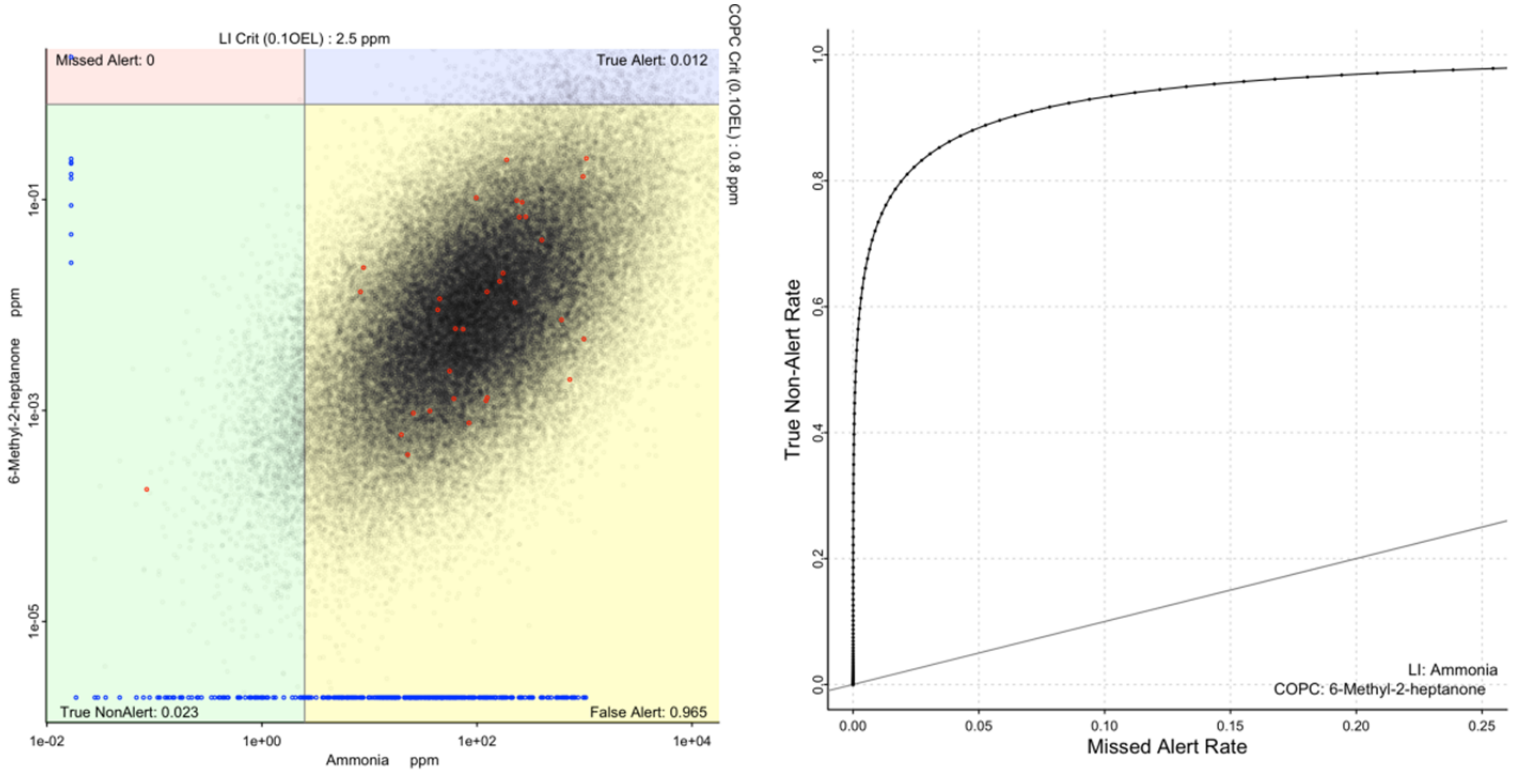

Figure C.9. Left: Scatterplot of 6-methyl-2-heptanone and ammonia measurements (red dots), probability density estimate (black dots), and non-paired or MDL measurements (blue dots) with associated alert quadrants designated by 10% OEL indication lines for each chemical. Right: ROC-like curve displays the change in statistical performance for 6-methyl-2-heptanone and ammonia in terms of paired true non-alert and missed alert probabilities obtained by increasing the LI alert level and noting the changes in these two.

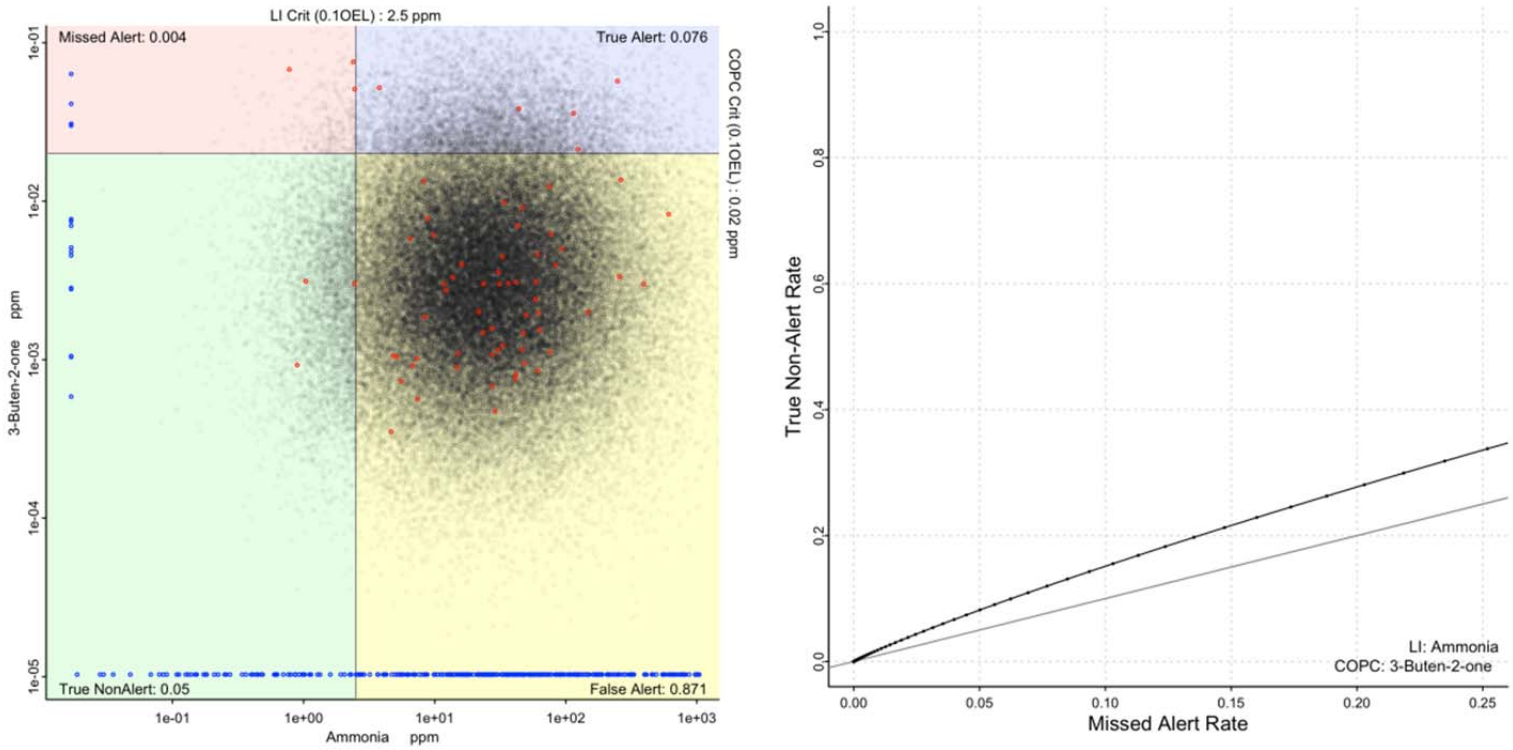

Figure C.10. Left: Scatterplot of 3-buten-3-one and ammonia measurements (red dots), probability density estimate (black dots), and non-paired or MDL measurements (blue dots) with associated alert quadrants designated by 10% OEL indication lines for each chemical. Right: ROC-like curve displays the change in statistical performance for 3-buten-2-one and ammonia in terms of paired true non-alert and missed alert probabilities obtained by increasing the LI alert level and noting the changes in these two.

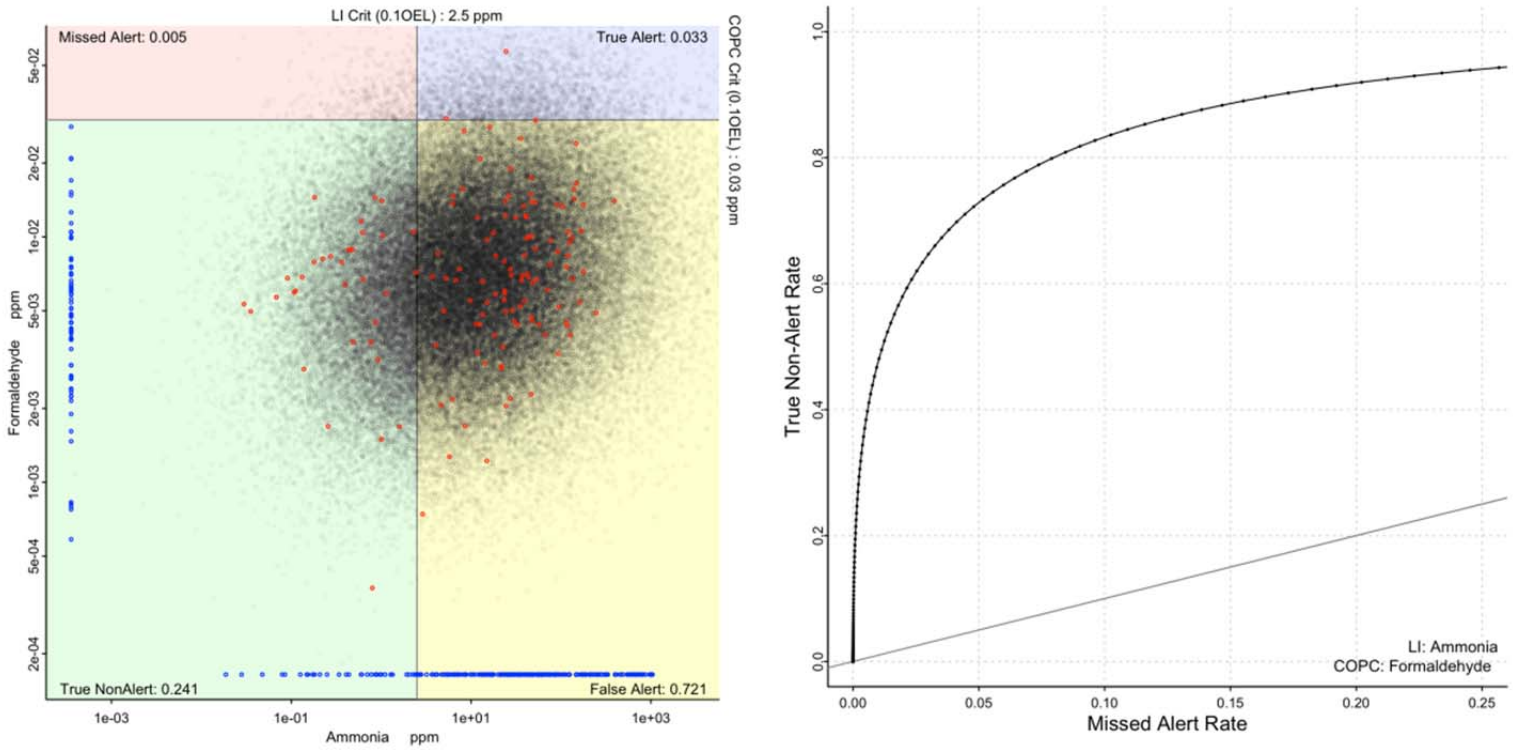

Figure C.11. Left: Scatterplot of formaldehyde and ammonia measurements (red dots), probability density estimate (black dots), and non-paired or MDL measurements (blue dots) with associated alert quadrants designated by 10% OEL indication lines for each chemical. Right: ROC-like curve displays the change in statistical performance for formaldehyde and ammonia in terms of paired true non-alert and missed alert probabilities obtained by increasing the LI alert level and noting the changes in these two.

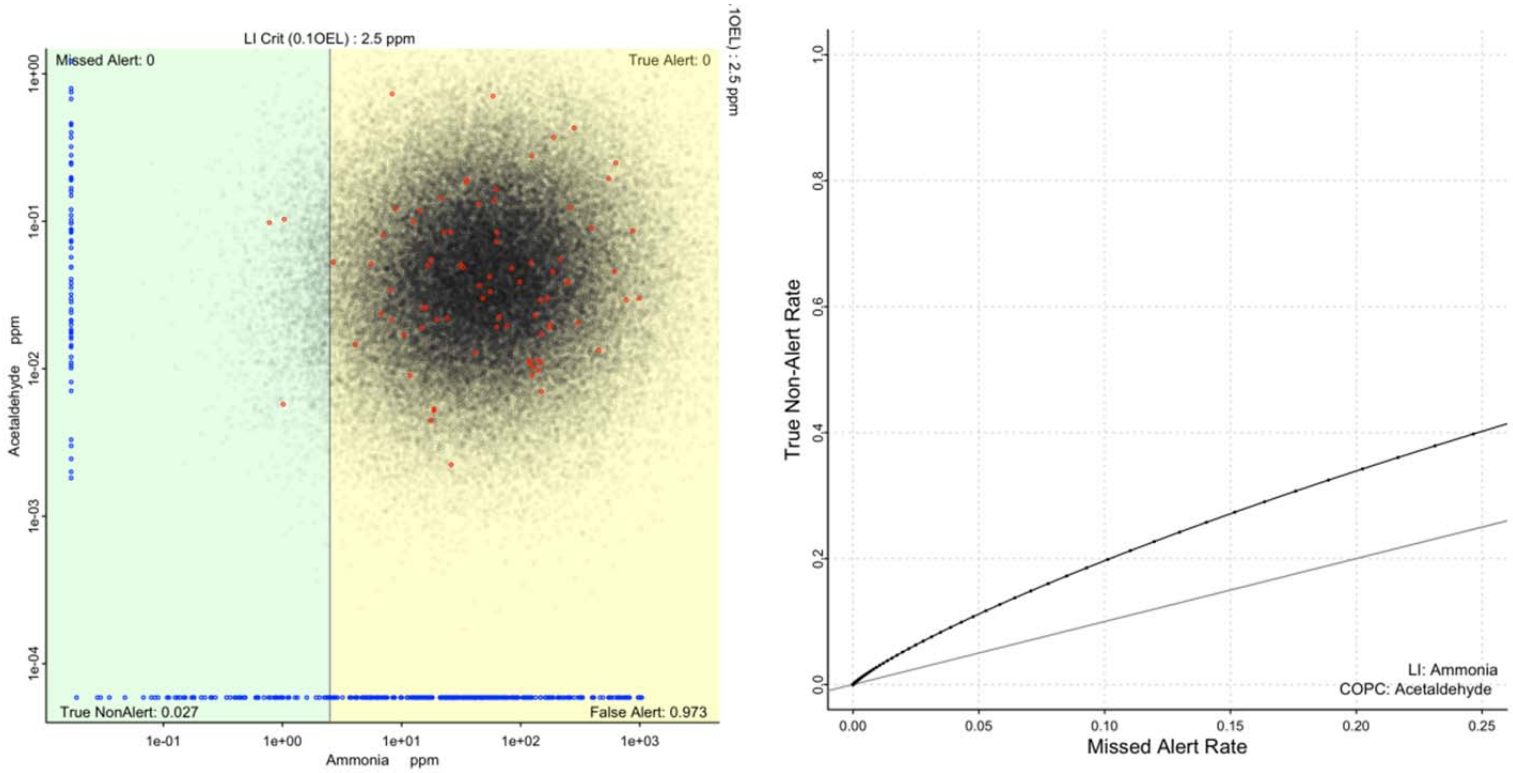

Figure C.12. Left: Scatterplot of acetaldehyde and ammonia measurements (red dots), probability density estimate (black dots), and non-paired or MDL measurements (blue dots) with associated alert quadrants designated by 10% OEL indication lines for each chemical. Right: ROC-like curve displays the change in statistical performance for acetaldehyde and ammonia in terms of paired true non-alert and missed alert probabilities obtained by increasing the LI alert level and noting the changes in these two.

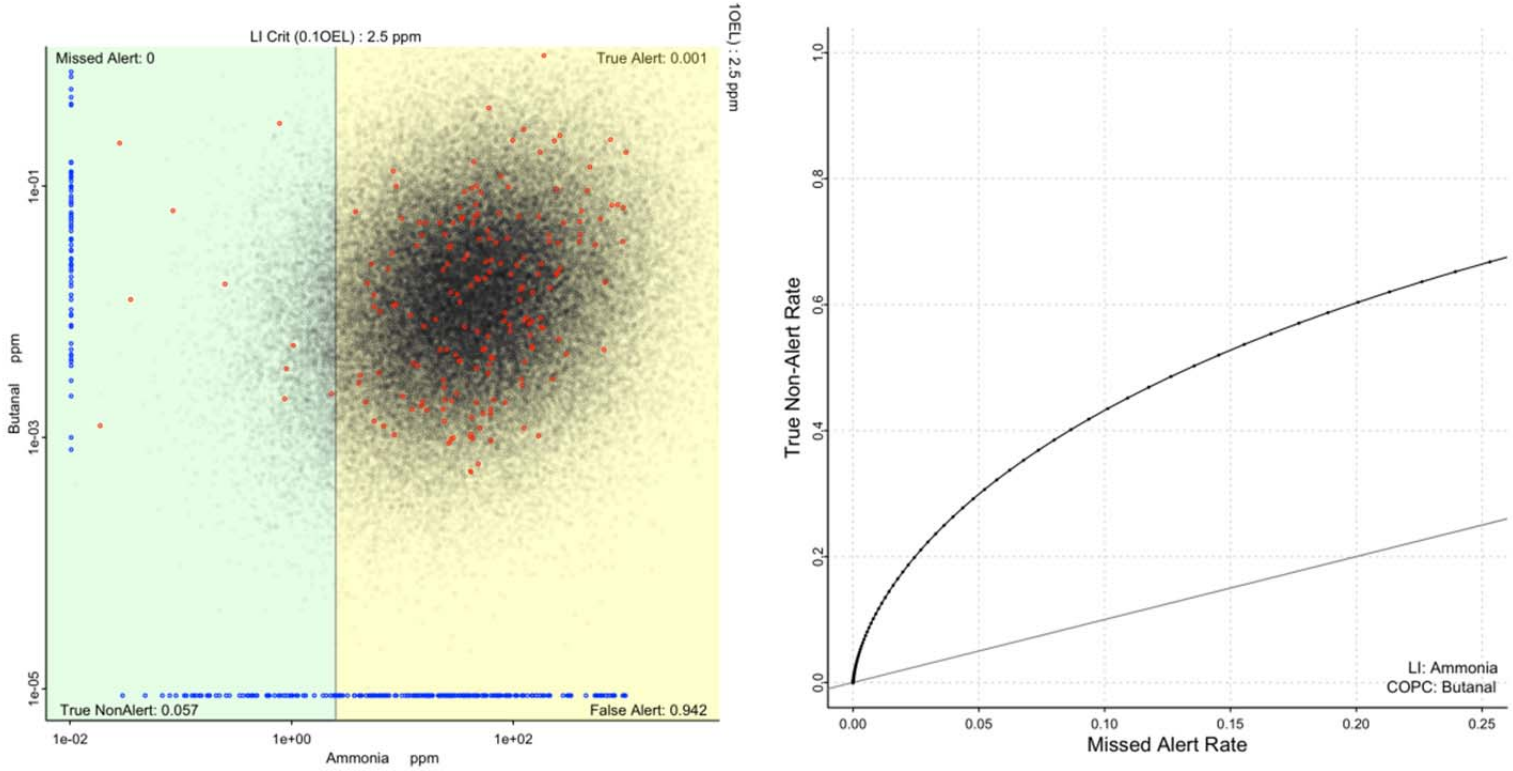

Figure C.13. Left: Scatterplot of butanal and ammonia measurements (red dots), probability density estimate (black dots), and non-paired or MDL measurements (blue dots) with associated alert quadrants designated by 10% OEL indication lines for each chemical. Right: ROC-like curve displays the change in statistical performance for butanal and ammonia in terms of paired true non-alert and missed alert probabilities obtained by increasing the LI alert level and noting the changes in these two.

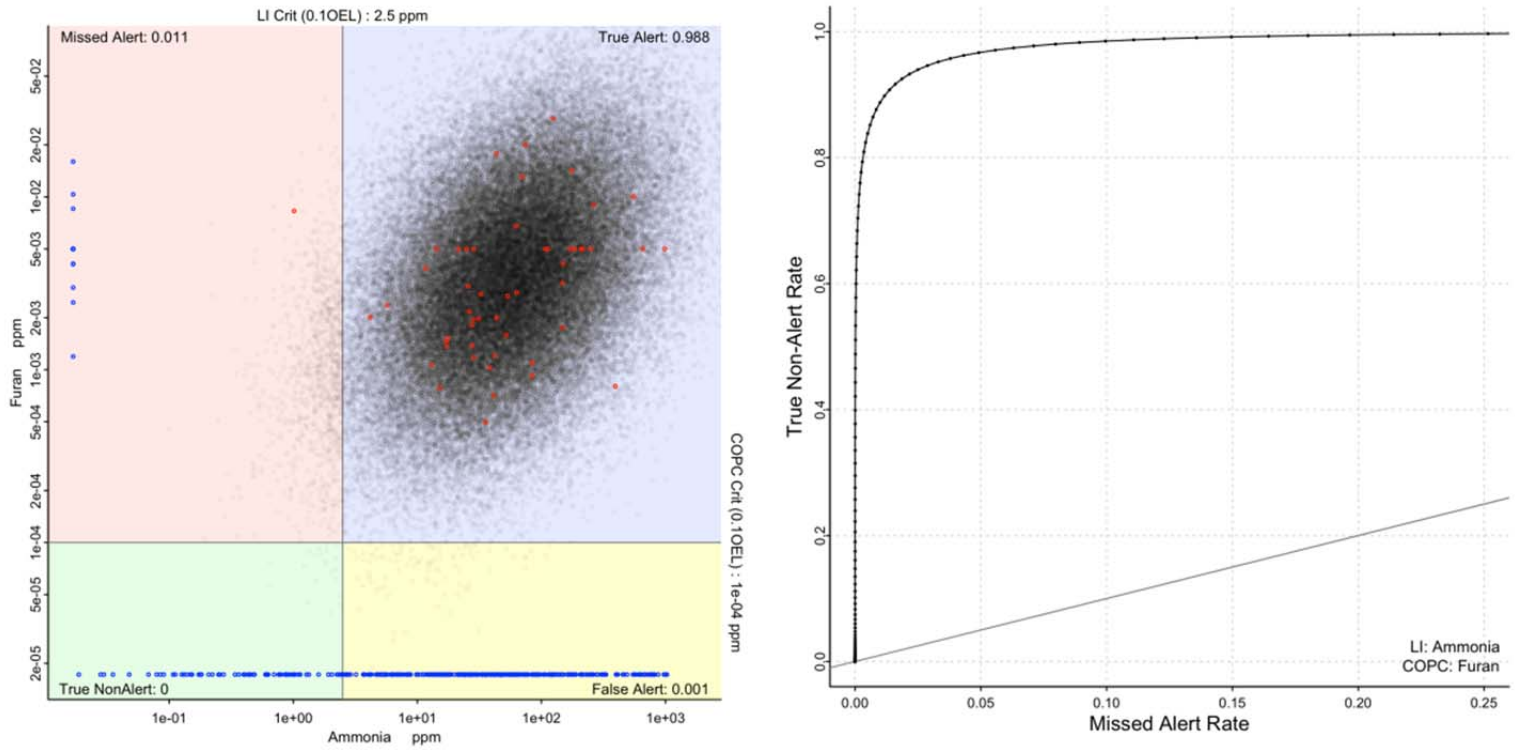

Figure C.14. Left: Scatterplot of furan and ammonia measurements (red dots), probability density estimate (black dots), and non-paired or MDL measurements (blue dots) with associated alert quadrants designated by 10% OEL indication lines for each chemical. Right: ROC-like curve displays the change in statistical performance for furan and ammonia in terms of paired true non-alert and missed alert probabilities obtained by increasing the LI alert level and noting the changes in these two.

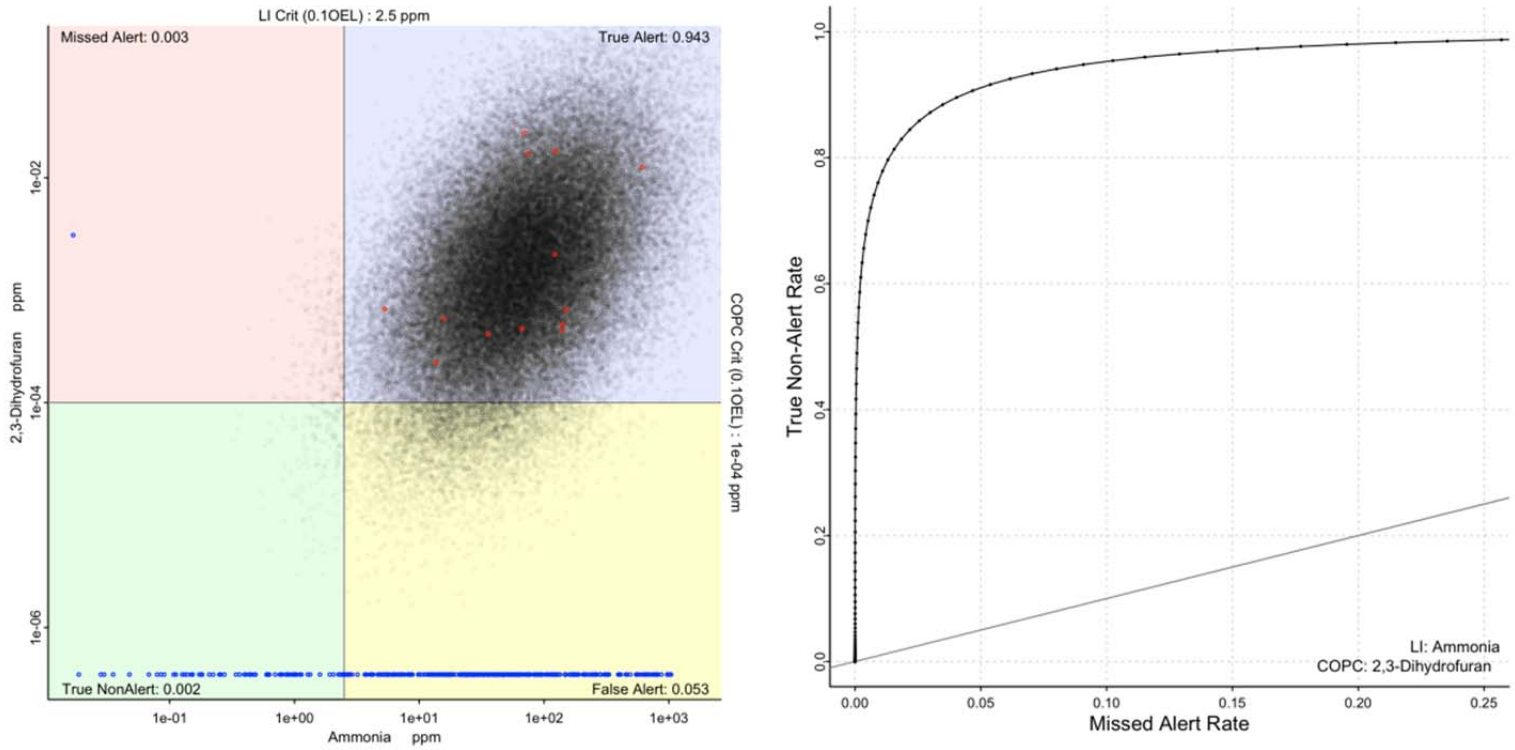

Figure C.15. Left: Scatterplot of 2,3-dihydrofuran and ammonia measurements (red dots), probability density estimate (black dots), and non-paired or MDL measurements (blue dots) with associated alert quadrants designated by 10% OEL indication lines for each chemical. Right: ROC-like curve displays the change in statistical performance for 2,3-dihydrofuran and ammonia in terms of paired true non-alert and missed alert probabilities obtained by increasing the LI alert level and noting the changes in these two.

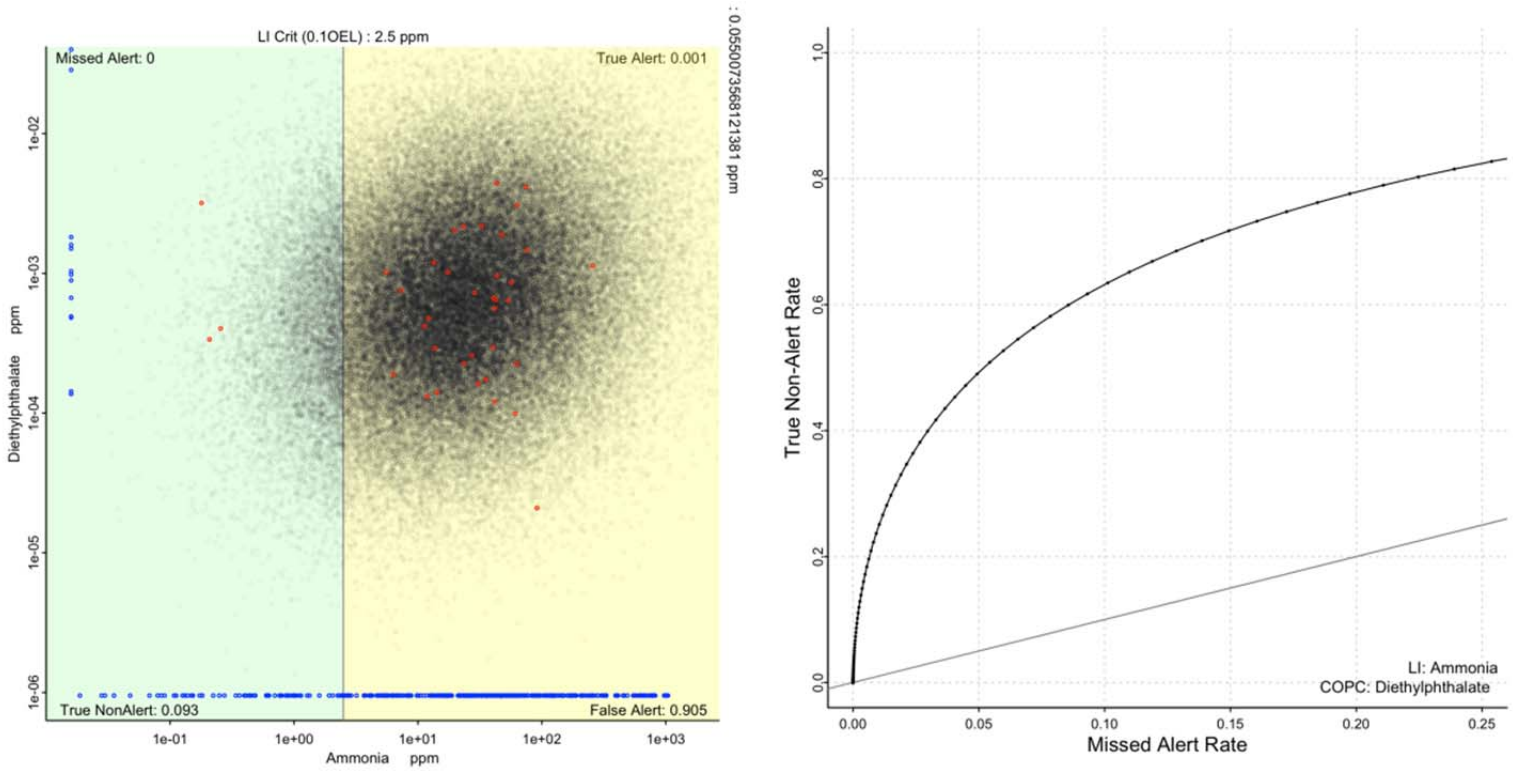

Figure C.16. Left: Scatterplot of diethylphthalate and ammonia measurements (red dots), probability density estimate (black dots), and non-paired or MDL measurements (blue dots) with associated alert quadrants designated by 10% OEL indication lines for each chemical. Right: ROC-like curve displays the change in statistical performance for diethylphthalate and ammonia in terms of paired true non-alert and missed alert probabilities obtained by increasing the LI alert level and noting the changes in these two.

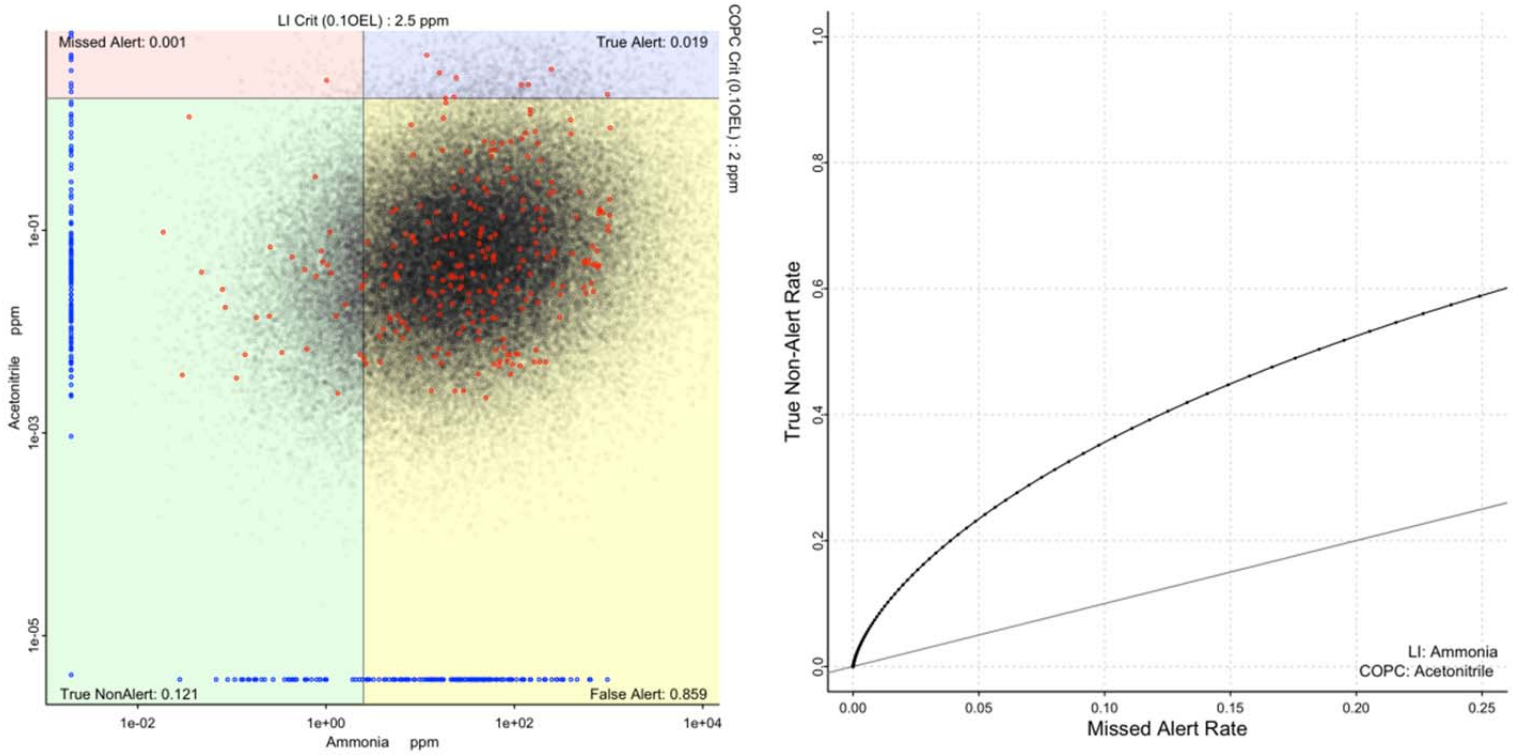

Figure C.17. Left: Scatterplot of acetonitrile and ammonia measurements (red dots), probability density estimate (black dots), and non-paired or MDL measurements (blue dots) with associated alert quadrants designated by 10% OEL indication lines for each chemical. Right: ROC-like curve displays the change in statistical performance for acetonitrile and ammonia in terms of paired true non-alert and missed alert probabilities obtained by increasing the LI alert level and noting the changes in these two.

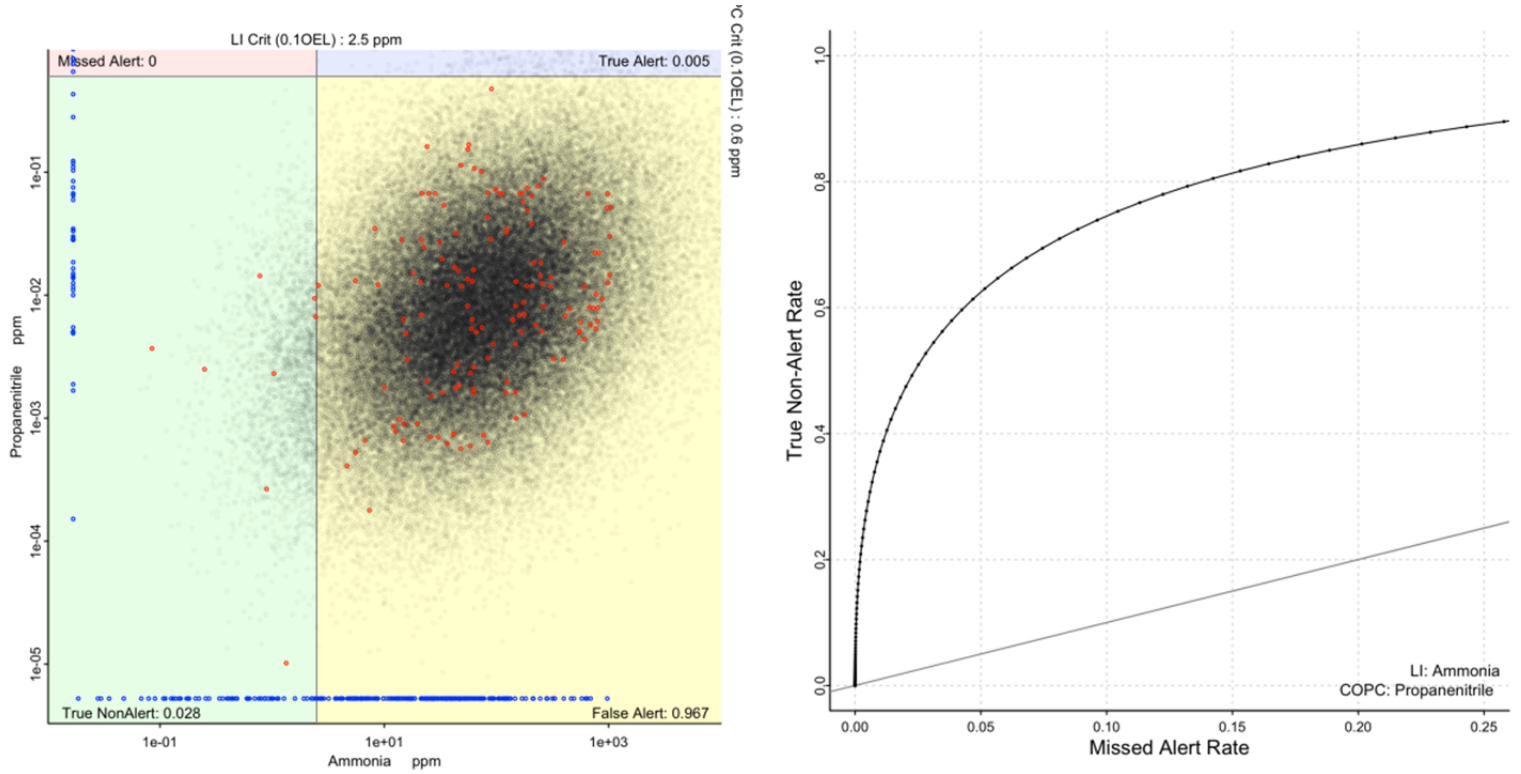

Figure C.18. Left: Scatterplot of propanenitrile and ammonia measurements (red dots), probability density estimate (black dots), and non-paired or MDL measurements (blue dots) with associated alert quadrants designated by 10% OEL indication lines for each chemical. Right: ROC-like curve displays the change in statistical performance for propanenitrile and ammonia in terms of paired true non-alert and missed alert probabilities obtained by increasing the LI alert level and noting the changes in these two.

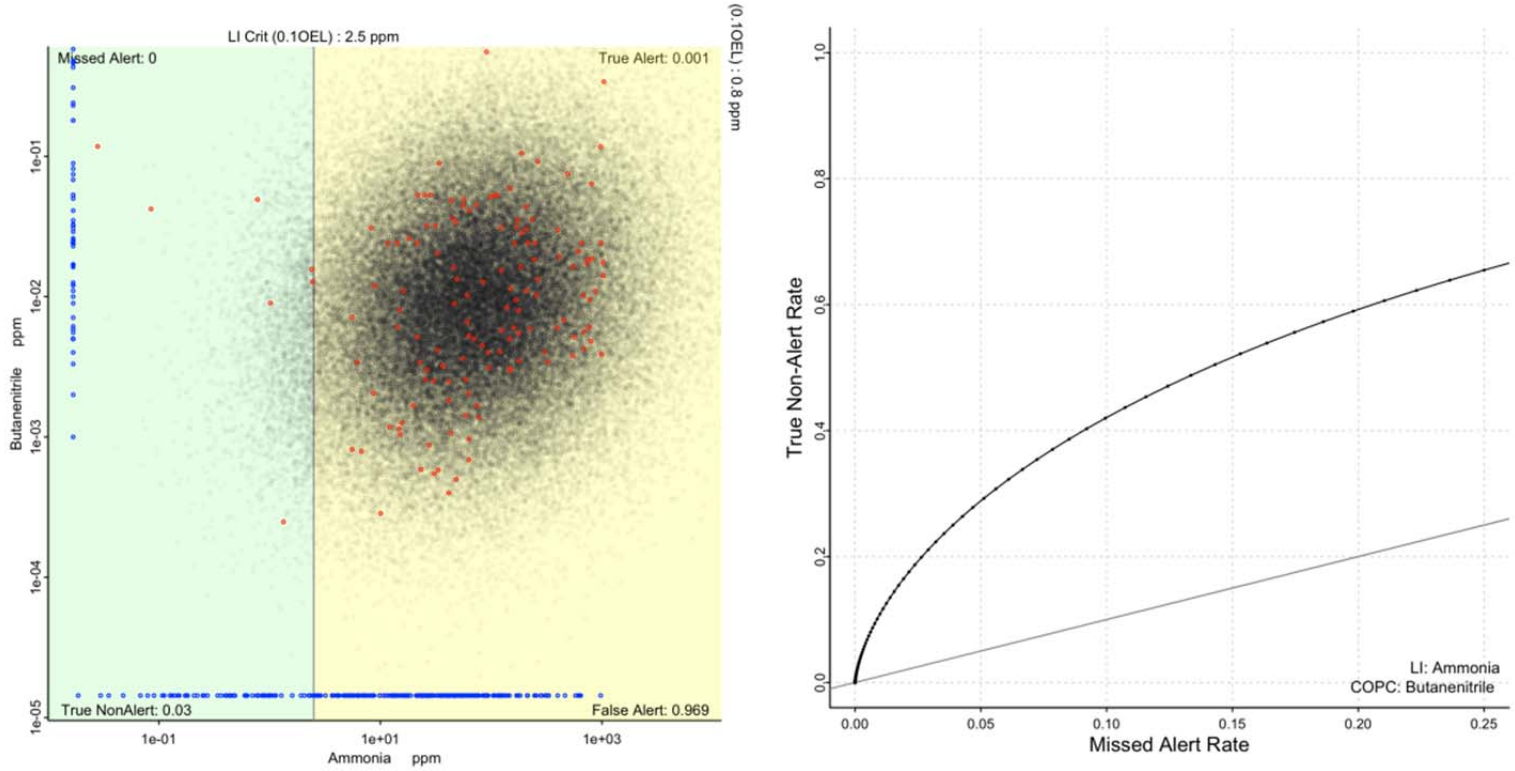

Figure C.19. Left: Scatterplot of butanenitrile and ammonia measurements (red dots), probability density estimate (black dots), and non-paired or MDL measurements (blue dots) with associated alert quadrants designated by 10% OEL indication lines for each chemical. Right: ROC-like curve displays the change in statistical performance for butanenitrile and ammonia in terms of paired true non-alert and missed alert probabilities obtained by increasing the LI alert level and noting the changes in these two.

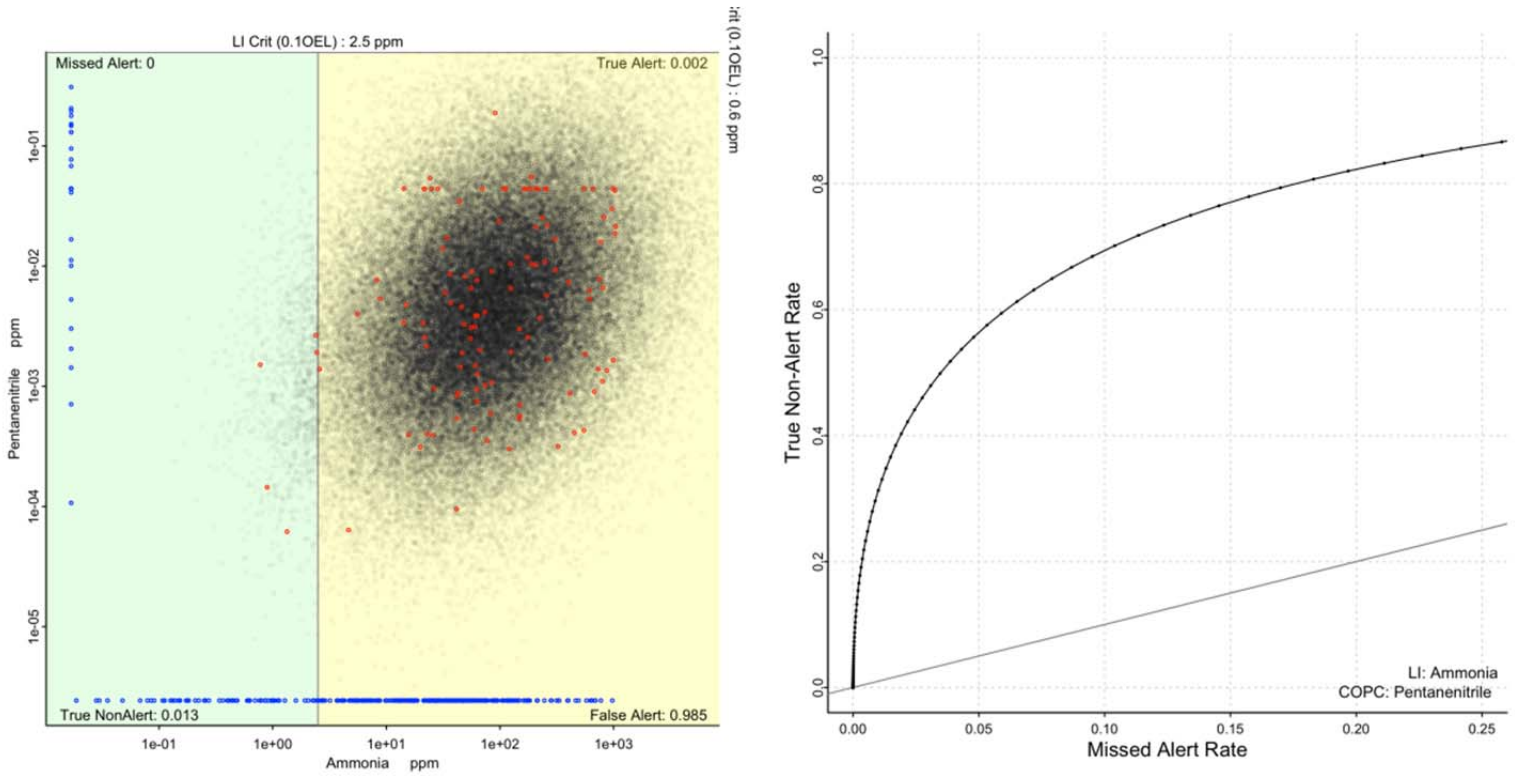

Figure C.20. Left: Scatterplot of pentanenitrile and ammonia measurements (red dots), probability density estimate (black dots), and non-paired or MDL measurements (blue dots) with associated alert quadrants designated by 10% OEL indication lines for each chemical. Right: ROC-like curve displays the change in statistical performance for pentanenitrile and ammonia in terms of paired true non-alert and missed alert probabilities obtained by increasing the LI alert level and noting the changes in these two.

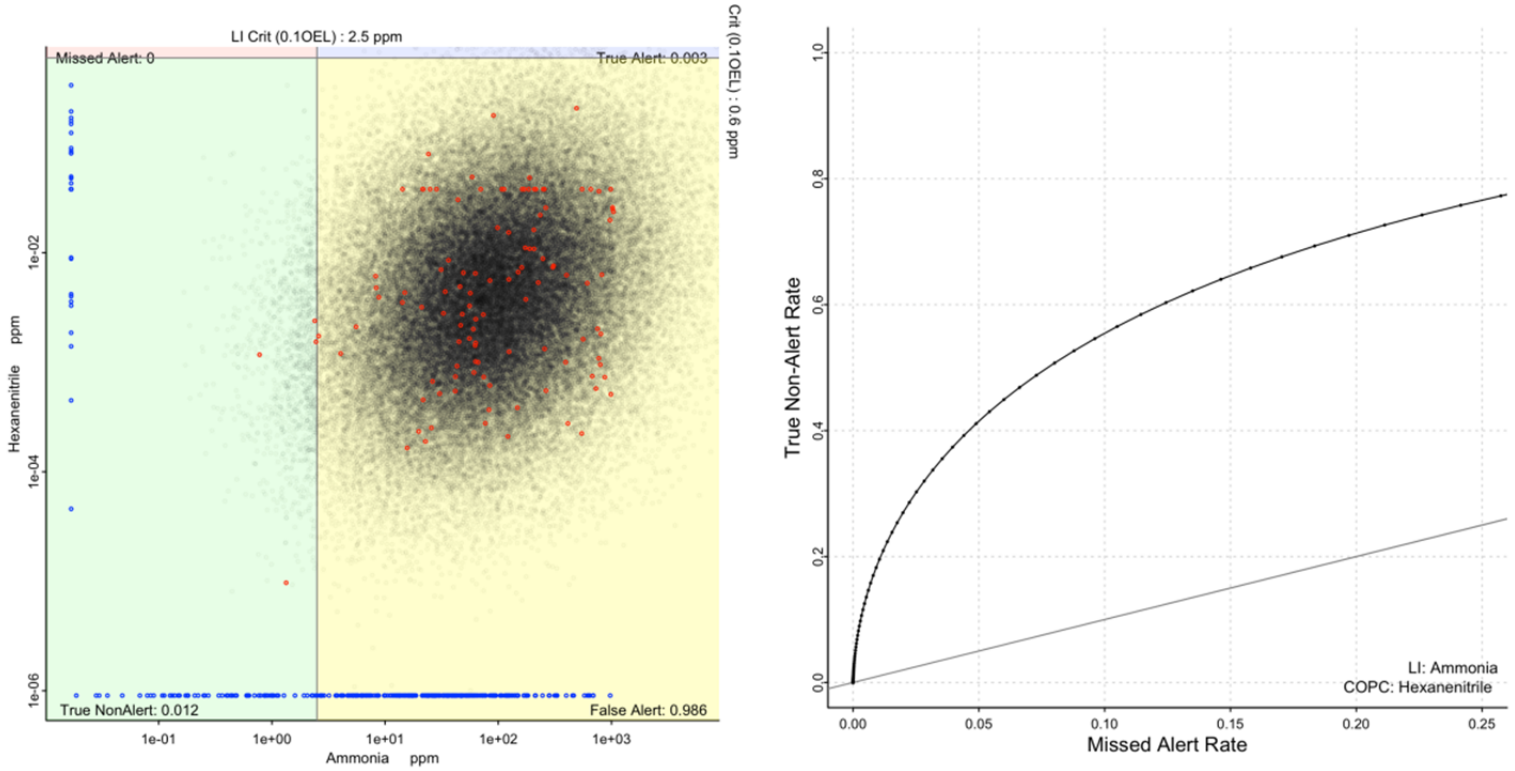

Figure C.21. Left: Scatterplot of hexanenitrile and ammonia measurements (red dots), probability density estimate (black dots), and non-paired or MDL measurements (blue dots) with associated alert quadrants designated by 10% OEL indication lines for each chemical. Right: ROC-like curve displays the change in statistical performance for hexanenitrile and ammonia in terms of paired true non-alert and missed alert probabilities obtained by increasing the LI alert level and noting the changes in these two.

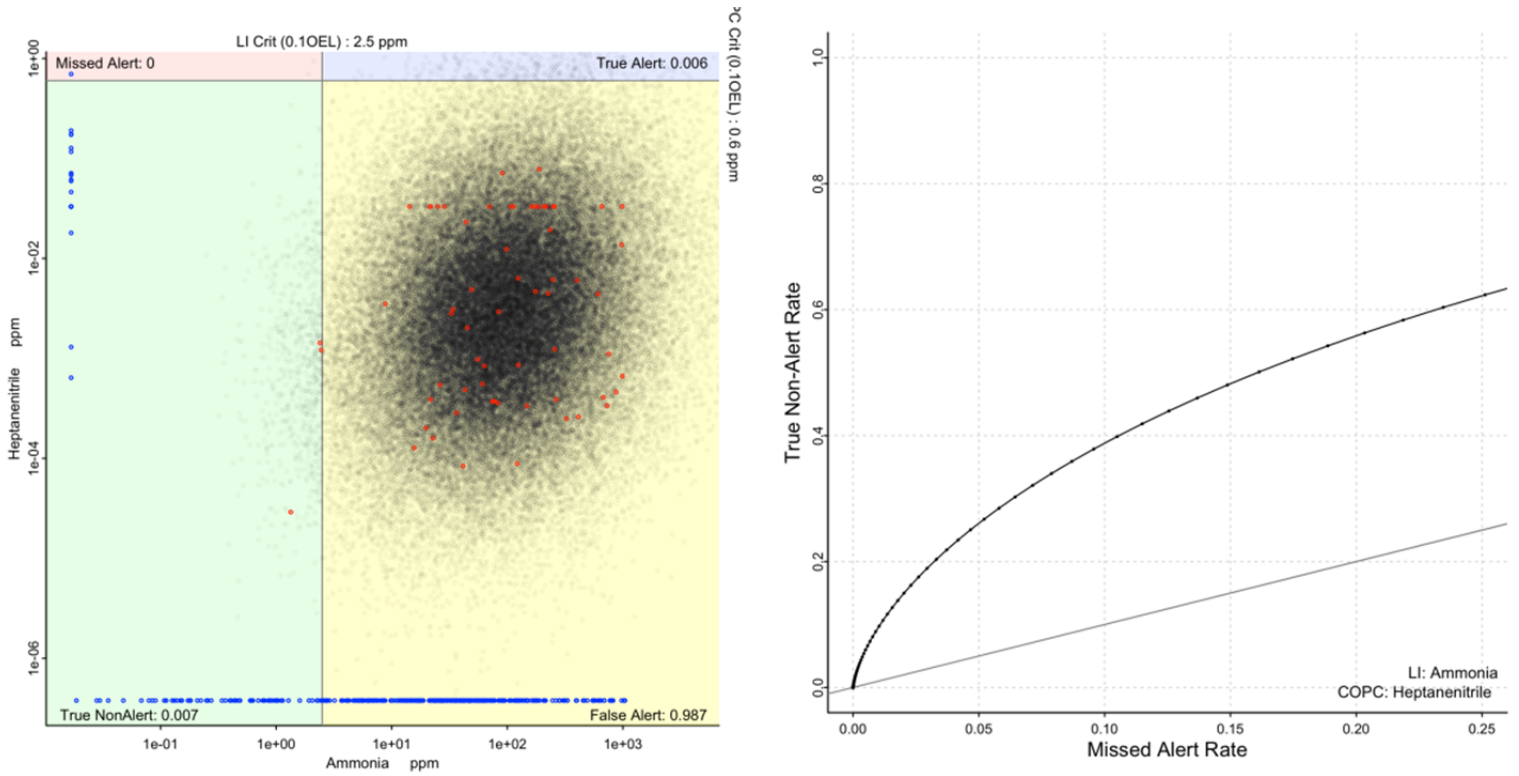

Figure C.22. Left: Scatterplot of heptanenitrile and ammonia measurements (red dots), probability density estimate (black dots), and non-paired or MDL measurements (blue dots) with associated alert quadrants designated by 10% OEL indication lines for each chemical. Right: ROC-like curve displays the change in statistical performance for heptanenitrile and ammonia in terms of paired true non-alert and missed alert probabilities obtained by increasing the LI alert level and noting the changes in these two.

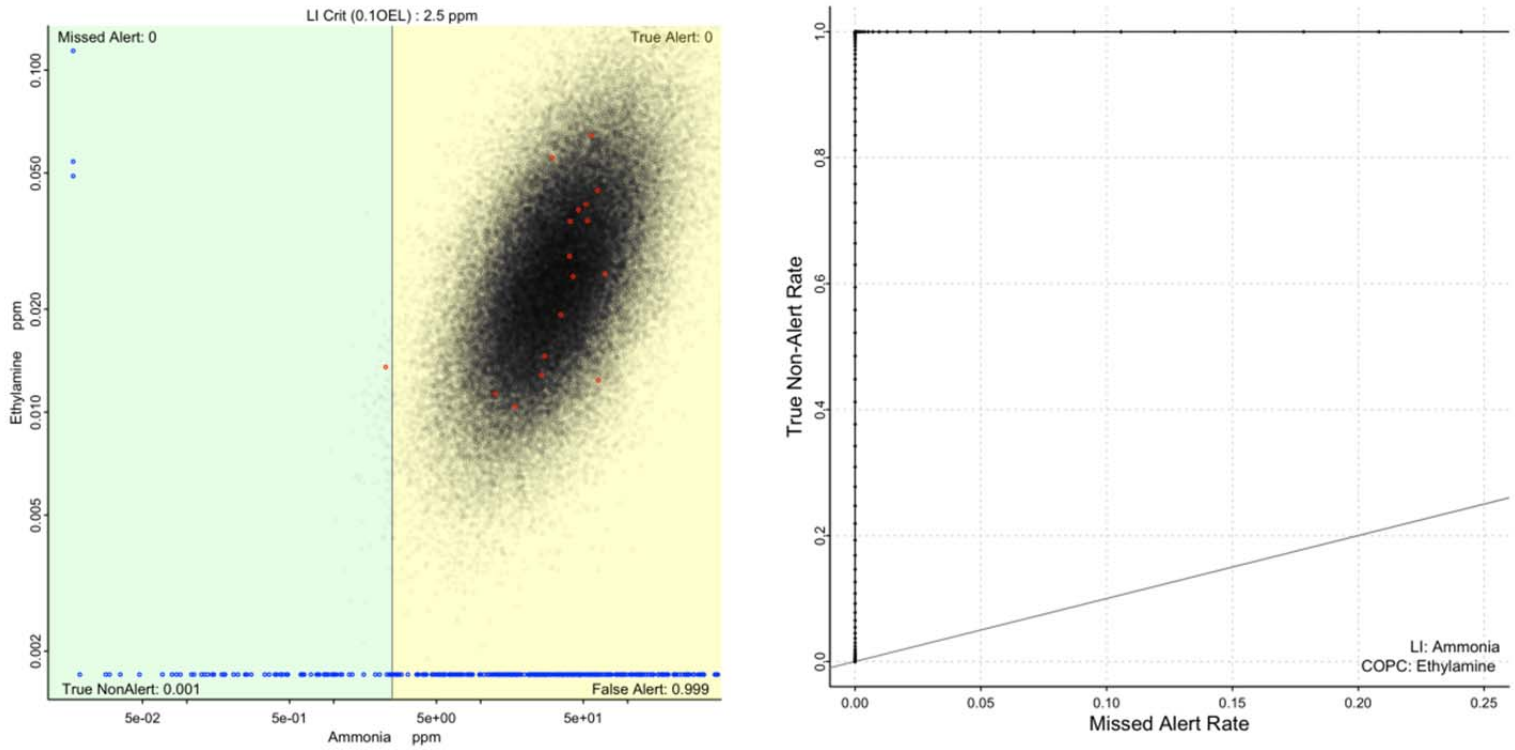

Figure C.23. Left: Scatterplot of ethylamine and ammonia measurements (red dots), probability density estimate (black dots), and non-paired or MDL measurements (blue dots) with associated alert quadrants designated by 10% OEL indication lines for each chemical. Right: ROC-like curve displays the change in statistical performance for ethylamine and ammonia in terms of paired true non-alert and missed alert probabilities obtained by increasing the LI alert level and noting the changes in these two.

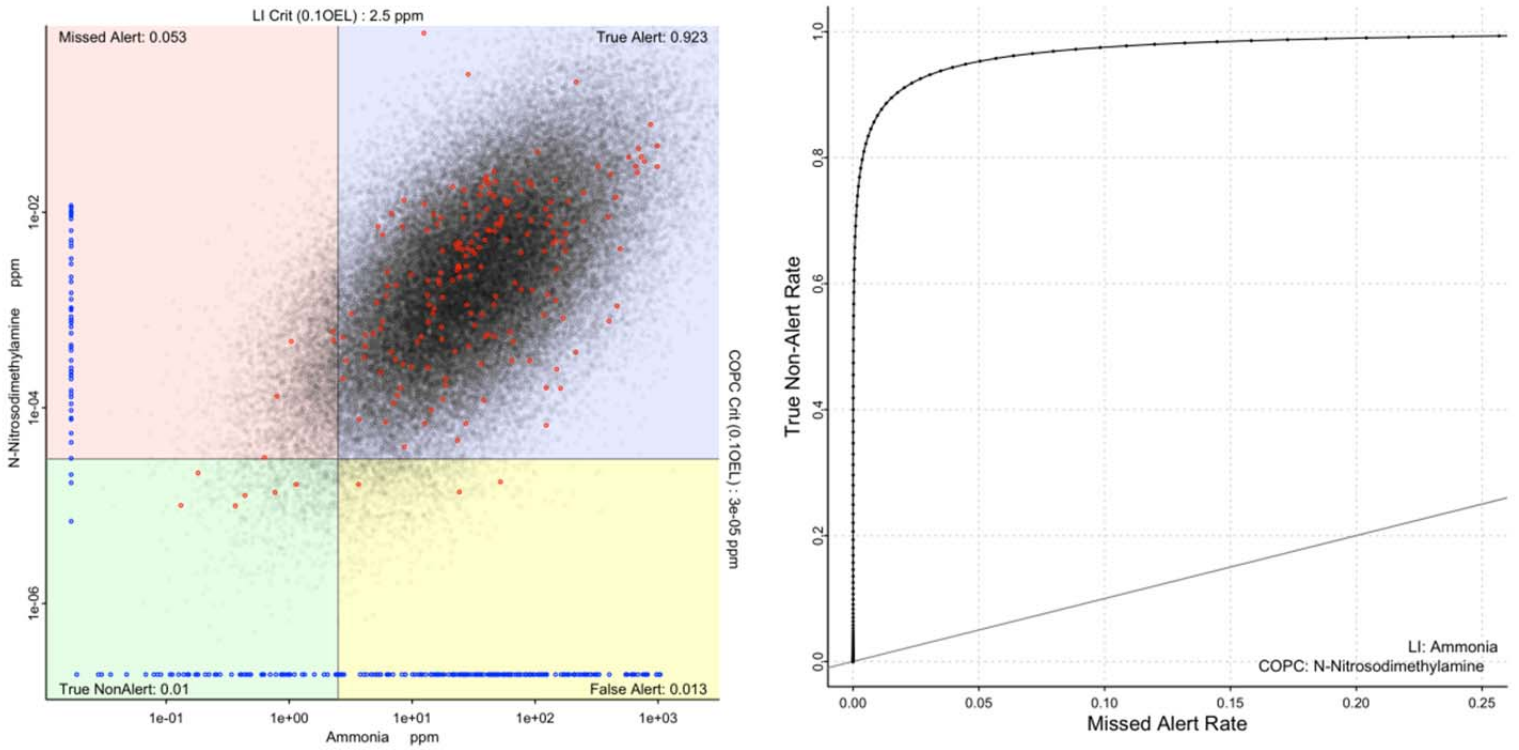

Figure C.24. Left: Scatterplot of n-nitrosodimethylamine and ammonia measurements (red dots), probability density estimate (black dots), and non-paired or MDL measurements (blue dots) with associated alert quadrants designated by 10% OEL indication lines for each chemical. Right: ROC-like curve displays the change in statistical performance for n-nitrosomethylamine and ammonia in terms of paired true non-alert and missed alert probabilities obtained by increasing the LI alert level and noting the changes in these two.

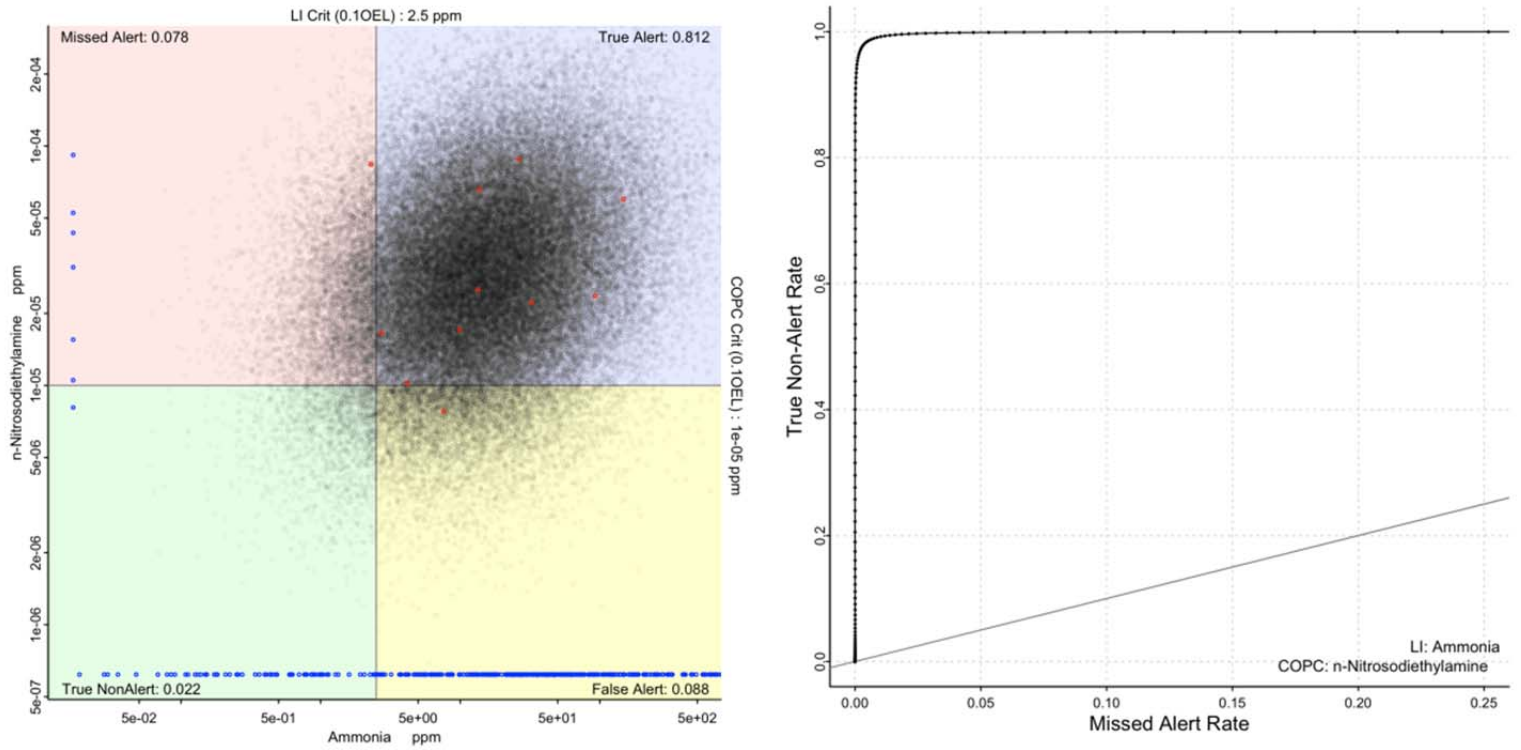

Figure C.25. Left: Scatterplot of n-nitrosodiethylamine and ammonia measurements (red dots), probability density estimate (black dots), and non-paired or MDL measurements (blue dots) with associated alert quadrants designated by 10% OEL indication lines for each chemical. Right: ROC-like curve displays the change in statistical performance for n-nitrosodiethylamine and ammonia in terms of paired true non-alert and missed alert probabilities obtained by increasing the LI alert level and noting the changes in these two.

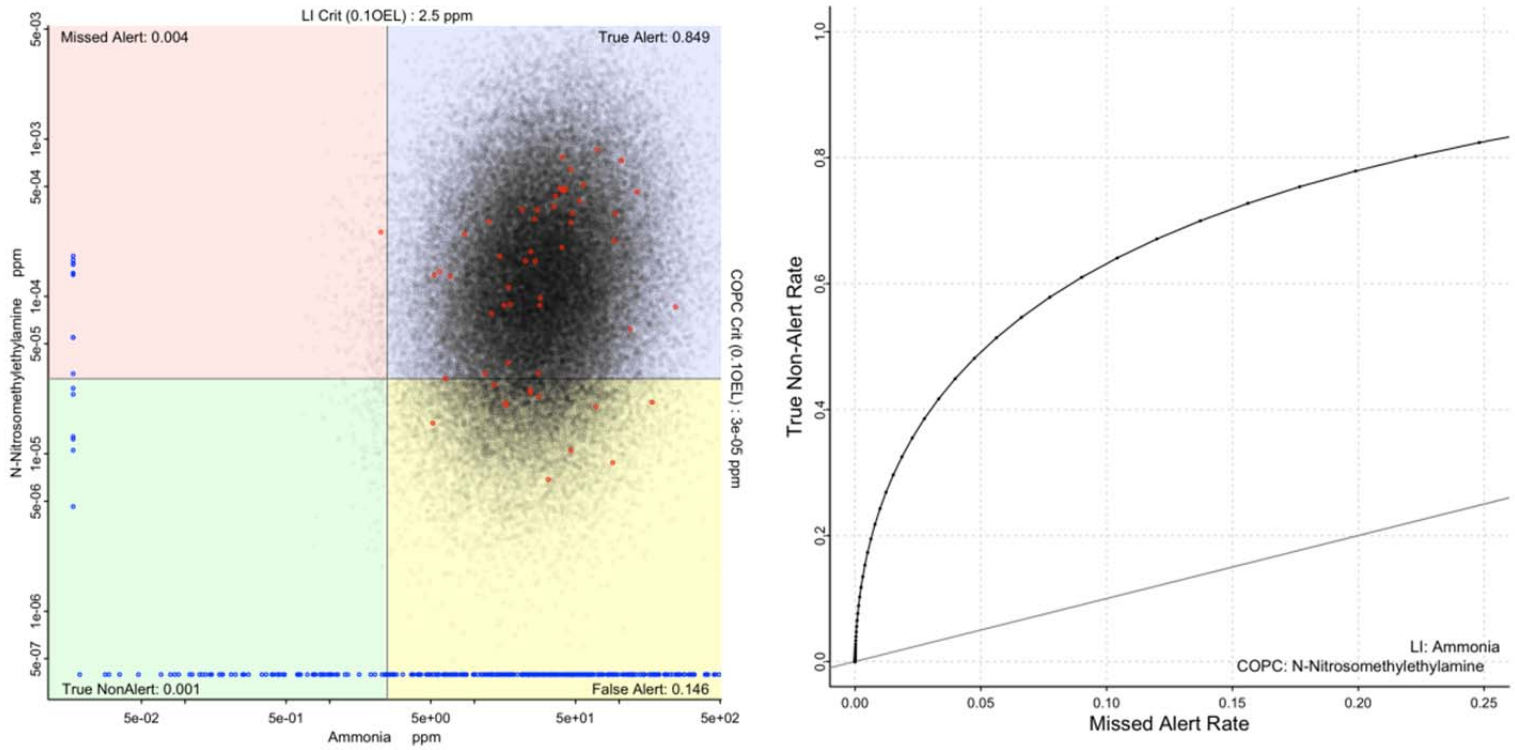

Figure C.26. Left: Scatterplot of n-nitrosomethylethylamine and ammonia measurements (red dots), probability density estimate (black dots), and non-paired or MDL measurements (blue dots) with associated alert quadrants designated by 10% OEL indication lines for each chemical. Right: ROC-like curve displays the change in statistical performance for n-nitrosomethylethylamine and ammonia in terms of paired true non-alert and missed alert probabilities obtained by increasing the LI alert level and noting the changes in these two.

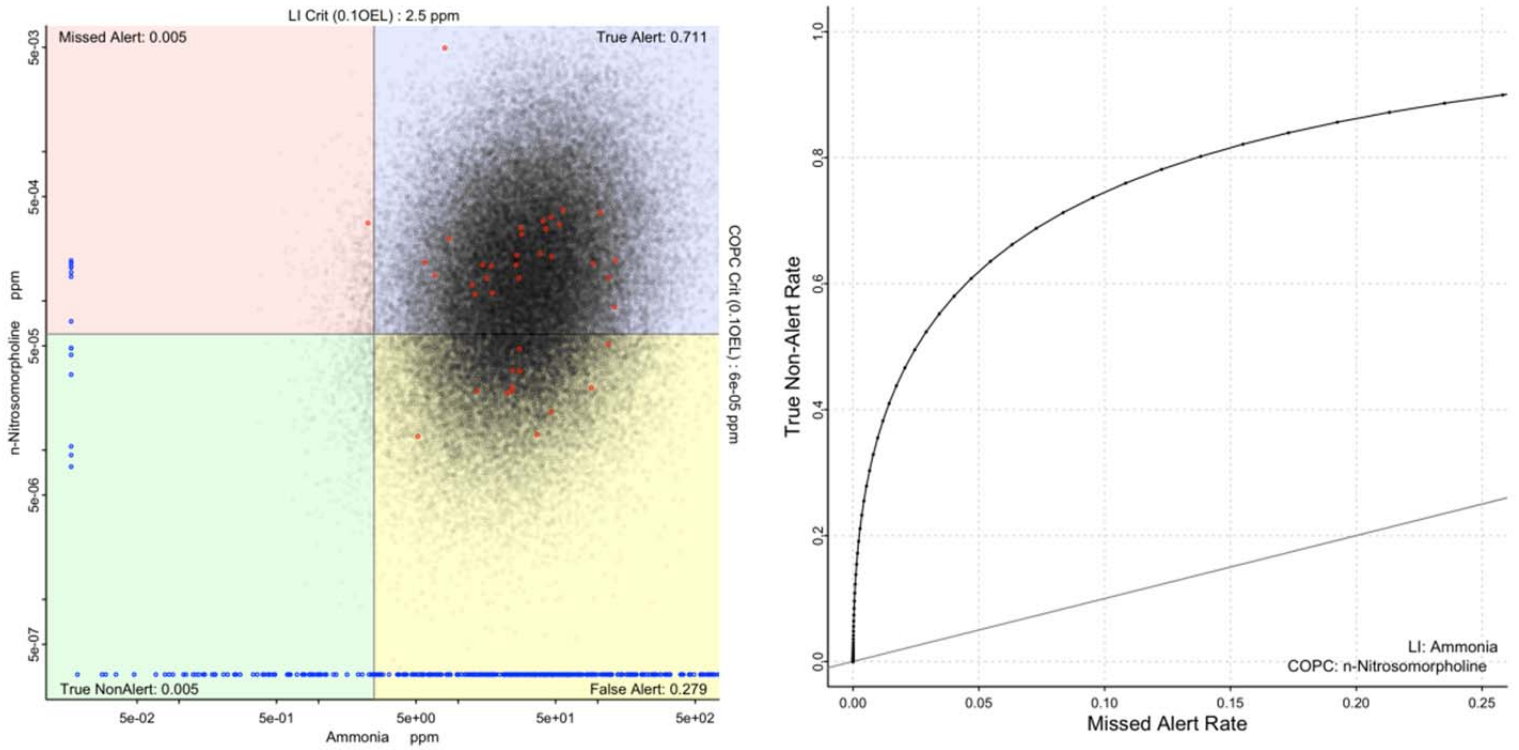

Figure C.27. Left: Scatterplot of n-nitrosomorpholine and ammonia measurements (red dots), probability density estimate (black dots), and non-paired or MDL measurements (blue dots) with associated alert quadrants designated by 10% OEL indication lines for each chemical. Right: ROC-like curve displays the change in statistical performance for n-nitrosomorpholine and ammonia in terms of paired true non-alert and missed alert probabilities obtained by increasing the LI alert level and noting the changes in these two.

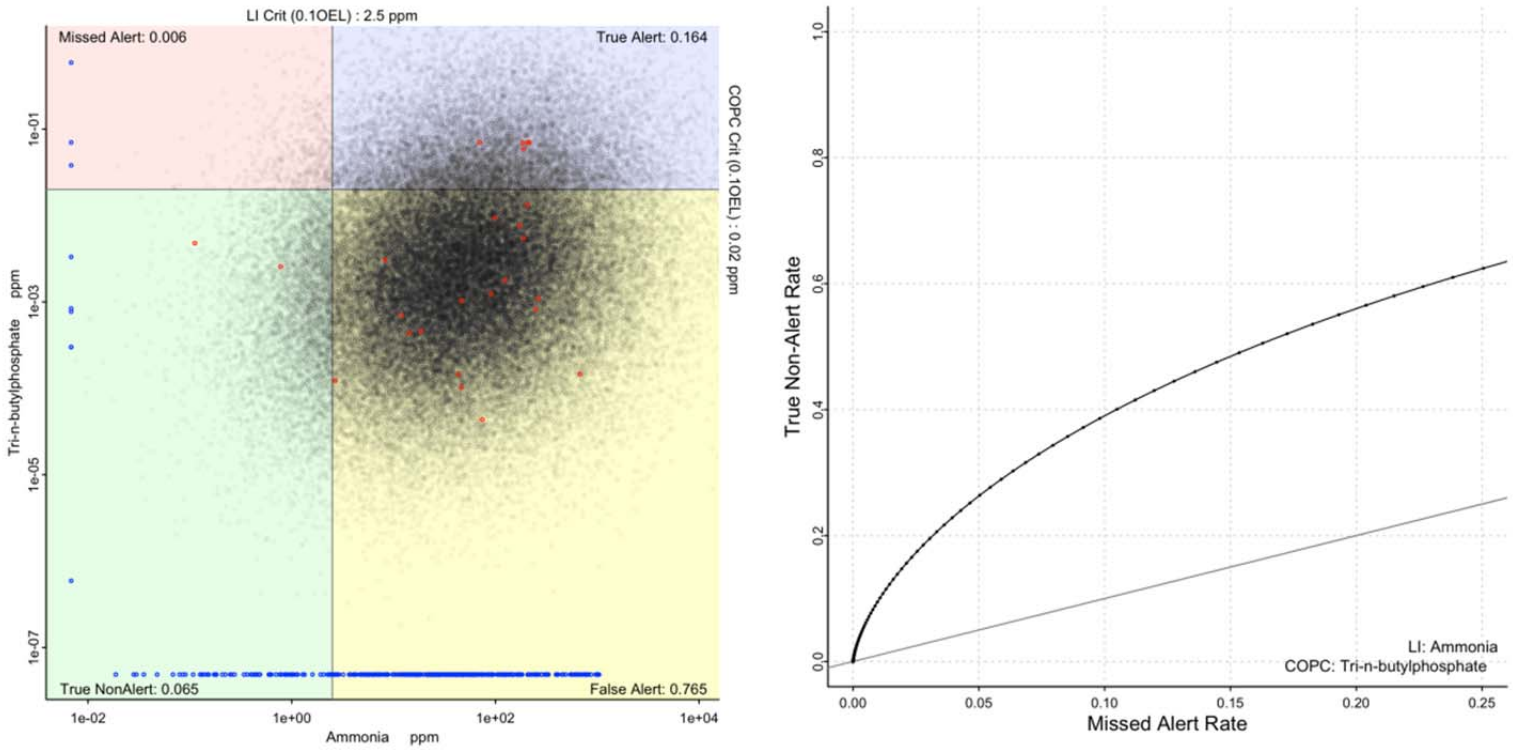

Figure C.28. Left: Scatterplot of tri-n-butylphosphate and ammonia measurements (red dots), probability density estimate (black dots), and non-paired or MDL measurements (blue dots) with associated alert quadrants designated by 10% OEL indication lines for each chemical. Right: ROC-like curve displays the change in statistical performance for tri-n-butylphosphate and ammonia in terms of paired true non-alert and missed alert probabilities obtained by increasing the LI alert level and noting the changes in these two.

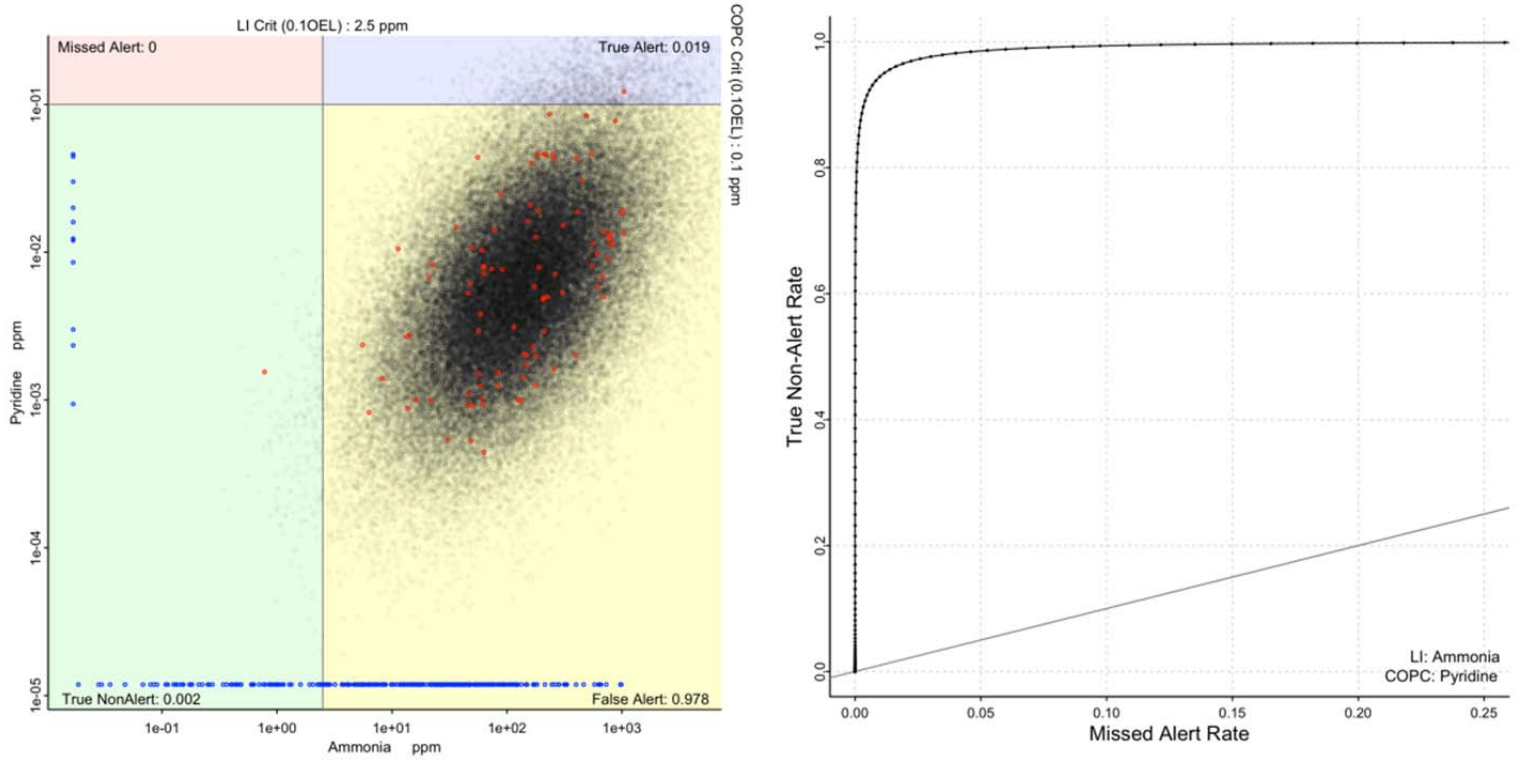

Figure C.29. Left: Scatterplot of pyridine and ammonia measurements (red dots), probability density estimate (black dots), and non-paired or MDL measurements (blue dots) with associated alert quadrants designated by 10% OEL indication lines for each chemical. Right: ROC-like curve displays the change in statistical performance for pyridine and ammonia in terms of paired true non-alert and missed alert probabilities obtained by increasing the LI alert level and noting the changes in these two.

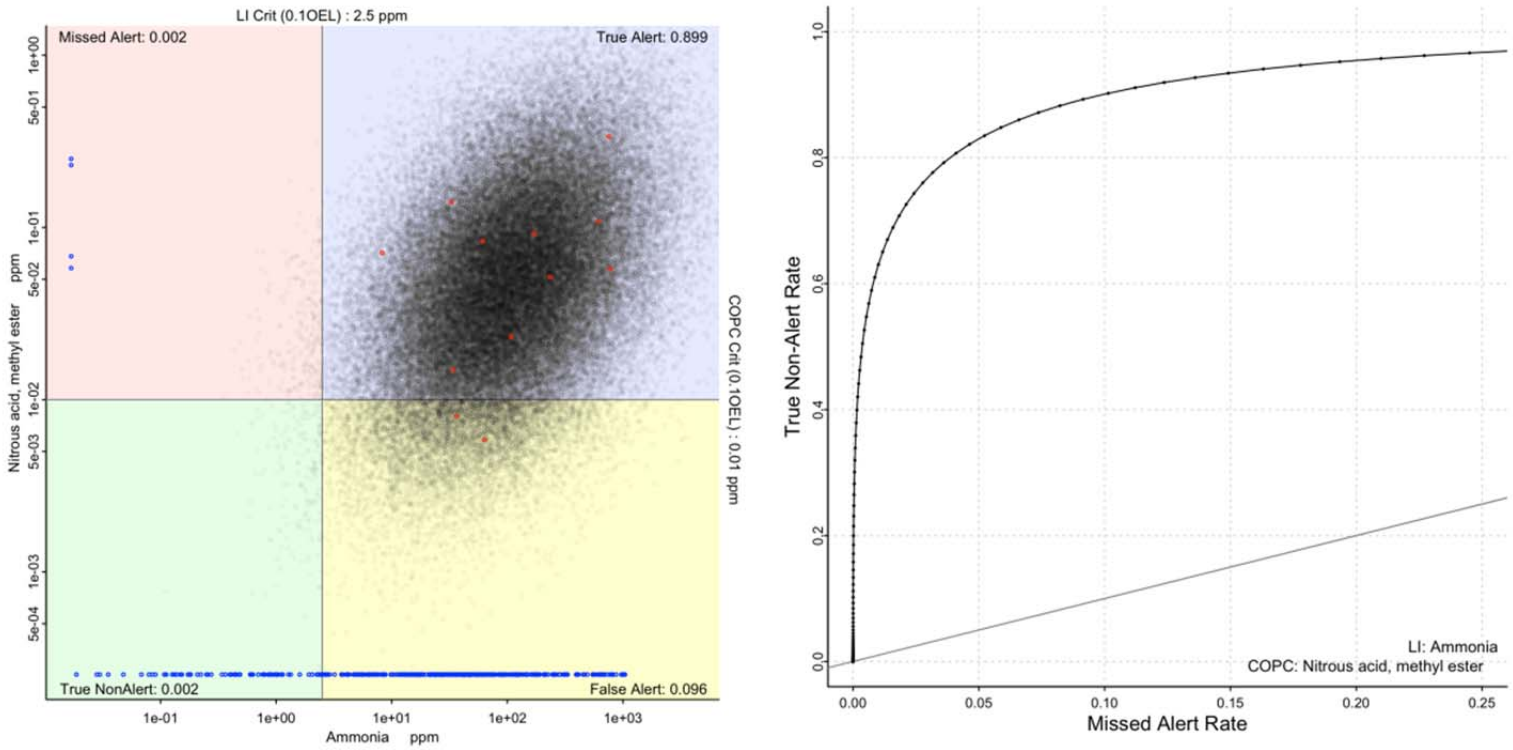

Figure C.30. Left: Scatterplot of methyl nitrate and ammonia measurements (red dots), probability density estimate (black dots), and non-paired or MDL measurements (blue dots) with associated alert quadrants designated by 10% OEL indication lines for each chemical. Right: ROC-like curve displays the change in statistical performance for methyl nitrate and ammonia in terms of paired true non-alert and missed alert probabilities obtained by increasing the LI alert level and noting the changes in these two.

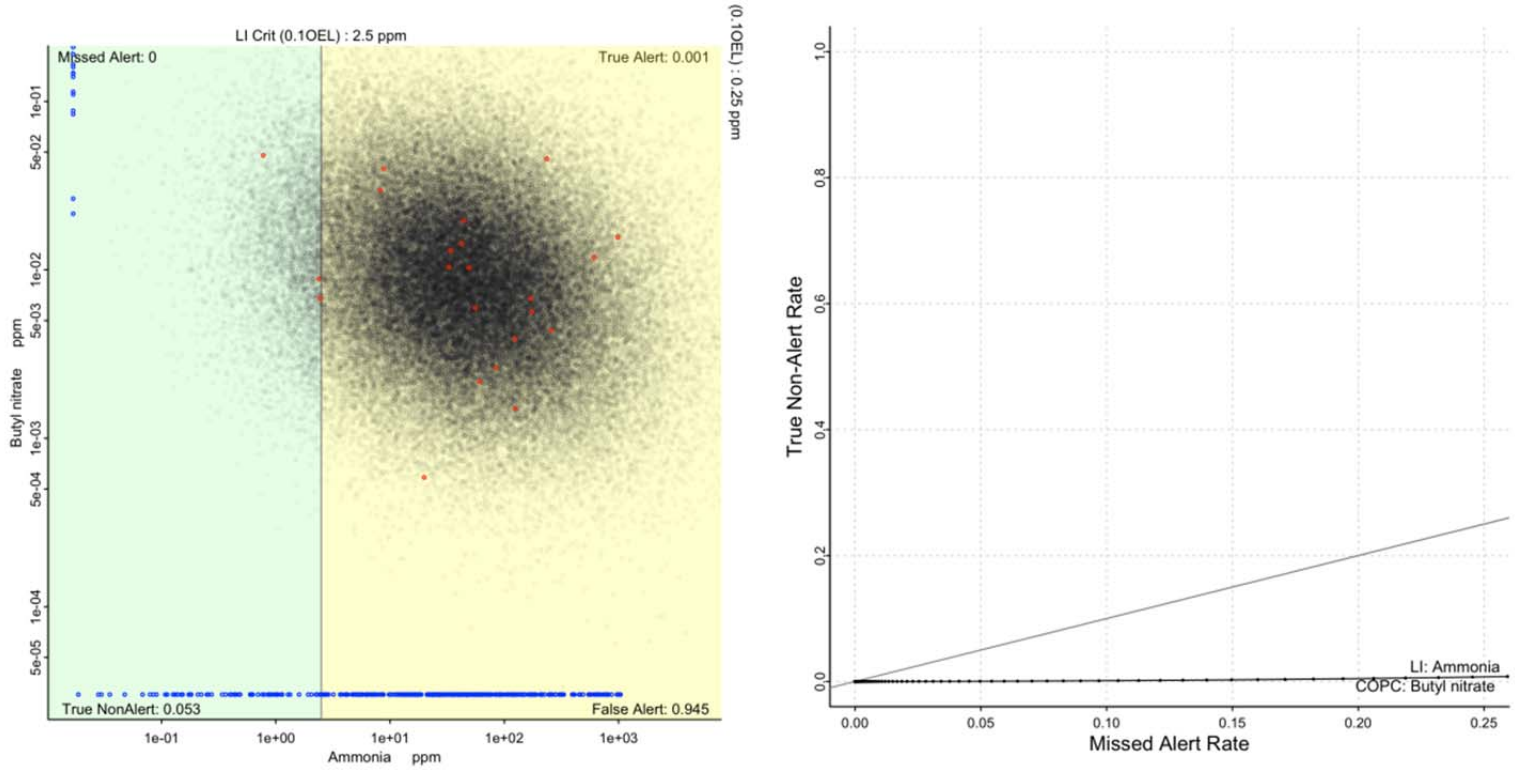

Figure C.31. Left: Scatterplot of butyl nitrate and ammonia measurements (red dots), probability density estimate (black dots), and non-paired or MDL measurements (blue dots) with associated alert quadrants designated by 10% OEL indication lines for each chemical. Right: ROC-like curve displays the change in statistical performance for butyl nitrate and ammonia in terms of paired true non-alert and missed alert probabilities obtained by increasing the LI alert level and noting the changes in these two.

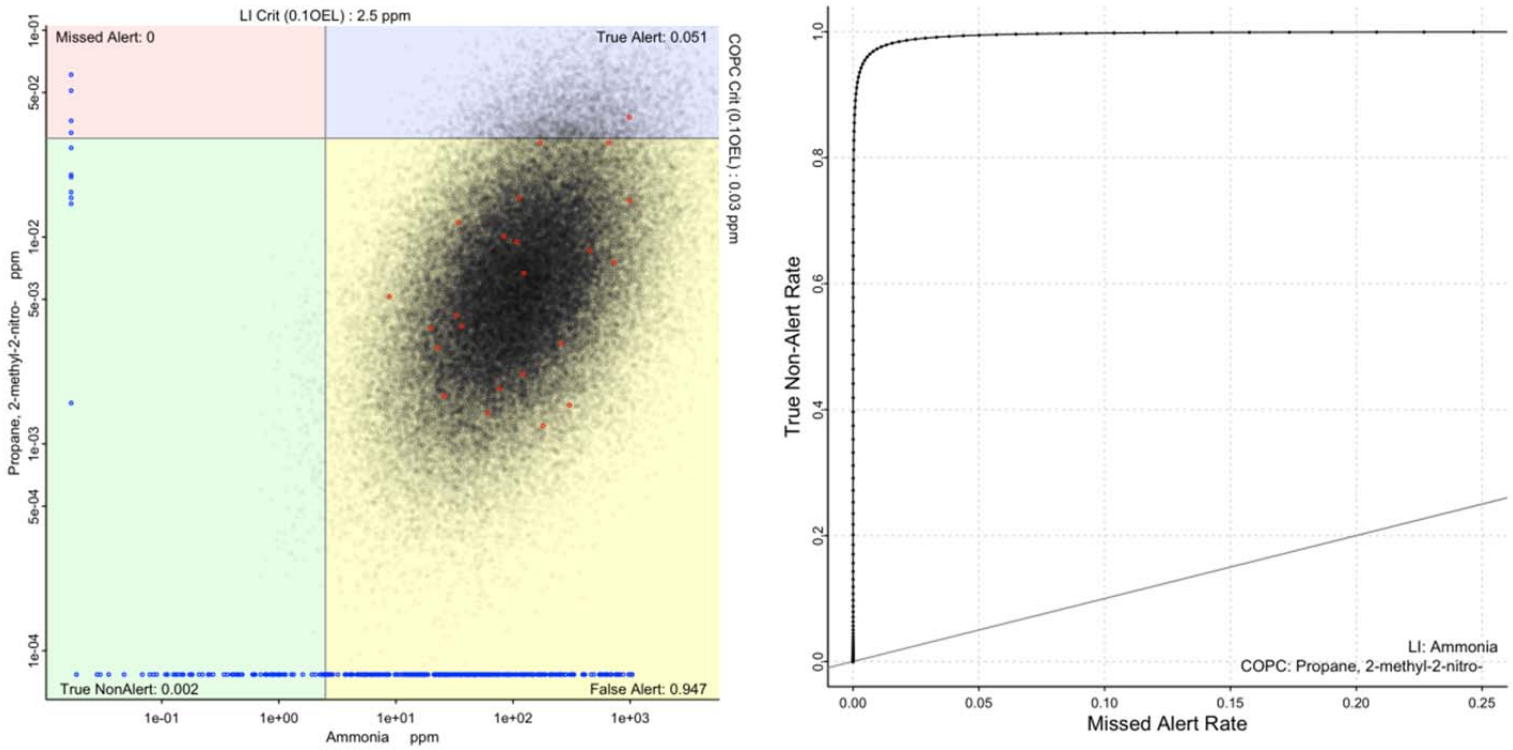

Figure C.32. Left: Scatterplot of 2-nitro-2-methylpropane and ammonia measurements (red dots), probability density estimate (black dots), and non-paired or MDL measurements (blue dots) with associated alert quadrants designated by 10% OEL indication lines for each chemical. Right: ROC-like curve displays the change in statistical performance for 2-nitro-2-methylpropane and ammonia in terms of paired true non-alert and missed alert probabilities obtained by increasing the LI alert level and noting the changes in these two.

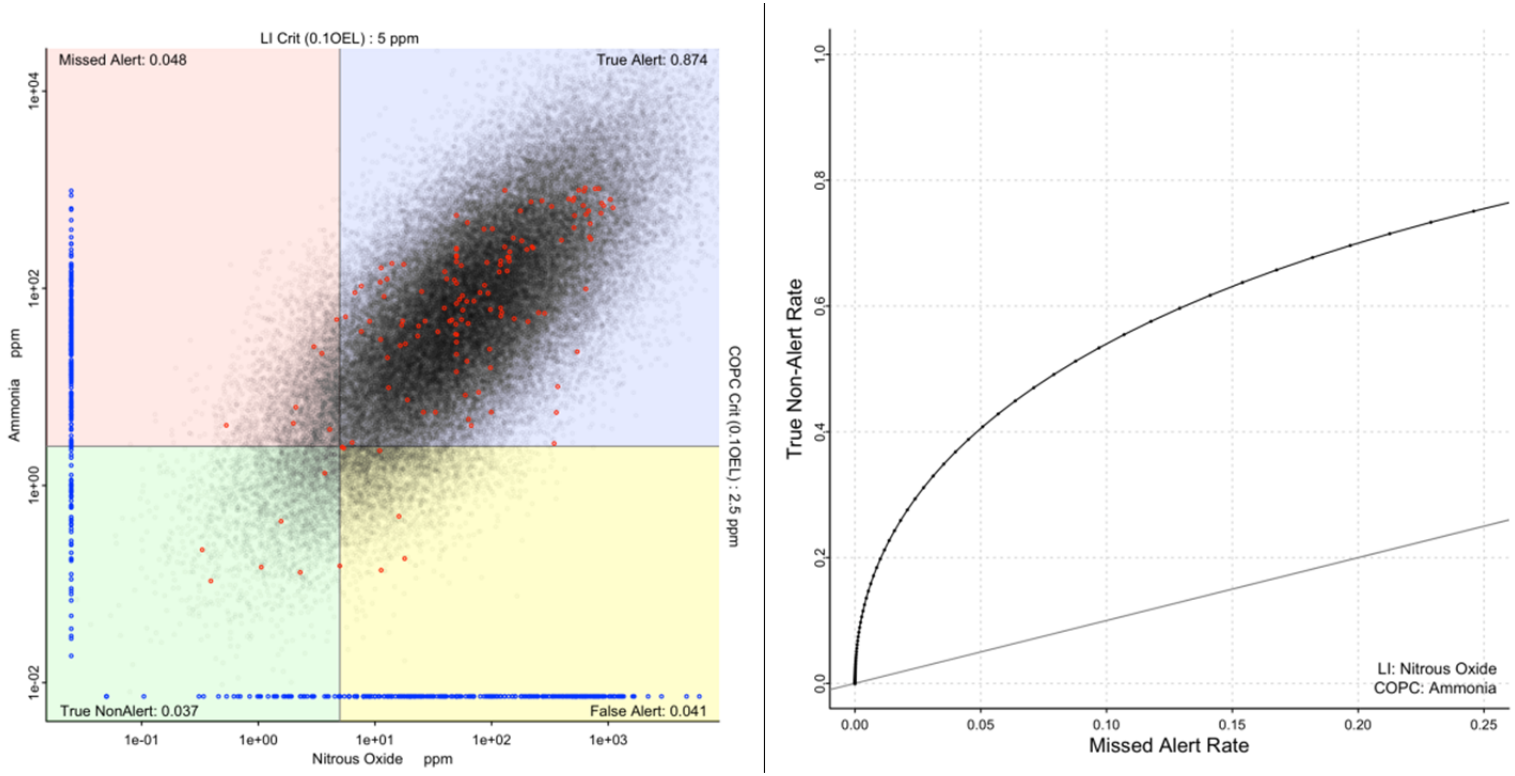

Figure C.33. Left: Scatterplot of ammonia and nitrous oxide measurements (red dots), probability density estimate (black dots), and non-paired or MDL measurements (blue dots) with associated alert quadrants designated by 10% OEL indication lines for each chemical. Right: ROC-like curve displays the change in statistical performance for ammonia and nitrous oxide in terms of paired true non-alert and missed alert probabilities obtained by increasing the LI alert level and noting the changes in these two.

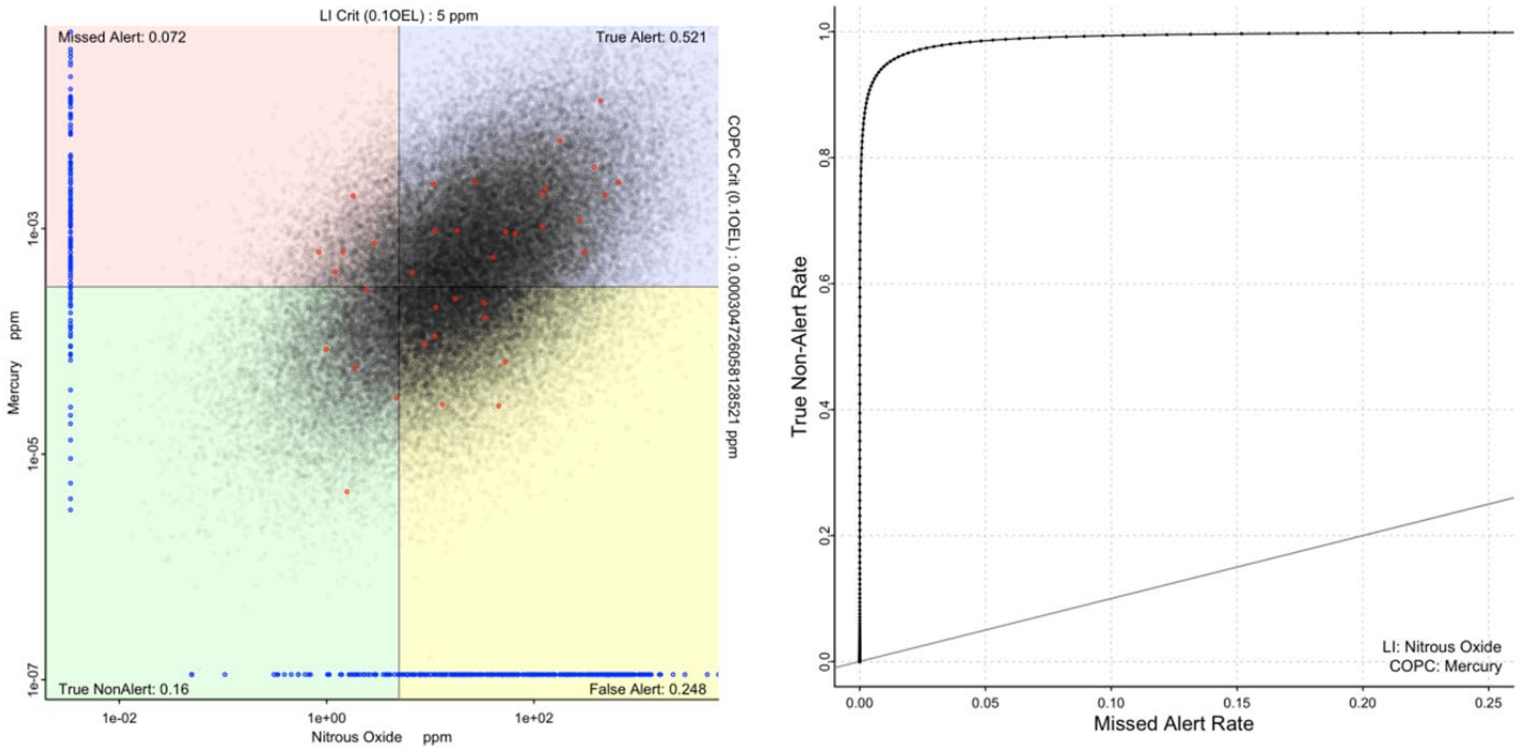

Figure C.34. Left: Scatterplot of mercury and nitrous oxide measurements (red dots), probability density estimate (black dots), and non-paired or MDL measurements (blue dots) with associated alert quadrants designated by 10% OEL indication lines for each chemical. Right: ROC-like curve displays the change in statistical performance for mercury and nitrous oxide in terms of paired true non-alert and missed alert probabilities obtained by increasing the LI alert level and noting the changes in these two.

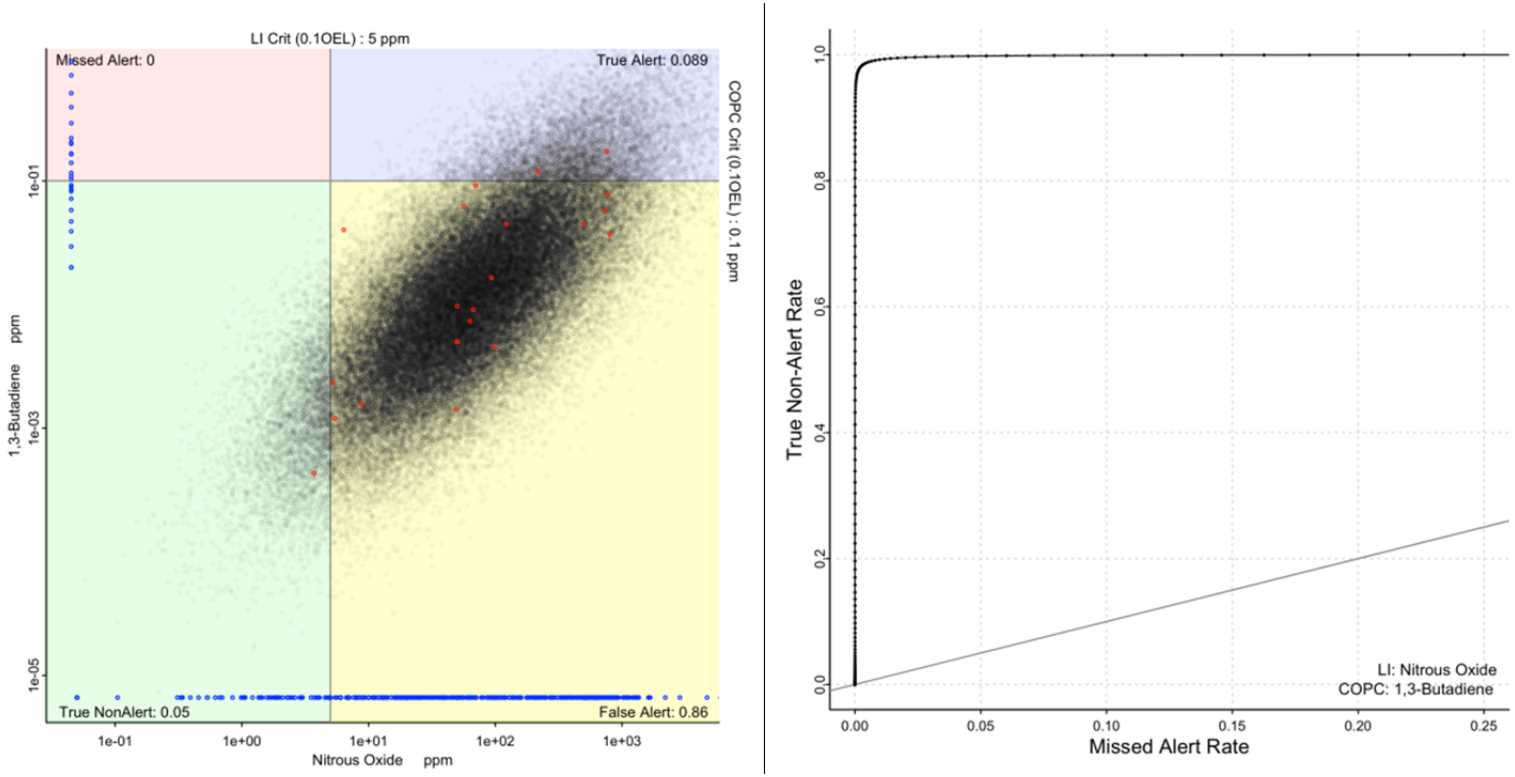

Figure C.35. Left: Scatterplot of 1,3-butadiene and nitrous oxide measurements (red dots), probability density estimate (black dots), and non-paired or MDL measurements (blue dots) with associated alert quadrants designated by 10% OEL indication lines for each chemical. Right: ROC-like curve displays the change in statistical performance for 1,3-butadiene and nitrous oxide in terms of paired true non-alert and missed alert probabilities obtained by increasing the LI alert level and noting the changes in these two.

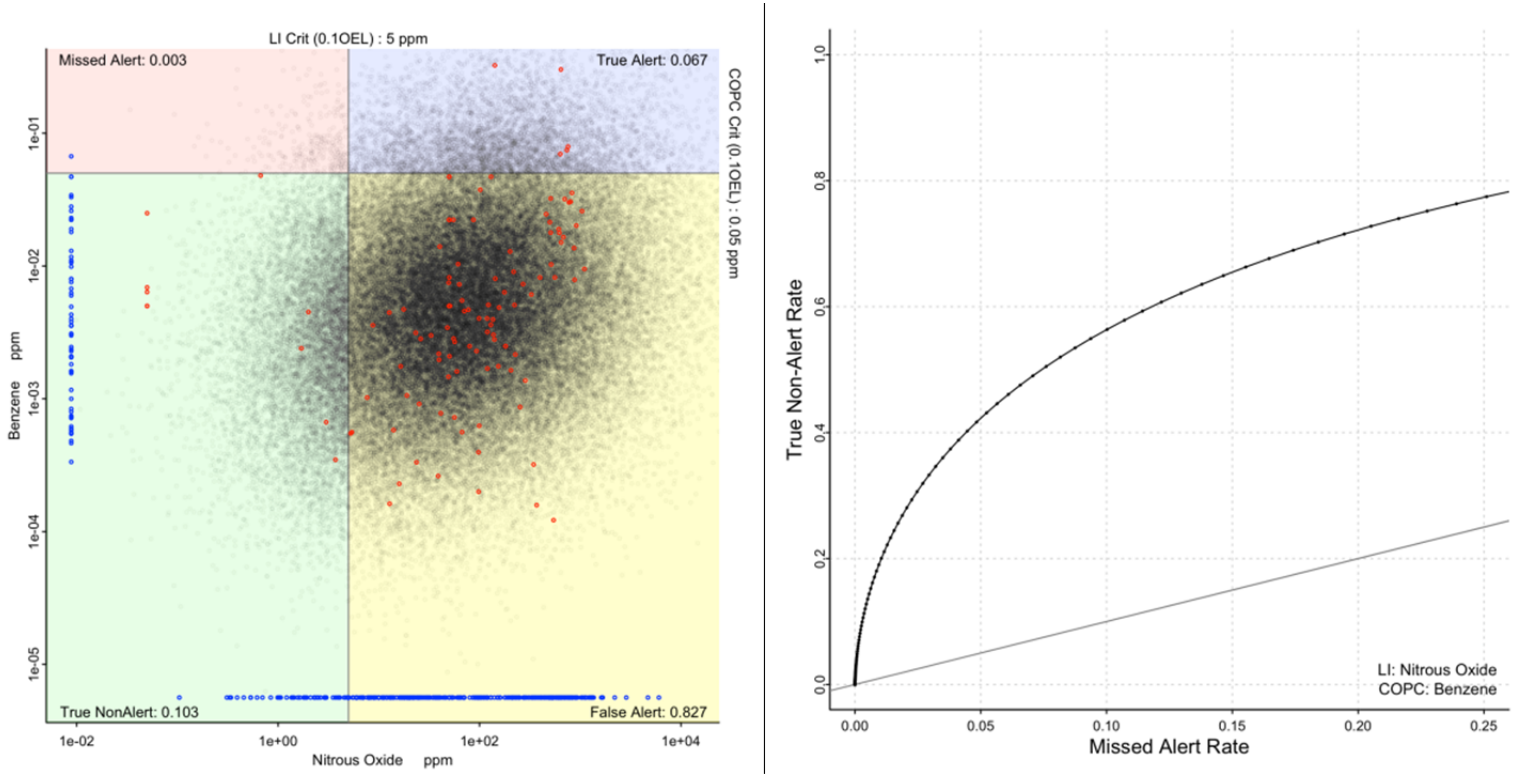

Figure C.36. Left: Scatterplot of benzene and nitrous oxide measurements (red dots), probability density estimate (black dots), and non-paired or MDL measurements (blue dots) with associated alert quadrants designated by 10% OEL indication lines for each chemical. Right: ROC-like curve displays the change in statistical performance for benzene and nitrous oxide in terms of paired true non-alert and missed alert probabilities obtained by increasing the LI alert level and noting the changes in these two.

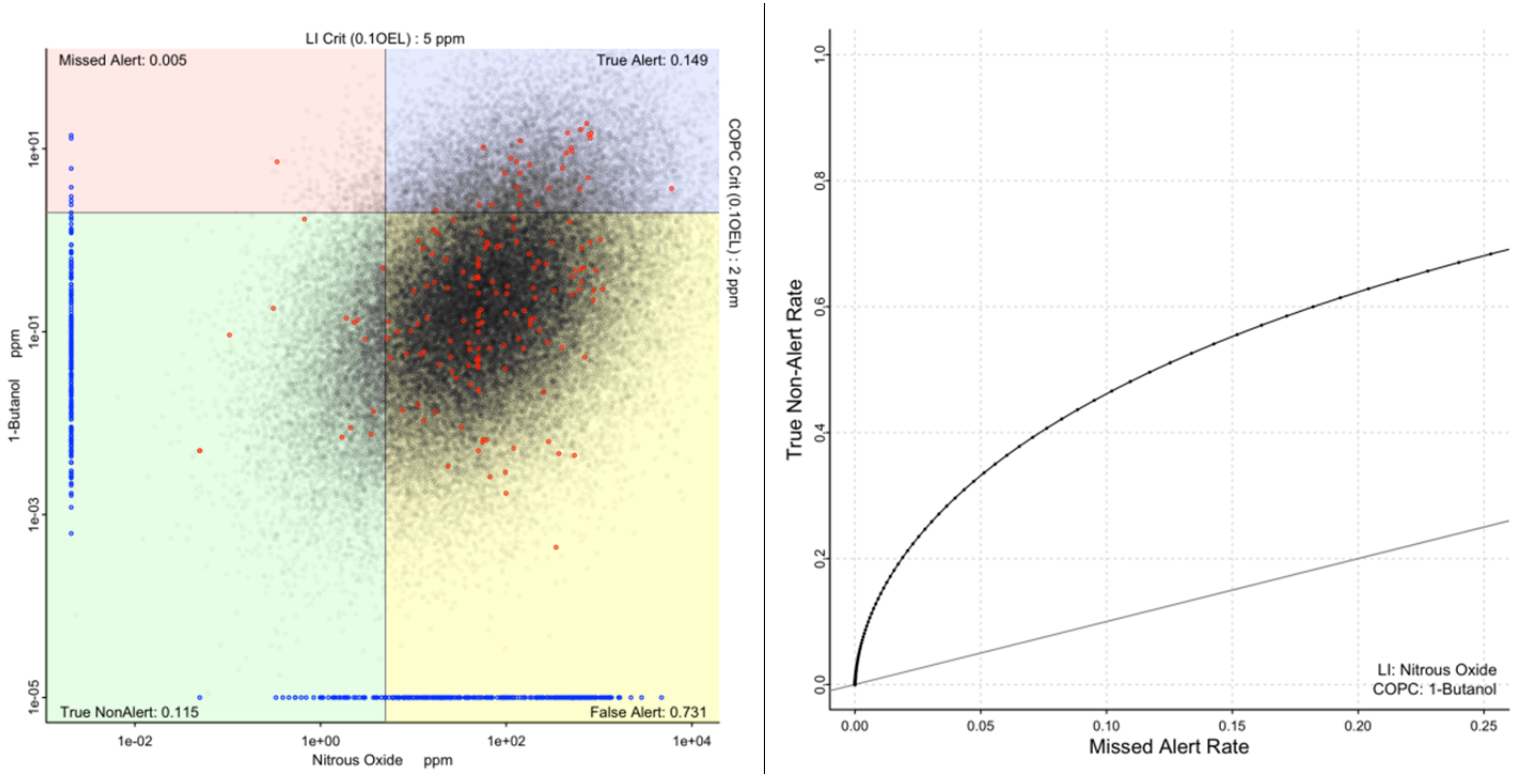

Figure C.37. Left: Scatterplot of 1-butanol and nitrous oxide measurements (red dots), probability density estimate (black dots), and non-paired or MDL measurements (blue dots) with associated alert quadrants designated by 10% OEL indication lines for each chemical. Right: ROC-like curve displays the change in statistical performance for 1-butanol and nitrous oxide in terms of paired true non-alert and missed alert probabilities obtained by increasing the LI alert level and noting the changes in these two.

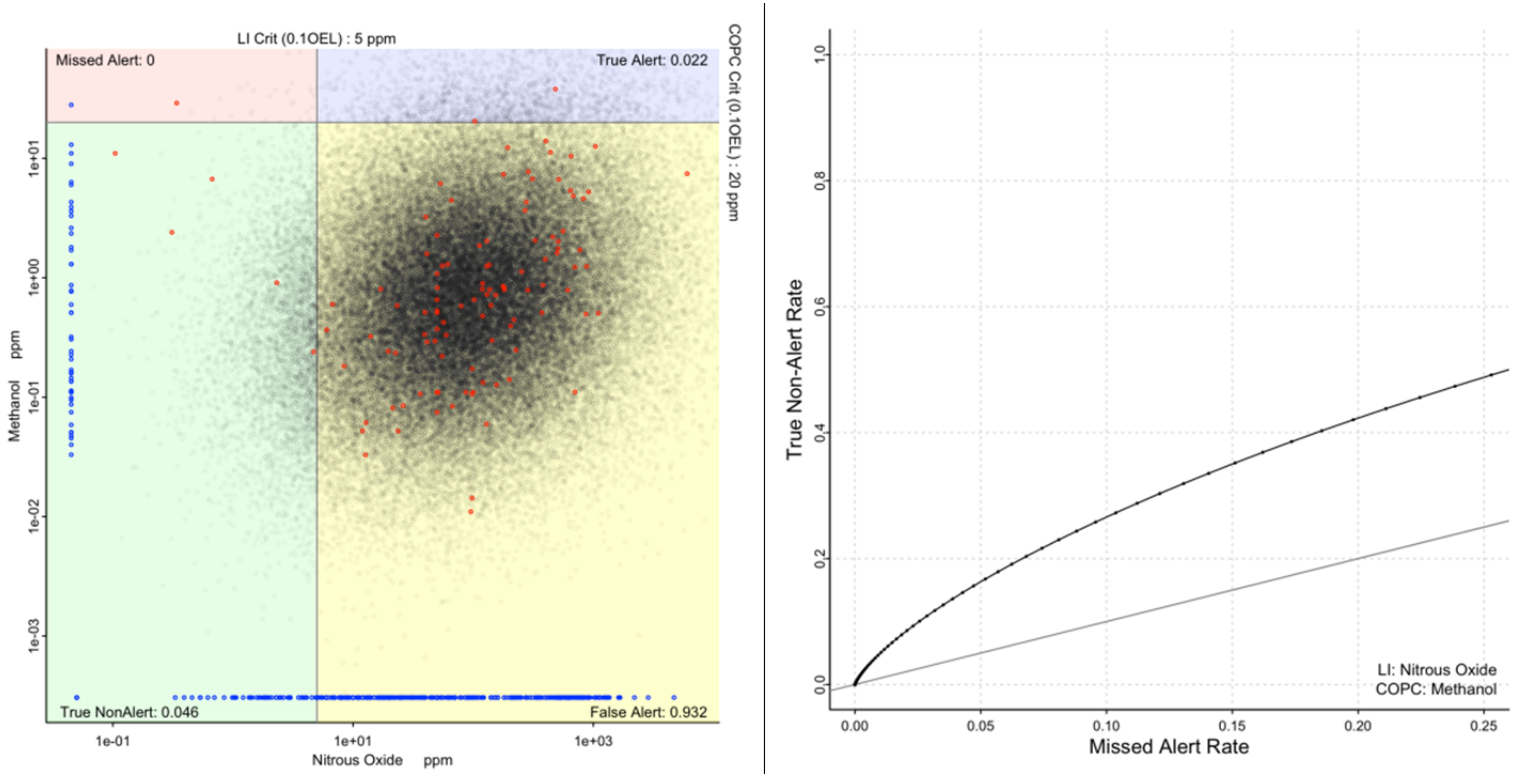

Figure C.38. Left: Scatterplot of methanol and nitrous oxide measurements (red dots), probability density estimate (black dots), and non-paired or MDL measurements (blue dots) with associated alert quadrants designated by 10% OEL indication lines for each chemical. Right: ROC-like curve displays the change in statistical performance for methanol and nitrous oxide in terms of paired true non-alert and missed alert probabilities obtained by increasing the LI alert level and noting the changes in these two.

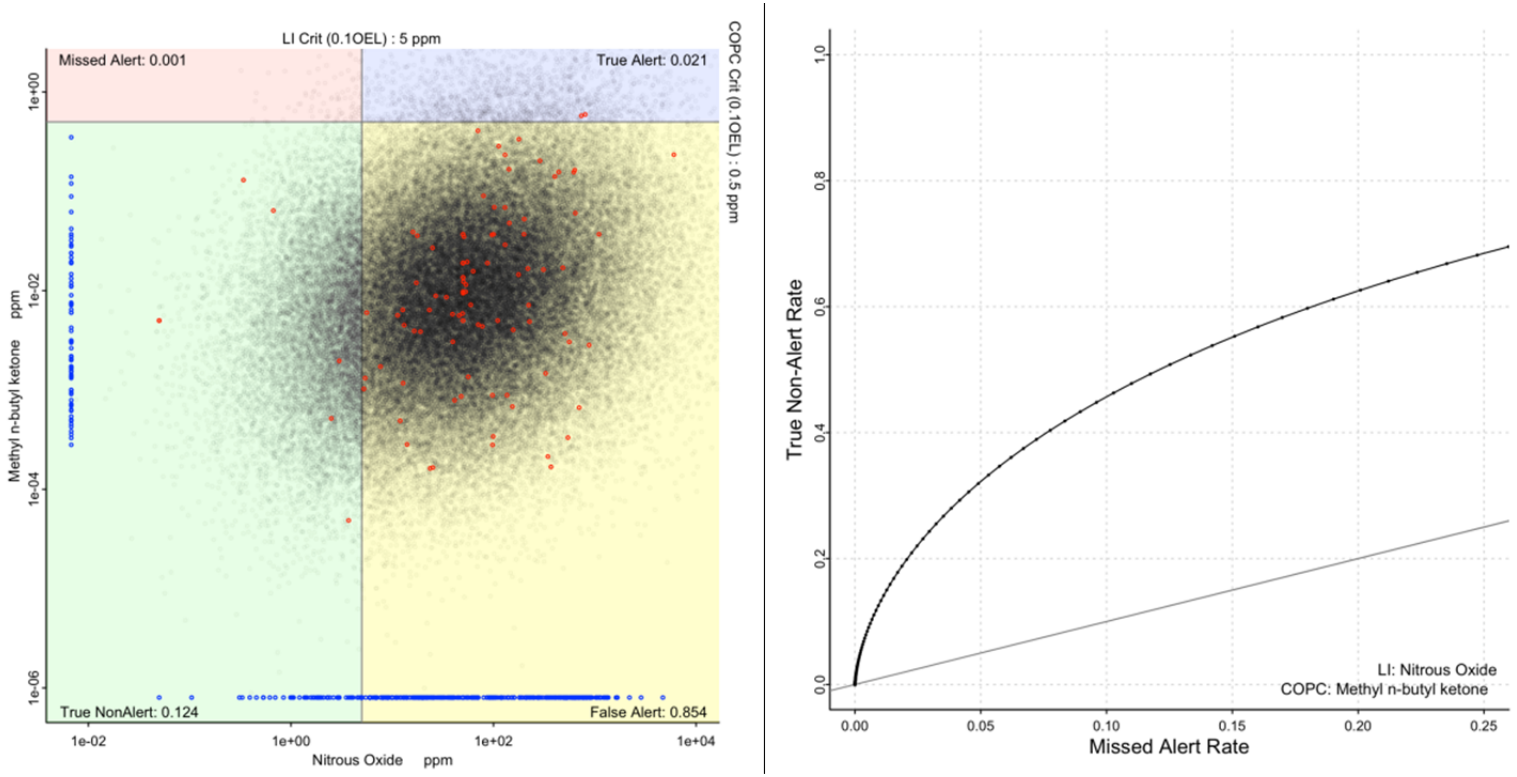

Figure C.39. Left: Scatterplot of methyl n-butyl ketone and nitrous oxide measurements (red dots), probability density estimate (black dots), and non-paired or MDL measurements (blue dots) with associated alert quadrants designated by 10% OEL indication lines for each chemical. Right: ROC-like curve displays the change in statistical performance for methyl n-butyl ketone and nitrous oxide in terms of paired true non-alert and missed alert probabilities obtained by increasing the LI alert level and noting the changes in these two.

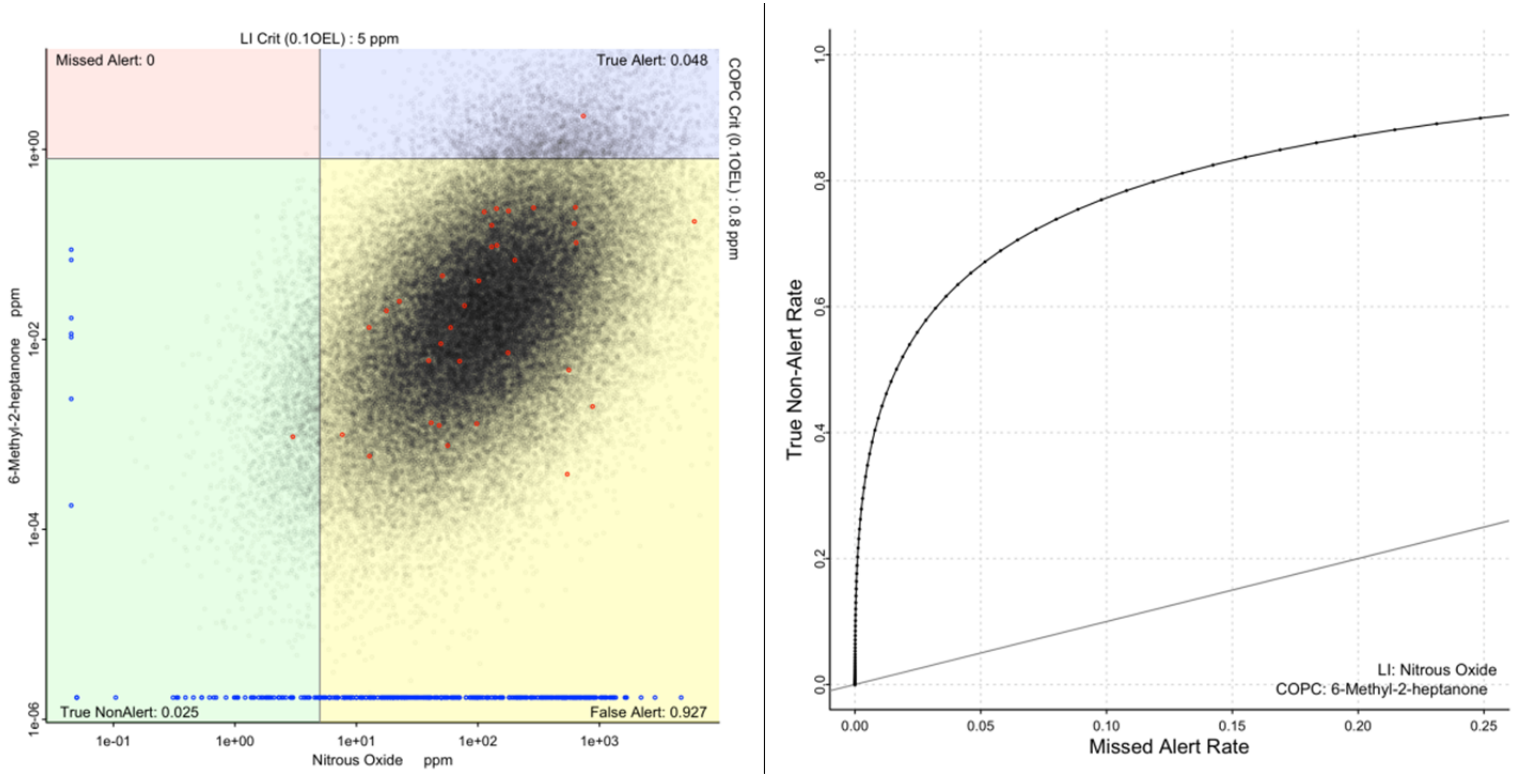

Figure C.40. Left: Scatterplot of 6-methyl-2-heptanon and nitrous oxide measurements (red dots), probability density estimate (black dots), and non-paired or MDL measurements (blue dots) with associated alert quadrants designated by 10% OEL indication lines for each chemical. Right: ROC-like curve displays the change in statistical performance for 6-methyl-2-heptanone and nitrous oxide in terms of paired true non-alert and missed alert probabilities obtained by increasing the LI alert level and noting the changes in these two.

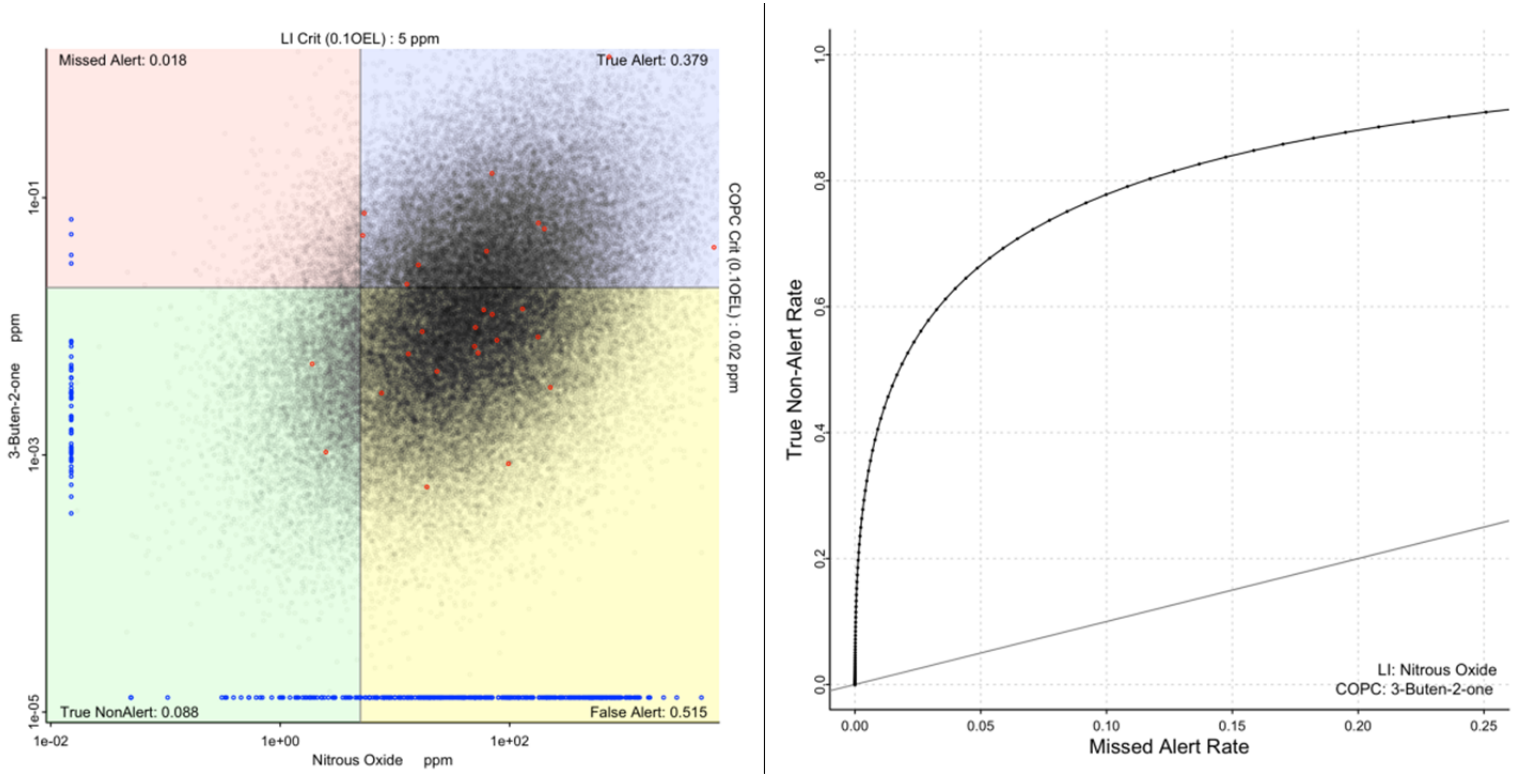

Figure C.41. Left: Scatterplot of 3-buten-2-one and nitrous oxide measurements (red dots), probability density estimate (black dots), and non-paired or MDL measurements (blue dots) with associated alert quadrants designated by 10% OEL indication lines for each chemical. Right: ROC-like curve displays the change in statistical performance for 3-buten-2-one and nitrous oxide in terms of paired true non-alert and missed alert probabilities obtained by increasing the LI alert level and noting the changes in these two.

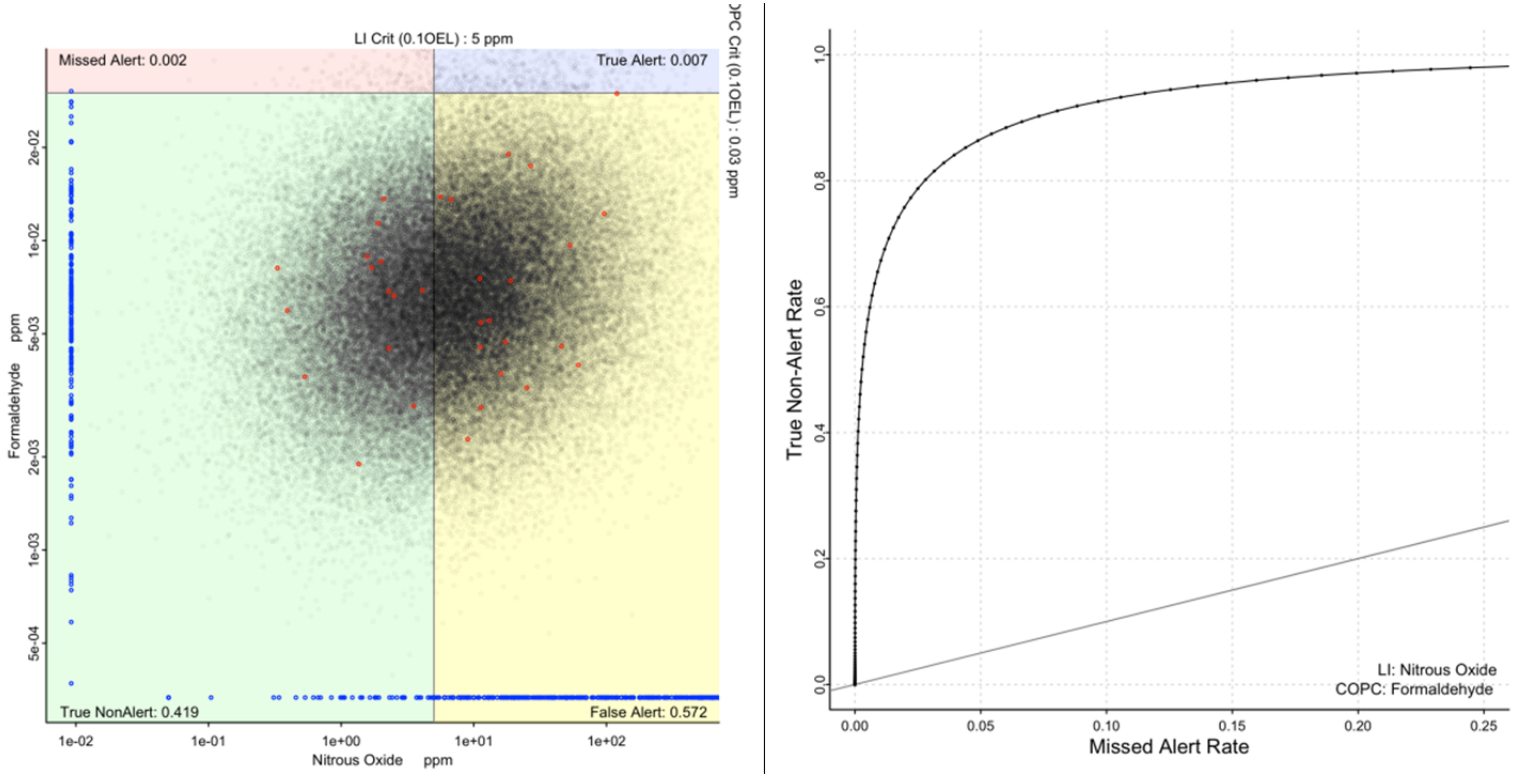

Figure C.42. Left: Scatterplot of formaldehyde and nitrous oxide measurements (red dots), probability density estimate (black dots), and non-paired or MDL measurements (blue dots) with associated alert quadrants designated by 10% OEL indication lines for each chemical. Right: ROC-like curve displays the change in statistical performance for formaldehyde and nitrous oxide in terms of paired true non-alert and missed alert probabilities obtained by increasing the LI alert level and noting the changes in these two.

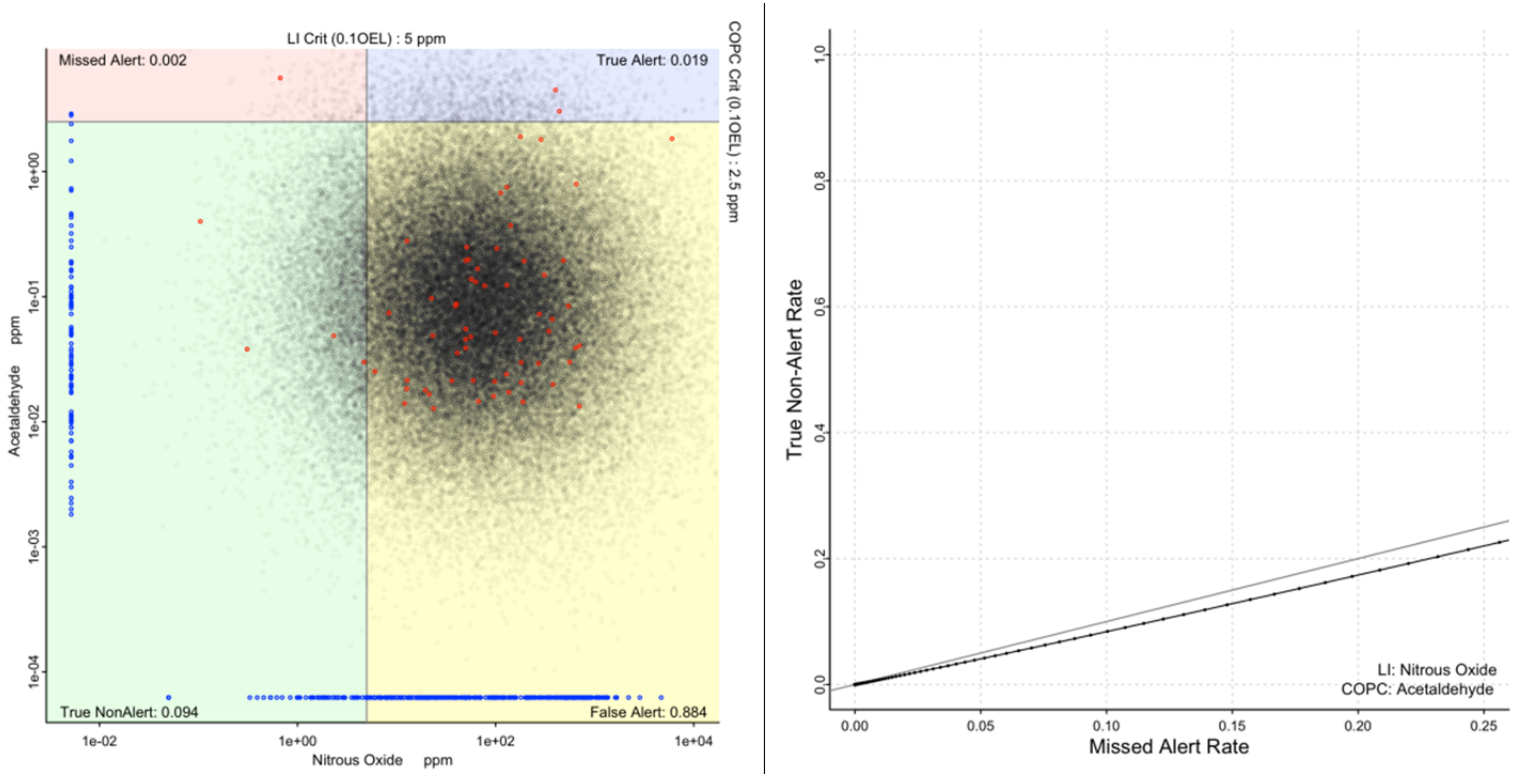

Figure C.43. Left: Scatterplot of acetaldehyde and nitrous oxide measurements (red dots), probability density estimate (black dots), and non-paired or MDL measurements (blue dots) with associated alert quadrants designated by 10% OEL indication lines for each chemical. Right: ROC-like curve displays the change in statistical performance for acetaldehyde and nitrous oxide in terms of paired true non-alert and missed alert probabilities obtained by increasing the LI alert level and noting the changes in these two.

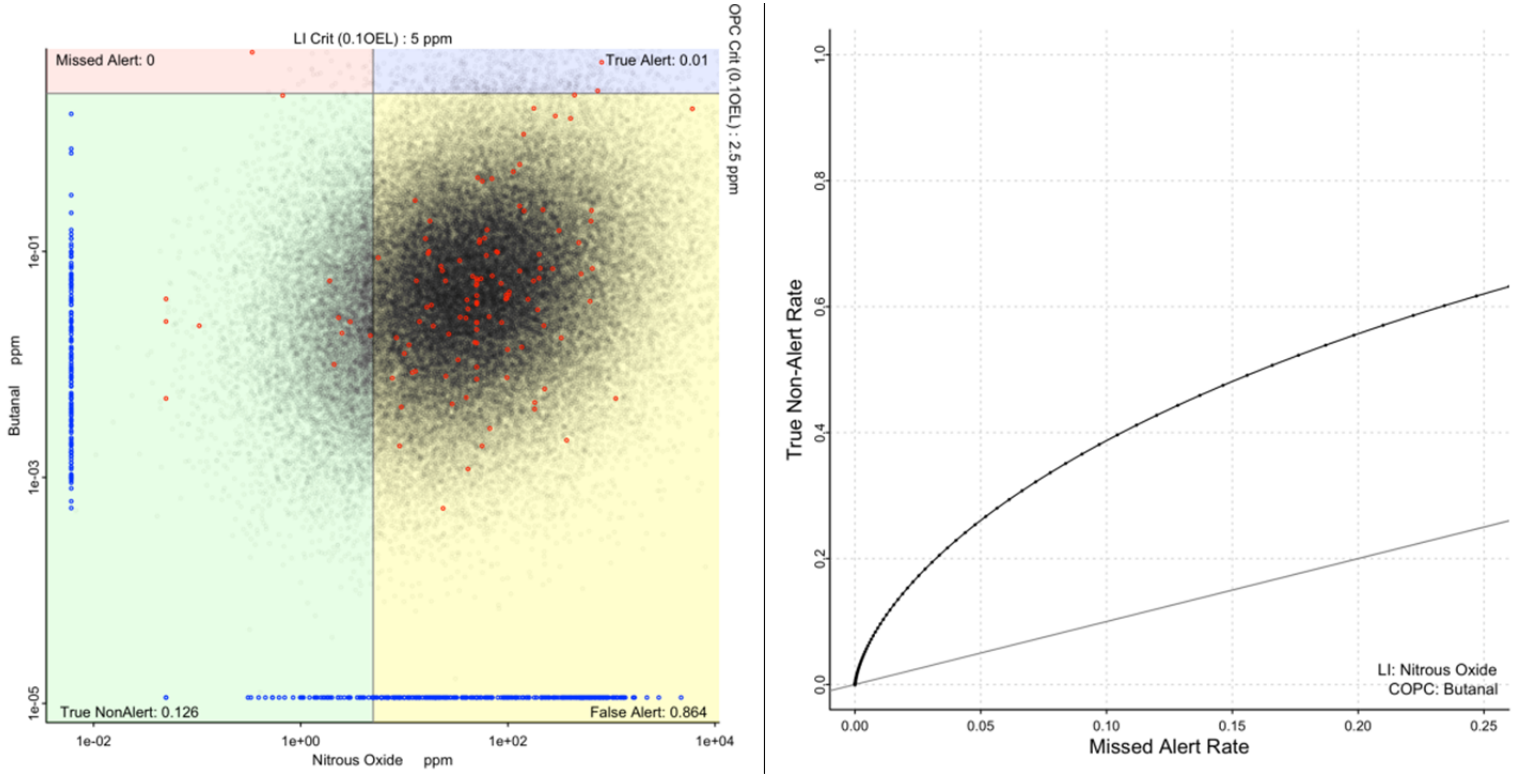

Figure C.44. Left: Scatterplot of butanal and nitrous oxide measurements (red dots), probability density estimate (black dots), and non-paired or MDL measurements (blue dots) with associated alert quadrants designated by 10% OEL indication lines for each chemical. Right: ROC-like curve displays the change in statistical performance for butanal and nitrous oxide in terms of paired true non-alert and missed alert probabilities obtained by increasing the LI alert level and noting the changes in these two.

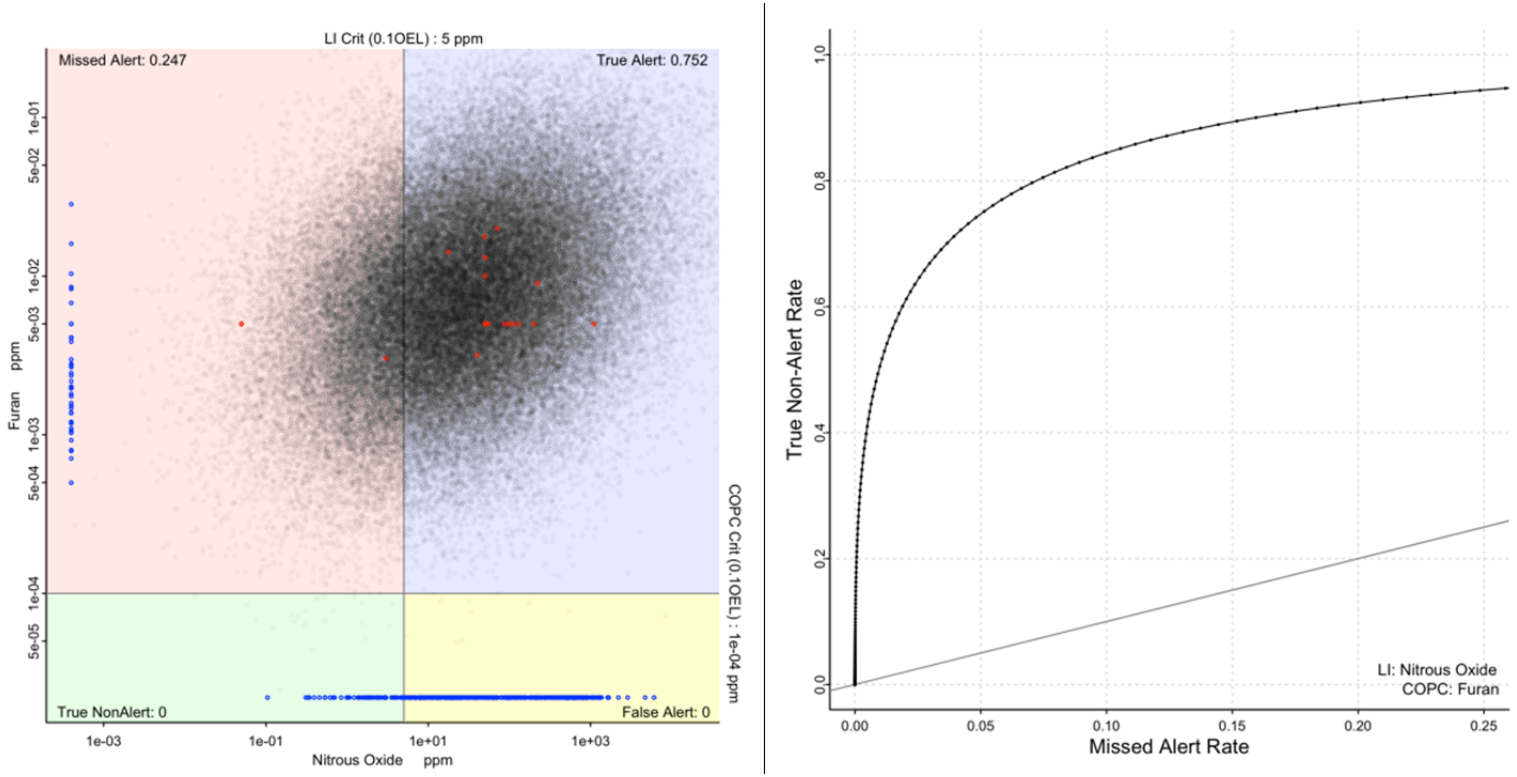

Figure C.45. Left: Scatterplot of furan and nitrous oxide measurements (red dots), probability density estimate (black dots), and non-paired or MDL measurements (blue dots) with associated alert quadrants designated by 10% OEL indication lines for each chemical. Right: ROC-like curve displays the change in statistical performance for furan and nitrous oxide in terms of paired true non-alert and missed alert probabilities obtained by increasing the LI alert level and noting the changes in these two.

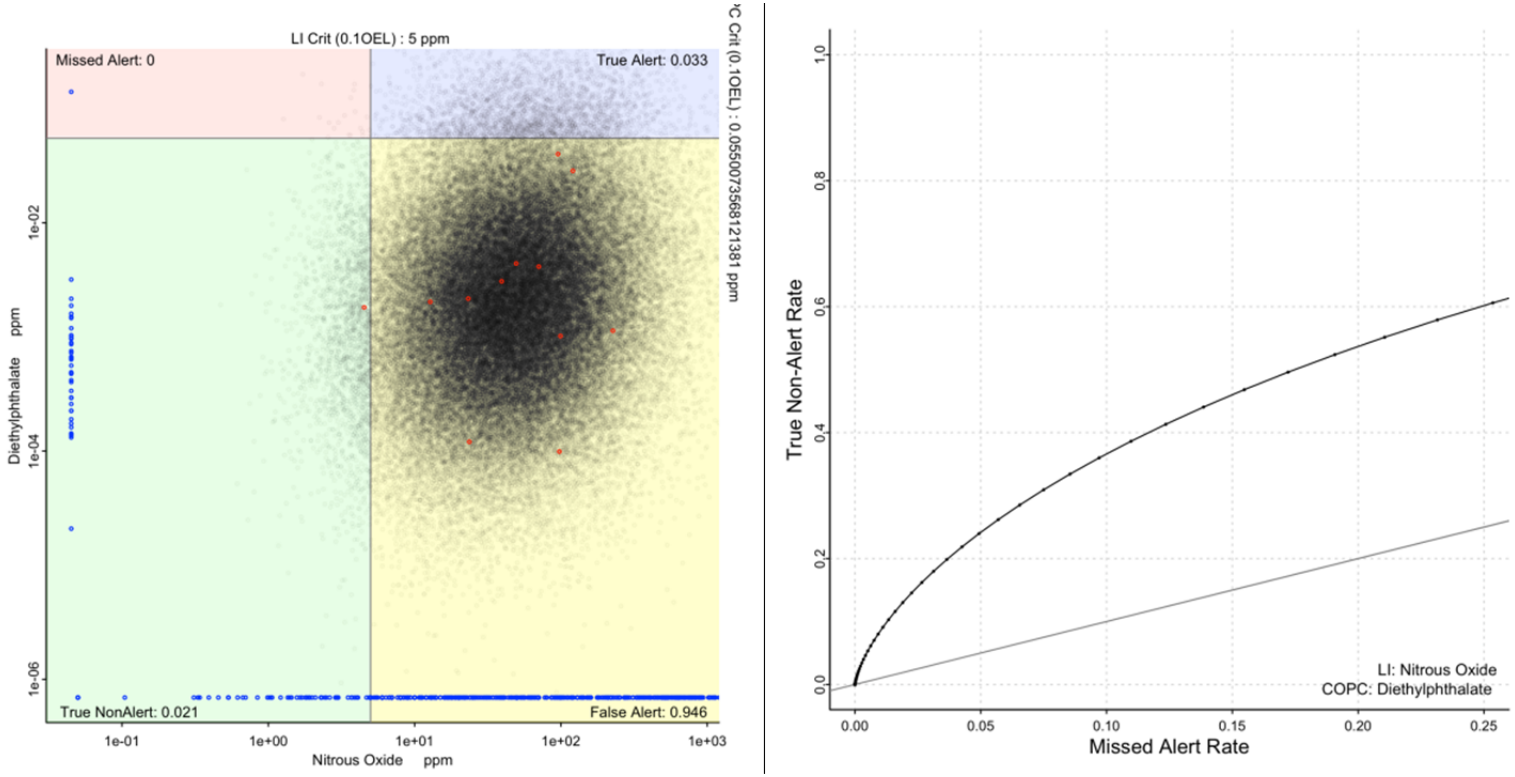

Figure C.46. Left: Scatterplot of diethylphthalate and nitrous oxide measurements (red dots), probability density estimate (black dots), and non-paired or MDL measurements (blue dots) with associated alert quadrants designated by 10% OEL indication lines for each chemical. Right: ROC-like curve displays the change in statistical performance for diethylphthalate and nitrous oxide in terms of paired true non-alert and missed alert probabilities obtained by increasing the LI alert level and noting the changes in these two.

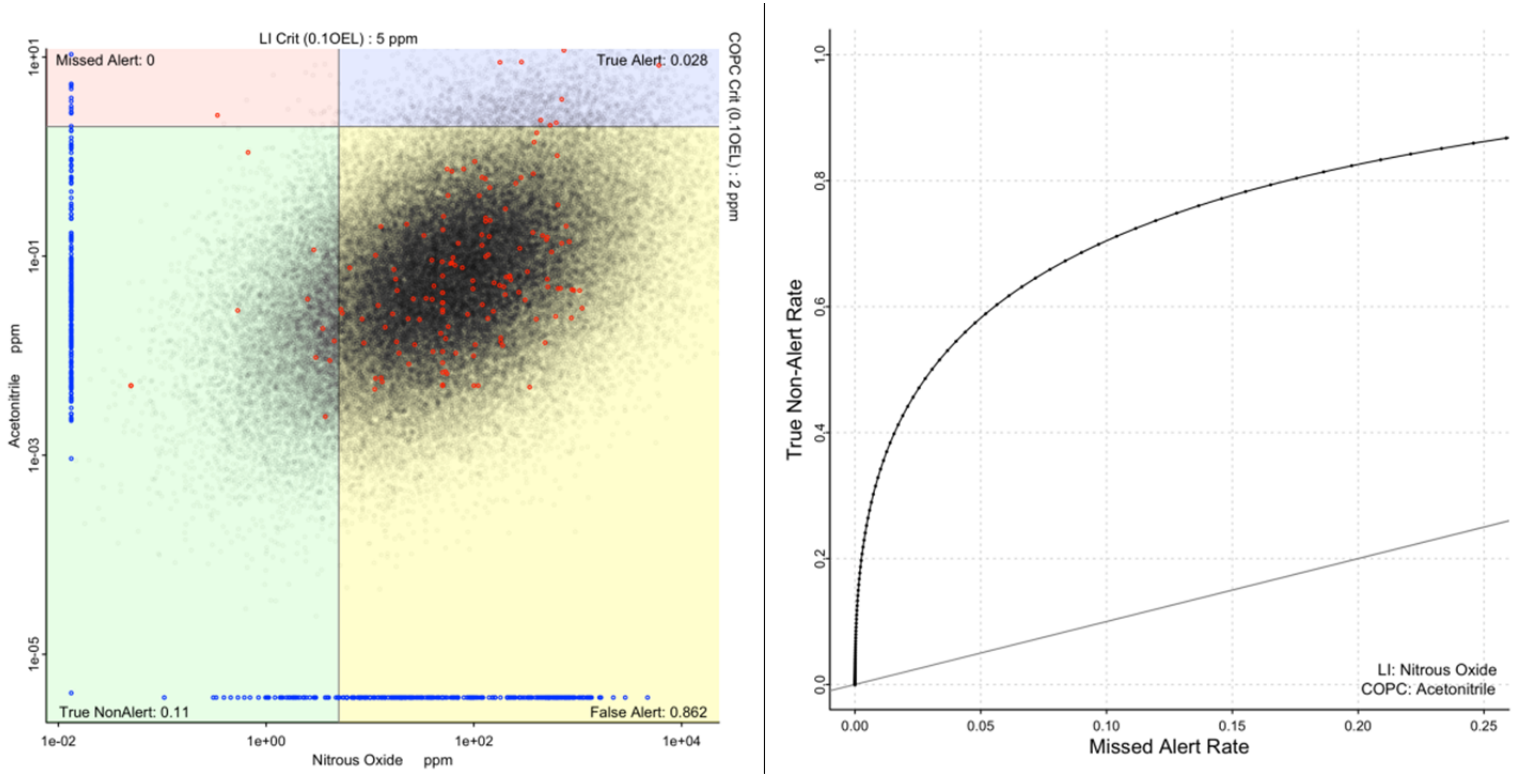

Figure C.47. Left: Scatterplot of acetonitrile and nitrous oxide measurements (red dots), probability density estimate (black dots), and non-paired or MDL measurements (blue dots) with associated alert quadrants designated by 10% OEL indication lines for each chemical. Right: ROC-like curve displays the change in statistical performance for acetonitrile and nitrous oxide in terms of paired true non-alert and missed alert probabilities obtained by increasing the LI alert level and noting the changes in these two.

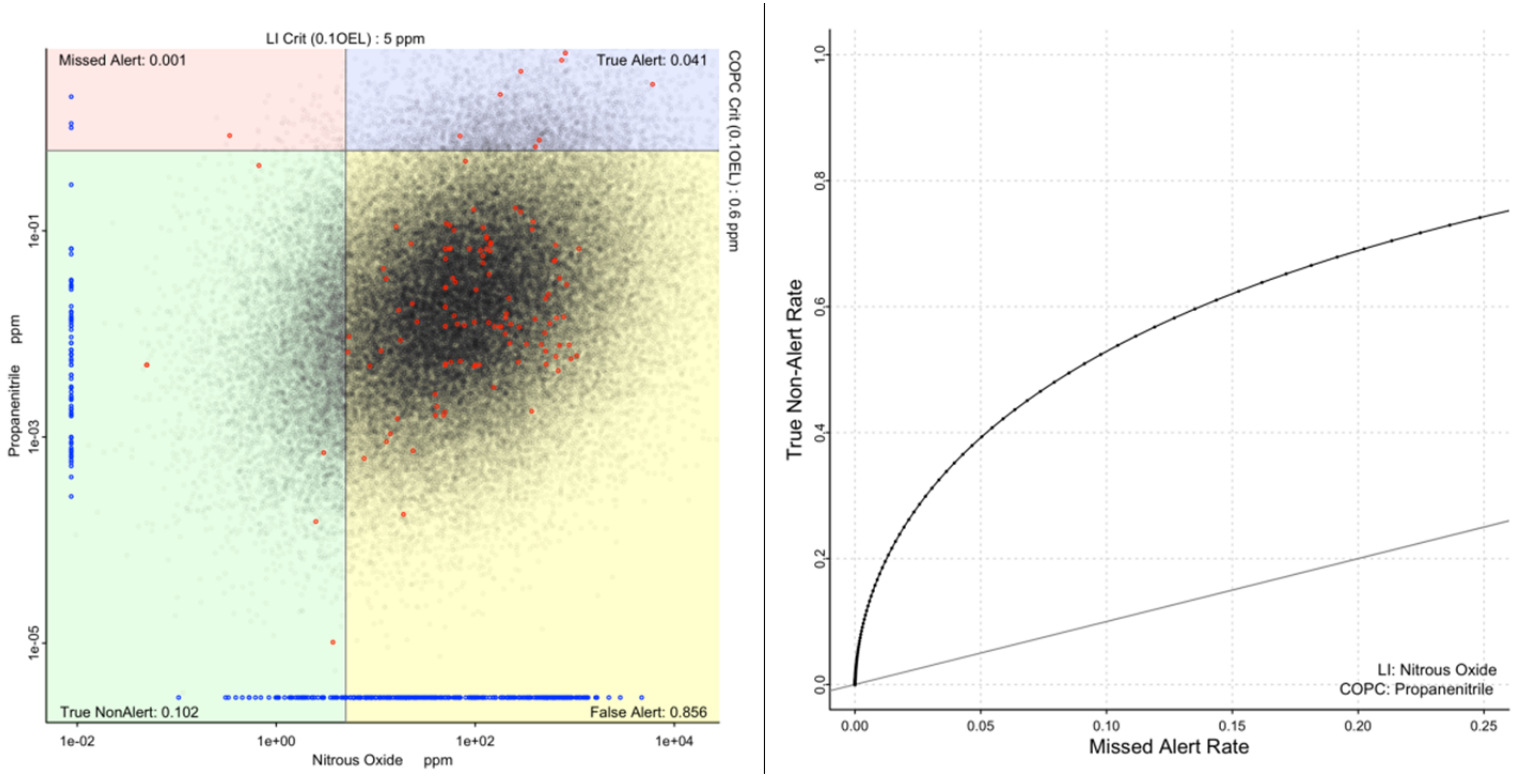

Figure C.48. Left: Scatterplot of propanenitrile and nitrous oxide measurements (red dots), probability density estimate (black dots), and non-paired or MDL measurements (blue dots) with associated alert quadrants designated by 10% OEL indication lines for each chemical. Right: ROC-like curve displays the change in statistical performance for propanenitrile and nitrous oxide in terms of paired true non-alert and missed alert probabilities obtained by increasing the LI alert level and noting the changes in these two.

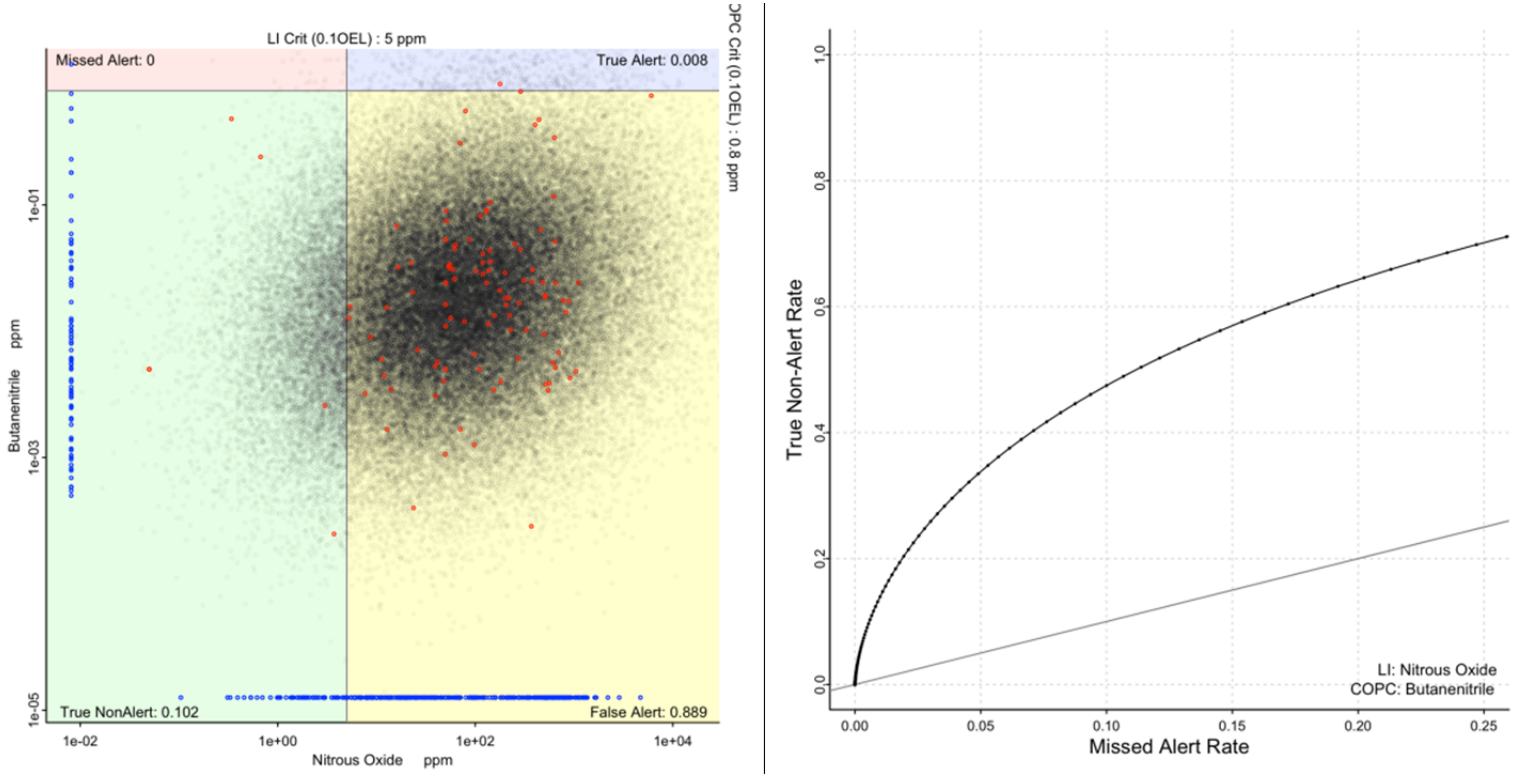

Figure C.49. Left: Scatterplot of butanenitrile and nitrous oxide measurements (red dots), probability density estimate (black dots), and non-paired or MDL measurements (blue dots) with associated alert quadrants designated by 10% OEL indication lines for each chemical. Right: ROC-like curve displays the change in statistical performance for butanenitrile and nitrous oxide in terms of paired true non-alert and missed alert probabilities obtained by increasing the LI alert level and noting the changes in these two.

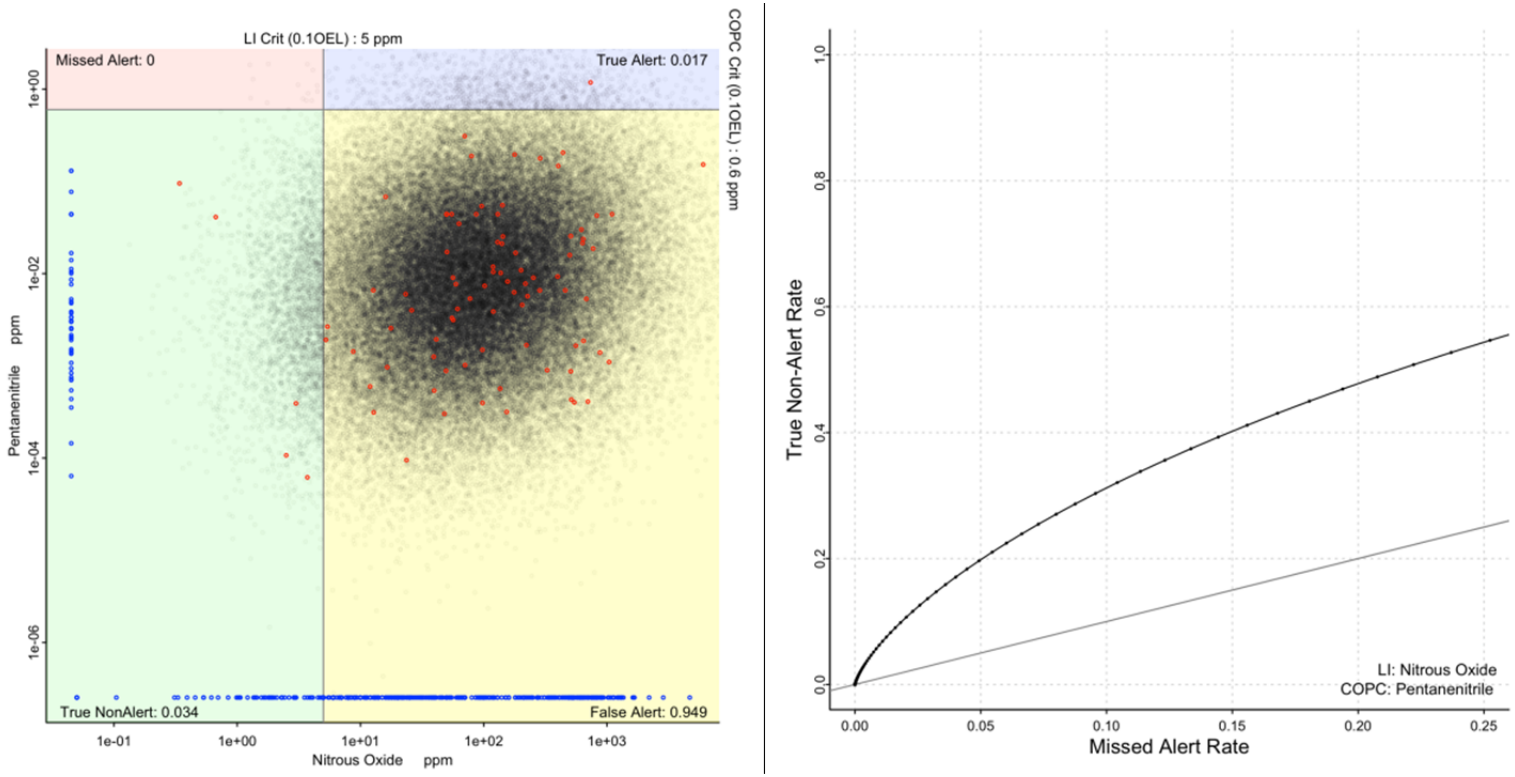

Figure C.50. Left: Scatterplot of pentanenitrile and nitrous oxide measurements (red dots), probability density estimate (black dots), and non-paired or MDL measurements (blue dots) with associated alert quadrants designated by 10% OEL indication lines for each chemical. Right: ROC-like curve displays the change in statistical performance for pentanenitrile and nitrous oxide in terms of paired true non-alert and missed alert probabilities obtained by increasing the LI alert level and noting the changes in these two.

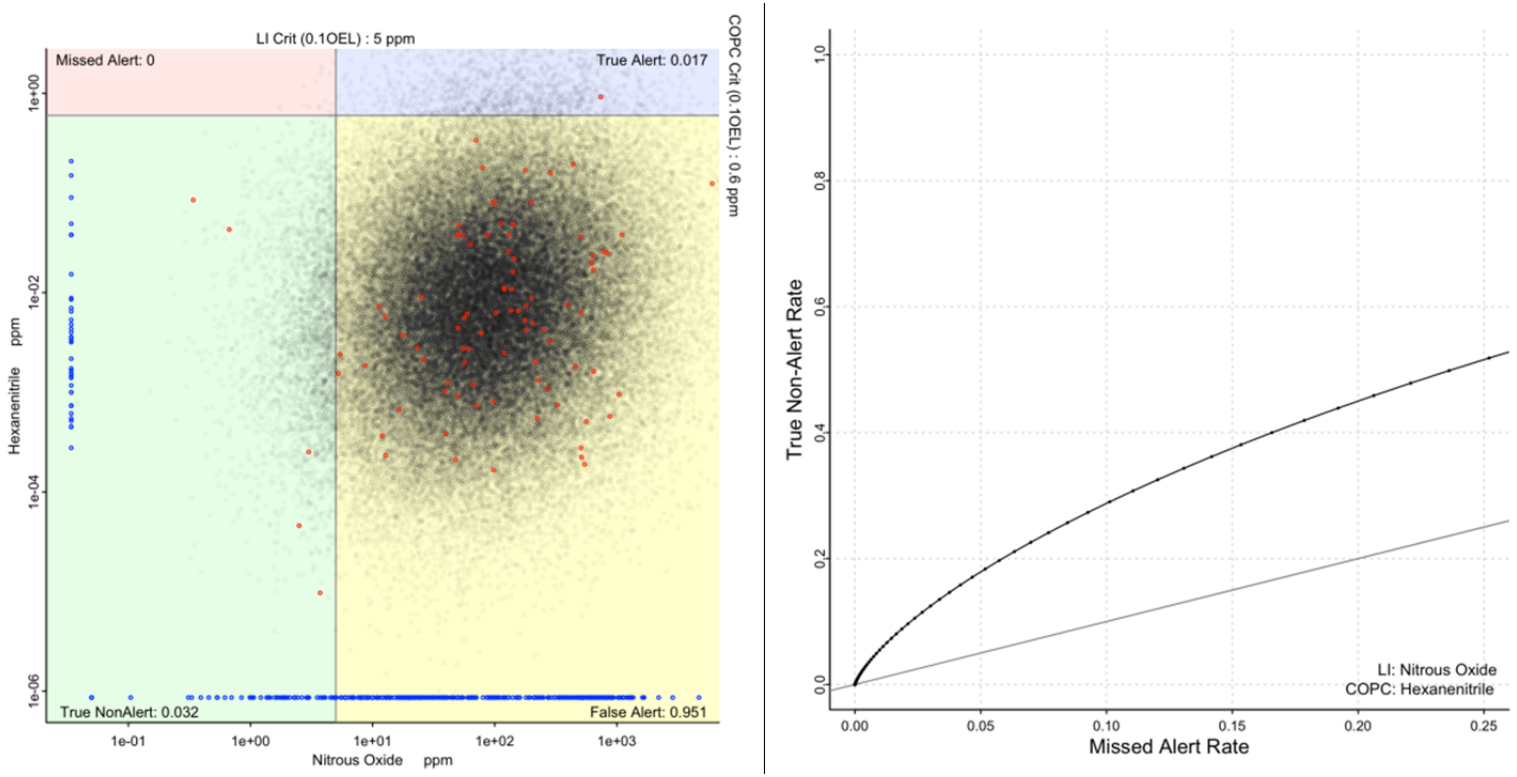

Figure C.51. Left: Scatterplot of hexanenitrile and nitrous oxide measurements (red dots), probability density estimate (black dots), and non-paired or MDL measurements (blue dots) with associated alert quadrants designated by 10% OEL indication lines for each chemical. Right: ROC-like curve displays the change in statistical performance for hexanenitrile and nitrous oxide in terms of paired true non-alert and missed alert probabilities obtained by increasing the LI alert level and noting the changes in these two.

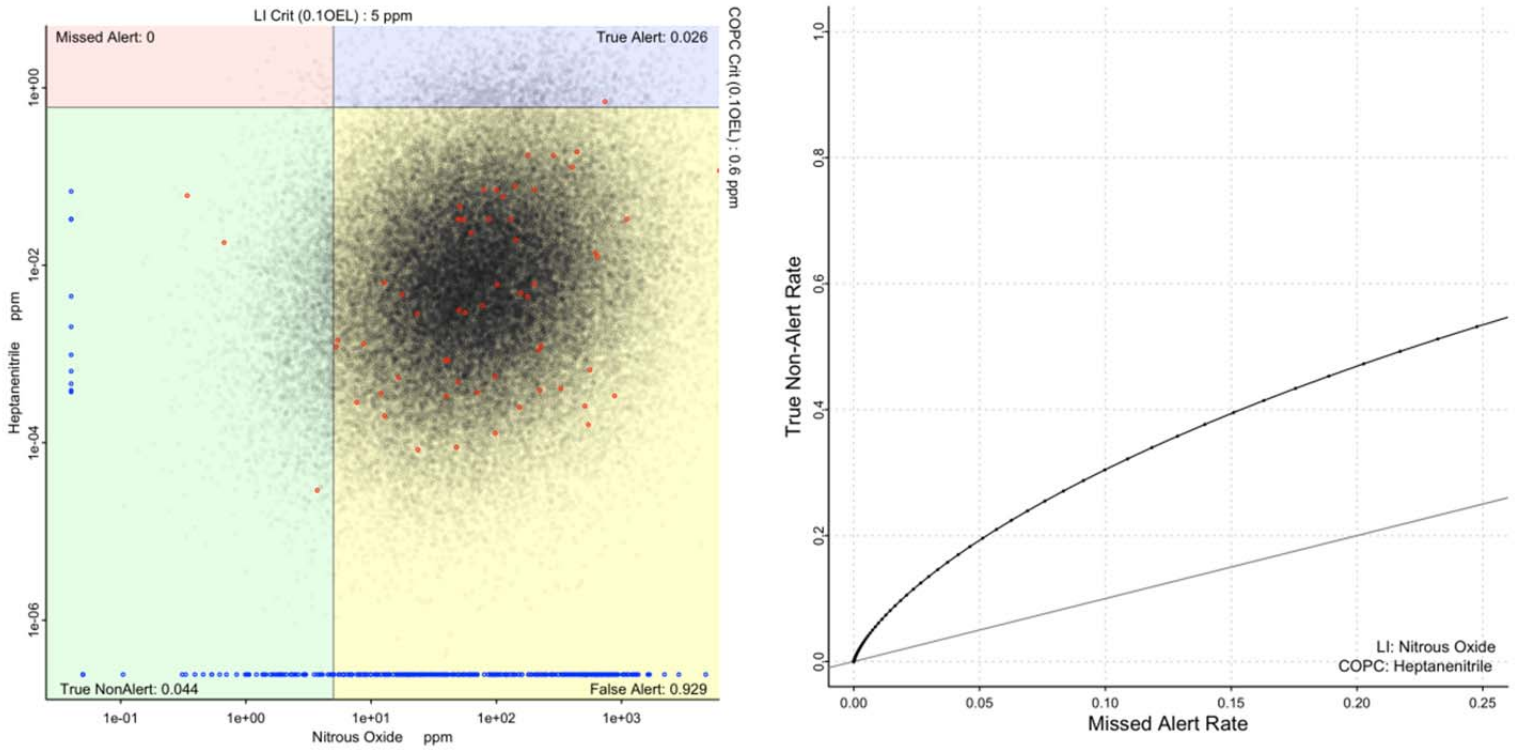

Figure C.52. Left: Scatterplot of heptanenitrile and nitrous oxide measurements (red dots), probability density estimate (black dots), and non-paired or MDL measurements (blue dots) with associated alert quadrants designated by 10% OEL indication lines for each chemical. Right: ROC-like curve displays the change in statistical performance for heptanenitrile and nitrous oxide in terms of paired true non-alert and missed alert probabilities obtained by increasing the LI alert level and noting the changes in these two.

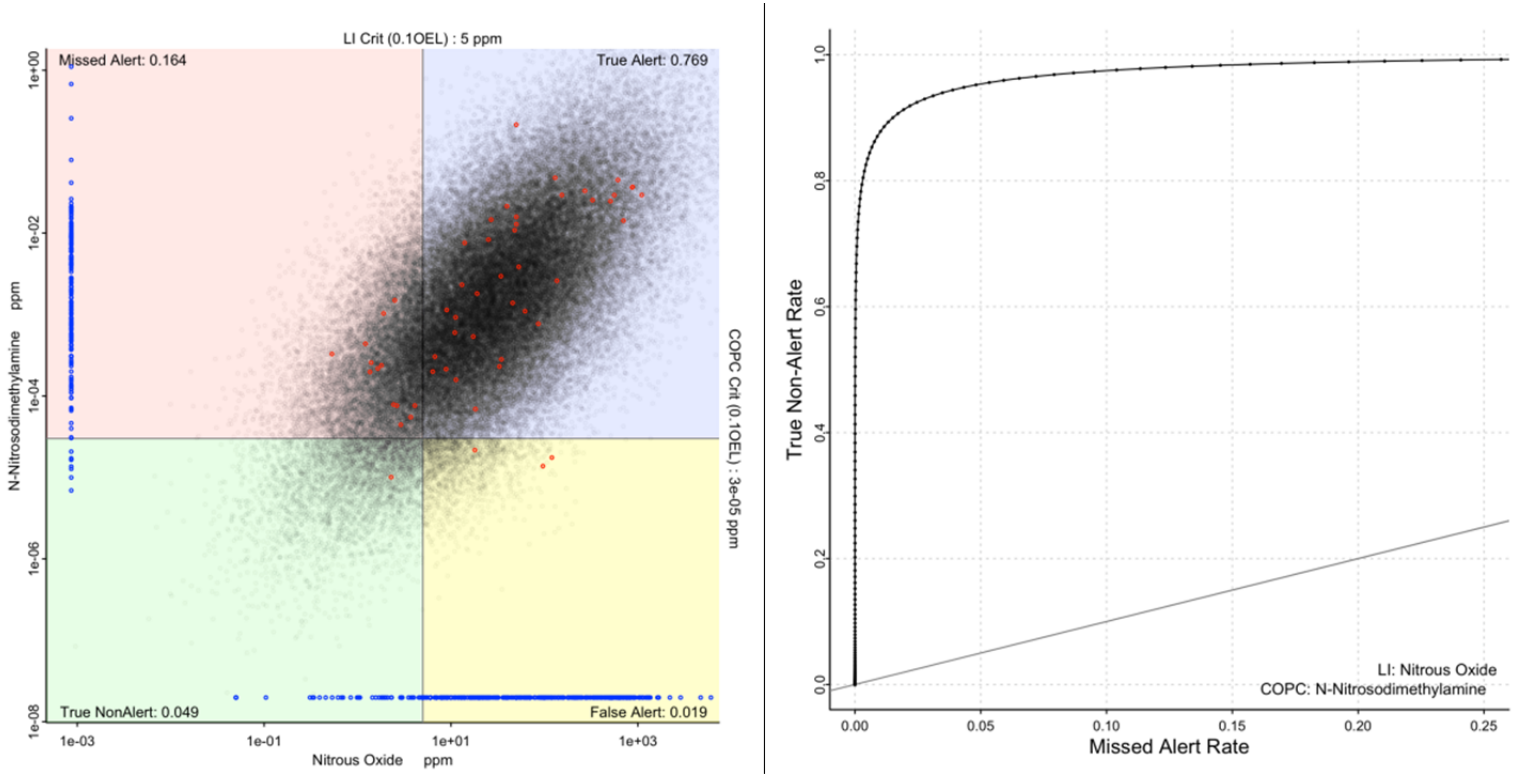

Figure C.53. Left: Scatterplot of n-nitrosodimethylamine and nitrous oxide measurements (red dots), probability density estimate (black dots), and non-paired or MDL measurements (blue dots) with associated alert quadrants designated by 10% OEL indication lines for each chemical. Right: ROC-like curve displays the change in statistical performance for n-nitrosodimethylamine and nitrous oxide in terms of paired true non-alert and missed alert probabilities obtained by increasing the LI alert level and noting the changes in these two.

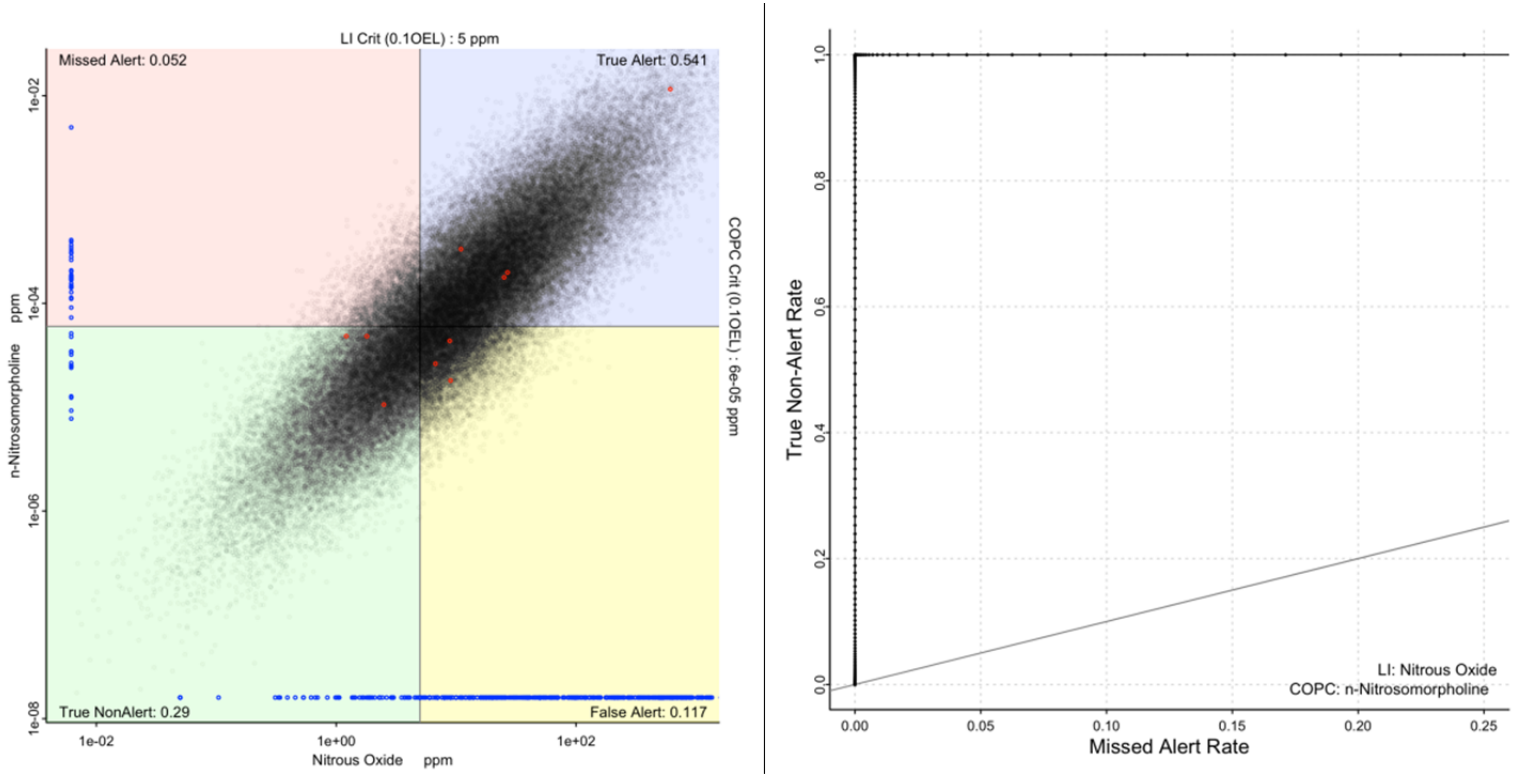

Figure C.54. Left: Scatterplot of n-nitrosomorpholine and nitrous oxide measurements (red dots), probability density estimate (black dots), and non-paired or MDL measurements (blue dots) with associated alert quadrants designated by 10% OEL indication lines for each chemical. Right: ROC-like curve displays the change in statistical performance for n-nitrosomorpholine and nitrous oxide in terms of paired true non-alert and missed alert probabilities obtained by increasing the LI alert level and noting the changes in these two.

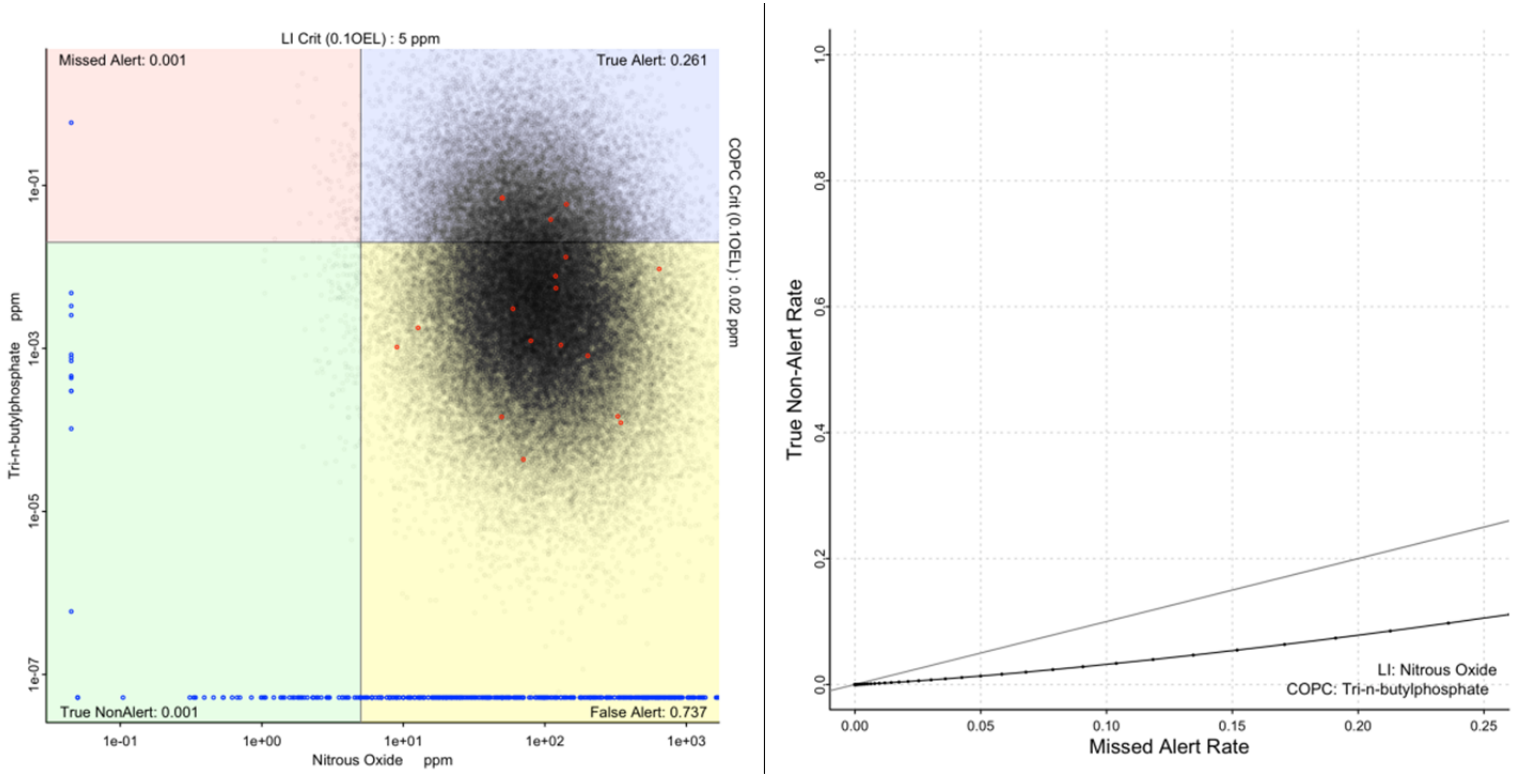

Figure C.55. Left: Scatterplot of tri-n-butylphosphate and nitrous oxide measurements (red dots), probability density estimate (black dots), and non-paired or MDL measurements (blue dots) with associated alert quadrants designated by 10% OEL indication lines for each chemical. Right: ROC-like curve displays the change in statistical performance for tri-n-butylphosphate and nitrous oxide in terms of paired true non-alert and missed alert probabilities obtained by increasing the LI alert level and noting the changes in these two.

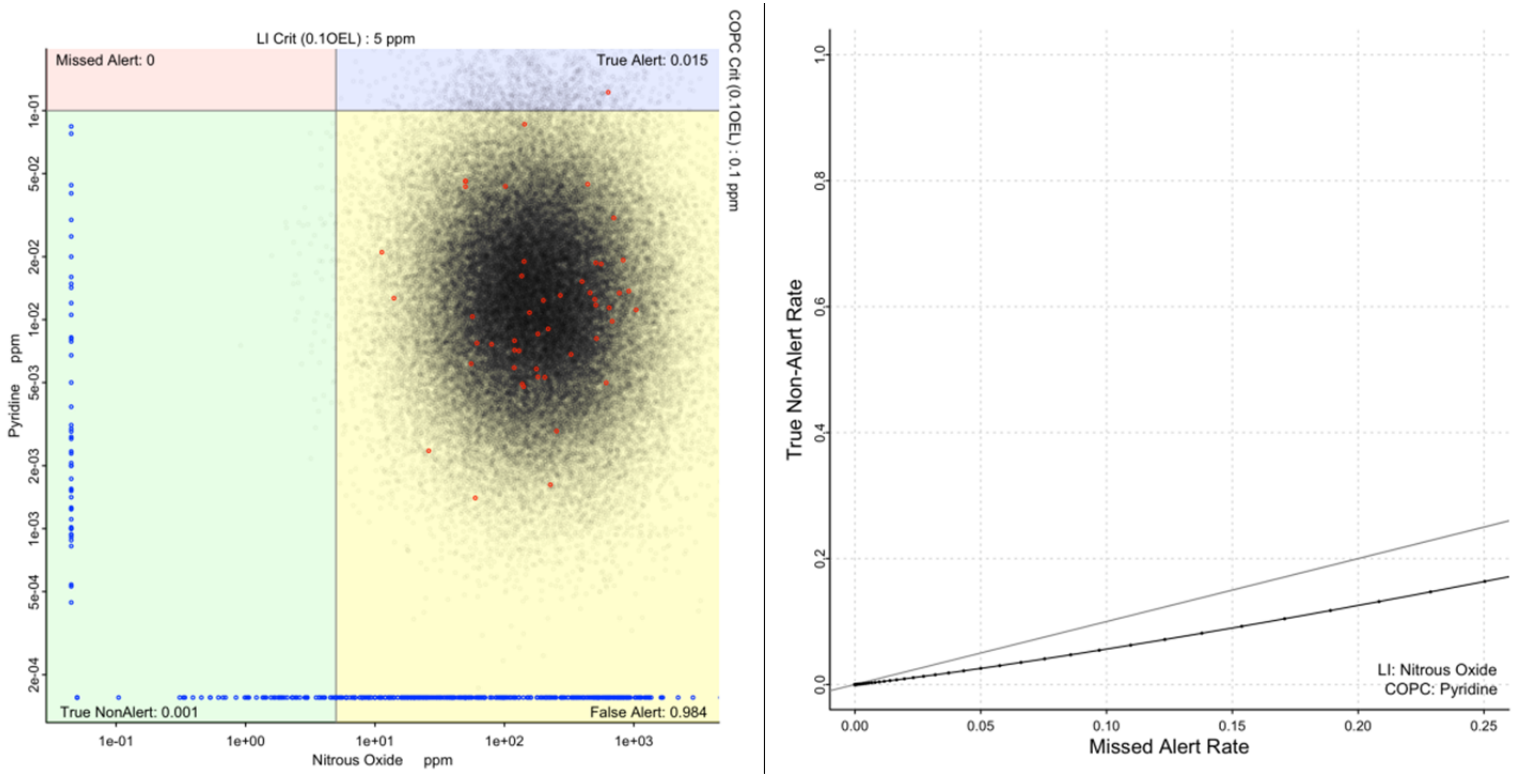

Figure C.56. Left: Scatterplot of pyridine and nitrous oxide measurements (red dots), probability density estimate (black dots), and non-paired or MDL measurements (blue dots) with associated alert quadrants designated by 10% OEL indication lines for each chemical. Right: ROC-like curve displays the change in statistical performance for pyridine and nitrous oxide in terms of paired true non-alert and missed alert probabilities obtained by increasing the LI alert level and noting the changes in these two.

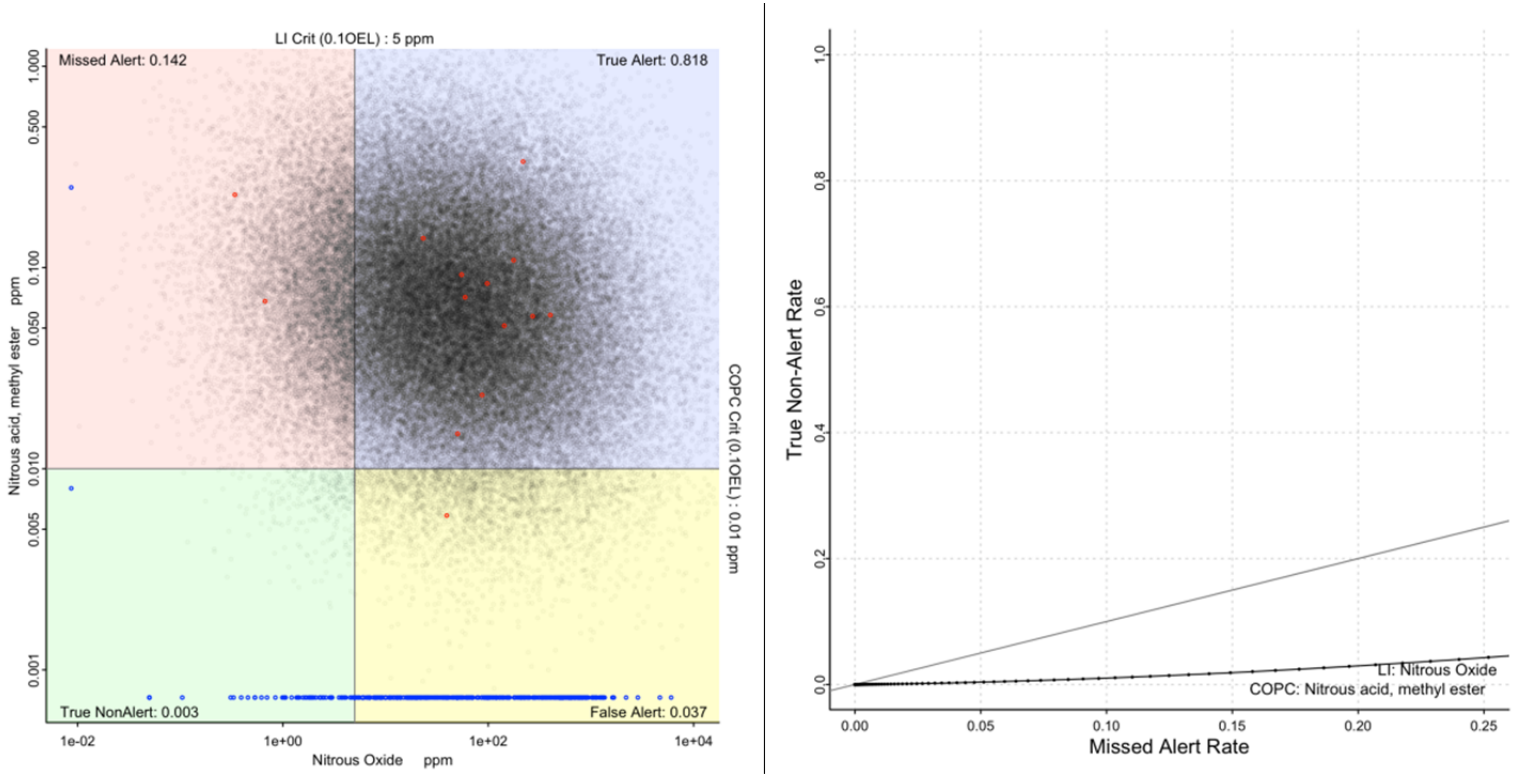

Figure C.57. Left: Scatterplot of methyl nitrite and nitrous oxide measurements (red dots), probability density estimate (black dots), and non-paired or MDL measurements (blue dots) with associated alert quadrants designated by 10% OEL indication lines for each chemical. Right: ROC-like curve displays the change in statistical performance for methyl nitrite and nitrous oxide in terms of paired true non-alert and missed alert probabilities obtained by increasing the LI alert level and noting the changes in these two.

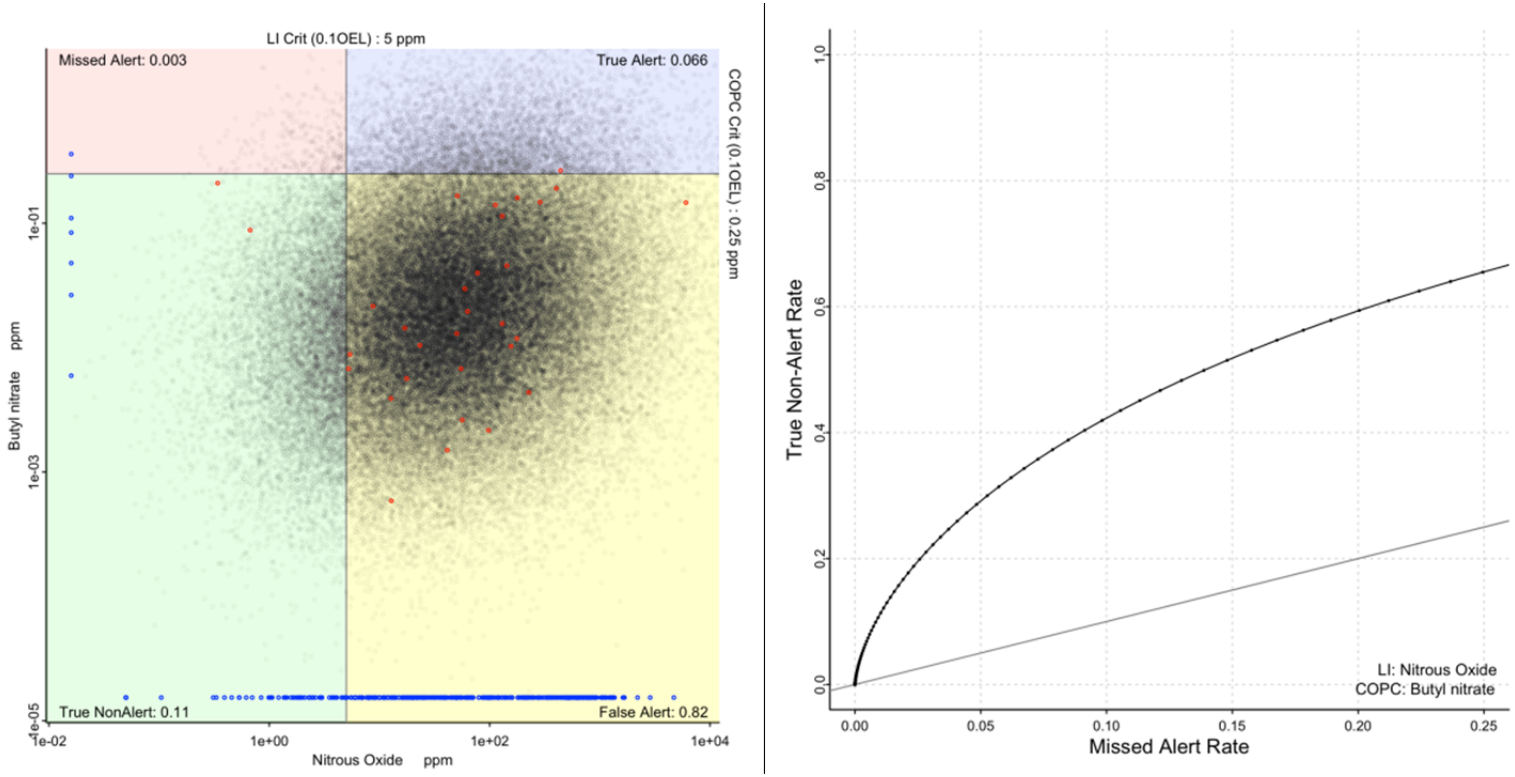

Figure C.58. Left: Scatterplot of butyl nitrate and nitrous oxide measurements (red dots), probability density estimate (black dots), and non-paired or MDL measurements (blue dots) with associated alert quadrants designated by 10% OEL indication lines for each chemical. Right: ROC-like curve displays the change in statistical performance for butyl nitrate and nitrous oxide in terms of paired true non-alert and missed alert probabilities obtained by increasing the LI alert level and noting the changes in these two.

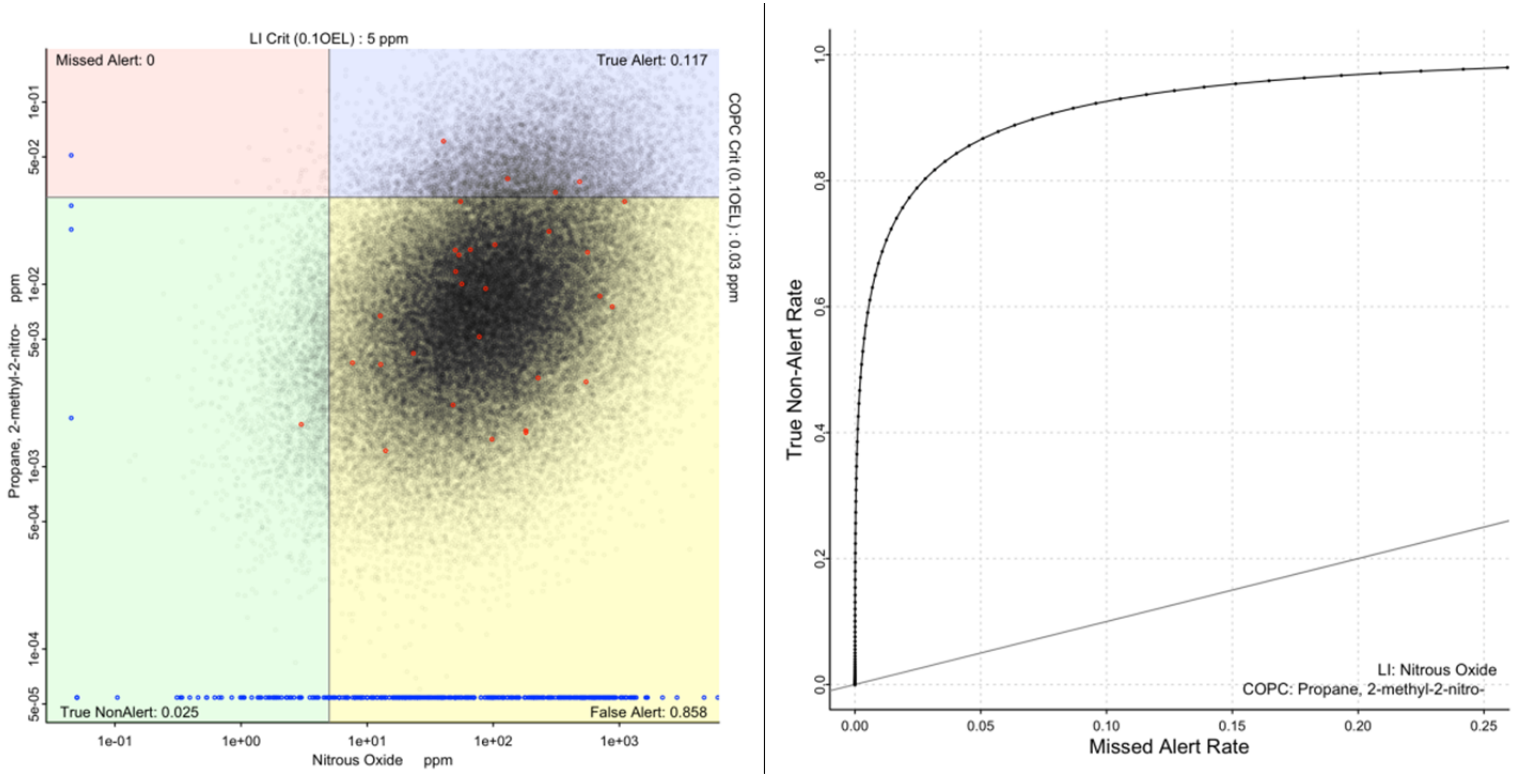

Figure C.59. Left: Scatterplot of 2-nitro-2-methylpropane and nitrous oxide measurements (red dots), probability density estimate (black dots), and non-paired or MDL measurements (blue dots) with associated alert quadrants designated by 10% OEL indication lines for each chemical. Right: ROC-like curve displays the change in statistical performance for 2-nitro-2-methylpropane and nitrous oxide in terms of paired true non-alert and missed alert probabilities obtained by increasing the LI alert level and noting the changes in these two.

Pacific Northwest
NATIONAL LABORATORY

Proudly Operated by **Battelle** *Since 1965*

U.S. DEPARTMENT OF
ENERGY

902 Battelle Boulevard
P.O. Box 999
Richland, WA 99352
1-888-375-PNNL (7665)

www.pnnl.gov